Response to NRR Request for Additional Information (dated June 23, 1994)
Concerning Core Shroud Cracking at
Dresden Unit 3
and
Quad Cities Unit 1

Commonwealth Edison Company

June 25, 1994

TABLE OF CONTENTS

ATTACHMENTS

ATTACHMENTS (Continued)

Question MS-1:

Provide for both Dresden, Unit 3, and Quad Cities, Unit 1, the number of effective full power years of operation.

Response MS-1:

Unit	Data Date	Effective Full Power Years
Dresden, Unit 2	March 1994	14.0454
Dresden, Unit 3	March 1994	13.4859
Quad Cities, Unit 1	March 1994	14.4397
Quad Cities, Unit 2	March 1994	13.9012

Question MS-2:

Provide information concerning the reactor coolant water chemistry for both units from the time of startup to the present and its effect on the core shroud cracking.

Response MS-2:

Attachments ____ are trends for Dresden, Units 2 & 3, and Quad Cities, Units 1 & 2. In Reference (b) ComEd addressed the issue of water chemistry. Water chemistry may have an effect on the time to initiation as well as crack growth rate. While initiation time is almost impossible to predict, the effect of conductivity on crack growth rates has been modeled by GE in the PLEDGE model, and the results were presented in the Dresden and Quad Cities H5 weld reports, see References (f) and (g).

Question MS-3:

Provide justification that the 45 degree Ultrasonic (UT) Transducer would reliably detect all cracks in the core shroud if the cracking is tight or geometry is unfavorable. In addition, the justification should provide a detailed explanation of why bounding flaw depth at the H5 weld is 1.24 inches.

Response MS-3:

See Reference (h). The physical characteristics of the cracks seen in the boat samples are such that a 45 degree ultrasonic shear wave will not be transmitted. Since the upper toe of the fillet weld can always be seen from below by the 45 degree UT shear wave, the cracks cannot be deeper than the intersection of the 45 degree shear wave with the weld fusion line. This effectively excludes a volume of material below the weld that cannot be cracked. For purposes of flaw evaluation, a defect is assumed to be everywhere outside this excluded volume. Significant margin is available even with this conservative assumption.

Question MS-4:

Provide justification to rule out cracking coming from the inside of the shroud at the H5 weld from the toe of the fillet weld.

Response MS-4:

The justification is provided in Reference (h).

Question MS-5:

Provide a map of the UT measurements on the H5 weld.

Response MS-5:

The map of the UT measurements are provided in Reference (i).

Question MS-6:

Provide a comparison of the Boiling Water Reactor Owners Group core shroud screening criteria to that used for the Dresden and Quad Cities core shroud inspection.

Response MS-6:

The approach used to perform the core shroud inspections at Dresden and Quad Cities provides the maximum information relevant to assuring core shroud integrity during all design basis events. This is achieved by verifying that sufficient uncracked shroud material (i.e. good metal) at each circumferential weld exists to ensure structural integrity of the shroud under all design basis events. This approach is referred to as "Qualified Shroud Based" (QSB) inspection. It is a modification of the BWROG standard inspection approach, Statistical Sample Based (SSB) inspection, which has been used and is primarily suited for inspections where cracking is not expected or expected to be infrequent.

Lessons learned on shroud inspection experiences at other BWR units led ComEd to evaluate the shroud cracking issue using a different strategy than has been traditionally used for many past industry cracking concerns. In this case, evaluations were performed to determine the best course of action if the initial assumption is that cracking will exist, particularly at older units with higher carbon content core shroud material. These evaluations resulted in the determination that, for the primary concern of core shroud integrity, the QSB inspection approach defined above maximizes assurance of core shroud integrity, yet minimizes inspection resources, outage duration, and radiation dose incurred to inspection personnel.

The QSB inspection approach relies on Linear Elastic Fracture Mechanics (LEFM) and/or Limit Load Analysis (LLA) plus conservative IGSCC growth rate of 5×10^{-5} in/hr to establish the required amount of evenly distributed uncracked material at each weld location to assure the structural integrity of the weld under all design basis events for a given operating interval. The LEFM/LLA results form the basis for the QSB initial inspection sample size which includes the number and location of inspection sites. All circumferential welds are included in the initial inspection sample. The nominal length of each inspection site ranges from 10 inches to 16 inches. With this approach uninspected locations are assumed to contain through-wall cracks. This is a conservative assumption since much of the uninspected locations may actually be uncracked or only partially cracked.

If visual inspection verifies sufficient uncracked material meeting the LEFM/LLA criteria, then the weld structural integrity is positively demonstrated. These crack free inspection sites also effectively bound possible crack length (i.e the length of uninspected weld areas). Any further inspections beyond this stage will be strictly discretionary and will be based completely on the cost effectiveness of the additional information to be obtained.

If the extent of uncracked material identified in the initial inspection fails to meet the weld specific LEFM/LLA criteria, additional sites will be inspected. The required number of additional sites and their distributed locations are again determined by LEFM and/or LLA plus conservative SCC growth rate, taking into account the existing uncracked material found at previously inspected sites. If visual inspection verifies sufficient uncracked material meeting the LEFM/LLA criteria, then the weld structural integrity is positively demonstrated. Any further inspections beyond this stage will be strictly discretionary and will be based completely on the cost effectiveness of the additional information to be obtained. This exercise will be repeated until the weld specific LEFM/LLA criteria are met or the complete weld circumference is inspected.

In practice, the manner in which the "sample expansion" described above is performed is analogous to cutting a pie into smaller pieces. Additional cutting of the pie only occurs in the arc segment of the pie encompassing the inspection site that fails the LEFM/LLA criteria. The number of "cuts" and the location of the "cuts" are determined by LEFM and/or LLA plus conservative IGSCC growth rate, taking into account the existing uncracked material found at previously inspected sites.

Additional conservatism are built into this QSB inspection approach, such as:

1. LLA is based on accepted ASME Section XI procedures for flawed austenitic stainless steel piping with appropriate code margins, although the shroud is not a primary pressure boundary,
2. Proximity rules of ASME Section XI are used to combine circumferential and/or vertical crack indications,
3. LEFM is applied in conjunction with LLA for welds in the core shroud "beltline" although it is not required for austenitic material at the fluence levels experienced by the Dresden and Quad Cities core shrouds.

In contrast, the SSB inspection approach uses a statistically based initial inspection sample. If crack indications are observed in the initial sample, the inspection will be extended in some fashion to additional locations on the same weld and to additional welds. This expansion of inspection results in the characterization of the observed crack indications, which is valuable information for future reference and possible repair decision. The expansion stops when no crack indications are observed and the analytical evaluations using LEFM and/or LLA are performed to determine the core shroud structural integrity based on available flaws characterization. However, this SSB approach and associated expansion may not always result in a 100% inspection of a weld. Therefore, the analytical evaluations could be based on the unconservative assumption that uninspected areas are uncracked.

The QSB inspection methodology discussed above was developed using sound and conservative technical bases. The results are positive demonstration of the core shroud structural integrity under all design basis events when the applicable inspection criteria are met. In hindsight, if the SSB inspection methodology was applied at Dresden and Quad Cities in lieu of the QSB approach, it is possible that the H5 weld would not have been inspected. ComEd has concluded that application of the QSB methodology is sound and results in identifying flawed weldments that require further evaluation.

The following table is a comparison of the Dresden/Quad Cities initial inspection plan for each shroud weld with that recommended by the BWROG Core Shroud Evaluation Inspection Strategy for a High Risk Plant. Section 6.0 of the BWROG Core Shroud Evaluation provides an inspection strategy designed to meet the intent of SIL 572 Rev.

10. As discussed in the BWROG plan, the recommendations were '"provided to utilities as a guide in developing their plant-specific inspection plans".

	Dresden Plan	Quad Cities Plan[Note 1]	BWROG Inspection Strategy
H1	4 Locations, 60 inches, 8.8% of Weld	4 Locations, 60 inches, 8.8% of Weld	No Inspection Recommended
H2	4 Locations, 60 inches, 8.8% of Weld	4 Locations, 60 inches, 8.8% of Weld	No Inspection Recommended
H3	4 Locations, 60 inches, 9.3% of Weld	4 Locations, 60 inches, 8.8% of Weld	8 Locations, 120 inches, 18.6% of Weld
H4	4 Locations, 60 inches, 9.3% of Weld	8 Locations, 120 inches, 18.6% of Weld	8 Locations, 120 inches, 18.6% of Weld
H5	4 Locations, 60 inches, 9.3% of Weld	8 Locations, 120 inches, 18.6% of Weld	No Inspection Recommended
H6	4 Locations, 60 inches, 9.6%, of Weld	4 Locations, 60 inches, 8.8% of Weld	No Inspection Recommended
H7	4 Locations, 78 inches, 12.5% of Weld	8 Locations, 114 inches, 18.2% of Weld	2 Locations, 10% of Weld
Vert Welds	No Inspection Performed	No Inspection Performed	1 weld only if cell already vacated
Summary	28 locations inspected on 7 welds, which represents 9.6% of the cumulative length of all circumferential welds in the shroud.	36 locations inspected on 7 welds, which represents 13% of the cumulative length of all circumferential welds in the shroud.	18 locations inspected on 3 welds, which represents 6.6% of the cumulative length of all circumferential welds in the shroud.

Note 1: Quad Cities requires more initial inspection locations than Dresden to demonstrate structural margin due to higher seismic loadings.

Question MS-7:

Is the Dresden and Quad Cities H5 fabrication similar to that of Brunswick (i.e., double V grooved, back gouged)?

Response MS-7:

Yes. The welds are termed single bevel double "V" weld joint geometries with fillet. The plate wall thickness at Dresden and Quad Cities is 2 inches instead of the 1.5 inches at Brunswick. The reinforcing fillet weld size at Dresden and Quad Cities is 1 inch, instead of the 0.75 inch at Brunswick Unit 1.

Question MS-8:

Provide verification of the dimension of the fillet weld.

Response MS-8:

Fillet dimensions were verified by following a quality control path of specification, written welding and inspection procedures, and by inspection verification and approval.

Question MS-9:

Provide justification that the crack growth rate in your June 13, 1994, submittal is bounded based on a water chemistry during the early years of operation at Dresden and Quad Cities. Could deeper cracks be expected based on water chemistry?

Response MS-9:

The bounding crack growth rate of $5X10^{-5}$ are taken from the appropriate chart published in NUREG 0313 rev. 2. This chart considers both high material susceptibility and abnormal water chemistries. It is the bounding crack growth rate used for the ComEd Structural Margin Assessment considering the variable water chemistry conditions.

Crack growth rates from References (f) and (g) are demonstrated to be bounding, since cracks growing at the 5E-5 in/hr rate would be through-wall in less than four cycles, yet UT has established that the H5 flaw is actually less than 1.24 in. deep. Further, the PLEDGE model predicted crack growth rates are very conservative when compared with recent EPRI data for operation at low levels of sulfate and chloride (also presented in References (f) and (g)).

Question MS-10:

Provide justification that crack propagation path predictions have correctly incorporated the effects of residual stresses. Could the crack propagate through an alternate path (i.e., up through the cylinder)?

Response MS-10:

See Attachment MS-10-1, the finite element model FEM of weld residual stresses. The predicted residual stress patterns are confirmed by boat sample metallography, in that the cracking appearance exhibits a transition from a high stress (planar) region into a region of lower stress (multibranched with extensive grain boundary encirclement) where crack growth rates would be predicted to fall by an order of magnitude in accordance with NUREG 0313, Rev. 2. Cracking would not propagate into the weld, because the shape of the residual stress field would be expected to favor cracking as observed in the core plate support ring, and the weld metal itself is considered to be immune from IGSCC by NUREG 0313, Rev. 2, due to its ferrite content and low carbon (see Attachment MS-10-2).

Question MS-11:

Provide stress distribution profile information across the H5 weld.

Response MS-11:

The stress distribution profile is provided in Attachment MS-10-1.

Question MS-12:

What is the status of the use of hydrogen addition to the reactor coolant at Dresden and Quad Cities.

Response MS-12:

In Reference (b), specifically Response (2) relative to Dresden, Unit 2, and Quad Cities, Unit 2, ComEd supplied the status of the use of hydrogen addition to the reactor coolant at Dresden Unit 2 and 3 and Quad Cities Unit 1 and 2.

Specifically, unlike Dresden Unit 3, Dresden Unit 2 has been operating with hydrogen injection beginning with operating cycle 9 (1983). Hydrogen injection has ranged from 1.0 - 1.5 ppm at approximately 90 % availability. Dresden Unit 3 does not operate with hydrogen addition.

Quad Cities Units 1 and 2 both have been operating with hydrogen injection beginning in November 1990. Hydrogen addition availability for Quad Cities Unit 1 has been 57 % and Quad Cities Unit 2 has been 44%. Hydrogen injection rates have ranged from 1.0 - 1.5 ppm.

Question MS-13:

Provide the detailed results of the Dresden and Quad Cities boat sample metallurgical analyses.

Response MS-13:

The details of the boat sample metallurgical analyses were presented on June 22, 1994, and will be presented again in the meeting planned for June 27, 1994. Further, details are included in Reference (h).

Question MS-14:

Provide a detailed justification and clarification for the basis of crack depth sizing based on the H5 weld geometry using only UT detection capability.

Response MS-14:

Reference (h) explains use of UT detection equipment (45 degree shear wave) to establish a zone of good metal which cracks have not penetrated. This is supported by boat sample results, which found flaws to be no deeper than 0.69 inch.

Question MS-15:

What are the fracture toughness properties in the short transverse direction for the heavy stainless steel plate of the top guide support ring and core plate support ring?

Response MS-15:

Only tensile properties are of significance to limit load analysis, and the short transverse properties of the austenitic stainless steel of the shroud do not vary significantly from the longitudinal properties. Data from Oak Ridge National Laboratory (ORNL) reported in Attachment MS-15-1 indicates that the short transverse tensile strength of the tested 304 plate was within 5% of the longitudinal tensile strength, and both were well above code minimums and the longitudinal tensile strength reported on the CMTR of the ORNL material. Based on this information it is reasonable to assume that austenitic stainless steel will meet Code minimums for S_m in the short transverse direction, and there will be no change in the Structural Margin Assessment or the margin of safety.

Question MS-16:

Justify why limit load analysis is appropriate for the stress distributions associated with the H5 weld and fillet finite element analysis. Is bending appropriately considered?

Response MS-16:

See References (f) and (g) which include the finite element model which shows that bending stresses in the remaining ligament are minimal, and membrane loading still applies.

Question MS-17:

What is the predicted/measured reduction in residual stresses with the cracking at the H5 weld?

Response MS-17:

See Attachment MS-10-1 for stress intensity vs. crack depth.

Question MS-18:

Provide an assessment of the operability margin against the uncertainties and approach used to size the H5 crack by UT.

Response MS-18:

Reference (h) explains the basis for stating that the maximum bounding flaw depth is less than 1.24 inches, and this is supported by the boat sample metallography results. The maximum allowable beginning-of-cycle allowable flaw depth is established by calculating an amount of crack growth based on operating cycle length and an assumed crack growth rate (CGR), and subtracting that from the maximum allowable end-of-cycle flaw depth, as established by structural margin assessment. See the previously submitted GE H5 evaluations, References (f) & (g). For Dresden's 24 month operating cycle, assuming 8000 hours/yr of operation, the amount of crack growth predicted ranges from: (a) 0.8 inch for the bounding NUREG 0313 CGR of 5E-5 in/hr, to (b) 0.2 inch for the PLEDGE model predicted CGR of 1.24E-5 in/hr, to as little as (c) 0.08 inch at the CGR predicted by NUREG 0313 for the 10 KSI-IN^{-2} stress intensity predicted by the residual stress analysis (Attachment MS-10-1) for a one inch deep flaw. This translates for Dresden to maximum allowable beginning-of-cycle flaw depths ranging from 2.14 inches to 2.86 inches. For Quad Cities, with its slightly smaller maximum end-of-cycle flaw depth and 18 month operating cycle, allowable beginning-of-cycle flaw depths range from 2.28 to 2.82 inches.

The operating margin to account for structural assessment uncertainty is the difference between the maximum allowable beginning-of-cycle flaw depth and the bounding assumed current flaw size of 1.24 inches. The operating margin for Dresden, depending on which crack growth rate is used, ranges from 0.9 to 1.62 inches, and for Quad Cities Unit 1 it ranges from 1.04 to 1.58 inches (see Attachments MS-18-1 and MS-18-2).

Even using the bounding 5E-5 in/hr CGR, which is at least a factor of 4 higher than CGRs believed to be realistic for current plant operating water chemistry conditions, there is large operating margin available to account for uncertainty in UT detection capability. As was pointed out in Reference (b), another compensatory factor against UT uncertainty is the application of Section XI safety factors for primary pressure boundaries in the structural margin assessment, even though the core shroud is not a primary pressure boundary. Other compensatory factors include: (1) the confirmation by metallography that actual flaw sizes in the boat samples taken from Dresden 3 and Quad Cities 1 are no deeper than .69 inch, and (2) the residual stress and applied stress intensity prediction (Attachment MS-10-1) indicate that CGRs will diminish significantly with depth based on NUREG 0313.

The foregoing operating margin assessment may be affected by ComEd technical audit activities is the input loads to the Structural Margin Assessment for Dresden. However, ComEd has concluded because of work to date that there will be minimal impact on operating margins. Our conclusion remains that the observed flaws represent no immediate safety concern, and all applicable ASME code safety margins will be maintained well beyond the end of the next operating cycle for both Dresden Unit 3 and Quad Cities Unit 1.

Question PR-1:

Provide the probabilities and basis of the design basis events as well as the data sources for the postulated event frequency. Also, provide the contribution to the core damage frequency and release frequency for these events.

Response PR-1:

Probabilities of design basis events:

	EVENT	DRESDEN FREQUENCY	QUAD CITIES FREQUENCY
1.	SSE	5.0E-5/yr	2.2E-5/yr
2.	Main Steamline Break	4.1E-8/yr	4.1E-8/yr
3.	Recirc Line Break	3.0E-4/yr	3.0E-4/yr
4.	#1 and #2 coincedently	5.6E-15/yr	2.5E-15/yr
5.	#1 and #3 coincedently	4.1E-11/yr	1.8E-11/yr

Bases of above probabilities:

1. The SSE frequency of exceedance was obtained from updated LLNL curves.

2. The frequency of an unisolable main steamline break was obtained from the IPEs.(1)

3. The frequency of a large LOCA was obtained from the IPEs.(1)

4. Derived as follows(2):
   (5.0E-5)/365 * (4.1E-8)/365 * 365 = DRESDEN
   (2.2E-5)/365 * (4.1E-8)/365 * 365 = QUAD CITIES

5. Derived as follows(2):
   (5.0E-5)/365 * (3.0E-4)/365 * 365 = DRESDEN
   (2.2E-5)/365 * (3.0E-4)/365 * 365 = QUAD CITIES

(1)*Section 4.1.1, Initiating Events; Individual Plant Examination Submittal, Reference (j) and (k).*

(2)*For purposes of these responses "coincident" is defined as occurring in the same 24 hour period.*

Contribution to core damage frequency and release frequency for design basis events:

The contribution to the core damage frequency and release frequency is presented in the IPEs for Dresden and Quad Cities(3). The values provided in the IPEs are for internal (non-seismic) initiators only. ComEd will not be able to address the frequency of seismic induced core damage or serious release until completion of the IPEEE. Even with completion of IPEEE, coincident seismic events and steamline breaks or recirculation line breaks as dual initiators are considered by ComEd to be low frequency events.

(3)*Section 4.6.2, Summary of Results; Individual Plant Examination Submittal, Reference (j) and (k).*

Question PR-2:

Are the shroud cracks in conjunction with the steamline break or recirculation pipe break events incorporated in the IPE study? If so, provide the information.

Response PR-2:

The shroud cracks are not incorporated in the IPE studies.

Question ME-1:

Provide complete structural/mechanical analysis of the core shroud, assuming worst-case degradation of the H5 weld up to and including a 360-degree thru wall crack at H5 for upset, emergency and faulted plant conditions (e.g., main steam line break (MSLB), recirculation line break (RCLB), SSE and most severe load combinations). Evaluate the effect of three-dimensional shroud movement (e.g., uplift/tilting and subsequent dropping, tilting, lateral motion, etc.) on the structural integrity and functionality of reactor internal components, equipment and support structures.

Analysis package should fully describe all analytical assumptions with justifications, conservatism, methodology (e.g., analytical models and boundary constraints, development and application of loads, stress and deflection calculations), and conclusions. Also provide information to verify that any computer codes used in the analysis have been properly benchmarked.

Response ME-1:

The examinations at the Dresden and Quad Cities stations have shown that the flaw at the H5 weld has only partially penetrated the wall of the shroud. Based on the results of extensive examinations ComEd has demonstrated through Structural Margin Assessments (References (f) and (g)) that the remaining ligaments including crack growth over the next operating cycle are structurally adequate. ComEd has determined the minimum required ligament for the shroud under all loading conditions. These analyses have included all design basis loads and in addition have considered additional load combinations that are more severe than what is defined in sections 3.9.3.1.1.2 of the Dresden and Quad Cities UFSAR's.

In addition to the Structural Margin Assessments, ComEd has assumed the condition of a fully severed shroud due to a 360 degree flaw at the H5 location (e.g. no ligament is remaining). This postulated shroud condition was analyzed to predict shroud behavior during accident conditions and evaluate the postulated loads resulting from these conditions. The results of these analyses were provided in References (b) and (c). Provided in the following discussions is a summary of the methodology, assumptions and judgements made. The detailed calculations, reports and justifications are also provided in the attachments. Additional discussion relevant to this question is provided in the response to Question RS-3.

A. Description of the loadings used and applicable load combinations.

The following loading conditions have been evaluated as part of the ligament calculations and for the safety assessment without the ligament:

Dead Loads - DL
Buoyancy - B
Normal Operation Pressure - N (7 psi Dresden, 8 psi Quad Cities)
Upset Pressure - U (7 psi Dresden, 8 psi Quad Cities)
Faulted Loads - F
MSLOCA (12 psi Dresden, 20 psi Quad Cities)
RRLOCA Pressure (7 psi Dresden, 8 psi Quad Cities)
RRLOCA Blowdown (17.2 Kip concentrated load)
RRLOCA Acoustic (175.0 Kip concentrated load)
Operating Basis Earthquake - OBE (horizontal and vertical)
Design Basis Earthquake - DBE (horizontal and vertical)

Provided in Attachment No. ME-1-1 is a copy of the applicable sections of the Dresden and Quad Cities UFSAR's defining the applicable design basis pressures, loads and load combinations for the shroud. The sections relevant to the shroud have been bubbled. Included as Attachment No. ME-1-2 is a free body diagram depicting the loads and the points of application on the shroud. Also included as part of this attachment are two summary worksheets that define the shroud section properties, loads, stresses and combined stresses in the wall of the shroud (CSSTRES1.XLS and CSSTRES2.XLS). Provided in the following section is a description of the methods used to calculate the loads used in the evaluations.

1. Dead Loads

   The self weight of the shroud and RPV internals have been calculated based on the design drawings and are the same as were used for the original design.

2. Buoyancy Loads

   The buoyancy loads have been calculated based on the relative density of the shroud components (0.29 lb./in^3) versus the density of water (0.036 lb./in^3).

3. Normal Operation Pressure

   The normal operating pressure was taken from the UFSAR (see Attachment No. ME-1-1) and was applied as a uniform pressure on the area of the shroud head (full inside diameter was used to calculate the total uplift force).

4. Upset Pressure

   The upset pressure was taken from the UFSAR (see Attachment No. ME-1-1) and was applied as a uniform pressure on the area of the shroud head (full inside diameter was used to calculate the total uplift force).

5. Faulted Loads

   Faulted pressure loads were taken from the UFSAR and applied as a uniform pressure on the area of the shroud head (full inside diameter). In addition to the internal pressure on the shroud head associated with the main steam (MS) and reactor recirculation (RR) LOCA the blowdown and acoustic loads associated with the RR LOCA have been calculated. The acoustic loads were calculated using the time history load profile in the UFSAR (see Attachment No. ME-1-1) and by proportioning the total force between the sections of the shroud above and below H5. Based on the relative geometry of the shroud 75% of the total load of 233 Kips has been assumed to act upon the portion of the shroud above H5. The blowdown loads have been calculated using a potential flow analysis to determine a net lateral force (17.2 Kips) acting above H5. See Attachment No. ME-1-3 for a detailed description of the methodology and assumptions used in calculating the blowdown and acoustic loads.

6. Seismic Loads

   The vertical seismic loads were calculated by multiplying the self weight by the vertical accelerations (0.133g DBE Dresden and 0.16g DBE Quad Cities). The horizontal seismic loads for the limit load evaluation (with a ligament) were extracted from the original time history analysis of the RPV and the RPV internals. The horizontal seismic movements for the safety assessment (postulated 360 degree flaw) were calculated using a parametric time history analysis with the original Quad Cities model. See Attachments No. ME-1-3 and ME-1-4 for a detailed description of the methodology and assumptions used in calculating the seismic displacements.

B. Limit Load Analysis With a Ligament

An evaluation was performed which determined allowable flaw depth, since UT examinations confirmed that the cracking was not through-wall. The purpose of this evaluation was to evaluate the indications found near the H5 weld from a structural standpoint. The cracking was assumed to be 360° around the circumference of the shroud for the purposes of this evaluation, since the indications discovered were seen at all accessible locations. Crack growth estimates were combined with the maximum bounding flaw depth of 1.24 inches to determine structural margin. Since the irradiation level is low, the fracture toughness is comparable to that of unirradiated material where ductile behavior governs. Therefore, limit load calculations which use ASME Code, Section XI safety factors were chosen as the appropriate technique for evaluating structural margins for this location. Further discussion of this approach is provided in References (f) and (g).

The limit load approach used was obtained from a net section collapse formulation. First, the neutral axis location was determined by equilibrating the force resulting from the applied membrane stress, Pm, in the uncracked cross section with the force resulting from a stress equal to the flow stress in the remaining ligament (uncracked region) at the crack cross section. The faulted load condition provided the limiting loads used in this calculation. Per Section XI of the ASME Code, a safety factor of 1.4 for the faulted condition was also included in these calculations.

The results showed that a crack depth of at least 96% (i.e., a/t = 0.96) of the shroud thickness can be tolerated while still maintaining all ASME Code structural margins for both the Dresden and Quad Cities Units. These results demonstrate that for Quad Cities at least a factor of 9.7 is available in terms of required area for a 18-month fuel cycle of operation with a bounding maximum flaw depth of 1.24 inches in the H5 weld. These results also demonstrate that for Dresden at least a factor of 16 is available for a 24-month operating cycle.

C. Safety Assessment For A Postulated Through Wall Flaw At H5

1. Shroud Movements Under Postulated Loading Conditions

The shroud lift calculations were performed for the Main Steam and Reactor Recirculation Line break and the details are provided in Attachments ME-1-9 and ME-1-10. These calculations considered the dynamic motion of the shroud and have been shown to be conservative (higher) compared to the detailed model which considered drag forces, buoyancy force, fluid momentum forces, and hydrodynamic masses.

The lateral movement by seismic excitation, acoustic loads during recirculation suction line break (RSLB) and the blowdown loads during RSLB were also calculated and the details of the calculation are shown in Attachment No. ME-1-3 and in the response to question RS-3. The results of all of the analysis are summarized in a table of the movements (see Attachment No. ME-1-8).

2. Seismic Calculations

See the response to question RS-3 for a detailed explanation.

3. Impact Calculation

Shroud impact calculations were performed using shroud lift values previously determined for a postulated main steam line guillotine break event with and without a safe shutdown earthquake (SSE) (see Attachments ME-1-5 and ME-1-6). A simplified second-order differential equation was used to evaluate the shroud impact velocity. Conservation of linear momentum was then applied to determine an effective impact velocity of the entire shroud on the shroud support legs. This velocity was used as an initial condition to a second-order mass-spring differential equation to determine the impact force and stress on the shroud and shroud support legs, assuming that the shroud support legs take the full dynamic load from the shroud drop and that the load is distributed equally. Elastic buckling calculations were also performed for the shroud support legs, and the elastic limit of the shroud support leg material was determined. These values were compared to the stresses calculated for the shroud and shroud support legs. See Attachment No. ME-1-7 for a detailed description of the methodology and assumptions used.

4. Functionality of Reactor Internal Components

See section 7 of Attachment No. ME-1-11 for a detailed description of the functionality of the RPV internal components.

Question RS-1:

What is the total flow value of the LPCI system under accident conditions (i.e., LOCA, large break and steamline break) with postulated worst-case single failure, and what are the limiting single failure assumptions applied and their impacts on injection flow?

Response RS-1:

The nominal design flows following reactor depressurization (<20 psig for both Dresden and Quad Cities) are approximately 5350 gpm for a single pump and 5000 gpm for multiple pump injection. With no single failures or equipment out of service conditions, the injecting equipment and flow rates are:

Equipment	Flow Rate (gpm)
"A" Core Spray	5350
"B" Core Spray	5350
"A" LPCI	5000
"B" LPCI	5000
"C" LPCI	5000
"D" LPCI	5000
Total	**30700**

The normal flow is representative of actual flows without operator intervention.

The total flow of the ECCS system under accident conditions with postulated limiting single failures is as follows.

Dresden - The ECCS systems consists of 2 trains powered from the unit and the swing diesel. Each train has the following:

System	Analytical Flow Rate
Core Spray (1 pump)	4500 gpm at 90 psid
LPCI (2 pumps)	4500 gpm/pump at 20 psid

Quad Cities - The ECCS systems consist of 2 trains powered from the unit and swing diesel. Each train has the following:

System	Analytical Flow Rate
Core Spray (1 pump)	4500 gpm at 90 psid
LPCI (2 pumps)	4500 gpm/pump at 20 psid

The limiting single failure assumption and the impact of that assumption on injection flow is as follows. In the design basis LOCA analysis, the single failures that prove most limiting from an injection flow (and resultant PCT) standpoint are:

1) Failure of a Diesel Generator - this failure can be caused by passive failure of the battery, or as a result of active failures in the diesel generator mechanical/electrical systems. This failure leads to a single injection train being available. (1 core spray plus two LPCI/RHR pumps (3 x 4500 gpm). This event is the limiting failure for the Quad Cities plants using GE best estimate LOCA methods.

2) Failure of the LPCI injection valves - prevents LPCI/RHR injection due to mechanical/electrical faults. This failure leads to core injection by two core spray pumps. (2 x 4500 gpm). This event is the limiting single failure for the Dresden plant using Siemens analysis methods.

Question RS-2:

What is the minimum core water level needed to assure adequate cooling following a DBA LOCA?

Response RS-2:

The minimum core height recommended by the NSSS vendor to ensure adequate cooling by convection to the steam generated in the lower core regions is the 2/3 core height (approximately 8 feet above the core support plate). This condition assumes that no core spray is available. With core spray available, adequate cooling is expected at levels below 2/3 core height.

Question RS-3:

Provide the operating and design basis faulted condition loads for the H5 weld. Identify the methodologies for determining the faulted condition loads and justify why the methodologies are appropriated (e.g., WHAM, RETRAN, approximate 3-D blow down flow analysis). Provide all assumptions with justification conservatism and initial and final conditions. In addition, provide all benchmarking and experimental data to justify use of all codes.

Response RS-3:

The design basis loads for all load cases are defined in the response to question ME-1. The methodology used to calculate these loads is also provided in the referenced response. The justification for the methodology used and a description of the applicable computer program validation is provided in the following discussion.

A. Acoustic loads due to a RRLOCA

The asymmetric acoustic loads applied to the shroud were conservatively calculated using a uniform acoustic load distribution. The WHAM code calculation was shown to be conservative (higher load magnitudes) in comparison to the experimental results, see Attachment No. RS-3-1 for a detailed description.

B. Blowdown loads due to a RRLOCA

The blowdown load was calculated using the potential flow method, and is described in Attachment No. RS-3-2. In comparison to the blowdown load shown in the UFSAR (reference question ME-1, Attachment No. 1) the calculated loads using the potential flow method are higher. The effects of the jet pumps with regard to the calculation of the blowdown force is currently being evaluated and will be submitted upon completion. This supplemental evaluation will be performed using the following two methods: (1) by modifying the potential flow calculation to include the effects of the jet pumps in the downcomer annulus, and (2) by performing a three-dimensional analysis using the TRACG code. This supplemental evaluation will be performed within 12 weeks.

When seismic excitation is not considered, no tipping occurs even if the blowdown load stays the same as the maximum acoustic load applied over the entire shroud. This indicates that the blowdown load calculated as described in Attachment No. RS-3-2 for the portion above H5 would have to be increased nearly 15 times before tipping would occur. By engineering judgement, ComEd has concluded that the supplemental evaluations are unlikely to change the conclusion that tipping does not occur when seismic excitation is not considered.

C. Seismic Loads

The seismic SSE maximum relative displacement between the RPV and the shroud for the case of a 360 degree through-wall crack at weld H5 was obtained from a base support, time history analysis of the Quad Cities primary structure east-west seismic model. The primary structure seismic model is a mathematical, center-line model comprised of standard beam elements and spring elements. The mathematical center-line model is a coupled composite model comprised of : (i) a detailed model of the RPV and internals, (ii) the reactor building and drywell, and (iii) the turbine building and accounts for the dynamic interaction between these various structures. The analytical model is identical to the original seismic licensing basis model contained in the Quad Cities FSAR except for appropriate modifications to account for the degraded H5 weld condition. A sketch of the analytical model is provided in Attachment No. ME-1-4.

The time history analyses were performed using the Level 2 Engineering Computer Program (ECP) SAP4GO7 which complies with all requirements of the GE Quality Assurance program.

The primary structure was subjected to the Quad Cities free-field, seismic SSE input motion normalized to a Zero Period Acceleration (ZPA) equal to 0.25g.

Two bounding analyses were performed to account for the 360 degree through-wall cracked condition at H5. The shroud was considered to be pin-connected at the weld elevation in the first analysis and roller-connected in the second analysis. In the first case only shear and not moment could be transferred across the cracked weld. In the second case neither shear nor moment could be transferred across the cracked weld. For both cases, very soft springs were added between the RPV and the shroud at both the top guide elevation and the core support plate elevation. The addition of the soft springs resulted in essentially zero change in the eigendata set for the uncracked model.

The soft springs were required to rid the model of the singularities introduced by the assumed pinned-connected and roller-connected conditions in the shroud at the H5 weld elevation. The resulting SSE forces in these springs were also divided by the soft spring stiffness to obtain the relative displacements between the RPV and the shroud at the top guide and the core support plate locations.

Question RS-4:

Provide unavailability data for the following ECCS scenarios:

1 core spray out;
1 LPCI out;
both core sprays out;
1 LPCI injection valve unavailable;
and common mode LPCI loop select logic unavailable.

Response RS-4:

The following data are overall failure probabilities from the ComEd plant IPE's (References (j) and (k)): the data includes contributions from maintenance and testing unavailabilities, failures to start and failures to run. The data is 1991 data.

	Dresden	Quad Cities
1 core spray out	1.4E-2	5.2E-2
1 LPCI out	2.6E-3	3.8E-3
both core spray out	2.2E-4	6.7E-3
1 LPCI injection	1.9E-3	1.5E-3

The IPE's does not include this common mode LPCI loop unavailability and it could not be extracted or created from the existing IPE data.

Question RQ-1:

In the May 26, 1994, meeting between the NRC and CECO concerning the core shroud, CECo indicated it would reevaluate continued operation after 6 months if the unit restart without repairing the H5 weld. Please provide the details of the proposed reevaluation and all other actions to be taken by CECo.

Response RQ-1:

Since April 26, 1994 the ComEd Dresden and Quad Cities Core Shroud Project Teams have been pursuing the best right answer for the core shroud cracks at the stations. During the last 8 weeks ComEd has performed exhaustive inspections and testing on the shrouds and has invented methods for doing so. In the process ComEd has learned more about the Dresden-3 and Quad Cities-1 core shrouds than is known about any other shrouds in the country. Throughout this process ComEd has focused on and has achieved uncompromising safety and technical excellence.

The weld thickness at the most significantly cracked shroud weld (H5) is 3 inches. ComEd has measured crack depths at this weld from physical boat samples of 0.69 inch. ComEd has determined what uncracked weld thickness would be required at the end of another full operating cycle to assure safety under all accident conditions considered for both Dresden and Quad Cities stations. This is the required weld thickness. Additional uncracked weld thickness is considered operating margin over and above the required thickness. These terms are illustrated on Figures RQ-1-1 and RQ-1-2. We have concluded that the Dresden-3 and Quad Cities-1 core shrouds have the required uncracked weld thickness to assure safe operation for a full operating cycle. Also, both stations have additional operating margin of at least 9.7 (QC) to 16 (Dr) times greater than the required thickness for a full operating period. For a 6-month operating period the operating margin is at least 13 (QC) to 26 (Dr) times greater than the required weld thickness.

Although a tremendous amount of work has been done during the past 8 weeks, more work also needs to be done. This technical problem has many details that remain to be rigorously completed. Additional analysis, testing and investigations by ComEd and the BWR Owner's Group will continue during the next 6 months. These additional results will not change the assurance of safe operation; however, the results may increase or decrease some of the conservatism in calculating operating margin, and may change some of our understanding of the detailed behavior of a degraded core shroud condition.

Additional work planned for the next 6 months includes scanning electron microscopic analysis of the boat samples from Dresden and Quad Cities to determine if the cracked H5 ring material has a microsegregated microstructure. ComEd plans to complete a technical audit of the analysis work performed by outside contractors in support of the shroud resolution process. ComEd plans to perform further study of dynamic effects in order to better understand the behavior of degraded core shrouds under design basis accident conditions. These plans include supporting three-dimensional modelling of the asymmetric flow conditions in the reactor vessel during the design-basis recirculation line break and the resulting loads on the shroud. The results of this additional work could increase or decrease the amount of operating margin currently available at the shroud H5 welds. These results could also change the understanding of the behavior of the shroud under design-basis accidents with a postulated through-wall 360 degree failure of the shrouds at the H5 welds.

Additional work planned for the next 6 months includes planning and preparation for a permanent comprehensive repair for the degraded core shrouds that will be an industry standard. Also, ComEd will support further analysis and qualification of the core shroud ultrasonic testing data and ultrasonic systems utilized to obtain the data. The objective of this analysis is to obtain better understanding of the ultrasonic testing uncertainties in the Dresden and Quad examinations and to quantify those uncertainties for future examinations. The results of this additional work could also increase or decrease the amount of operating margin currently available at the H5 welds.

The results of the fall 1994 industry BWR shroud inspections will also be considered by ComEd. These results could impact the priority of repairs or other resolution efforts

Recognizing that the additional work needs to be done, ComEd has established a conservative 6-month administrative operating period for both Dresden-3 and Quad Cities-1 before making any additional inspections or repairs to the shrouds at these units.

The results of the additional analyses and testing and their impact on the degree of operating margin or consequences for these units will be reviewed by ComEd as soon as the results are available and ComEd may extend the administrative operating period for up to 24 months. Alternatively, if the results indicate that the margins are reduced to unacceptable levels (see Figure RQ-1-3 for an illustration) then ComEd will revise the following resolution priorities and schedules for Dresden and Quad Cities Stations; these revisions will be appropriate to the magnitude of changes in operating margins, including immediate shutdown of the affected units:

1. **Quad Cities Unit 2**-Initially Inspect and/or Repair in Spring 1995.
2. **Dresden Unit 2**-Initially Inspect and/or Repair in Spring 1995.
3. **Quad Cities Unit 1**-Reinspect and/or Repair in Fall 1995.
4. **Dresden Unit 3**-Reinspect and/or Repair in Spring 1996.

Figure RQ-1-1

Illustration of Dresden Unit - 3 Core Shroud (H5 Weld) Operating Margin

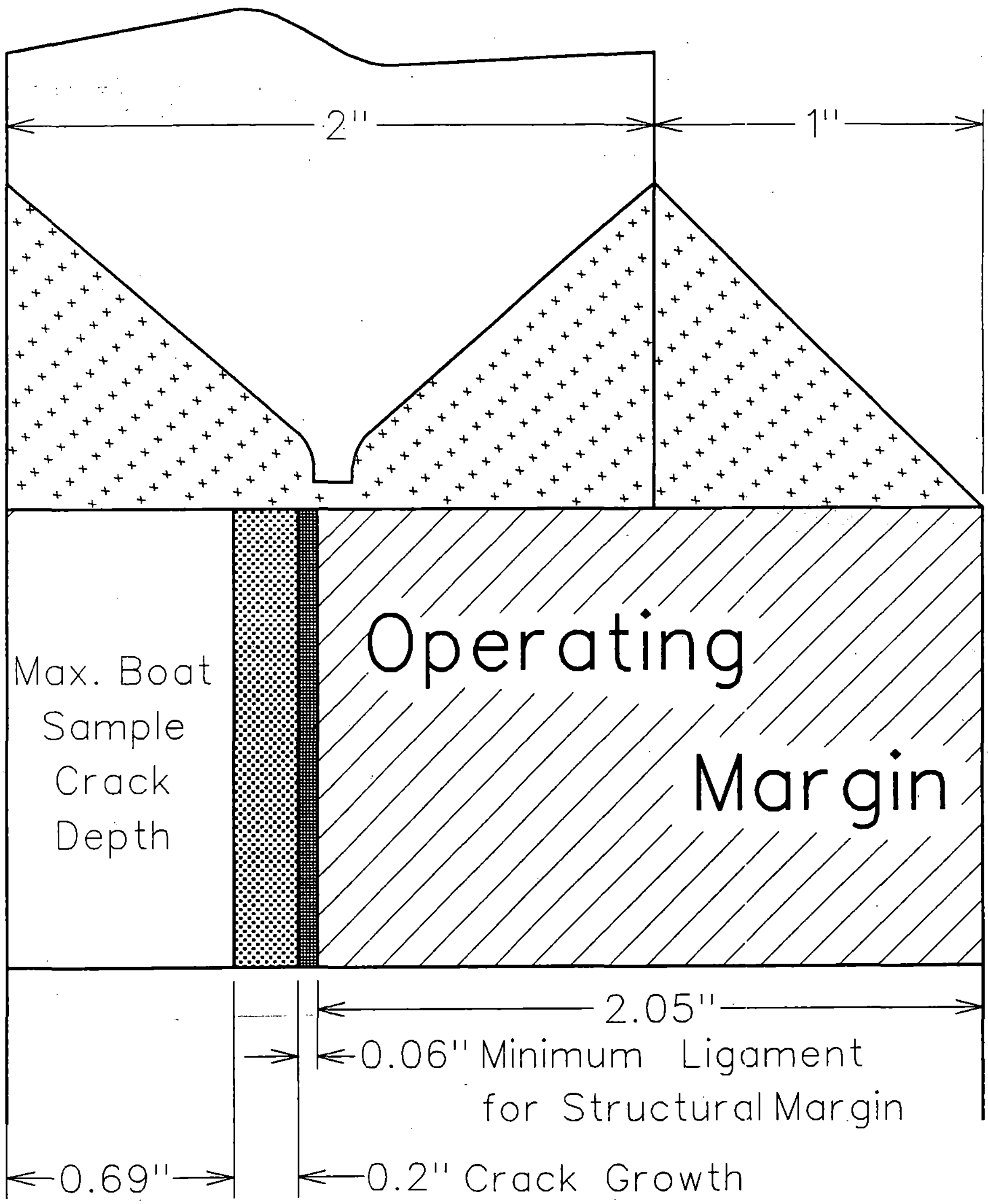

*Assumptions

a: 24 month operation cycle.

b: Pledge model crack growth rate of 1.24 X 10^{-5}

Figure RQ-1-2

Illustration of Quad Cities Unit-1 Core Shroud (H5 Weld) Operating Margin

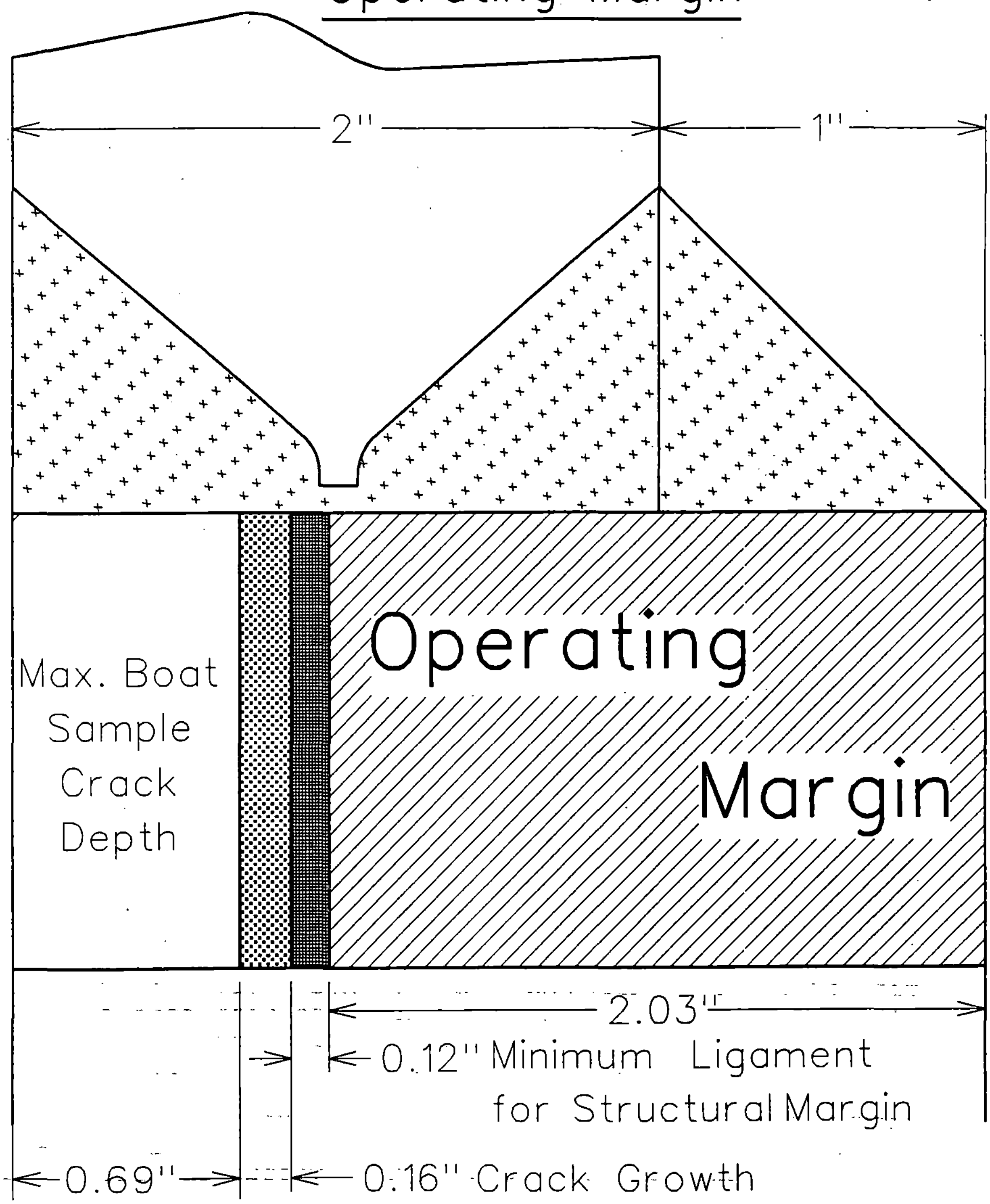

*Assumptions

a. 18 month operation cycle.

b: Pledge model crack growth rate of 1.32 X 10 $^{-5}$

Figure RQ-1-3
Illustration of Brunswick Unit-1 Core Shroud (H3 Weld) Operating Margin

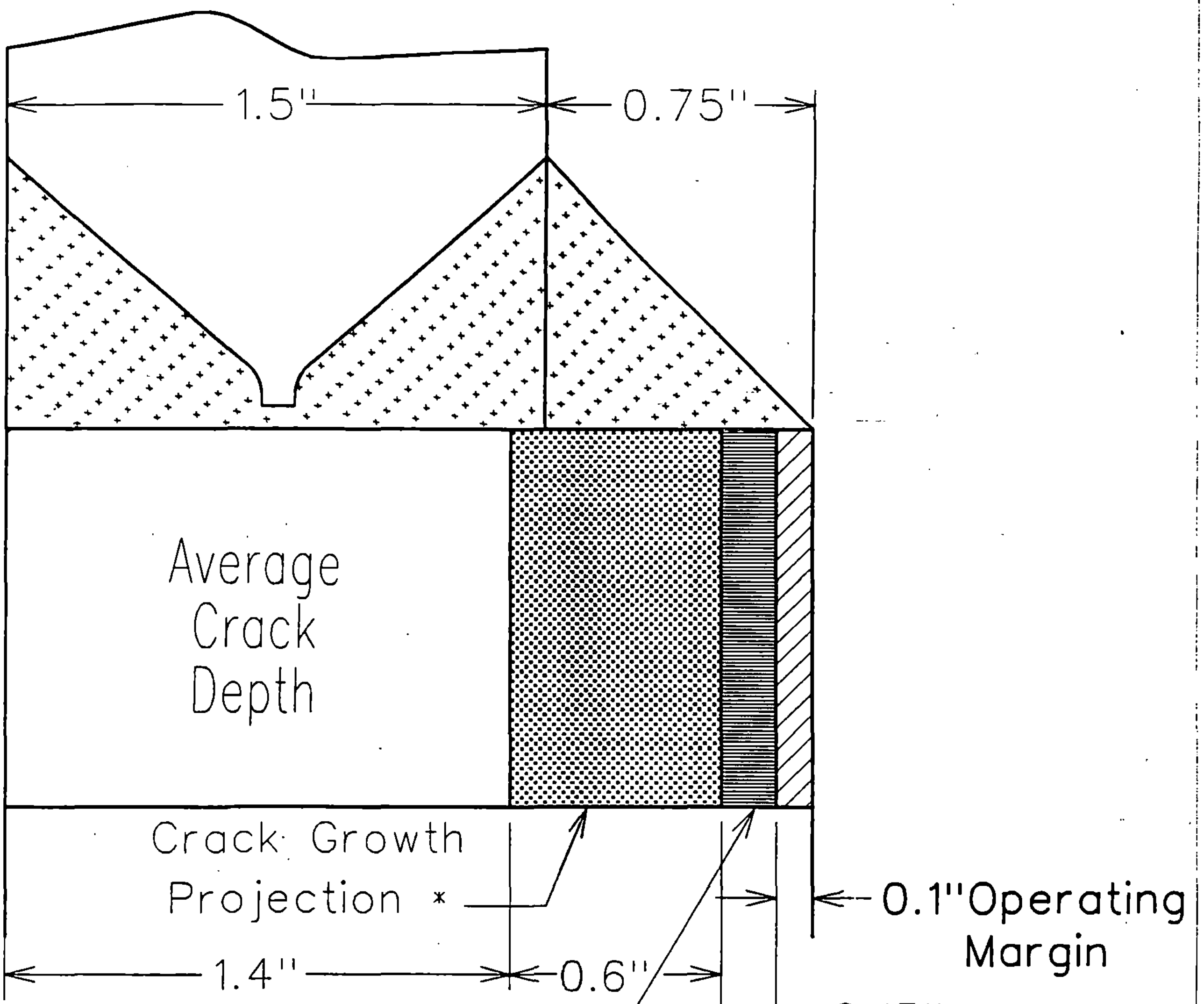

*Assumptions

a: 18 month operation cycle.

b: Bounding crack growth rate of 5 X 10^{-5}

Attachment MS-2-1 Conductivity Trends

Quad Cities Unit 1 Reactor Water Conductivity Mean Values

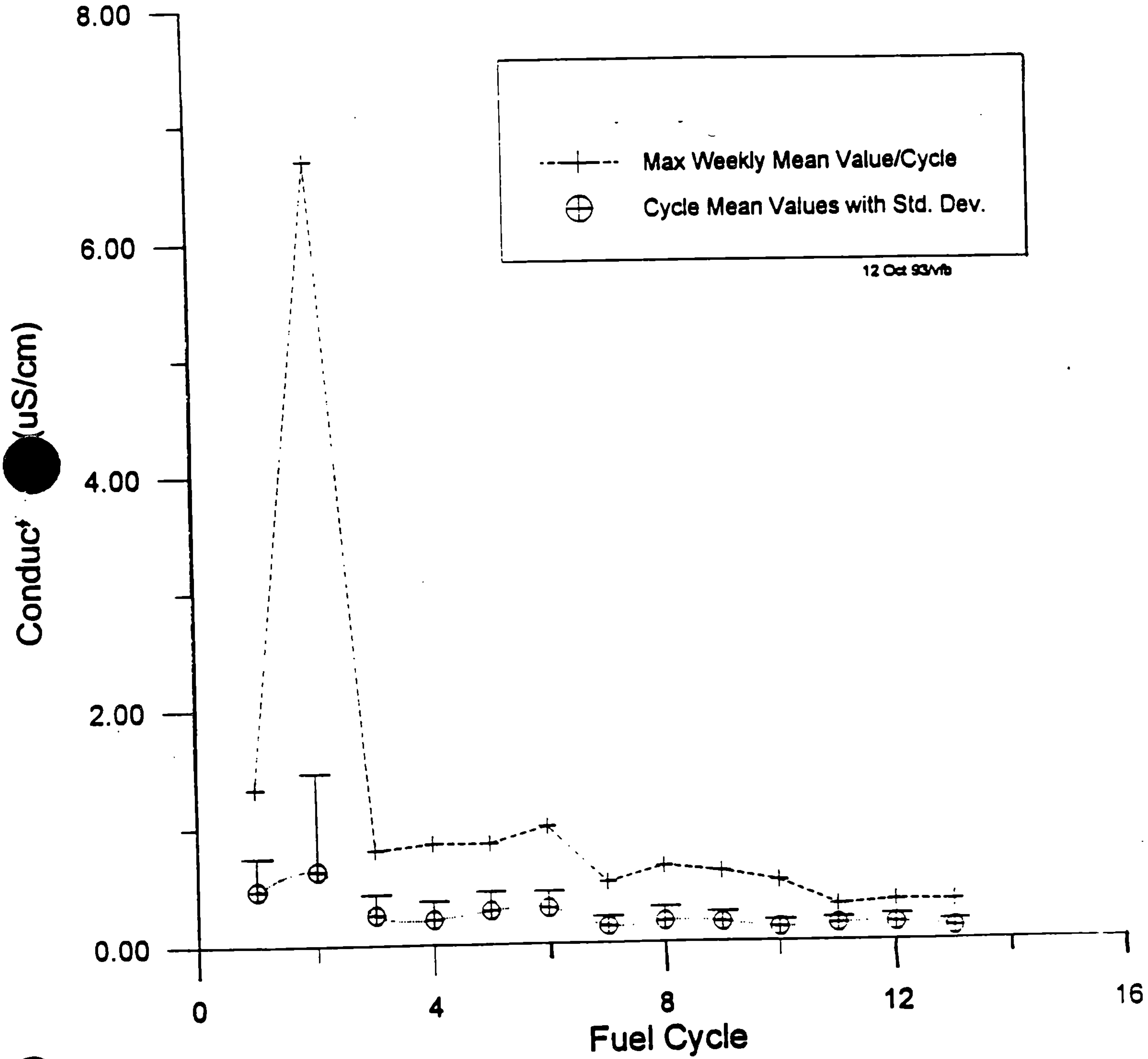

Quad Cities Unit 2 Reactor Water Conductivity Mean Values

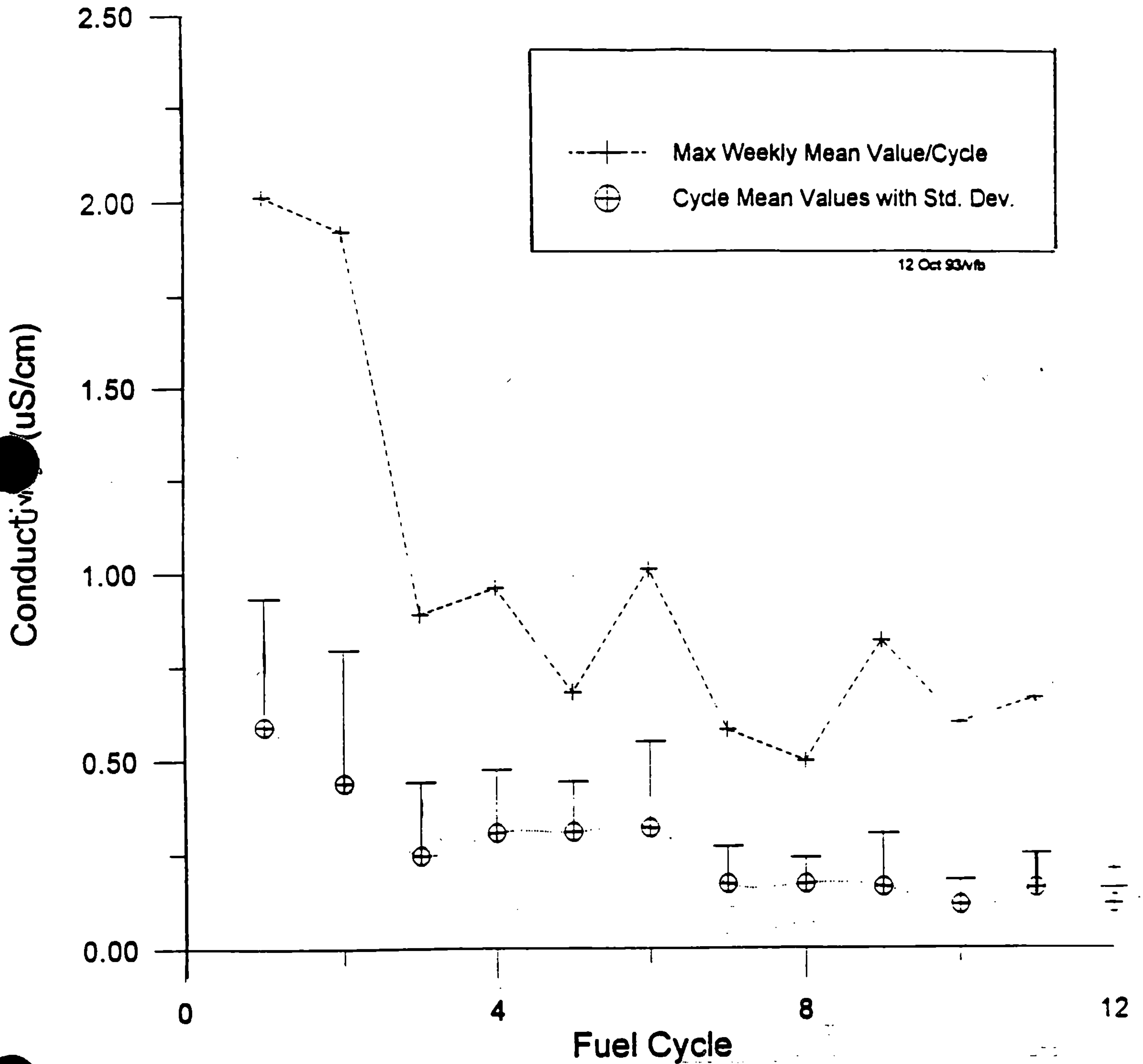

Dresden Unit 2 Reactor Water Conductivity Mean Values

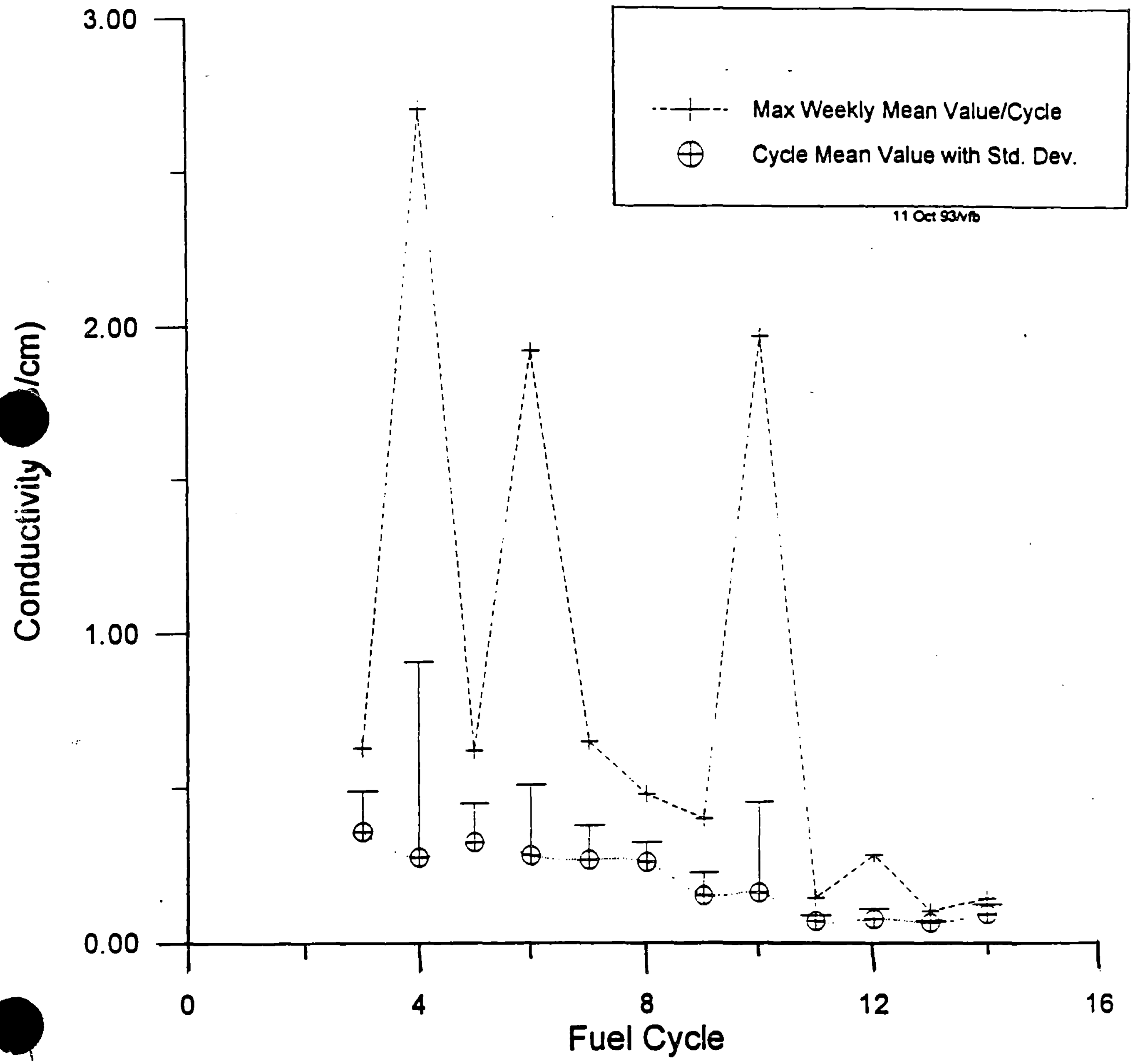

Dresden Unit 3 Reactor Water Conductivity Mean Values

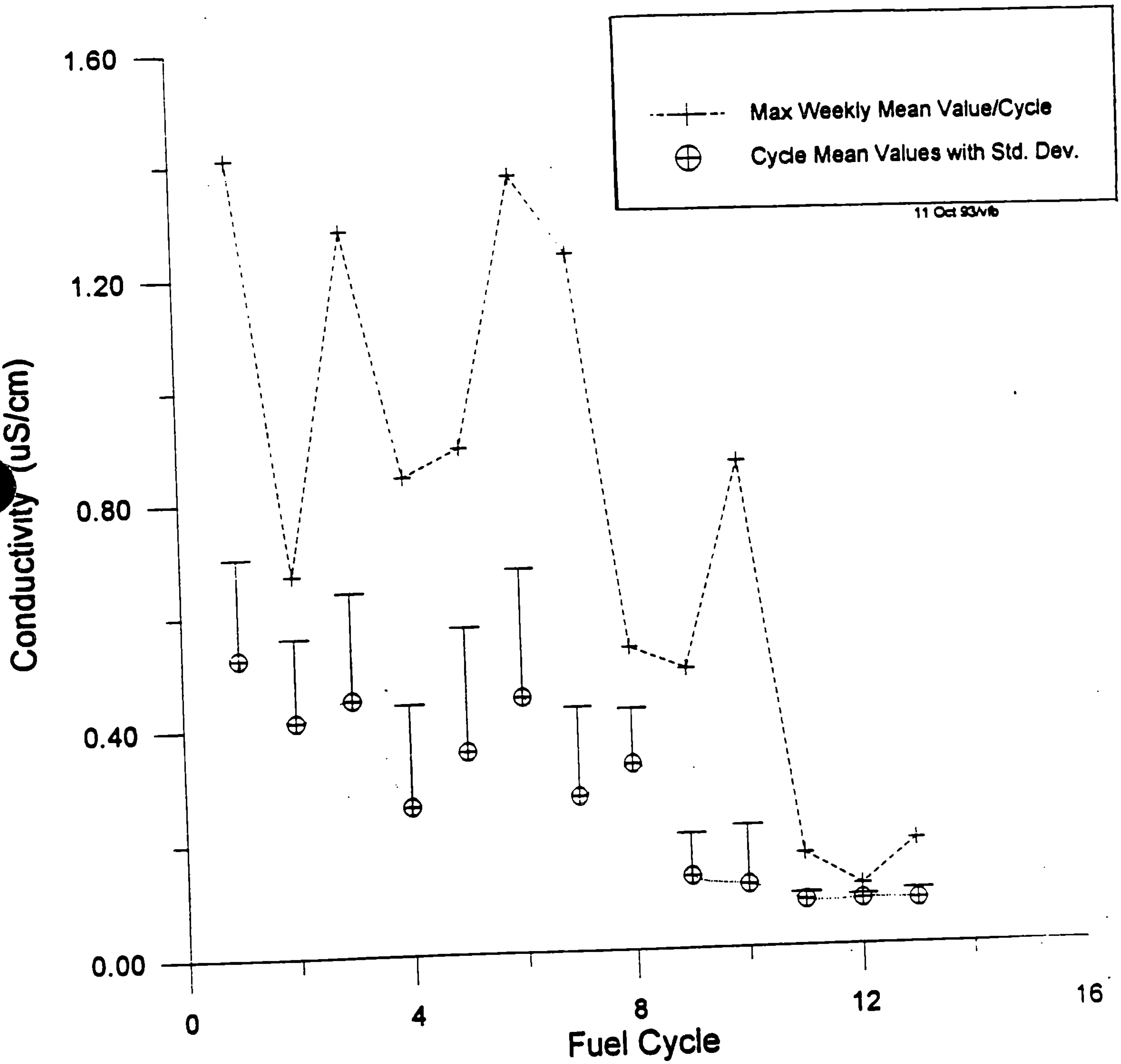

Commonwealth Edison
Dresden Nuclear Power Station
6500 North Dresden Road
Morris, Illinois 60450
Telephone 815/942-2920

Attachment MS-3-1 **GE UT White Paper**

June 24, 1994
VPLTR 94-0027

Mr. William T. Russell, Director
Office of Nuclear Reactor Regulation
U.S. Nuclear Regulatory Commission
Washington, D.C. 20555

Attn: Document Control Desk

Subject: Dresden Nuclear Power Station Unit 3
Quad Cities Nuclear Power Station Unit 1
Clarification of Ultrasonic Examination Methods Used at Dresden Unit 3 and Quad Cities Unit 1 to Address Core Shroud Cracking at the H5 Weld
NRC Docket No. 50-249 and 50-254

Reference: Meeting between Commonwealth Edison (J. Williams, P.Piet, et. al.) and the NRC Staff (R. Capra, T. Sullivan, et. al.), dated June 21, 1994.

Dear Mr. Russell:

In the referenced meeting, ComEd met with the NRC staff to discuss issues concerning the core shroud cracking at Dresden and Quad Cities Stations. During the meeting, ComEd discussed specific issues regarding the ultrasonic (UT) examination methods used to establish the depth of uncracked material in the core shrouds. The purpose of this letter is to supplement material presented during the referenced meeting and to present ComEd's exclusion zone approach (attached).

ComEd's approach is based upon the receipt of consistent geometry signals when examining the H5 fillet weld with UT. If a flaw were to penetrate the sound path of the transducer during the examination of the inner diameter (ID) of the fillet weld region, recognizable responses would be detected. The exclusion zone approach is similar to that utilized by the EPRI NDE center to detect Intergranular Stress Corrosion Cracking (IGSCC). ComEd's approach is discussed in more detail in the attachment to this letter.

The NRC staff expressed concerns regarding the potential transparency of a flaw using ComEd's approach near a crack tip. It was noted that this phenomenon may have occurred during the qualification of other plants' core shroud UT techniques. ComEd's methodology detected shallow crack indications along with the ID fillet weld using 45° shear wave UT. These flaws were determined by boat sample evaluation to be IGSCC, demonstrating the detectability of IGSCC with 45° shear wave UT. Because the ID fillet weld was observed in each of the more than 2000 stepped transducer scans performed on the H5 weld, it is unlikely that a crack-like defect intersecting the central beam path would remain transparent along the entire inspected length.

The exclusion zone approach requires that no significant cracking be present at the inside surface of the H5 weld. ComEd did not identify any indications of cracking during the UT examinations of the H5 welds at Dresden Unit 3 or Quad Cities Unit 1.

Therefore, ComEd concludes that the exclusion zone approach is a valid and conservative technique for determining a bounding crack depth for the H5 weld, because: the ID fillet weld was consistently identified during the UT examinations; the metallography results show the cracks to be relatively open and exhibit grain encirclement, and the technique is very sensitive to grain boundaries; the bounding flaw represents the largest flaw that could possibly exist; and flaws shadowing the root is an established flaw detection method.

To the best of my knowledge and belief, the statements contained in this response are true and correct. In some respects, these statements are not based on my personal knowledge, but obtained information furnished by other ComEd employees, contractor employees, and consultants. Such information has been reviewed in accordance with company practice, and I believe it to be reliable.

Please direct any questions you may have concerning this response to this office.

Sincerely,

M D Lyster

Michael D. Lyster
Site Vice-President
Dresden Station

Attachment: Ultrasonic Examination Methods - Dresden Unit 3 and Quad Cities Unit 1

cc: J.B. Martin, Regional Administrator - RIII
C. Miller, Senior Resident Inspector - Quad Cities
M.N. Leach, Senior Resident Inspector - Dresden
C.P. Patel, Project Manager - NRR
J.F. Stang, Project Manager - NRR
R. Hermann, NRR
Office of Nuclear Facility Safety - IDNS

(L:\VPLTR\0027.94)

GE Nuclear Energy

June 24, 1994

Mr. Joe D. Williams, Project Manager
Dresden Shroud Project
Dresden Nuclear Power Station
ComEd

Subject: Ultrasonic Examination Methods Report, Dresden 3 and Quad Cities 1.

Dear Mr. Williams,

Attached please find the Subject Report, as authored by Mr. Tony R. Jaschke, GE Nuclear Energy UT Level III.

The report describes an alternate approach to establishing with certainty the depth of uncracked material in the Core Shroud H5 Weld of the subject reactors.

John E.Nash
GE Site Services Manager
Dresden Station

ULTRASONIC EXAMINATION METHODS

As used at Dresden 3 and Quad Cities 1

Introduction

An inconsistency between the depth of flaws determined by UT sizing techniques versus the actual measured depths determined by examination of boat sample cross-sections was discovered at the H5 weld location during the recent ultrasonic examination of the Dresden 3 and Quad Cities 1 shrouds. An alternate approach was developed to establish with certainty the depth of uncracked material in the shroud. This alternate approach is identified as the exclusion zone approach and is the subject of this report.

45° shear wave exclusion zone

The examination recorded fillet weld geometry with both the 45° shear (as well as 60° RL) transducer, because of the shroud geometry at the H5 weld (see Figure 1). The geometry signals were from the fillet weld on the ID surface. This weld geometry gave an excellent benchmark indication on the system C-scan using both 45° shear and 60° RL search units. It is the 45° shear that is used as the primary exclusion zone transducer.

Figure 2 shows the 45° sound pattern including beam spread and how it can insonify the entire ID fillet weld region. The technical basis for establishing an exclusion zone is the fact that during normal examination of the weld, geometric signals were consistently recorded from the fillet weld. If a flaw were to penetrate the sound path of the 45° transducer while the transducer was insonifying the ID fillet weld region, 2 responses would be recorded on the acquisition system:

1. The response amplitude from the ID fillet weld region would be noticeably reduced by the flaw.
2. An indication response of the shorter metal path to the flaw, than to the ID fillet weld, would be observed.

During acquisition and analysis of these data, the examiner and analyst would recognize these indication responses and record them as part of the final data package.

This detection method is directly analogous to techniques taught at the EPRI NDE center for IGSCC detection. For example, when an operator finds a signal that obscures the response from the weld root geometry, he can be confident that the signal is a crack. Conversely, if no signal obscures the response from the weld root geometry, it is concluded that no crack is present between the 45° shear wave transducer and the weld root. This premise is fundamental to IGSCC crack detection using a 45° shear wave. Figure 3 below displays this concept for the H5 weld configuration. In this case a flaw intersects the 45° sound beam at its mid point, obscuring ~ 50% of the sound energy, which would both reduce the amplitude response from the ID fillet weld, and produce a response from the flaw at a shorter metal path.

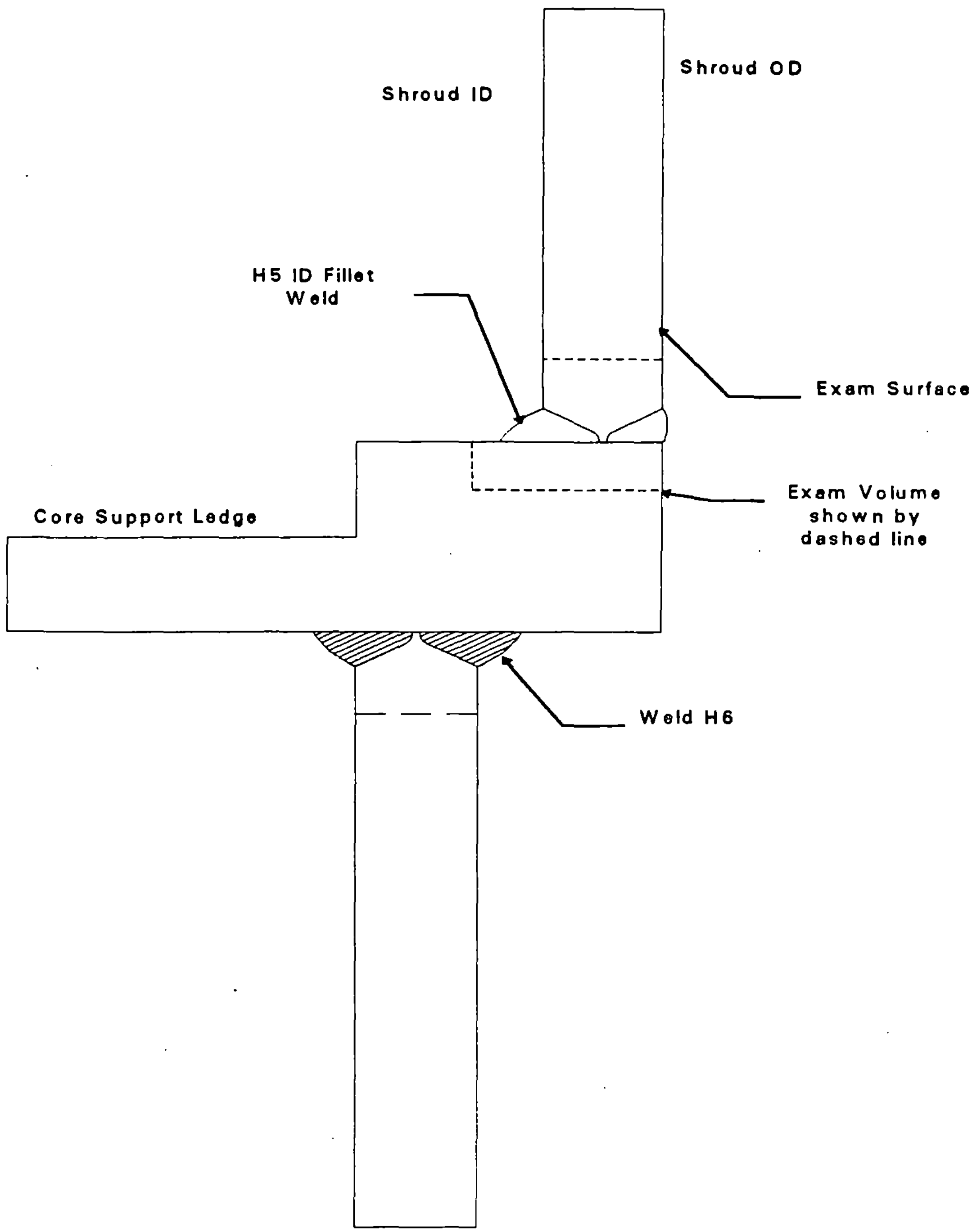

Figure 1 - H5 Weld Geometry

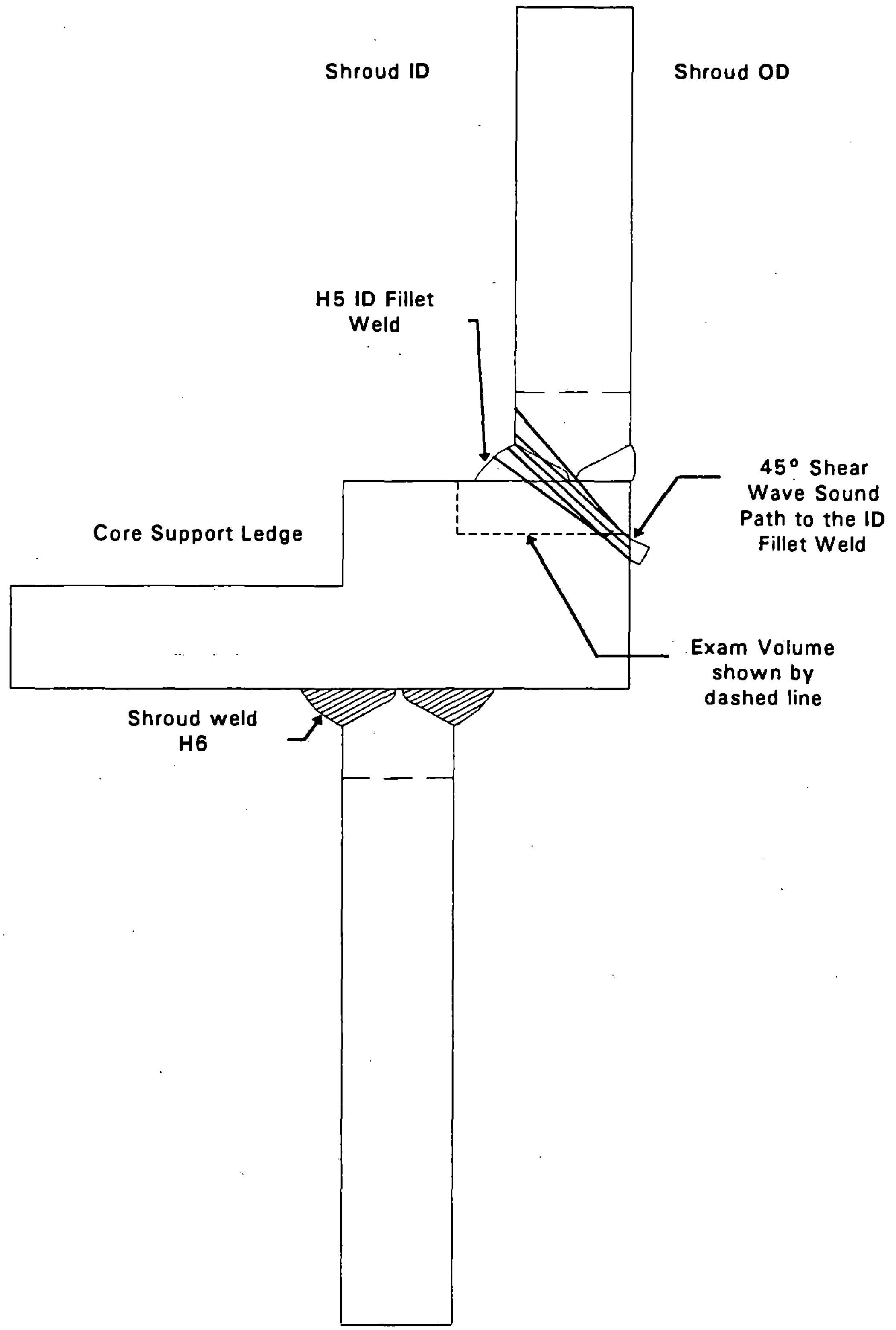

Figure 2 - 45° Shear Wave No Flaw

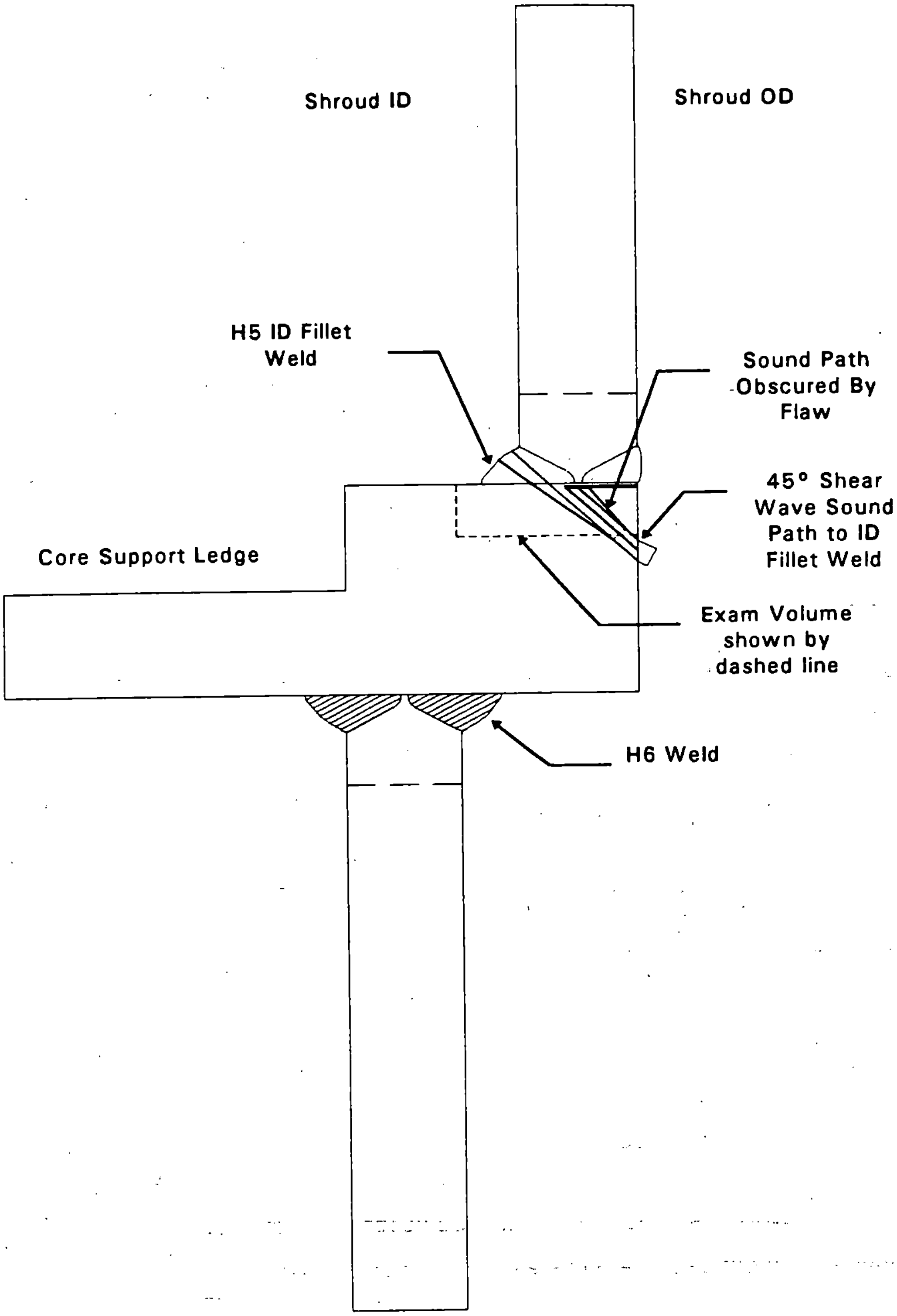

Figure 3 - 45° Shear Wave with Flaw

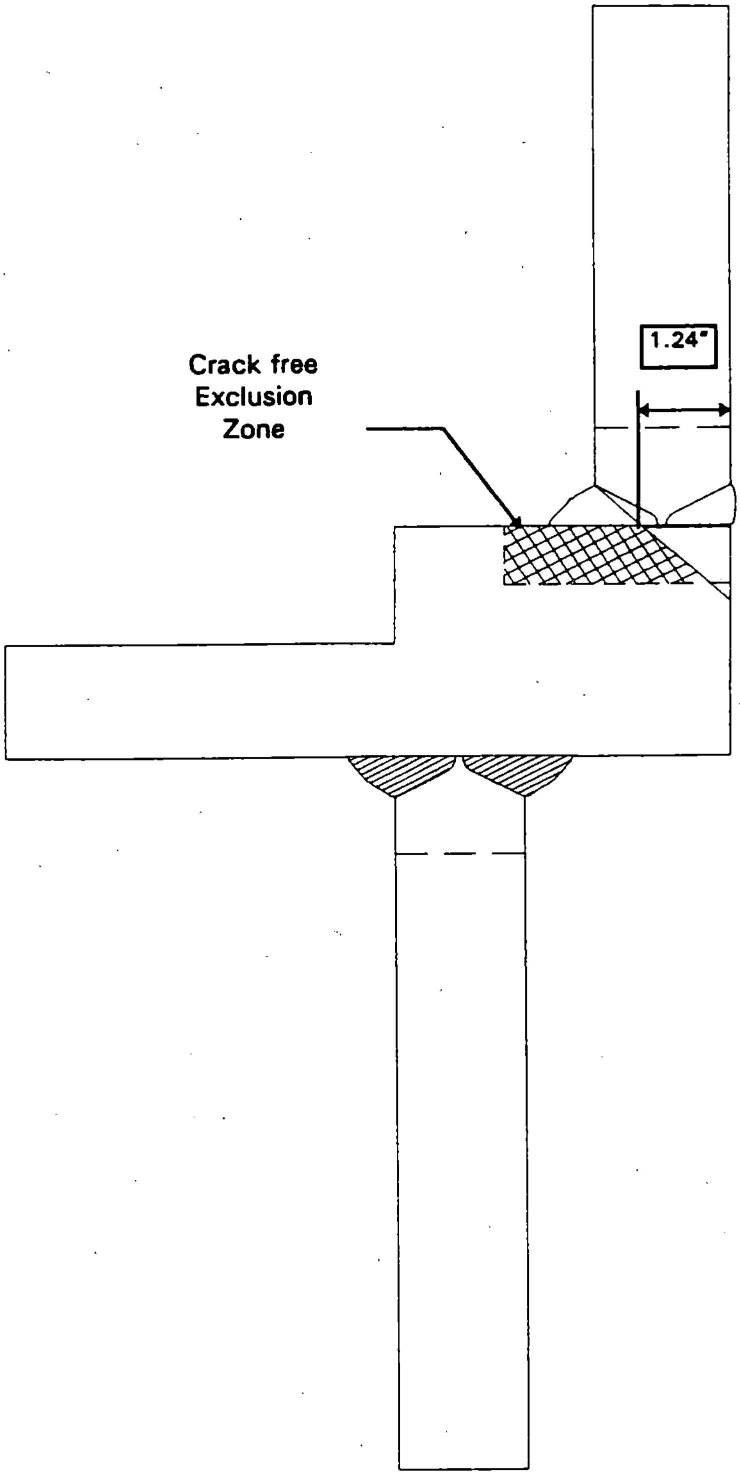

Figure 4 - Definition of "Crack Free" Exclusion Zone Based on 45° Shear Wave Examination

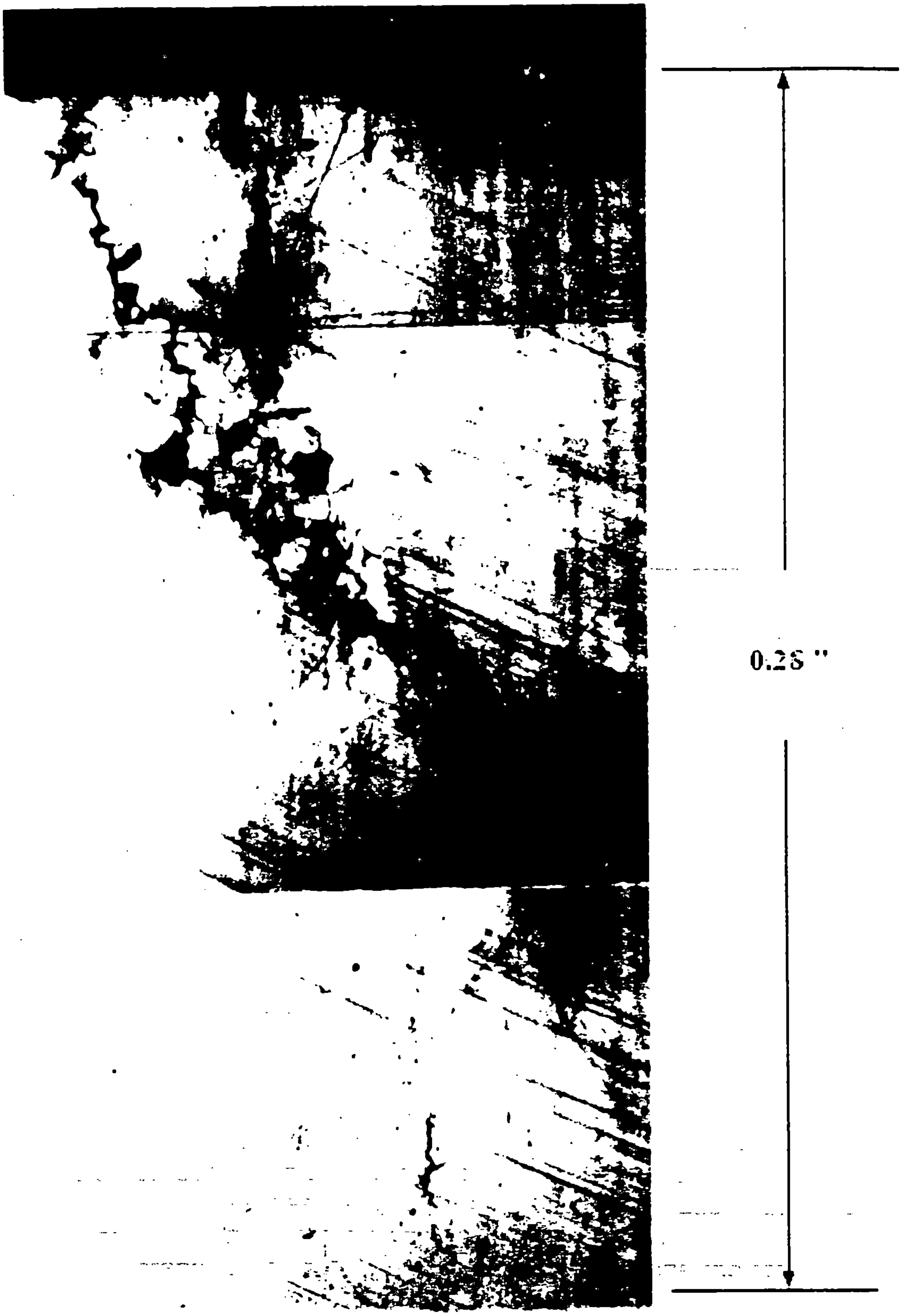

Figure 5 - Quad Cities Unit 1, 154 Degree Azimuth Showing Intergranular Cracking, Branching and Grain Encirclement

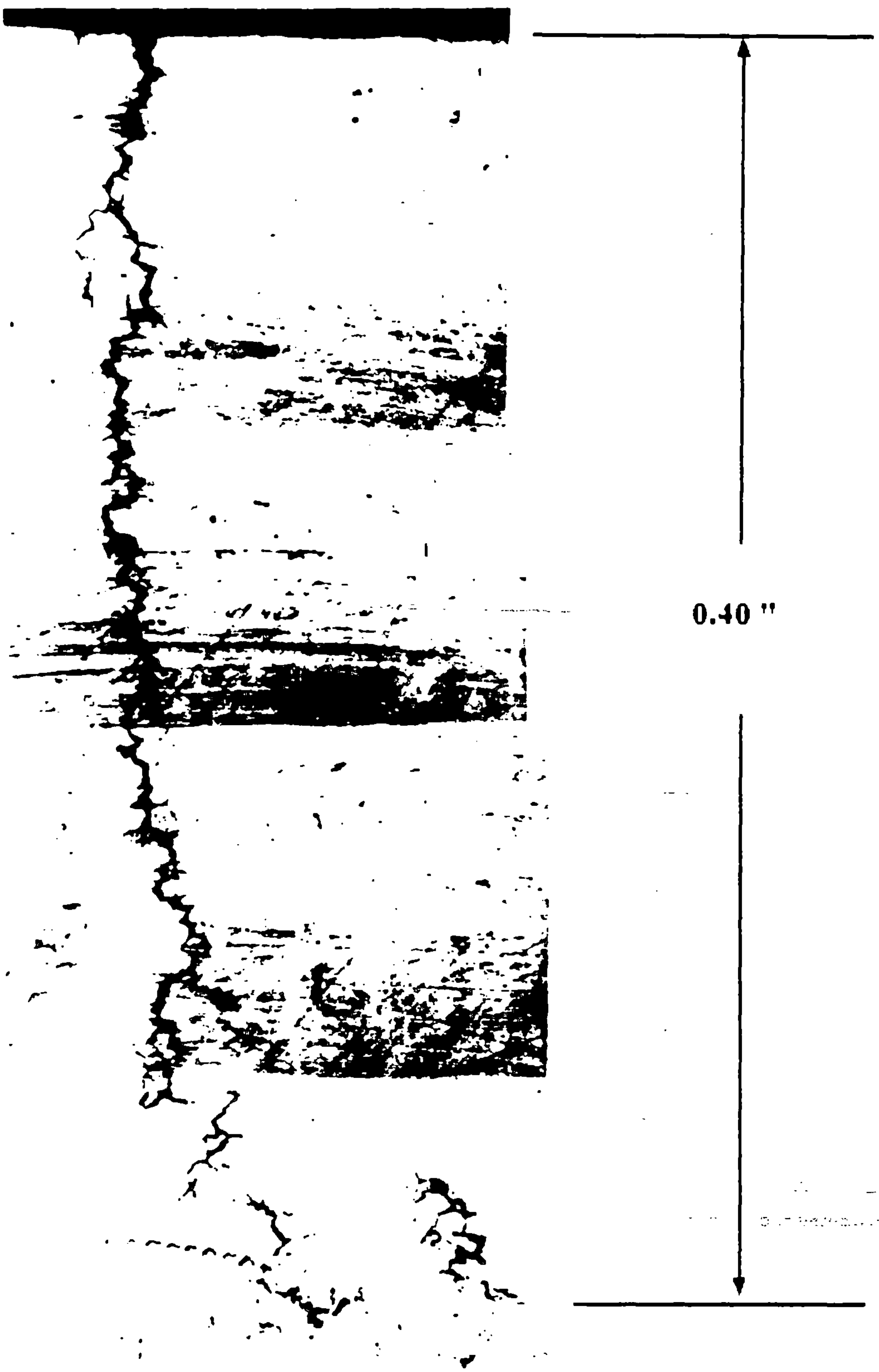

Figure 6 - Quad Cities Unit 1, 342 Degree Azimuth Showing Intergranular Cracking, Branching and Grain Encirclement

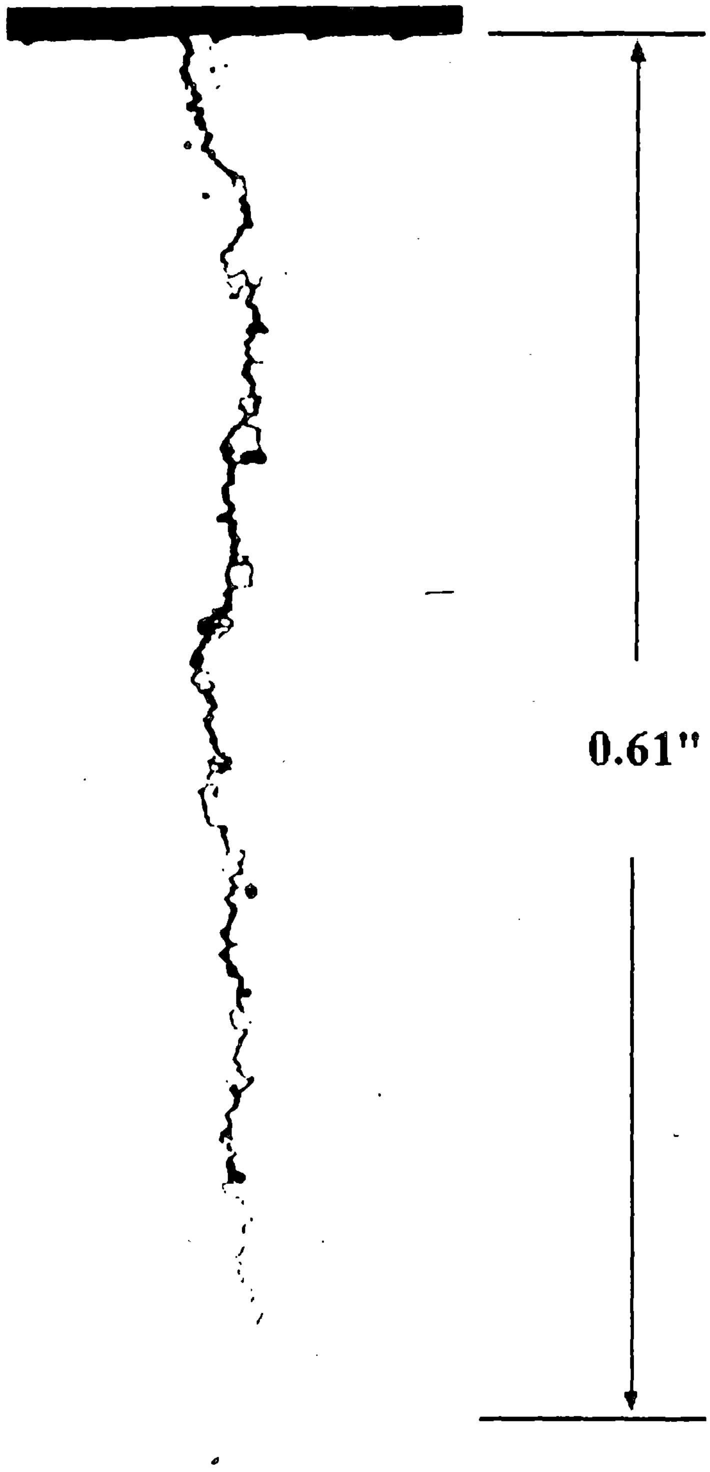

Figure 7 - Dresden Unit 3, 153 Degree Azimuth Showing Open Intergranular Cracking and Minor Branching

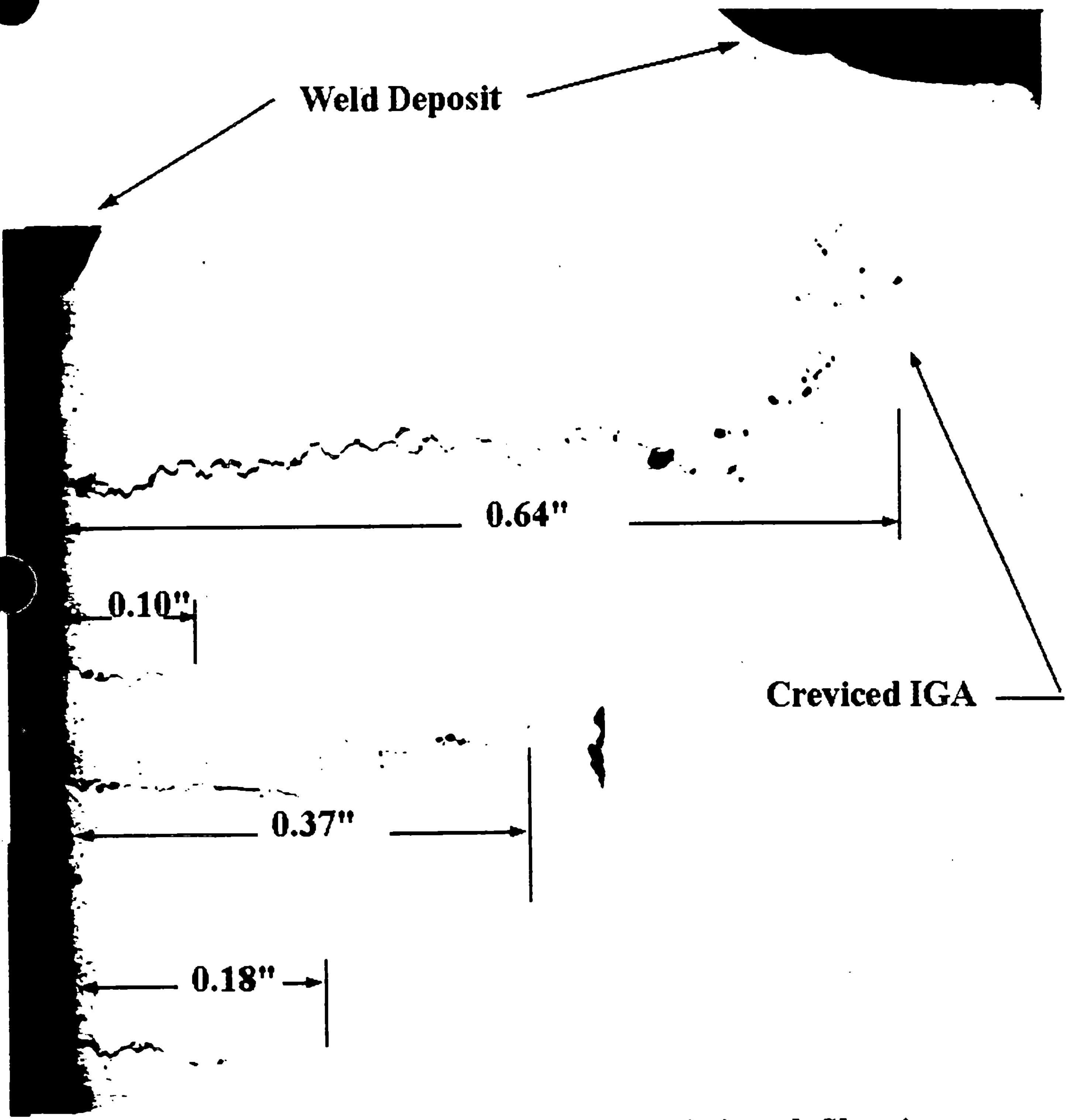

Figure 8 - Dresden Unit 3, 324 Degree Azimuth Showing Multiple Crack Initiation, Open Cracks, Branching and Grain Encirclement

Transmission of sound through flaws

A note of concern for the exclusion zone approach has been raised based on the notion that the crack would be transparent to the sound beam near the crack tip. It was noted that this phenomenon may have occurred during the qualification of Time of Flight Diffraction (TOFD) techniques for the Brunswick shroud UT. Through conversations with the team members involved with this TOFD qualification, including EPRI NDE Center personnel, it was determined that the sound transmission through cracks referred to was observed with the lateral wave produced using the TOFD technique. This lateral wave is a longitudinal wave, whereas the 45° search unit discussed for this application is a shear wave. Shear waves reflect sound energy from multifaceted flaws more strongly than longitudinal waves. Additionally, the crack morphology, as evidenced in the Dresden and Quad Cities boat samples, show these cracks to be open, with some grain encirclement from corrosion, enhancing sound reflection. Figures 5 through 8 show example cracks from each of the 4 boat samples taken at Dresden 3 and Quad Cities 1.

Empirical data supporting the 45° shear wave crack detection is available in shroud exams performed to date with the OD Tracker system. Shallow crack indications (determined to be IGSCC by evaluation of boat samples at Dresden 3 and Quad Cities 1) were detected with the 45° shear wave transducer, with the response from the ID fillet weld also present. Since the ID fillet weld was observed in each of the more than 2000 stepped transducer scans, it is unlikely that any crack-like defect intersecting the central beam path would not have been seen. Therefore, the 1.24 inch bounding limit on crack size is assured.

Detection of flaws at the inside surface of the H5 weld lower toe

Assurance of the depth of uncracked material established by the exclusion zone requires that no significant cracking be present at the inside surface of the H5 weld lower toe. The 45° shear wave scans the entire fillet weld region including the intersection with the Core Support Plate Ring. This intersection is readily apparent in the recorded data, as are reflections from minor surface irregularities such as machining marks on the ring. This establishes a high sensitivity for detection of cracking and it is the judgment of the Level III analysts that cracks would be reliably detected. No indications of cracking from the inside surface were noted during the UT examinations of the H5 welds at Dresden Unit 3 or Quad Cities Unit 1.

Conclusion

The 45° shear wave technique for determining a zone of sound metal is a valid technique. The technical justification behind this opinion is as follows:

- The 45° shear wave search unit consistently recorded the ID fillet weld during the examination.
- The 60° RL also recorded this fillet weld geometry.
- The metallography results show that these cracks are relatively open and exhibit grain encirclement. The flaw branches extensively in several instances.
- The 45° shear wave is very sensitive to grain boundaries. Crack morphology as seen in figures 5 through 8 show grain encirclement, and multifaceted flaws. The

45° shear wave would reflect sound energy from the multifaceted flaws, which would then be recorded by the system as crack tip reflections and/or as interference with the fillet weld reflection. Empirical data from boat sample evaluations indicates that the shallow flaws detected by 45° shear wave were IGSCC.

- The 1.24"flaw exclusion is based conservatively on the center of the beam. The previous figures show that approximately 50% of the sound energy, including beam spread, would be blocked from the fillet weld for a 1.24" flaw. This dimension represents the largest flaw that could possibly exist and still see the fillet intersection with the vertical cylinder.
- Sound transmission through a crack (if it occurred) would be further attenuated in this application because of the two-way transmission through the crack to the fillet weld and back to the transducer.
- Flaws shadowing the root is an established flaw detection method.

Attachment MS-10-1 GE FEM, GLS-94-12

GE Nuclear Energy

Structural Mechanics Projects
175 Curtner Avenue M/C 747
San Jose, CA 95125
Phone: (408) 925-5382
FAX: (408) 925-1150

GLS 94-12
June 17, 1994

cc: S. Ranganath
H. Mehta
DRF 137-0010-7
(GE-NE-523-A69-0594)

TO: **Tom Spry, ComEd**
FAX: (815) 942-2920, X-2922

Gary

FROM: **Gary L. Stevens -- GE San Jose**

SUBJECT: Stress Intensity Factor Distribution at the Shroud H5 Weld

---

This letter documents the results of an evaluation to determine stress intensity factor as a function of crack depth in the vicinity of the shroud H5 weld.

Weld Residual Stress Distribution

Based on prior finite element model analysis for the shroud H3 weld location, the weld residual stress distribution shown in Figure 1 was utilized for this evaluation applicable to weld H5. The stress distribution shown in Figure 1, although derived for the H3 weld location, was considered to be a reasonable approximation of the stress pattern for the H5 location because of the geometric similarities between the two locations (i.e., full penetration butt weld backed by a fillet weld, shroud cylinder attached to a support ring, etc.). The H3 and H5 welds are in fact mirror images of each other, each possessing identical dimensions. Therefore, it is reasonable to assume that the residual stress patterns obtained by finite element analysis for either weld would be similar.

The prior analysis which determined the residual stress distribution for the H3 weld region utilized techniques similar to those described in Reference 1. The nugget area heating method was employed to the full-penetration and fillet welds (using multiple passes) on a two-dimensional, axisymmetric finite element model using ANSYS (Reference 2) of the H3 weld region to determine the temperature distribution resulting from the simulated welding process. This was followed by an elastic-plastic stress analysis to obtain the final residual stress pattern resulting from the welding process. The resulting vertical (or shroud axial) stress pattern is shown in Figure 1.

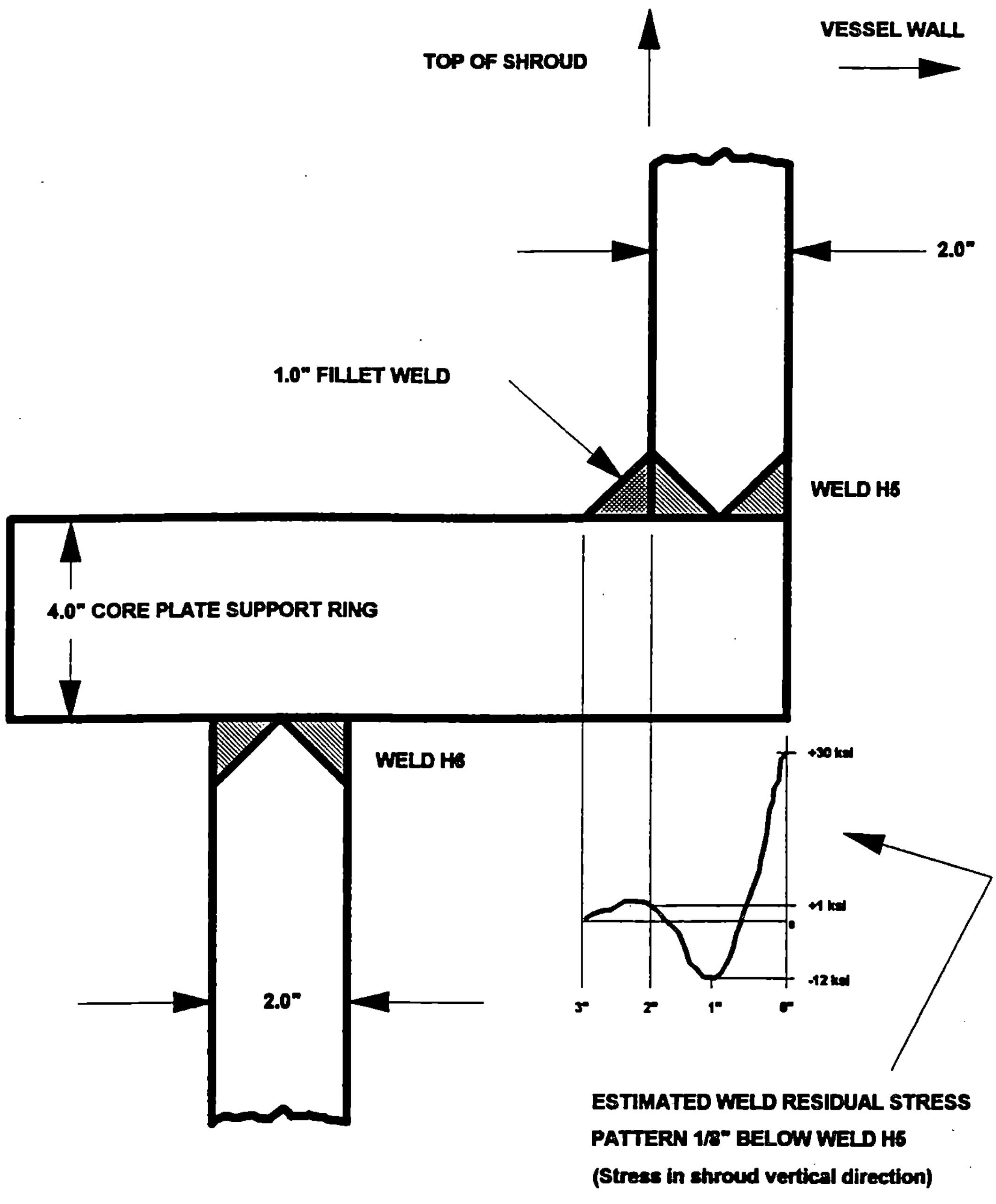

Figure 1: Estimated Weld Residual Stress Distribution for Weld H5

Only sustained stresses are considered for determining the stress intensity factor profile for this evaluation; as a result, seismic stresses are not included. The axial pressure stress of 0.178 ksi (Reference 3) applicable to the H5 weld location for normal/upset conditions was superimposed on the residual stress profile shown in Figure 1. Deadweight stresses were neglected since they are compressive in nature. The Buchalet-Bamford method (Reference 4) was employed for calculating stress intensity factor as a function of crack depth for the resulting stress profile. The resulting stress intensity factor profile as a function of crack depth is shown in Figure 2.

REFERENCES

[1] EPRI Report No. NP-3479-LD, "Last-Pass Heat Sink Welding," Project T109-3, Electric Power Research Institute, Palo Alto, CA, March 1984.

[2] G. J. DeSalvo and R. W. Gorman, ANSYS Engineering Analysis System User's Manual, Swanson Analysis Systems, Inc., Houston, PA, Revision 4.4a, May 1, 1989.

[3] GE Report GENE-523-05-0194, Revision 0, "Evaluation and Screening Criteria for the Dresden 2 and 3 Shrouds," W.F. Weitze, GE Nuclear Energy, March 1994.

[4] C. B. Buchalet and W. H. Bamford, "Stress Intensity Factor Solutions for Continuous Surface Flaws in Reactor Pressure Vessels," *Mechanics of Crack Growth*, ASTM STP 590, American Society for Testing and Materials, 1976, pp. 385-402.

Figure 3: Stress Intensity as a Function of Crack Depth

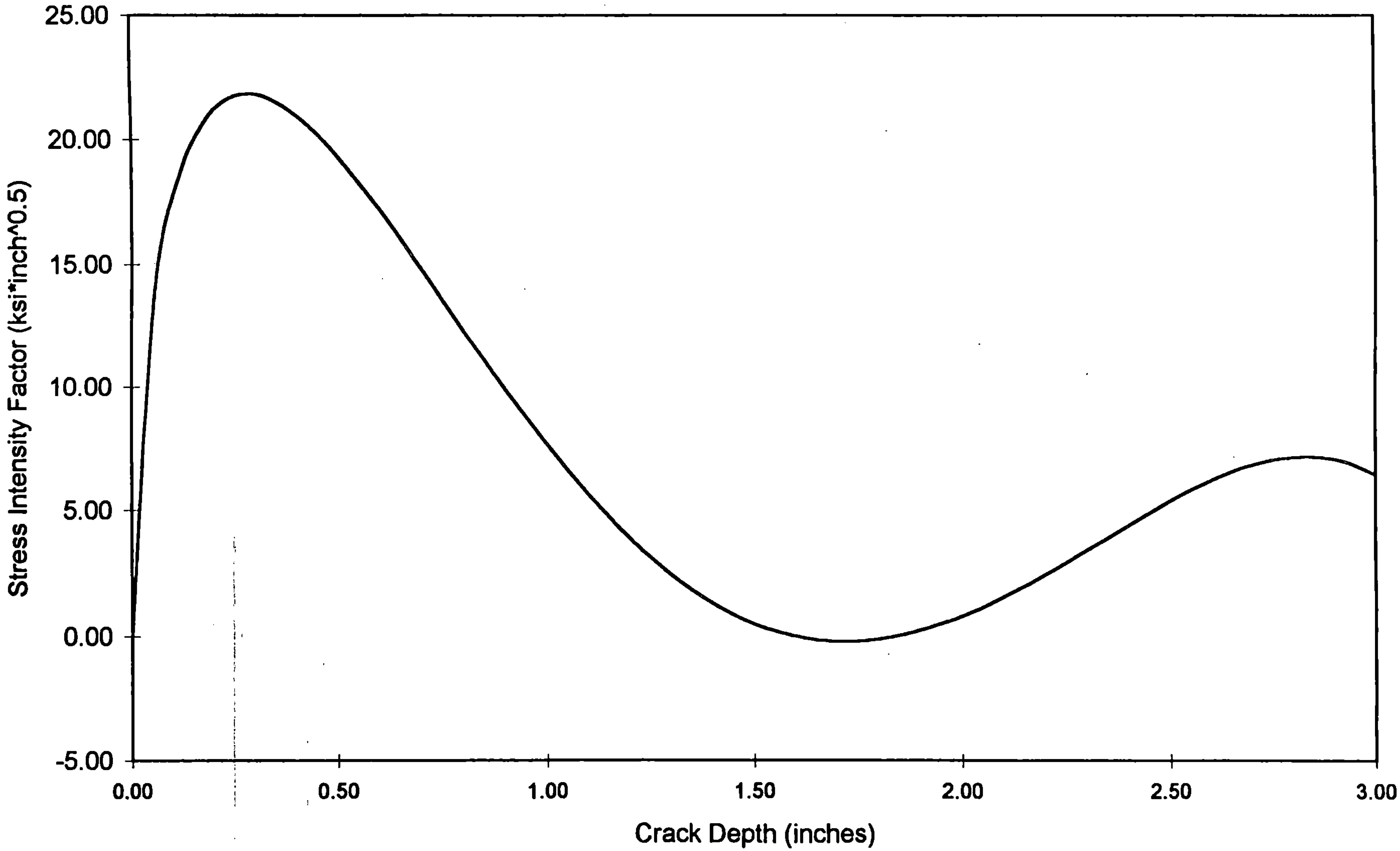

June 11, 1994

Attachment MS-10-2 Estimate of Ferrite Content

To: Tom Spry

From: Dick Smith REL

Subject: Estimate of Ferrite Content for Dresden Unit 3 Core Shroud Welds

The ferrite contents for the subject welds have been estimated from the Delta Ferrite Content diagram given in Figure NB-2433.1-1 of the 1989 Edition of ASME B&PV Code Section III, Division 1. Compositions of the weldments are taken from available CMTR's from Willamette Iron and Steel records for Job No. 660510. The process is Submerged Arc Welding using ⅛ inch diameter wire. Three heats were identified with this job although individual heats could not be associated with individual welds. All welding consumable materials identified were from Sandvik Steel Inc. and were designated as ASTM 371-62 (Type 308-L). This also called Sandvik 3R17. Wire was spooled on 60# reels. It is assumed that these heats represent the filler used in the H5 weld.

Heat No.	C	Si	Mn	P	S	Cr	Ni	Ni_{EQUI}	Cr_{EQUI}
7-06635	.020	.50	1.62	.006	.010	20.5	9.7	12.91	21.25
7-06278	.023	.35	1.70	.008	.011	20.4	9.8	13.14	20.925
7-06601	.021	.41	1.66	.012	.008	20.4	9.3	12.56	21.015

The equivalents were plotted on the attached diagram (referenced above) and a range of ferrite contents determined to represent what might be expected for the welds in the core shroud. The range is 9.0% to 10.75% ferrite (FN 10 - 12).

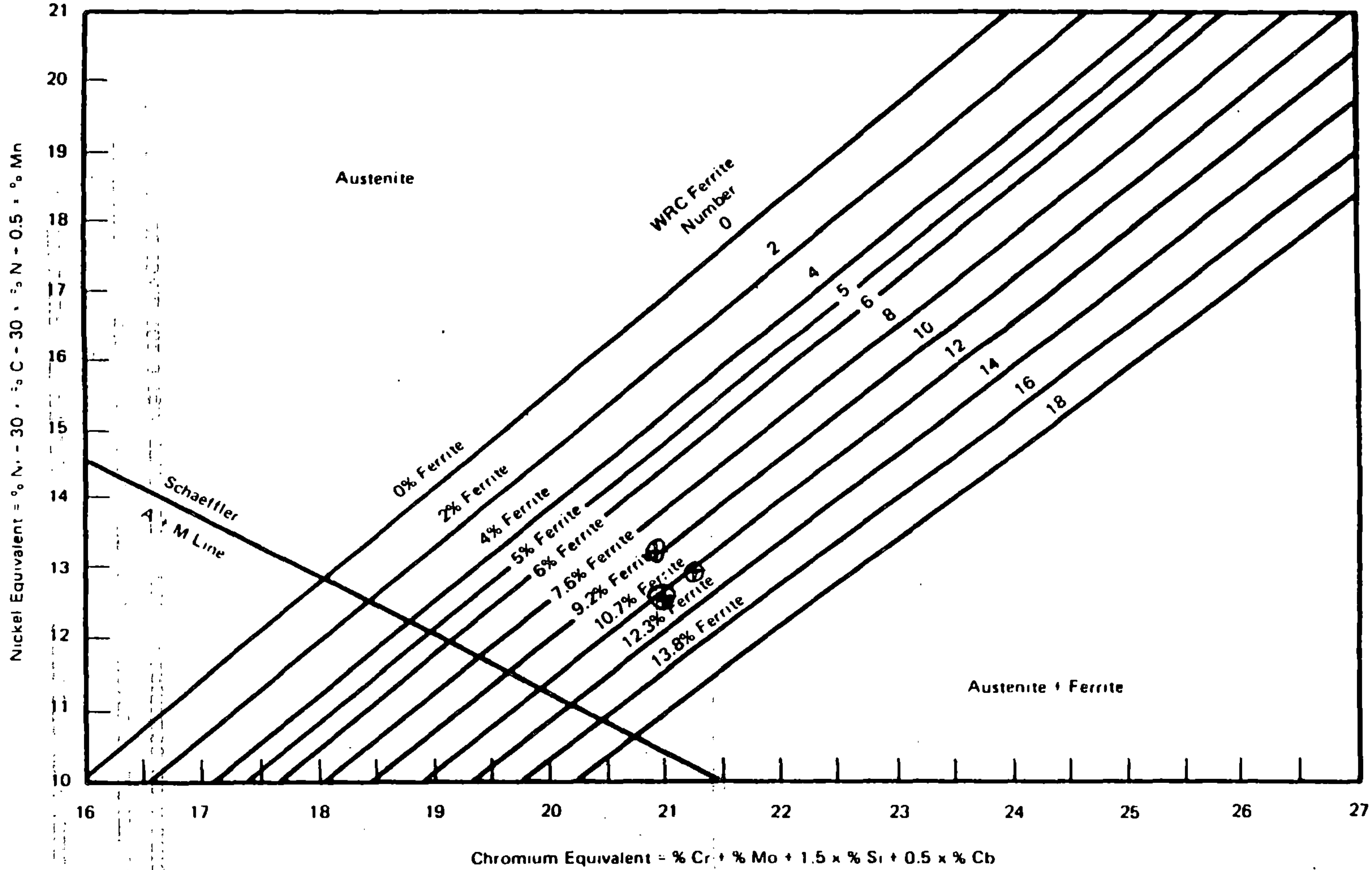

GENERAL NOTE:
The actual nitrogen content is preferred. If this is not available, the following applicable nitrogen value shall be used.
(a) GMAW welds 0.08% (except self-shielding flux cored electrode GMAW welds 0.12%).
(b) welds of other process 0.06%.

FIG. NB-2433.1-1 DELTA FERRITE CONTENT

SANDVIK STEEL, INC.

SOLD TO

DAVIS WELDING PRODUCTS, INC.
P.O. BOX 4243
PORTLAND, OREGON

SHIPPED TO

WILLAMETTE IRON AND STEEL
2800 NW FRONT AVENUE
PORTLAND, OREGON

11 38 52 0

CUSTOMER ORDER NO W 0273 DATE 11/23/66

REQ. NO MARKS:

VIA Cons. Frt.

TERMS 1/2 10 DAYS 30 DAYS NET

INVOICE NO 193033 DATE 12/30/66

ORDER NO. P-0241

SOURCE Paterson stock SALESMAN

REMIT TO SANDVIK STEEL INC. P.O. BOX 2232 CHURCH STREET STATION NEW YORK, N.Y.

F.O.B. Portland, Oregon

DESCRIPTION	QUANT. ORDERED	QUANTITY BACK ORDERED	QUANTITY SHIPPED	UNIT PRICE	TOTAL AMOUNT
SANDVIK 2R17 (TYPE 308L) STAINLESS WELDING WIRE					
3/8" dia. x 60 lb. coil on 4" x 12" lp bound rings	2 Skids Gr.Wt. 2460#				

660510

Heat No.	C	Si	Mn	P	S	Cr	Ni
706635	.020	.50	1.62	.026	.010	20.5	9.7 %

MAT'L-CERTS-CHECKED (WC)

ORDER COMPLETE PARTIAL DELIVERY X

.93

Willamette Iron & Steel
~~2800 N West Front Avenue~~
Portland, Oregon

~~Your Specification No.~~ ~~5000 Lbs.~~

Our Order .... No. 15169-L

Our Invoice .... No. 555443
11/30/66

CERTIFICATE OF ANALYSIS

Material: Type 308-L (SANDVIK 3R17) Welding Wire
on 60# Reels, to ASTM 371-62.

2356.6 Lbs. 1/8" dia.

Cast No.	C %	Si %	Mn %	P %	S %	Cr %	Ni %
7-05635	.020	.50	1.62	.006	.010	20.5	9.7

660518

RECEIVED
MAR 16 1967
Willamette Q. C. Dept.

MATL-CERTS-CHECKED QC

SANDVIK STEEL, Inc.

B. A. Fernaeus

Börje A. Fernaeus

SANDVIK STEE' INC.

Willamette Iron & Steel
2800 N. West Front Avenue
Portland, Oregon

Your Order No. 21773
Your Specification No. 5000 Lbs.
Our Order No. 15169-L
Our Invoice No. 58777 1/13/

CERTIFICATE OF ANALYSIS

Material: Type 308-L (SANDVIK 3R17) Welding Wire
on 60# Reels, To ASTM 371-62.
353.0 Lbs 1/8" dia.

Cast No.	C %	Si %	Mn %	P %	S %	Cr %	Ni %
7-06278	.023	.35	1.70	.008	.011	20.4	9.8

660510

RECEIVED
MAR 16 1967
Willamette Q. C. Dept.

MAT'L-CERTS-CHECKED

SANDVIK STEEL, Inc.

~~B. A. Ferneous~~

MAT'L-CERTS-CHECKED

Willamette Iron & Steel
2800 N.West Front Avenue
Portland, Oregon

Your Specification No. 5000 Lbs
Our Order No. 15169-L
Our Invoice No. 555.443
11/30/66

CERTIFICATE OF ANALYSIS

Material: Type 308-L (SANDVIK 3R17) Welding Wire
on 60# reels. To ASTM 371-62.
2313.5 Lbs. 1/8" dia.

Cast No.	C %	Si %	Mn %	P %	S %	Cr %	Ni %
7-06635	.020	.50	1.62	.006	.010	20.5	9.7
7-06601	/021	.41	1.66	.012	.008	20.4	9.3

660510

RECEIVED
MAR 16 1967
Willamette Q. C. Dept.

MATL-CERTS-CHECKED

SANDVIK STEEL, Inc.

B. A. Fernaeus

Börje A. Fernaeus

SANDVIK STEEL, INC.

Willamette Iron & Steel
2800 N.West Front Avenue
Portland, Oregon

Your Order .... No. 21773

Your Specification No. 5000 Lbs

Our Order .... No. 15169-L

Our Invoice .... No. 555.443
11/30/66

CERTIFICATE OF ANALYSIS

Material: Type 308-L (SANDVIK 3R17) Welding Wire
on 60# reels. To ASTM 371-62.
2313.5 Lbs. 1/3" dia.

Cast No.	C %	Si %	Mn %	P %	S %	Cr %	Ni %
7-06635	.020	.50	1.62	.006	.010	20.5	9.7
7-06601	/021	.41	1.66	.012	.008	20.4	9.3

MATL-CERTS-CHECKED

SANDVIK STEEL, Inc.

B. A. Fernaeus

B. A. Fernaeus

MEMORANDUM

June 19, 1994

Attachment MS-15-1 Short Transverse Tensile Properties

To: Core Shroud Team File

From: Richard Smith R. E. Smith

Subject: Short Transverse Tensile Properties for ASTM A-240 Heavy Plate Austenitic Stainless Steel

This memorandum documents my telephone conversation with Mr. Robert Swinderman of Oak Ridge National Laboratory regarding my request for information on tensile properties of austenitic stainless steel plate in the through-thickness orientation. Bob indicated that he had properties developed for the Breeder Program and that a report could be made available to support us. Unfortunately, it will take some time to locate the report. His recollection was that very little difference, if any, exists for the highly ductile austenitic stainless steel, and that directional property differences are within the scatterband for measurement.

In the meantime, he reported to me some test data he had measured for a 2 inch plate of annealed material. This plate had been formed into a hemispherical head for a pressure vessel. The head required the use of several penetrations and through-thickness properties had been required. The plate material was ASME SA-240 in the annealed condition delivered with CMTR's and prolongations for testing. The following properties are tabulated based upon the telephone conversation:

Measured Property	Test Orientation	Test Value
Ultimate Tensile Strength		
a. CMTR	Longitudinal	77.4 ksi
b. Prolongation	Longitudinal	85.4 ksi
c. Anneal @ 1093°C	Longitudinal	78.3 ksi
d. Test Piece	**Short Transverse**	**81.6 ksi**
Reduction In Area	Short Transverse	66.14%
Elongation	Short Transverse	102%
Hardness		R_B 55-69
Grain Size		1 to 2

Bob was going out of town for a few days, but when he returned he would search for the test data. He does have a few test pieces left of the short transverse orientation. Interestingly, GE had called this week for information on the same topic. This test result was pulled for him. I believe his last name was Hampton . I will pursue this issue further next week.

Operating Margin for Dresden Unit - 3 Core Shroud (H5 Weld)

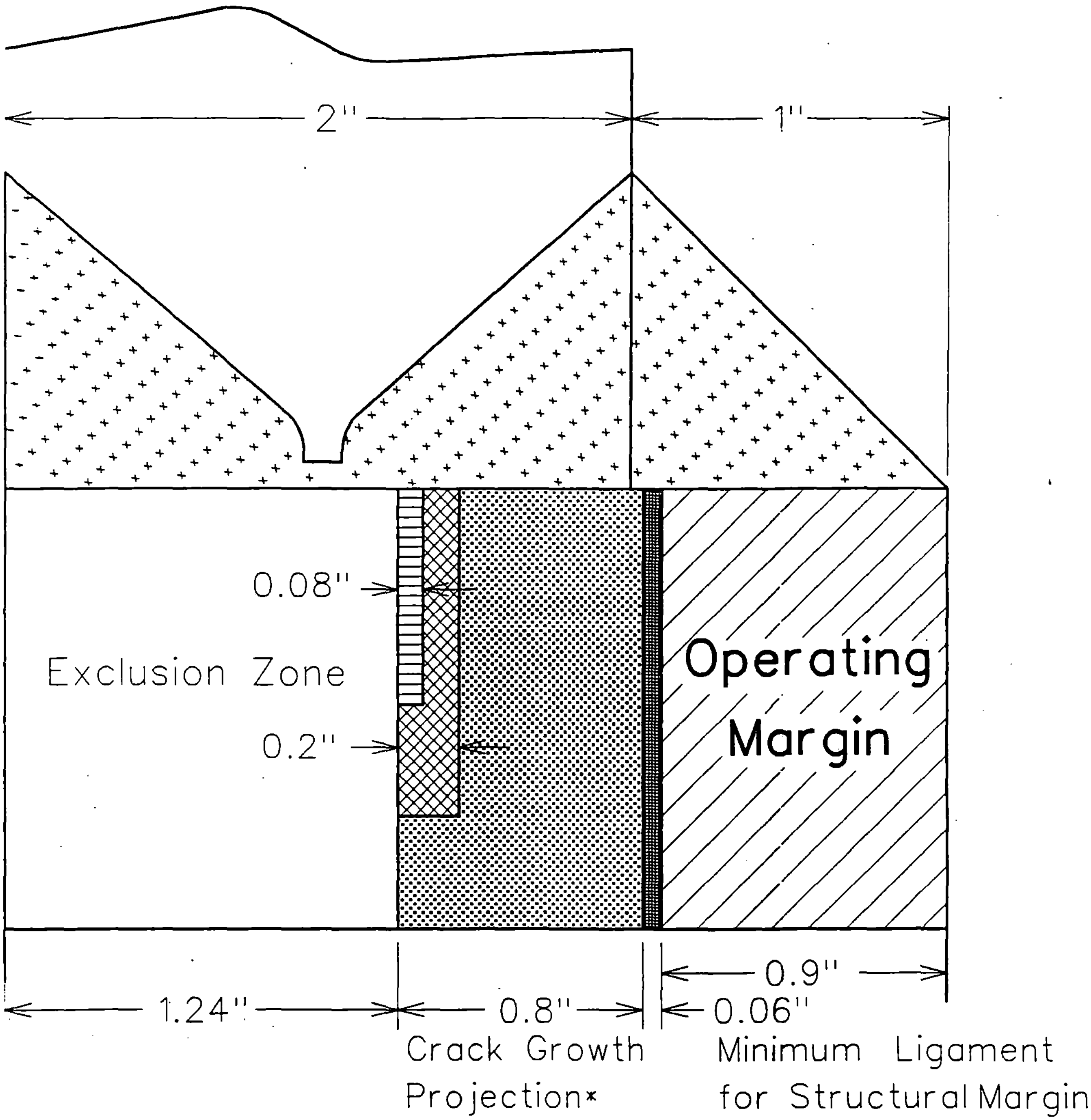

0.8" = 5E-5 in/hr Crack Growth Rate

0.2" = 1.24E-5 in/hr Crack Growth Rate

0.08" = 5.2E-6 in/hr Crack Growth Rate

*Assumptions

a. 24 month operation cycle.

Operating Margin for Quad Cities Unit-1 Core Shroud (H5 Weld)

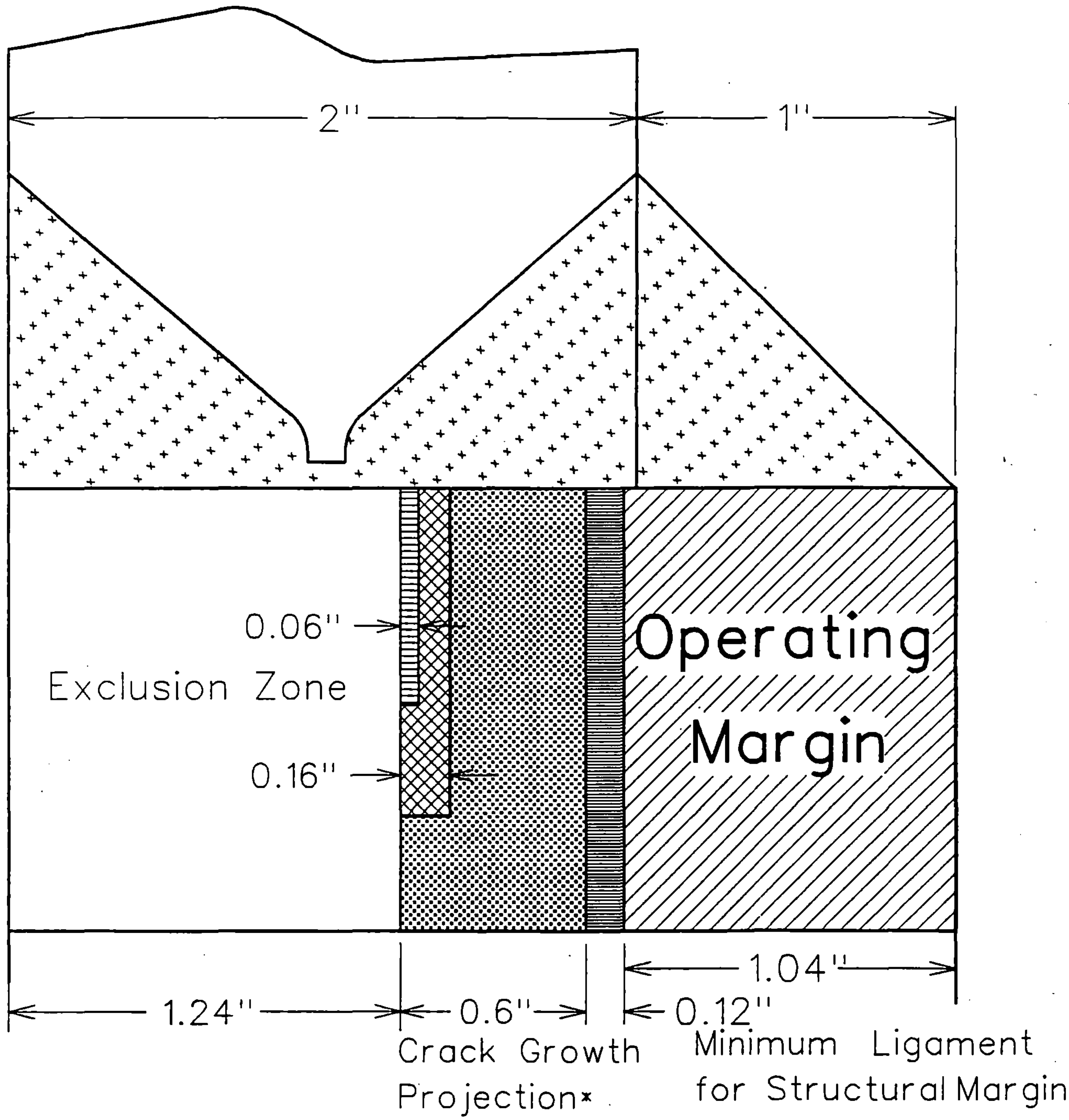

0.6" = 5E-5 in/hr Crack Growth Rate

0.16" = 1.32E-5 in/hr Crack Growth Rate

0.06" = 5.2E-6 in/hr Crack Growth Rate

*Assumptions

a. 18 month operation cycle.

3.9.3.1.1 Reactor Pressure Vessel and Supports

The reactor vessel is described in Section 5.3. The reactor vessel is supported by a steel skirt. The top of the skirt is welded to the bottom of the vessel. The base of the skirt is continuously supported by a ring girder fastened to a concrete foundation, which carries the load through the drywell to the reactor building foundation slab.

Stabilizer brackets, located below the vessel flange, are connected to tension bars with flexible couplings (see Figure 3.9-1). The bars are then connected through the drywell to the concrete structure outside the drywell to limit horizontal vibration and to resist seismic and jet reaction forces. The bars are designed to permit axial expansion.

3.9.3.1.1.1 Acceptance Criteria

The Dresden reactor pressure vessels were designed according to ASME Section III, 1963 Edition, including the Summer 1964 Addenda, plus code case interpretations pertaining to primary nuclear reactor vessels applicable on February 8, 1965 (see Appendix 5A). Applicable code cases and exceptions are described in Section 3.2.

Design of the primary reactor vessel supports was governed by the ASME Code, the American Institute for Steel Construction (AISC) Structural Steel Code, the American Concrete Institute (ACI) Code.

3.9.3.1.1.2 Design Loadings

Information regarding the design transients and fatigue evaluation of the reactor pressure vessel is presented in Section 3.9.1.1.

This subsection describes the loads and load combinations applicable to the design of the reactor pressure vessel internals and supports.

The applicable loads for the reactor vessel internals and supports, and for the emergency core cooling system equipment and piping covered in Section 3.9.3.1.2.2, are defined as follows:

D = Dead load of structure and equipment plus any other permanent loads contributing stress, such as soil or hydrostatic loads or operating pressures, and live loads expected to be present when the plant is operating.

P = Pressure due to loss-of-coolant accident (LOCA).

R = Jet force or pressure on structure due to rupture of any one pipe.

H = Force on structure due to thermal expansion of pipes under operating conditions.

Attachment 1
page of

E = Operating basis earthquake (OBE) load, ground horizontal g = 0.12. vertical g = 0.08.

T = Thermal loads on containment due to LOCA.

E' = Safe shutdown earthquake (SSE) load, ground horizontal g = 0.24, vertical g = 0.16.

Following are the load combinations used for the reactor vessel and vessel supports.

Reactor Primary Internals

D + E	Stresses which occur as a result of the maximum possible combination of loadings encountered in operational conditions; they are within the stress criteria of ASME Section III, Class A Vessel.
D + E'	The primary stresses and primary plus secondary stresses are examined on a rational basis taking into account elastic and plastic strains. These strains are limited to preclude failure by deformation which would compromise any of the engineered safeguards or prevent safe shutdown of the reactor.
P + D	Primary stresses are within the stress criteria of ASME Section III, Class A. The primary stresses and primary plus secondary stresses are examined on a rational basis taking into account elastic and plastic strains. These strains are limited to preclude failure by deformation which would compromise any of the engineered safeguards or prevent safe shutdown of the reactor.

Reactor Primary Vessel Supports

D + H + E	Stresses remain within Code allowables without the usual increase for earthquake loadings (AISC for structural steel; ACI for reinforced concrete).
D + H + R + E	Stresses do not exceed: • 150% of AISC allowables for structural steel • 90% of yield stress for reinforcing bars • 85% of ultimate stress for concrete
D + H + E'	No functional failure — usually stresses do not exceed the yield point of the material for steel or the ultimate strength of the concrete. If these limits are exceeded energy absorption capacity is determined and compared to the energy input from the earthquake. The design is such that energy absorption capacity exceeds energy input.

Attachment 1
page of

Table 3.9-18

RPV INTERNALS PRESSURE DIFFERENTIAL DUE TO RECIRCULATION LINE RUPTURE

Major Component	Maximum dP (psi)	Design Capability dP (psi)[1]
Shroud Support[2]	25 (initial)	100
Guide Tube	17 (initial)	68
Lower Shroud[(2)]	25 (initial)	185
Upper Shroud[(2)]	7 (initial)	185
Core Plate	17 (initial)	50
Shroud Head Assembly	9 7 *	25

*Note: This typographical error was identified in the FSAR. GE calculations used the 7 psi value.

Notes:

1. This is the pressure differential consistent with ASME Code allowable stresses. For primary loading, considerably higher differentials can be sustained before failure.

2. Core cooling dependent.

Attachment 1
page of

Table 3.9-20

RPV INTERNALS PRESSURE FORCES

Major Component	Pressure Force	Initial Value (psi)
Shroud Support	P_1-P_4	25
Guide Tube	P_1-P_3	17
Core Plate	P_1-P_3	17
Lower Shroud	P_1-P_4	25
Upper Shroud	P_3-P_4	7
Shroud Head Assembly	P_3-P_4	7
Jet Pump Diffuser	P_1-P_4	25

Notes:

1. Refer to Figure 3.9-5 (BWR Internal Configuration) for location of pressure nodes.

Attachment 1
page of

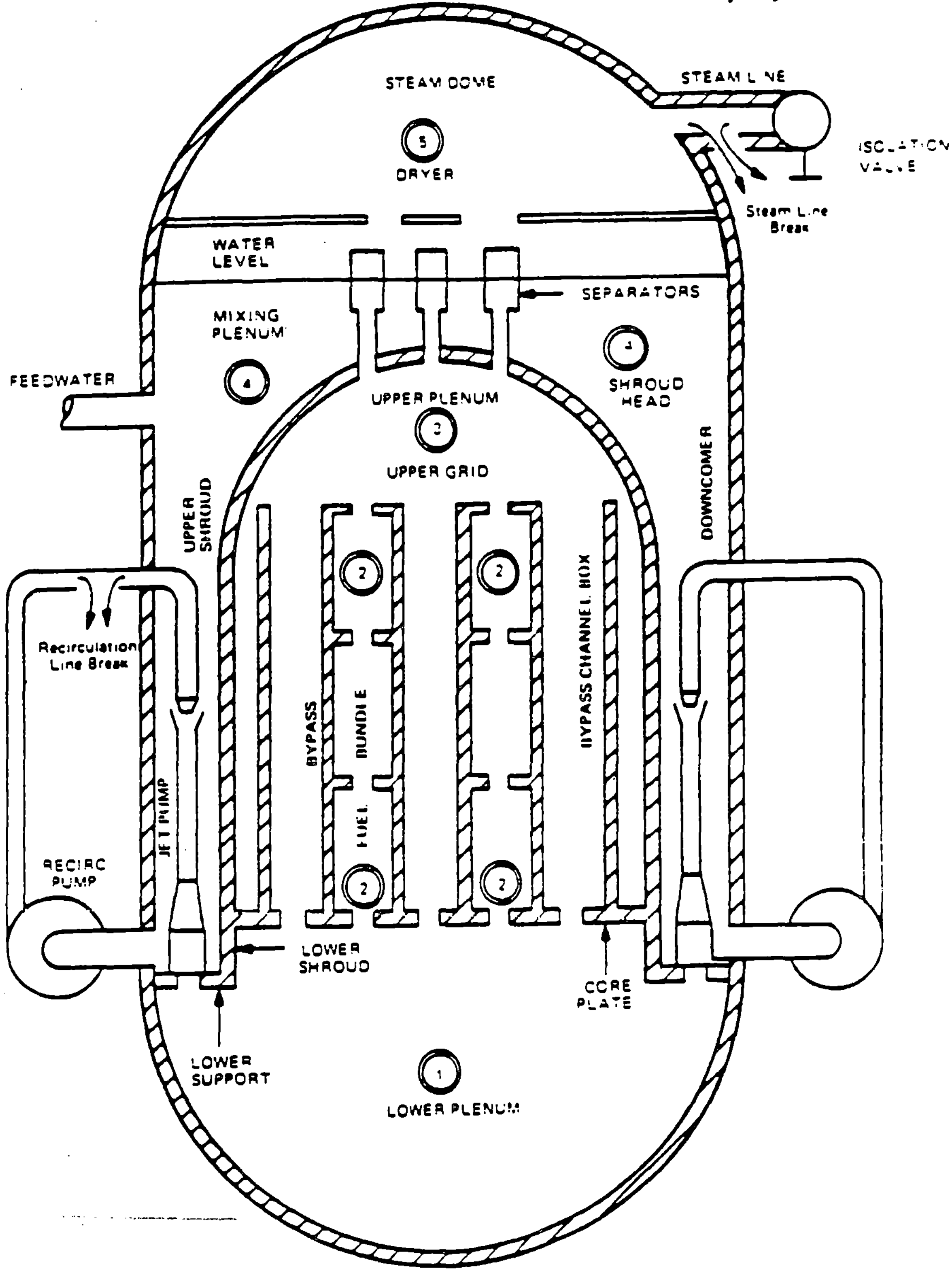

DRESDEN STATION
UNITS 2 & 3

BWR INTERNAL CONFIGURATION
WITH JET PUMP

FIGURE 3.9-5

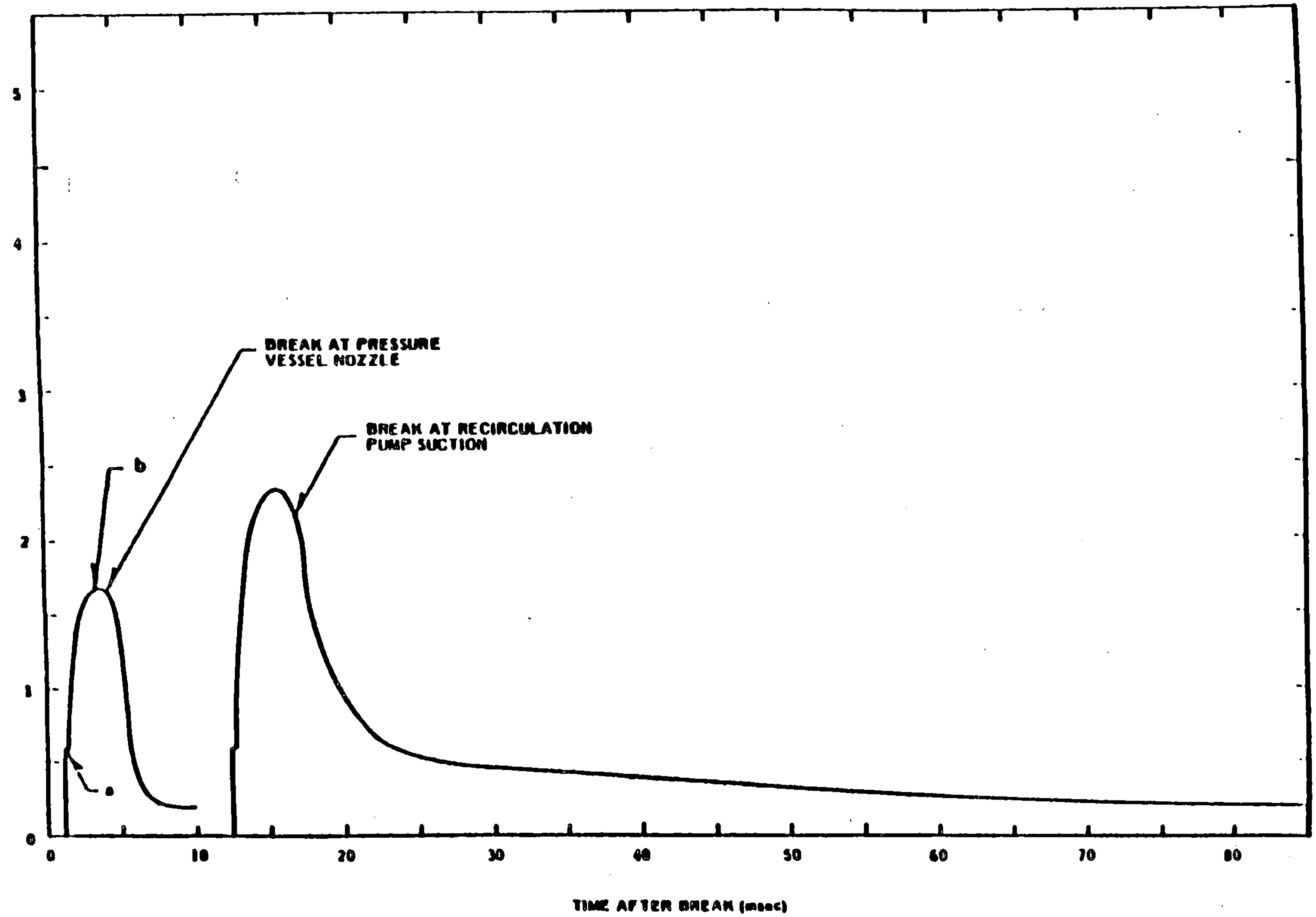

DRESDEN STATION
UNITS 2 & 3

REACTOR VESSEL SHROUD FORCE
FOLLOWING RECIRCULATION LINE BREAK

FIGURE 3.9-6

Attachment 1
Page of 1

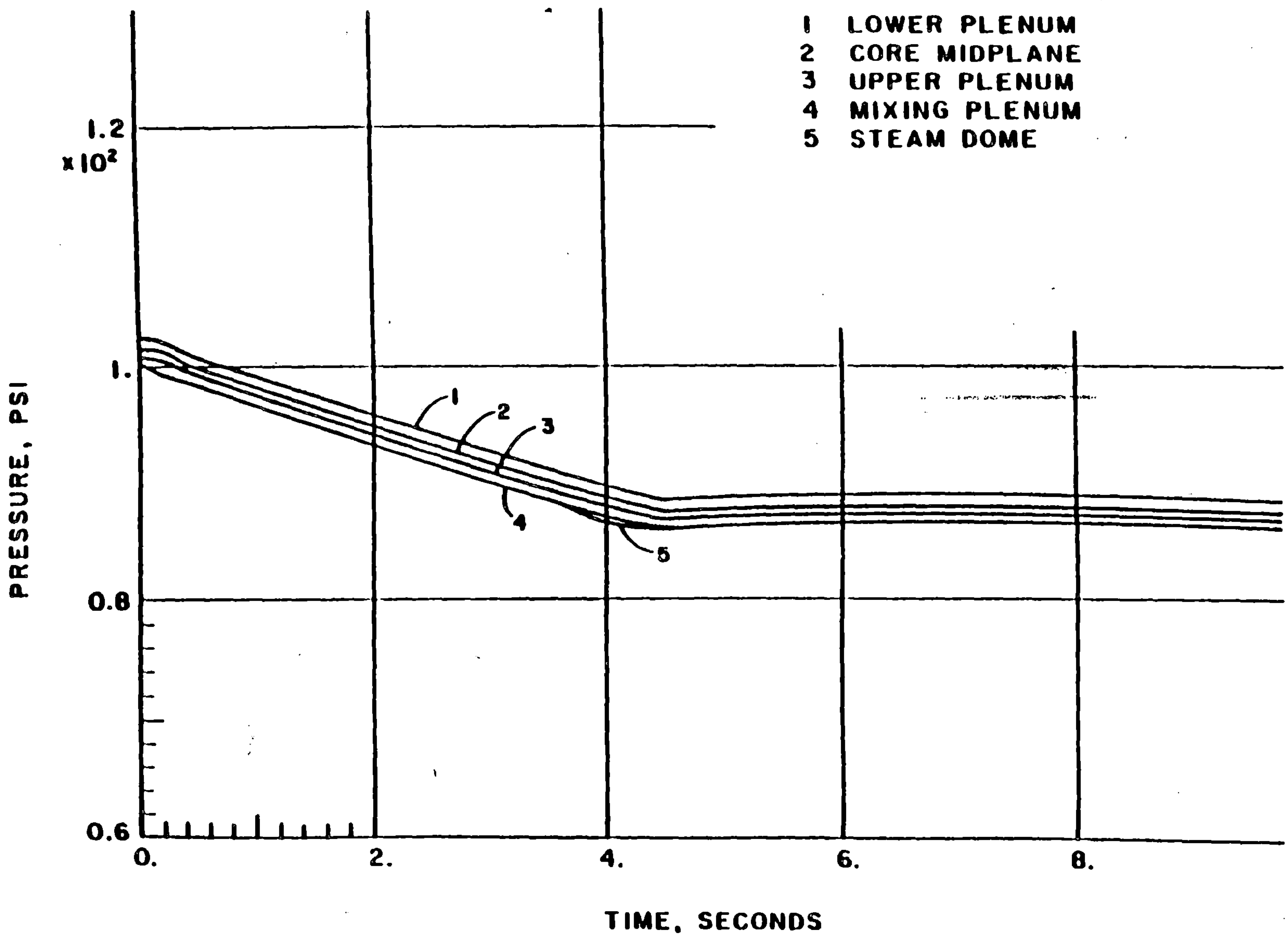

DRESDEN STATION
UNITS 2 & 3
BLOWDOWN TRANSIENT REACTOR
PRESSURE FROM 2527 MWt

FIGURE 3.9-7

Attachment
Page of 1

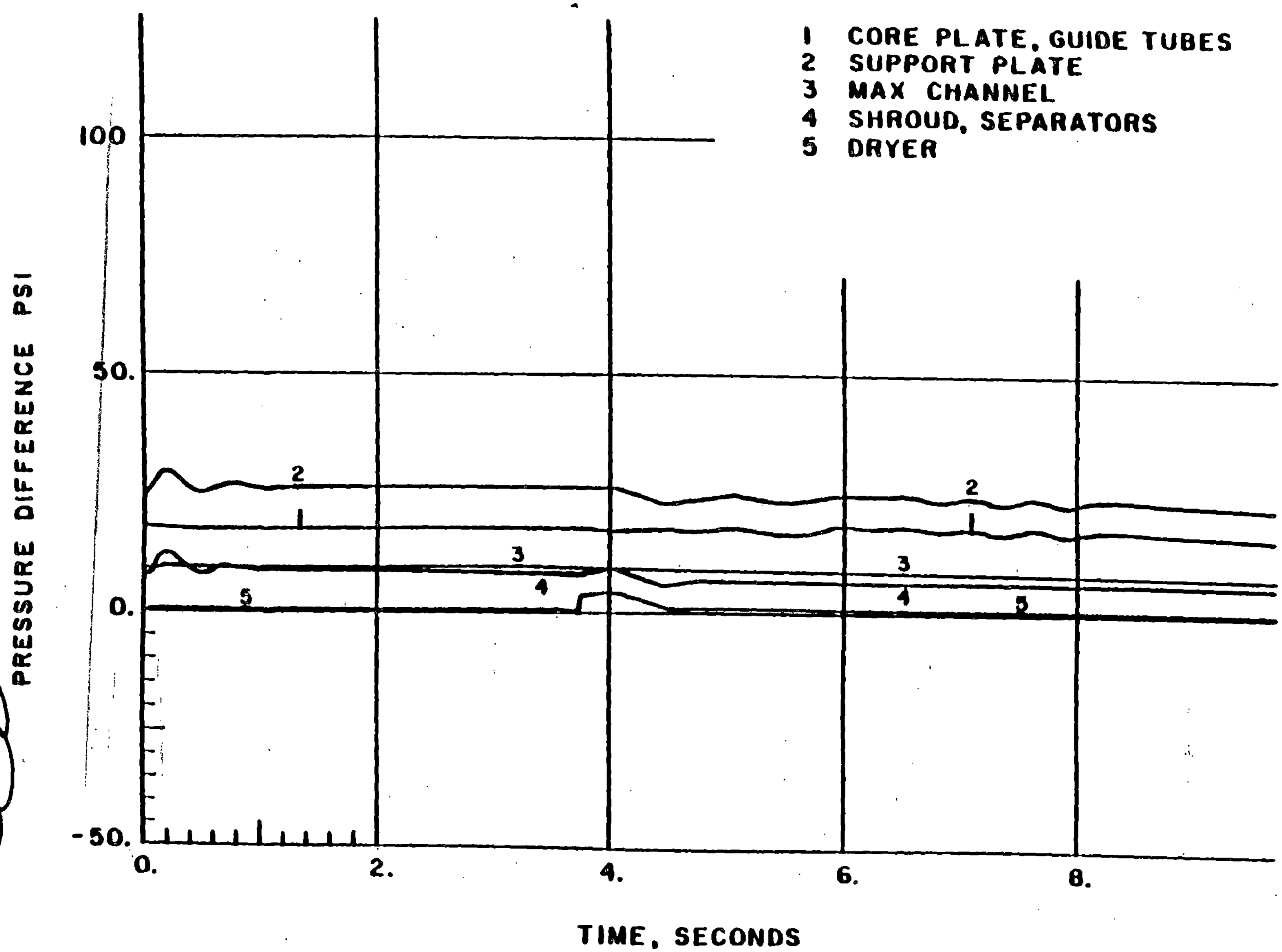

DRESDEN STATION
UNITS 2 & 3
BLOWDOWN TRANSIENT REACTOR
DIFFERENTIAL PRESSURE FROM 2527 MWt
FIGURE 3.9-8

Attachment 1
Page of

Attachment 1
page of

The following subsections have been organized to provide a discussion of the design for the reactor vessel and vessel supports (Section 3.9.3.1.1), mechanical equipment (Section 3.9.3.1.2) and piping (Section 3.9.3.1.3). Fatigue evaluation of the reactor vessel was discussed previously in Section 3.9.1.1.1.

As defined in Section 3.2, mechanical systems and components which have been designated as safety Class I are either vital to safe plant shutdown or systems and components whose failure could cause significant release of radioactivity. Throughout this section use of the term "Class I" refers to this classification basis and not to ASME Code classifications. See section 3.2 for definition of all safety classifications.

3.9.3.1.1 Reactor Pressure Vessel and Supports

The reactor vessels at Quad Cities Station Unit 1 and 2 are described in Section 5.3. The reactor vessel is supported by a steel skirt. The top of the skirt is welded to the bottom of the vessel. The base of the skirt is continuously supported by a ring girder fastened to a concrete foundation, which carries the load through the drywell to the reactor building foundation slab.

Stabilizer brackets, located below the vessel flange, are connected to tension bars with flexible couplings. The bars are then connected through the drywell to the concrete structure outside the drywell to limit horizontal vibration and to resist seismic and jet reaction forces. The bars are designed to permit axial expansion.

3.9.3.1.1.1 Acceptance Criteria

The Quad Cities reactor pressure vessels were designed according to the ASME Code, Section III, 1965 Edition, including the Summer 1965 Addenda. Applicable code cases and exceptions to the Summer 1965 Addenda are described in Section 3.2.

Design of the primary reactor vessel supports was governed by the ASME Code, the American Institute for Steel Construction (AISC) Structural Steel Code, the American Concrete Institute (ACI) Code, and by special requirements and standards set forth to provide safety assurance in the event of specific occurrences not covered by the various codes.

3.9.3.1.1.2 Design Loadings

Information regarding the design transients and fatigue evaluation of the reactor pressure vessel is presented in Section 3.9.1.1.

This subsection describes the loads and load combinations applicable to the design of the reactor pressure vessel and vessel supports.

The applicable loads for the reactor vessel and supports are defined as follows:

Attachment 1
page of

D = Dead load of structure and equipment plus any other permanent loads contributing stress, such as soil or hydrostatic loads or operating pressures and live loads expected to be present when the plant is operating.

P = Pressure due to loss-of-coolant accident (LOCA).

R = Jet force or pressure on structure due to rupture of any one pipe.

H = Force on structure due to thermal expansion of pipes under operating conditions.

T = Thermal load on containment, reactor vessel, and internals due to LOCA.

E = Operating basis earthquake (OBE) load, ground horizontal g=0.12. vertical g=0.08.

E′ = Design basis earthquake (DBE) load, ground horizontal g=0.24, vertical g=0.16.

L = Wind live load beyond normal building code requirements.

Following are the load combinations used for the reactor vessel and vessel supports.

Reactor Vessel and Primary Internals

D + E — Stresses which occur as a result of the maximum possible combination of loadings encountered in operational conditions are within the stress criteria of ASME Code, Section III, Class A Vessel.

D + E′ — The primary, and primary plus secondary stresses take into account elastic and plastic strains. These strains are limited to preclude failure by deformation which would compromise any of the engineered safeguards or prevent safe shutdown of the reactor.

P + D + T — Primary stresses are within the stress criteria of ASME Code, Section III Class A. The primary and primary plus secondary stresses are examined and take into account elastic and plastic strains. These strains are limited to preclude failure by deformation which would compromise any of the engineered safeguards or prevent safe shutdown of the reactor.

For the reactor vessel, primary stresses have been limited to 90% of the material yield strength.

Reactor Primary Vessel Supports

D + H + E — Stresses remain within Code allowables without the usual increase for earthquake loadings (AISC for structural steel, ACI for reinforced concrete).

D + H + R+ E — Stresses do not exceed :
- 150% of AISC allowables for structural steel.
- 90% of yield stress for reinforcing bars.
- 85% of ultimate stress for concrete.

Attachment 1
Page of

Table 3.9-19

REACTOR INTERNAL PRESSURE DIFFERENTIALS

Component	Δ P At Turbine-Generator Design Power	Maximum Δ P Following A Steam Line Break	Maximum Δ P Following a Recirculation Line Break
Shroud support	25	43	25
Guide tube	17	30	17
Core plate	17	30	17
Lower shroud	25	43	25
Upper shroud	8	20	8
Shroud head	8	20	8
Dryers	2	4 [Note 1]	2
Channel box	9	16	9

Notes:

1. Evaluated from the outside steam-line break described in Chapter 15.

Attachment 1
page of

Table 3.9-20

PRESSURE FORCES ACTING ON MAJOR REACTOR INTERNAL COMPONENTS

Major Component	Pressure Force[Note 1]
Shroud support	P_1-P_4
Guide tube	P_1-P_3
Core plate	P_1-P_3
Lower shroud	P_1-P_4
Upper shroud	P_1-P_4
Shroud head	P_3-P_4
Jet pump diffuser	P_1-P_4

Notes:

1. Refer to Figure 4.1-2; subscripts refer to model nodes shown on Figure 3.9-7.

Attachment 1
page of

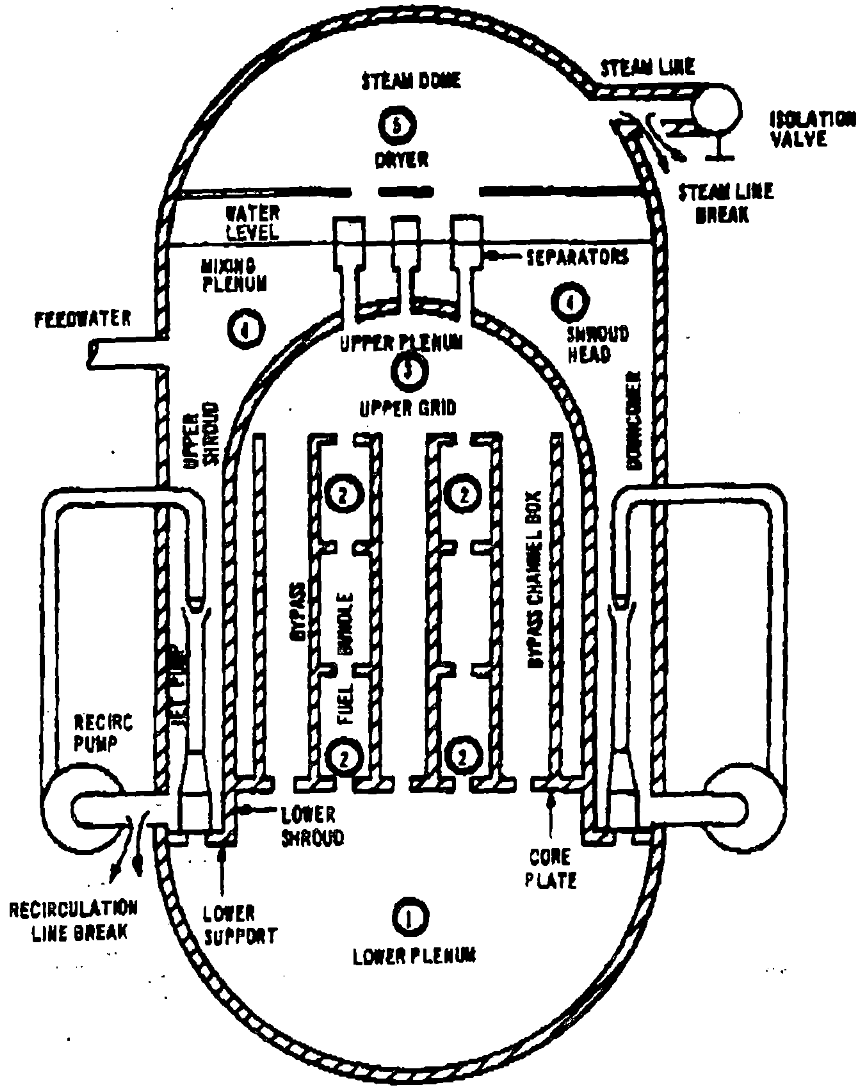

QUAD CITIES STATION UNITS 1 & 2
BWR REACTOR INTERNAL CONFIGURATION WITH JET PUMP
FIGURE 3.9-11

Attachment 1
Page of

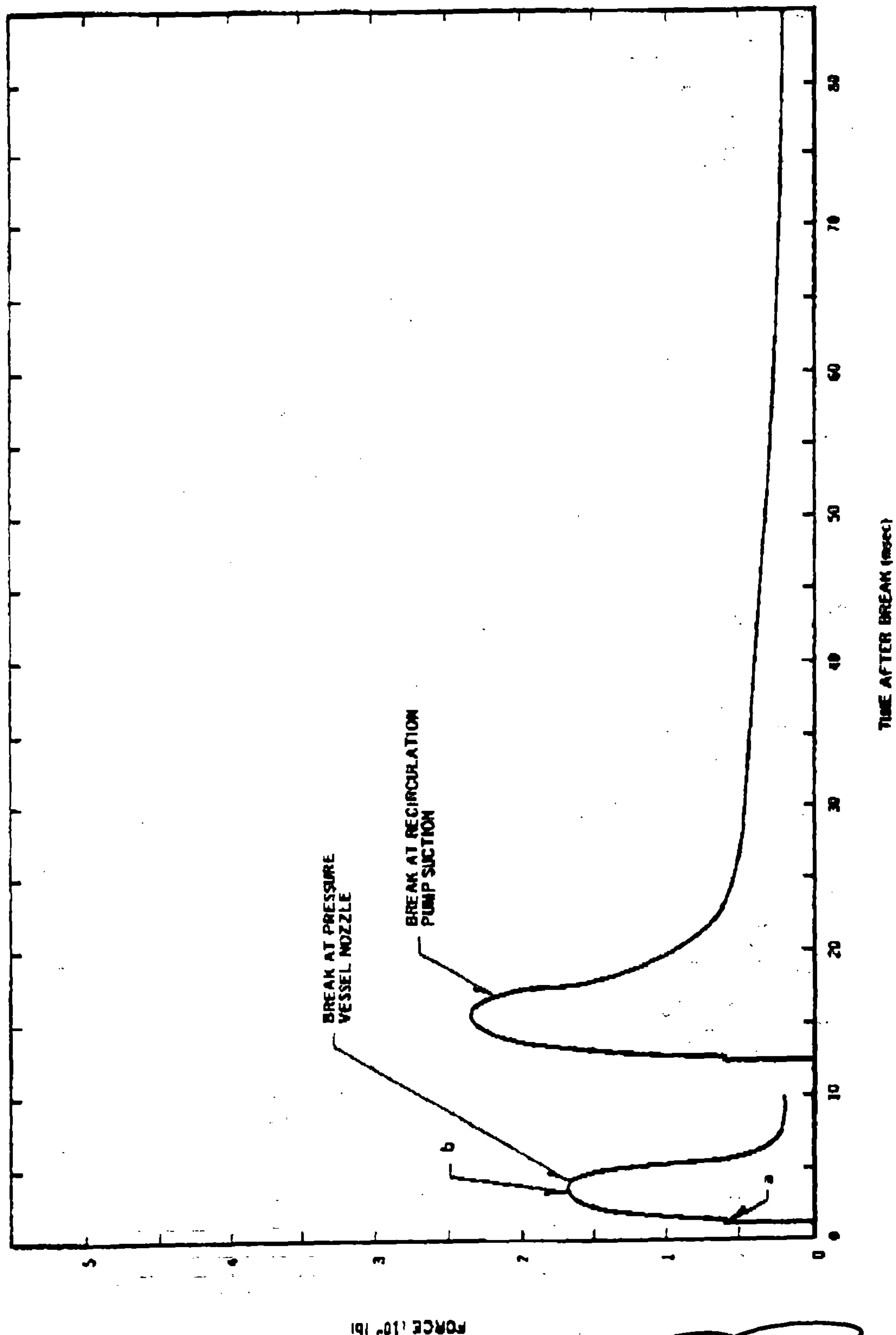

QUAD CITIES STATION
UNITS 1 & 2

REACTOR VESSEL SHROUD FORCE FOLLOWING
RECIRCULATION LINE BREAK

FIGURE 3.9-12

Attachment 1
page of

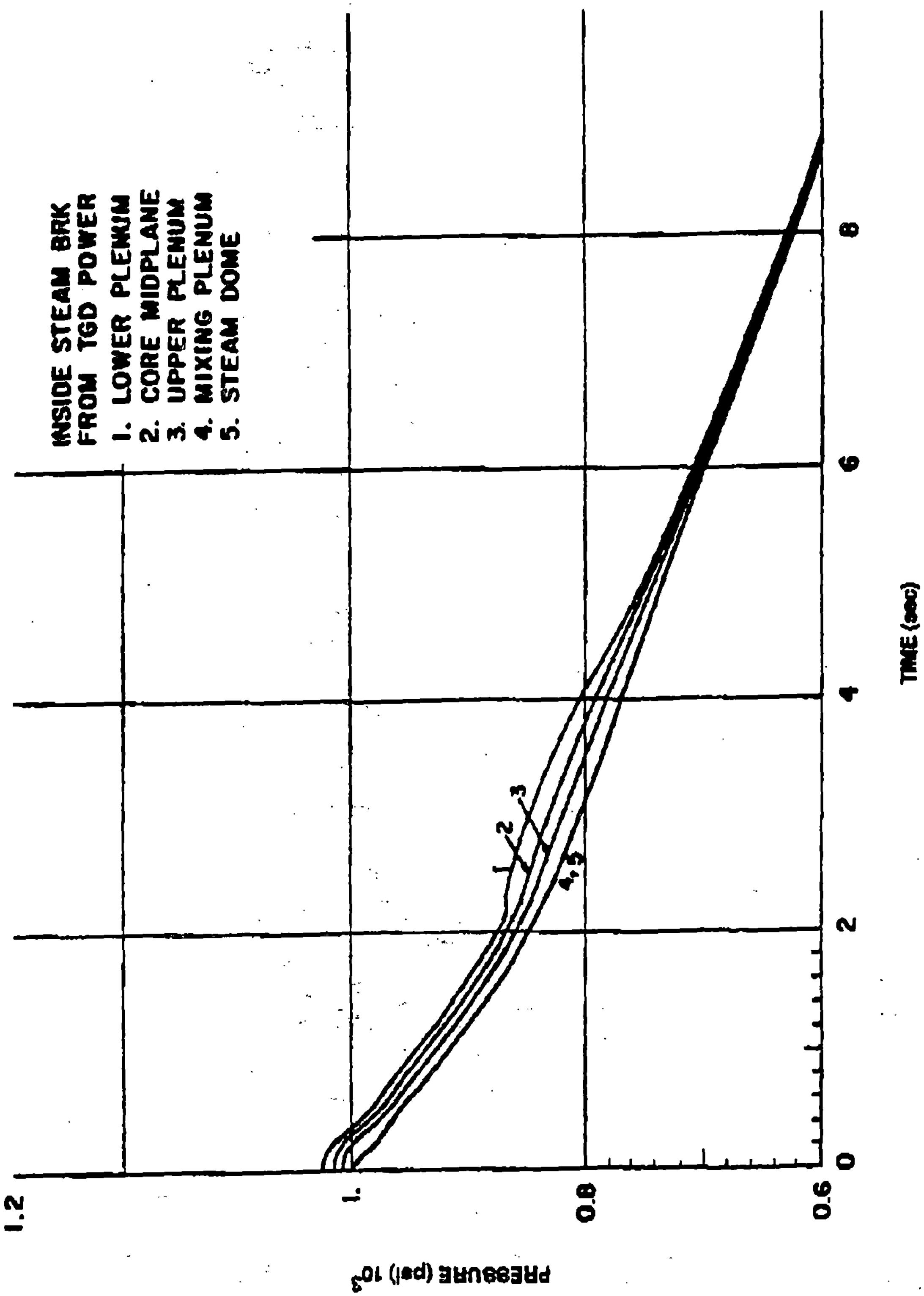

QUAD CITIES STATION UNITS 1 & 2
BLOWDOWN TRANSIENT REACTOR PRESSURE FROM 2511 MWT
FIGURE 3.9-13

Attachment 1
page of

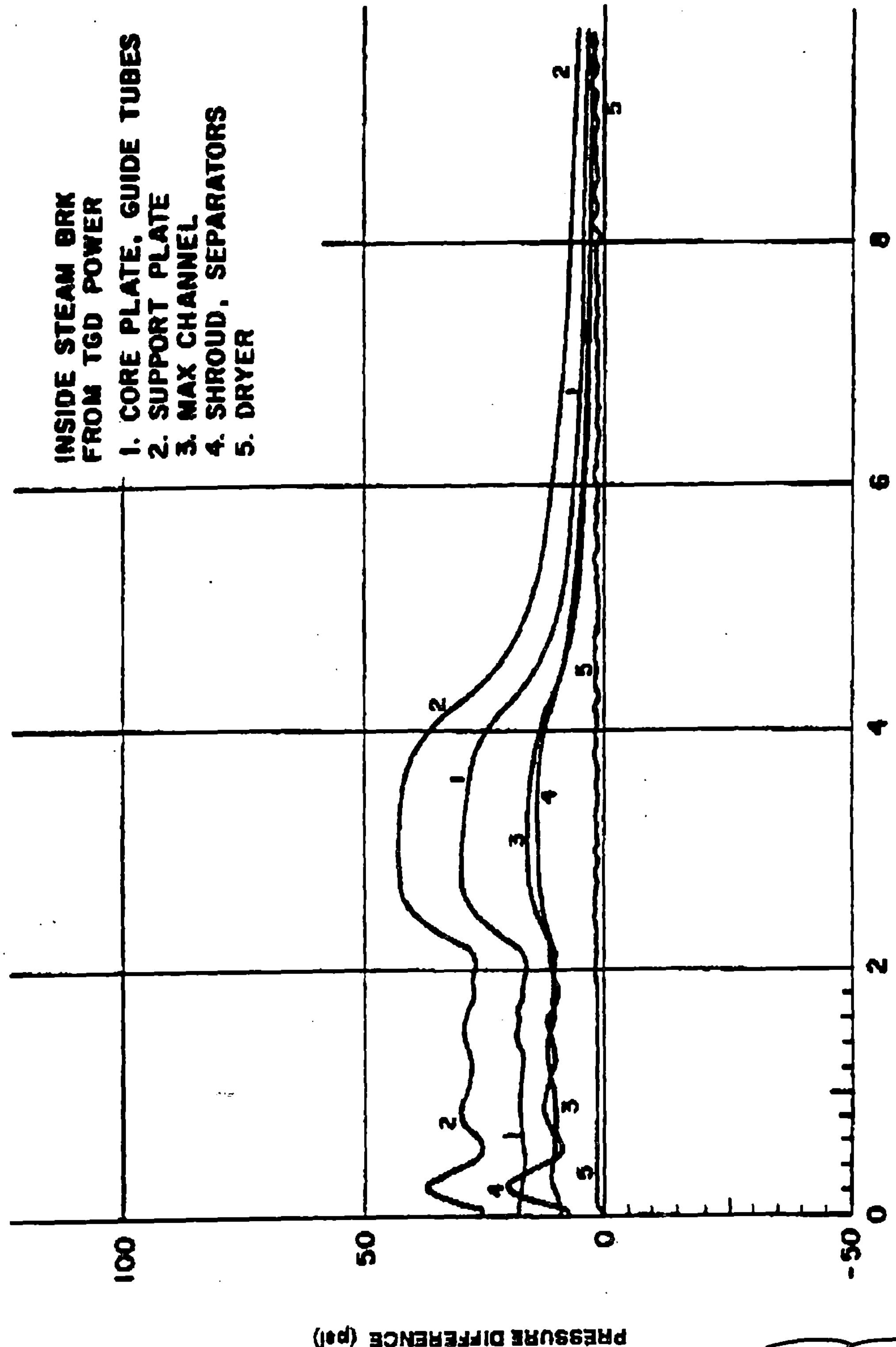

QUAD CITIES STATION
UNITS 1 & 2

BLOWDOWN TRANSIENT REACTOR DIFFERENTIAL PRESSURE FROM 2511 MWT

FIGURE 3.9-14

FREE BODY DIAGRAM
RR LOCA BLOWDOWN LOADS

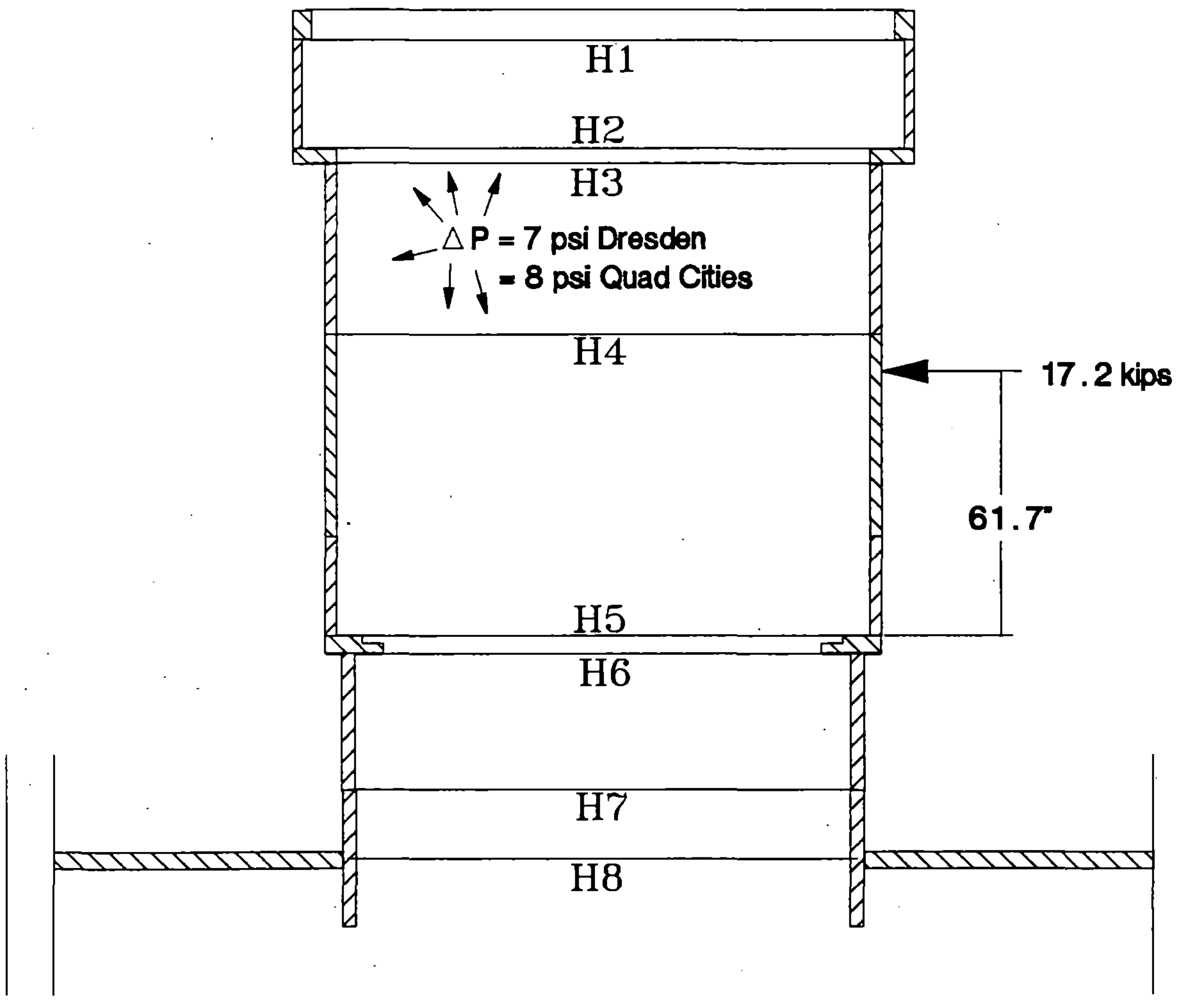

FREE BODY DIAGRAM
RR LOCA ACOUSTIC LOADS

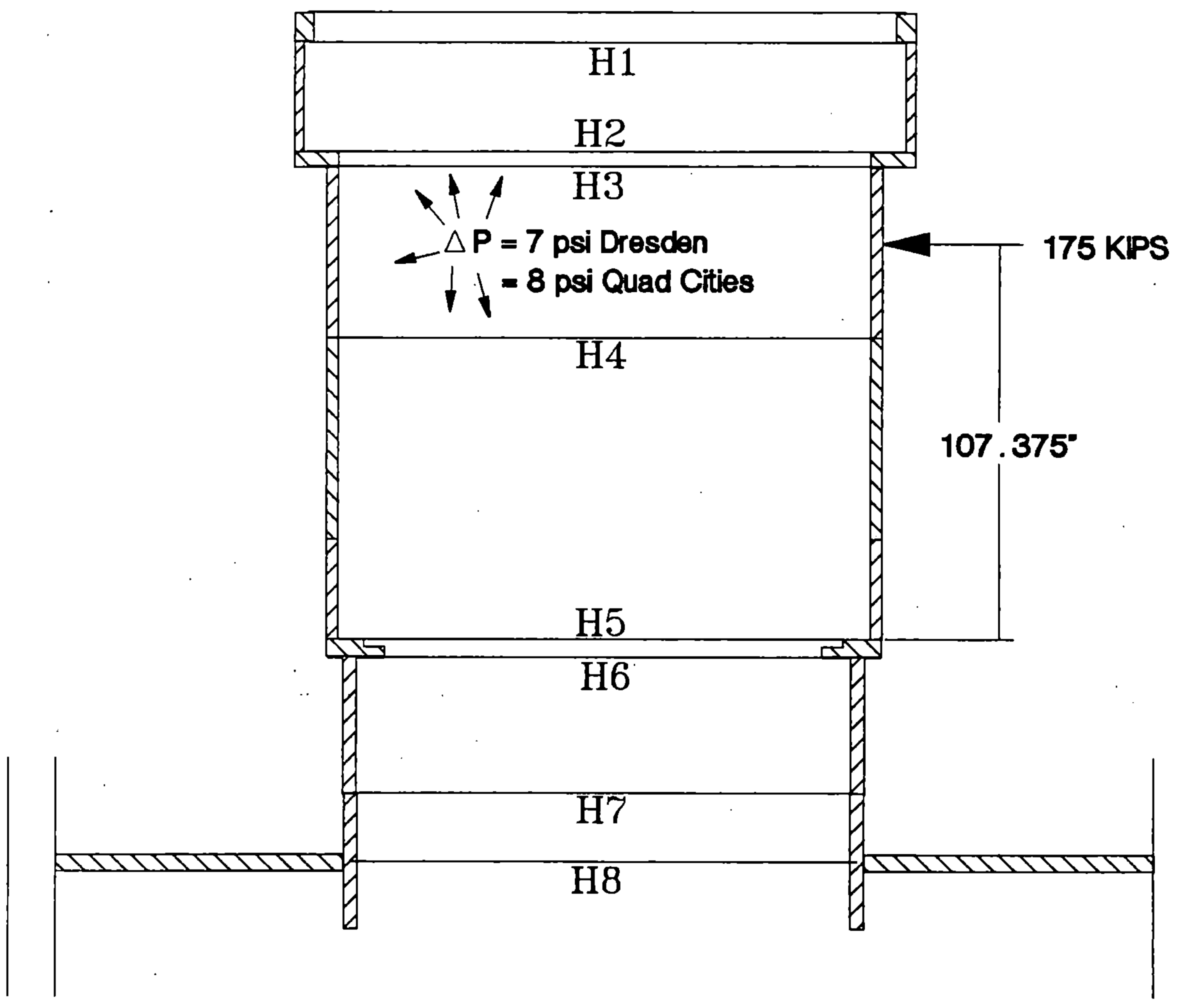

FREE BODY DIAGRAM
SEISMIC LOADS

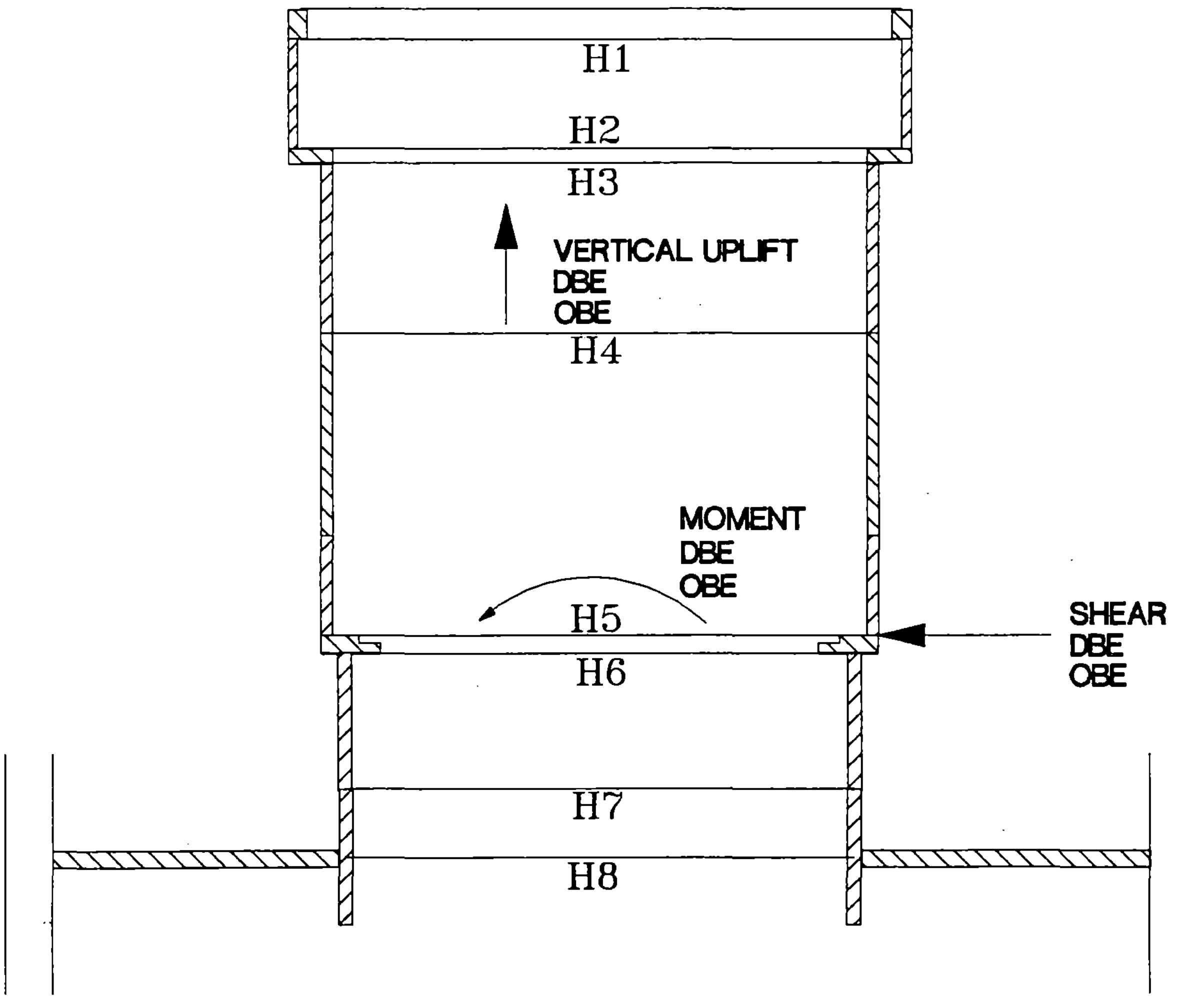

Dresden Core Shroud Summary of Loads and Stresses At Each Horizontal Weld Location COMED Design Review

Shroud Weld Designation	Combined Stresses DL+B+N (Psi)	Combined Stresses DL+B+U+OBE (Psi) Compression	Combined Stresses DL+B+U+OBE (Psi) Tension	Combined Stresses DL+B+F MS LOCA (Psi)	Combined Stresses DL+B+SSE (Psi) Compression	Combined Stresses DL+B+SSE (Psi) Tension	Combined Stresses DL+B+F+SSE MS LOCA (Psi) Compression	Combined Stresses DL+B+F+SSE MS LOCA (Psi) Tension
H1	-46.673	-13.981	-100.778	-180.434	205.993	32.399	-115.034	-288.629
H2	-28.212	50.491	-131.140	-161.973	316.478	-46.784	-4.549	-367.811
H3	-6.004	90.285	-128.184	-131.716	362.590	-74.348	60.881	-376.057
H4	41.751	379.197	-328.860	-83.961	892.666	-523.450	590.957	-825.159
H5	105.150	690.430	-522.961	-20.562	1451.739	-975.023	1150.030	-1276.732
H6	120.489	763.791	-567.155	N/A	1577.769	-1084.123	N/A	N/A
H7	133.777	1079.870	-858.682	N/A	2196.641	-1680.463	N/A	N/A
H8	119.298	1017.398	-820.016	N/A	2066.826	-1608.001	N/A	N/A

References: GE-NE-523-05-0194 Dre.-3 Evaluation and Screening Criteria for H5 Weld
GE-NE-523-A69-0594 Dre.-3 Evaluation of the Indications for the H5 Weld

Symbols:
DL= Dead Loads
B= Buoyancy Forces
U= Upset Loads Due To A 7 psi Dp
F= Faulted Loads Due To A 12 psi Dp (MS LOCA)
RR LOCA= Lateral Loads And Induced Bending Due To A RR Line Break

Inputs:
Vertical OBE = 0.0667g
Vertical DBE = 0.1333g
Density Water= 0.036
Density Shroud= 0.290

Prepared By: T. J. Behringer *T.J. Behringer* Date: 6/21/94

Reviewed By: J. A. Dawn *J. Dawn* Date: 6/21/94

Approved By: J. D. Williams *JDW* Date: 6/24/94

Attachment 2
Page of

Dresden Core Shroud Summary of Loads and Stresses At Each Horizontal Weld Location COMED Design Review

Shroud Weld Designation	Combined Stresses DL+B+F+SSE RR LOCA Blowdown (Psi) Compression	Combined Stresses DL+B+F+SSE RR LOCA Blowdown (Psi) Tension	Combined Stresses DL+B+F+SSE RR LOCA Accoustic (Psi) Compression	Combined Stresses DL+B+F+SSE RR LOCA Accoustic (Psi) Tension
H1	18.727	-154.867	18.727	-154.867
H2	129.212	-234.050	129.212	-234.050
H3	186.593	-250.345	186.593	-250.345
H4	716.669	-699.447	716.669	-699.447
H5	1291.798	-1167.076	1560.034	-1435.311
H6	N/A	N/A	N/A	N/A
H7	N/A	N/A	N/A	N/A
H8	N/A	N/A	N/A	N/A

Attachment 2
Page of

Prepared By:	T. J. Behringer	T. J. Behringer	Date:	6/21/94
Reviewed By:	J. A. Dawn	J. Dawn	Date:	6/21/94
Approved By:	J. D. Williams	J D Will	Date:	6/24/94

Dresden Core Shroud Summary of Loads and Stresses At [illegible]n Horizontal Weld Location COMED Design Review

Shroud Weld Designation	OBE Moment (In-Kips)	DBE Moment (In-Kips)	RR LOCA Moment Blowdown (In-Kips)	RR LOCA Moment Accoustic (In-Kips)	Shear OBE (Kips)	Shroud Weight (Kips)	Buoyant Force (Kips)	Vertical OBE Uplift (Kips)	Vertical DBE Uplift (Kips)	Effective Weight OBE (Kips)	Effective Weight DBE (Kips)
H1	3.240E+03	6.480E+03	N/A	N/A	25.00	219.87	-27.29	-14.67	-29.31	177.91	163.27
H2	6.780E+03	1.356E+04	N/A	N/A	186.00	248.74	-30.88	-16.59	-33.16	201.27	184.70
H3	7.220E+03	1.444E+04	N/A	N/A	186.00	250.14	-31.05	-16.68	-33.34	202.40	185.74
H4	2.340E+04	4.680E+04	N/A	N/A	193.00	320.41	-39.78	-21.37	-42.71	259.26	237.92
H5	4.010E+04	8.020E+04	1.061E+03	1.879E+04	327.00	413.70	-51.36	-27.59	-55.15	334.75	307.20
H6	4.140E+04	8.280E+04	1.130E+03	1.949E+04	327.00	415.61	-51.59	-27.72	-55.40	336.30	308.62
H7	6.030E+04	1.206E+05	2.087E+03	2.923E+04	366.00	434.58	-53.95	-28.99	-57.93	351.65	322.70
H8	6.430E+04	1.286E+05	2.275E+03	3.114E+04	366.00	434.58	-53.95	-28.99	-57.93	351.65	322.70

Prepared By: T. J. Behringer T. J. Behringer Date: 6/21/94

Reviewed By: J. A. Dawn J. Dawn Date: 6/21/94

Approved By: J. D. Williams J D Williams Date: 6/24/94

Attachment 2
Page of

Dresden Core Shroud Summary of Loads and Stresses At Each Horizontal Weld Location COMED Design Review

Shroud Weld Designation	Horizontal Bending OBE Pbs (Psi)	Horizontal Bending DBE Pbs (Psi)	Dead Load Stresses Pmd (Psi)	Buoyancy Stresses Pmb (Psi)	Vertical OBE Stresses (Psi)	Vertical DBE Stresses (Psi)	Upset & Normal(7Psi) Pressure Stresses Pm (Psi)	MS LOCA Faulted(12Psi) Pressure Stresses Pm (Psi)	RRLOCA Bending Stresses Blowdown Pbrrl1 (Psi)	RRLOCA Bending Stresses Accoustic Pbrrl2 (Psi)
H1	43.40	86.80	160.520	-19.927	-10.707	-21.397	-187.266	-321.028	N/A	N/A
H2	90.82	181.63	181.597	-22.543	-12.113	-24.207	-187.266	-321.028	N/A	N/A
H3	109.23	218.47	194.086	-24.093	-12.946	-25.872	-175.997	-301.709	N/A	N/A
H4	354.03	708.06	248.610	-30.862	-16.582	-33.140	-175.997	-301.709	N/A	N/A
H5	606.69	1213.38	320.995	-39.848	-21.410	-42.789	-175.997	-301.709	16.056	284.292
H6	665.47	1330.95	332.394	-41.263	-22.171	-44.308	-170.643	N/A	18.165	313.297
H7	969.28	1938.55	347.566	-43.146	-23.183	-46.330	-170.643	N/A	33.544	469.769
H8	918.71	1837.41	308.947	-38.352	-20.607	-41.183	-151.298	N/A	32.511	444.988

Prepared By: T. J. Behringer *T.J. Behringer* Date: 6/21/94

Reviewed By: J. A. Dawn *J. Dawn* Date: 6/21/94

Approved By: J. D. Williams *J D Williams* Date: 6/24/94

Attachment 2
Page of

Quad Cities Core Shroud Summary of Loads and Stresses At Each Horizontal Weld Location COMED Design Review

Shroud Weld Designation	Combined Stresses DL+B+N (Psi)	Combined Stresses DL+B+U+OBE (Psi) Compression	Combined Stresses DL+B+U+OBE (Psi) Tension	Combined Stresses DL+B+F MS LOCA (Psi)	Combined Stresses DL+B+SSE (Psi) Compression	Combined Stresses DL+B+SSE (Psi) Tension	Combined Stresses DL+B+F+SSE MS LOCA (Psi) Compression	Combined Stresses DL+B+F+SSE MS LOCA (Psi) Tension
H1	-73.425	-16.748	-155.785	-394.452	253.947	-24.126	-281.099	-559.172
H2	-54.964	85.886	-224.870	-375.992	440.754	-180.757	-94.292	-715.803
H3	-31.147	140.932	-234.278	-332.856	514.149	-236.271	11.300	-739.120
H4	16.608	648.798	-655.359	-285.101	1482.128	-1126.187	979.279	-1629.036
H5	80.007	1222.321	-1113.665	-221.702	2565.773	-2106.198	2062.924	-2609.046
H6	96.111	1349.028	-1209.989	N/A	2796.965	-2321.069	N/A	N/A
H7	109.399	1897.982	-1734.794	N/A	3881.584	-3383.966	N/A	N/A
H8	97.684	1773.218	-1627.283	N/A	3621.664	-3179.337	N/A	N/A

References: GE-NE-523-02-0194 QC-1 Evaluation and Screening Criteria for H5 Weld
GE-NE-523-A79-0594 QC-1 Evaluation of the Indications for H5 Weld

Symbols:
DL = Dead Loads
B = Buoyancy Forces
U = Upset Loads Due To A 8 psi Dp
F = Faulted Loads Due To A 20 psi Dp (MS LOCA)
RR LOCA = Lateral Loads And Induced Bending Due To A RR Line Break

Inputs:
Vertical OBE = 0.08g
Vertical DBE = 0.16g
Density Water = 0.036
Density Shroud = 0.290

Prepared By: T. J. Behringer *T. J. Behringer* Date: 6/21/94

Reviewed By: J. A. Dawn *J. Dawn* Date: 6/21/94

Approved By: J. D. Williams *JDWell* Date: 6/24/94

Attachment 2
Page of

Shroud Weld Designation	Combined Stresses DL+B+F+SSE RR LOCA Blowdown (Psi) Compression	Combined Stresses DL+B+F+SSE RR LOCA Blowdown (Psi) Tension	Combined Stresses DL+B+F+SSE RR LOCA Accoustic (Psi) Compression	Combined Stresses DL+B+F+SSE RR LOCA Accoustic (Psi) Tension
H1	39.928	-238.144	39.928	-238.144
H2	226.736	-394.775	226.736	-394.775
H3	313.010	-437.410	313.010	-437.410
H4	1280.988	-1327.327	1280.988	-1327.327
H5	2380.890	-2323.393	2648.925	-2591.629
H6	N/A	N/A	N/A	N/A
H7	N/A	N/A	N/A	N/A
H8	N/A	N/A	N/A	N/A

Prepared By:	T. J. Behringer	T. J. Behringer	Date:	6/21/94
Reviewed By:	J. A. Dawn	J Dawn	Date:	6/21/94
Approved By:	J. D. Williams	J D Wil	Date:	6/24/94

Attachment 2
Page of

Quad Cities Core Shroud Summary of Loads and Stresses At Each Horizontal Weld Location COMED Design Review

Shroud Weld Designation	Weld Elevation (Inches)	Shroud Outside Radius (In.)	Shroud Inside Radius (In.)	Shroud Thickness (In.)	Shroud Area (In.^2)	Shroud Centerline Section Modulus (In.^3)
H1	391.375	110.000	108.000	2.000	1369.734	7.466E+04
H2	357.875	110.000	108.000	2.000	1369.734	7.466E+04
H3	355.375	103.560	101.560	2.000	1288.807	6.610E+04
H4	266.375	103.560	101.560	2.000	1288.807	6.610E+04
H5	191.125	103.560	101.560	2.000	1288.807	6.610E+04
H6	187.125	100.500	98.500	2.000	1250.354	6.221E+04
H7	131.500	100.500	98.500	2.000	1250.354	6.221E+04
H8	120.531	100.625	98.375	2.250	1406.648	6.999E+04

Prepared By: T. J. Behringer *T. J. Behringer* Date: 6/21/94

Reviewed By: J. A. Dawn *J. A. Dawn* Date: 6/21/94

Approved By: J. D. Williams *J D Williams* Date: 6/24/94

Attachment 2
Page of

Quad Cities Core Shroud Summary of Loads and Stresses At Each Horizontal Weld Location COMED Design Review

Shroud Weld Designation	OBE Moment (In-Kips)	DBE Moment (In-Kips)	RR LOCA Moment Blowdown (In-Kips)	RR LOCA Moment Accoustic (In-Kips)	Shear OBE (Kips)	Shroud Weight (Kips)	Buoyant Force (Kips)	Vertical OBE Uplift (Kips)	Vertical DBE Uplift (Kips)	Effective Weight OBE (Kips)	Effective Weight DBE (Kips)
H1	5.190E+03	1.038E+04	N/A	N/A	43.00	219.87	-27.29	-17.59	-35.18	174.99	157.40
H2	1.160E+04	2.320E+04	N/A	N/A	338.00	248.74	-30.88	-19.90	-39.80	197.96	178.06
H3	1.240E+04	2.480E+04	N/A	N/A	338.00	250.14	-31.05	-20.01	-40.02	199.08	179.07
H4	4.310E+04	8.620E+04	N/A	N/A	415.00	320.41	-39.78	-25.63	-51.27	255.00	229.37
H5	7.720E+04	1.544E+05	1.061E+03	1.879E+04	604.00	413.70	-51.36	-33.10	-66.19	329.25	296.15
H6	7.960E+04	1.592E+05	1.130E+03	1.949E+04	604.00	415.61	-51.59	-33.25	-66.50	330.77	297.52
H7	1.130E+05	2.260E+05	2.087E+03	2.923E+04	592.00	434.58	-53.95	-34.77	-69.53	345.87	311.10
H8	1.190E+05	2.380E+05	2.275E+03	3.114E+04	592.00	434.58	-53.95	-34.77	-69.53	345.87	311.10

Attachment 2
Page of

Prepared By: T. J. Behringer *T. J. Behringer* Date: 6/21/94

Reviewed By: J. A. Dawn *J. A. Dawn* Date: 6/21/94

Approved By: J. D. Williams *J D Williams* Date: 6/24/94

Quad Cities Core Shroud Summary of Loads and Stresses At Each Horizontal Weld Location COMED Design Review

Shroud Weld Designation	Horizontal Bending OBE Pbs (Psi)	Horizontal Bending DBE Pbs (Psi)	Dead Load Stresses Pmd (Psi)	Buoyancy Stresses Pmb (Psi)	Vertical OBE Stresses (Psi)	Vertical DBE Stresses (Psi)	Upset & Normal(8Psi) Pressure Stresses Pm (Psi)	MS LOCA Faulted(20Psi) Pressure Stresses Pm (Psi)	RRLOCA Bending Stresses Blowdown Pbrrl1 (Psi)	RRLOCA Bending Stresses Accoustic Pbrrl2 (Psi)
H1	69.52	139.04	160.520	-19.927	-12.842	-25.683	-214.018	-535.046	N/A	N/A
H2	155.38	310.76	181.597	-22.543	-14.528	-29.056	-214.018	-535.046	N/A	N/A
H3	187.61	375.21	194.086	-24.093	-15.527	-31.054	-201.140	-502.849	N/A	N/A
H4	652.08	1304.16	248.610	-30.862	-19.889	-39.778	-201.140	-502.849	N/A	N/A
H5	1167.99	2335.99	320.995	-39.848	-25.680	-51.359	-201.140	-502.849	16.056	284.292
H6	1279.51	2559.02	332.394	-41.263	-26.592	-53.183	-195.020	N/A	18.165	313.297
H7	1816.39	3632.78	347.566	-43.146	-27.805	-55.610	-195.020	N/A	33.544	469.769
H8	1700.25	3400.50	308.947	-38.352	-24.716	-49.432	-172.912	N/A	32.511	444.988

Attachment 2
Page of

Prepared By:	T. J. Behringer	T. J. Behringer	Date:	6/21/94
Reviewed By:	J. A. Dawn	J. Dawn	Date:	6/21/94
Approved By:	J. D. Williams	J D Well	Date:	6/24/94

Attachment ME-1-3 Calculation DRF A00-05652

GE Nuclear Energy

ENGINEERING ANALYSIS VERIFICATION COVER SHEET

(Reference EOP 42-6.00 and EOP 25-6.00) Sheet. 1 of 1

DRF No./Section: A00-05652, Section 15

Subject: Asymmetric Load Analysis for Core Shroud Assembly without H5 Weld

1 **VERIFICATION STATEMENTS** Designated Verifier: D. Henrie

1A APPLICATION. (System/Project/Program)

Asymmetric Load Analysis to show the extent of the shroud motion during LOCA with SSE and acoutic load (recirculation suction line break only) for Dresden and Quad Cities Plants

1B METHOD OF VERIFICATION. Checking, Alternate Calc., Indiv. Design Review*, Team Design Review, Test (underline as needed); Other (describe)

1C SCOPE. Identify what is to be verified (e.g., level of detail).
Verify by the method described in 1B, that the output (1E) has been correctly generated in accordance with the referenced inputs (1D) and that the results (1E) are reasonable and adequate for the application described in 1A above.

1D INPUTS Identify any GE and external interfaces and requirements, assumptions, input documents, test analyses, reasons for changes.

1. Dresden UFSAR, Section 3-9,
2. GE Drawing, 104R861
3. Computer Runs: Case 11 = 6407T, Case 12 = 3340V, Case 13 = 2179U, Case 14 = 2180U, Case 15 = 2865V, Case 16 = 2866V

1E OUTPUTS. Identify output document(s) or analysis to be verified.

The attached write-up (Supplement 3 to GE-NE-A00-05652-03)

1F Responsible Engineer: H. Choe Hwang Choe Date: 6/7/94 Comp. 523
(print name and sign)

2 **INDEPENDENT VERIFICATION**

Comments: No Yes (See Attached) — write up revised per comments Hwang Choe 6/13/94

2A VERIFICATION STATEMENT. The method and scope of verification are appropriate and the same as stated in 1B and 1C. The inputs are appropriate and are the same as identified in 1D. All comments and technical issues are resolved. The verification establishes that the analysis output identified in 1E is correct and is adequate for its intended application as identified in 1A.

2B Independent Verifier: D. Henrie / DKHenrie Date: 6/8/94 Comp. 523
(print name and sign)
DKH signed the writeup 6/13/94

3 **APPROVAL OF VERIFICATION**

3A MANAGER'S APPROVAL: All design requirements have been identified and all technical issues are adequately resolved. The verification described in the above Sections 1 and 2 is sufficient to issue/apply the results

3B Resp. Manager or Delegate S. Ranganath SRanganath Date: 6/9/94 Comp. 523
(print name and sign)
SR 6/13/94

4A Are there attached sheets for 1A,1B,1C,1D,1E,2A,3A? (circle as applicable)

*This does not constitute a design review per the requirements of Procedure 40-7.00

SUPPLEMENT 3 (Rev. 1) TO GE-NE-A00-05652-03

Asymmetric Loads on Core shroud Assembly with a 360° Through-Wall Crack at H5 Weld Location

As part of safety assessment regarding the crack indications found near H5 weld in Dresden 3 and Quad Cities 1, asymmetric loads and the resulting motions of the core shroud assembly are evaluated. The following loads are considered: differential pressure between the inside and the outside of the shroud during LOCA, seismic acceleration during SSE, blowdown load (only for recirculation suction line break), and acoustic load (only for recirculation suction line break). This evaluation also assumes that a 360 ° through-wall crack exists at the H5 weld location. The analysis has been performed using the bounding conditions for Quad Cities 1 and Dresden 3.

The main contributor for the lateral motion or rotational (tipping) motion is caused by the seismic acceleration. The blowdown load caused by break flow through the recirculation suction line is primarily confined over the projected recirculation line area and is approximately 20,000 lbf (Reference 6 of GE-NE-A00-05652-03), and has nearly no effect on the shroud assembly above the H5 weld. Therefore, the blowdown load will not be discussed in this evaluation. The two main discussion items are: Shroud motion due to acoustic loads during recirculation suction line break LOCA, and Shroud motion due to seismic loads during recirculation line break LOCA or main steam line break LOCA. In addition, ability of the control rods to insert is discussed.

1. Acoustic Load and Shroud Motion

This load is due to an instantaneous break of the recirculation suction line. Such a load is unrealistic in the sense that it takes a finite time for the break to occur, at least 100 milliseconds. However, a hypothetical instantaneous break is considered as the source of a bounding load. The asymmetric load is caused by the fact that the sound wave takes finite time to travel from the broken suction line side to the unbroken suction line side of the annulus. The duration of the load is extremely short, about 5 milliseconds, as shown in Figure 3.9-6 of the Dresden UFSAR (Reference 6). The acoustic load has a higher load distribution on the lower portion of the shroud. However, the acoustic load distribution is assumed to be uniform between the jet pump base plate and the top of the shroud head. Above the shroud head, there is almost no acoustic load due to the large cross sectional area that attenuates the acoustic wave. Therefore, the assumption made provides a bounding lateral force and a bounding overturning moment to the shroud assembly above the H5 weld.

The result of this evaluation on the acoustic load indicates that the force acting on the shroud assembly above H5 is less than 75 % of the total force calculated for the shroud. The total force on the shroud is provided as a function of time in Figure 3.9-6 of Reference 6. The point of application of the resultant horizontal acoustic load is less than 107 inches above the H5 weld. During the recirculation suction line break, the core shroud assembly does not lift and retains substantial downward load, approximately 75 kips for Dresden and 37 kips for Quad Cities, even after the pressure difference across the shroud under the SSE load has been considered. Substantial resisting forces exist with the downward load due to the irregular mating surfaces along the crack both in radial and circumferential directions. Therefore, the shroud assembly is constrained from lateral movement. More likely motion of the shroud assembly is rotating (tipping) motion of the assembly pivoted on one side of the H5 weld crack area. The resulting lateral motion near the top of the shroud assembly associated with this rotating motion is very small, approximately twenty thousandth of an inch, because the duration of the load is very short, and hence small impulse. The restoring moment by the downward load sets back the shroud assembly in the vertical position. In conclusion, the lateral motion of the shroud assembly due to the acoustic load is essentially zero even if a 360° through-wall crack is present at H5. Practically, the addition of the acoustic load to seismic and other LOCA loads does not change the shroud motion.

Furthermore, it can be concluded that the acoustic load does not result in any plastic deformation of the shroud assembly.

The main steam line break LOCA is not discussed for this load because the asymmetric acoustic loading of the shroud occurs only with the recirculation line break LOCA.

2. Seismic Load and Shroud Motion

The core shroud pressure drop during the recirculation suction line break under SSE seismic excitation does not lift the core shroud assembly above H5 and allows substantial downward load, approximately 75 kips for Dresden and 37 kips for Quad Cities, even after the peak pressure difference across the shroud during SSE has been considered. Substantial resisting forces exist with the downward load due to the irregular mating surfaces along the crack both in radial and circumferential directions. Therefore, the shroud assembly is not likely to move laterally. More likely motion of the shroud assembly is rotating (tipping) motion of the assembly pivoted on one side of the H5 weld crack area. The lateral motion near the top of the shroud assembly due to this rotating motion is calculated to be less than 3/4 inch. The displacement of this magnitude does not interfere with any reactor internals.

When the main steam line break is considered with the SSE excitation, the shroud assembly lifts, less than 2 inches for Dresden 3 and less than 8 inches for Quad Cities 1. The seismic acceleration is transmitted to the shroud assembly before the lift, but is no longer applicable once it is lifted. One evaluation has been done with the shroud assembly mounted on a frictionless roller. This analysis shows less than 0.6 inch lateral movement. Based on this analysis, the maximum velocities of the shroud assembly, and engineering judgment, the lateral displacement is expected to be less than 3/4 inch. The displacement of this magnitude does not interfere with any reactor internals.

3. Insertion of Control Rods

The control rods insert fully because the core geometry is maintained and the lateral relative displacement between the shroud and the reactor pressure vessel is small, less than 3/4 inch. Even with 8 inches of lift anticipated during the main steam line break concurrent with SSE, fuel bundles and the top guides stay engaged and the core lattice is maintained. The height of the top guide is over 14 inches and any lift less than this retains the fuel bundles within the top guide cavity. The fuel bundles are not expected to be lifted by the top guide because the friction between the top guide and the fuel channel is not high and the fuel bundles stay within the top guide cavity by gravity alone. The core geometry is maintained during this event.

Also a summary of various safety functions for several postulated scenarios are provided in the attached table. This table has been created in cooperation with CECo.

Prepared By Hwang Choe 6/13/94
H. Choe

Verified By D K Henrie 6/13/94
D. K. Henrie

Approved By S Ranganath 6/13/94
S. Ranganath

CORE SHROUD LOSS OF H5 WELD

Design Basis Accidents	Anticpated Movement			Rod Insertion	Core Reflood	Core Spray	SBLC
	Lateral	Vertical	Moment(Tip)				
Design Basis Earthquake (SSE)	None at the H5 weld location. 3/4" at the top of the shroud.	None	3/4" maximum displacement (laterally)	Rods Insert After Tipping, Timing Not Signifcantly Affected	Floodable Volume Maintained, ECCS Systems Available	System Function Not Affected	No Boron Density Change
Main Steam Line Break	None	4" Quad Cities 0" Dresden	None	Insertion Completed After Shroud Comes Down, Timing Not Significantly Affected	Floodable Volume Maintained	Dre. CS not Affected, QC Potential Failure OF CS Riser Or Sparger, Injection Into RPV Allows Long Term Cooling	No Boron Density Change
Recirculation Line Break	None	None	None	Rods Insert, Timing Not Affected	Very Small Gap 1-2 Mils, 40GPM Bypass Analysis Unaffected	Core Spray Not Affected	N/A

Additional Scenarios Considered	Anticpated Movement			Rod Insertion	Core Reflood	Core Spray	SBLC
	Lateral	Vertical	Moment(Tip)				
Main Steam Line Break Plus DBE	3/4" maximum displacement.	8" Quad Cities 2" Dresden	3/4" maximum displacement (laterally)	Rod Insertion Complete After and While Shroud Comes Down, Oscillitory Velocity Profile, Timing Affected	Floodable Volume Maintained	Dresden CS Function Not Affected, QC Potential Failure Of CS Riser Or Sparger, Injection Into RPV Will Allow Long Term Cooling	No Boron Density Change
Recirc. Line Break Plus DBE (Low PRA Without Adding Single Failure Criteria)	None at the H5 weld location. 3/4" at the top of the shroud.	None	3/4" maximum displacement (laterally)	Rods Insert After Tipping, Timing Not Significanly Affected	Bounded By Calc. Assuming 1/4" Open All Around (Bypass Flow Small)	Core Spray Function Not Affected	N/A

Subject	Originator	Date
QUAD CITIES 1&2 AND DRESDEN 2&3 SAFETY ASSESSMENT	DK Henrie	6/10/94
Number	**Verifier**	**Date**

BOUNDING LATERAL SHROUD DISPLACEMENT RELATIVE TO RPV DUE TO ASYMMETRIC ACOUSTIC LOAD AND TO SEISMIC SSE

(Alternate Calculation)

PURPOSE

The purpose of this calculation is to verify the upper bound shroud lateral displacements relative to the RPV given in Section 15 of DRF A00-05652, "Asymmetric Load Analysis for Core Shroud Assembly without H5 Weld", for Dresden and Quad Cities.

Bounding relative displacements are calculated for: (1) Asymmetric Acoustic Load due to recirculation suction line break, and (2) Seismic SSE excitation.

ASYMMETRIC ACOUSTIC LOAD

Methodology. Based on a fundamental structural dynamics principle, it i[s] first demonstrated that the displacement of the shroud due to the acoustic load is small. Then based on a very conservative calculation, an upper bound value for the small lateral displacement is obtained.

Deamplification. As has been demonstrated ad infinitum, both theoretically by analy[sis] and empirically by dynamic test, the structural responce is significantly deamplified relative to the input excitation whenever a low-frequency structure is excited b[y] a high frequency excitation. The extent of the deamplification is dependent on the ratio of the dominant characteristic frequency of the excitation to the predominant (generally fundamental) natural frequency of the structure and on the ratio of the duration of the impulse to the dominant natural period of the structure.

Subject | Originator DK Henrie | Date 6/11/94
Number | Verifier | Date

The acoustic load resultant force time history on the shroud due to a recirculation suction line break for Dresden 2 and 3 is given in Figure 3.9-6 of the Dresden 2 & 3 USAR. The USAR figure is given in Figure 1 of this calculation. Figure 1 is representative of both Dresden and Quad Cities for purpose of the present evaluation.

From Figure 1, it is observed that the resultant acoustic load on the shroud corresponds to an impulse load with a characteristic frequency $f_c > 50$ Hz; ie $f_c = 1/T = 1/0.02 = 50$ Hz.

The shroud fundamental frequency for the uncracked weld condition is 6.69 Hz and that for a 360° through-wall crack for weld H5 is 0.073 Hz. These values come from eigen-analyses of the seismic, licensing basis, primary structure model for Quad Cities 1 & 2. The values are representative of both Quad Cites and Dresden for the present evaluation.

The eigen summary table for the uncracked weld case is given by Table 1. The summary table for a 360° through-wall crack at H5 with the shroud pin-connected at H5 is given by Table 2 and with the shroud on a roller at H5 by Table 3.

Denoting the characteristic frequency of the acoustic impulse by Ω, (>50 Hz) and the duration by t_d, ($\cong 0.020$ sec), and the structurally dominant natural (fundamental) frequency and natural period of the shroud by ϖ, (< 0.073 Hz), and T, ($> 1/0.073 = 13.7$ sec); respectively, we have

$$\Omega/\varpi \geq 50/0.073 = 685 \qquad \ldots (1)$$

and

$$t_d/T \leq 0.020/13.7 = 0.0015 \qquad \ldots (2)$$

The maximum possible structural dynamic amplification occurs for harmonic excitation of a Simple Harmonic Oscillator (SHO) in which the excitation frequency is equal to oscillator frequency. In addition, the excitation must be for a sufficient number of cycles to allow for the resonant build-up. As discussed above, the response of the SHO is deamplified relative to that of the harmonic input motion if the driving frequency is sufficiently high relative to the oscillator frequency. The corresponding dynamic amplification curve, taken from Bigg's "Introduction to Structural Dynamics", is given in Figure 2.

The dynamic amplification from Figure 2 for the frequency ratio calculated in Eq. (1) is essentially zero. If the same SHO was excited by the acoustic force time history impulse in Figure 1, the dynamic amplification would be even lower. Farthermore, the dynamic amplification of the cracked shroud excited by the acoustic impulse is even lower than that for the SHO excited by the acoustic impulse.

Figures 3 and 4, also taken from Biggs, give the dynamic amplifications of a SHO excited by impulses more nearly representative of the acoustic impulse. Figure 4 provides the closest approximation of the two. Again, the dynamic amplification of a SHO excited by any of the impulse loads of Figures 3 and 4 is essentially zero for the period ratio calculated in Eq. (20). The dynamic amplification of the shroud excited by any of the Figure 3 and 4 impulse loads would be even lower. Since the Figure 3 and 4 impulse load are approximately representative of the acoustic load, it follows that the dynamic amplification of the shroud, excited by the acoustic load, is also essentially zero.

<u>Conclusion.</u> Based on the foregoing discussion, it follows that the dynamic amplification of the Dresden or Quad Cities shroud is approximately zero when excited by the acoustic impulse time history given in Figure 1. Therefore, the expected displacement of the shroud due to the acoustic loading is also close to zero.

Subject	Originator DKHenrie	Date 6/11/94
Number	Verifier	Date

Shroud Bounding Lateral Displacement. The following calculations provide an independent demonstration of the foregoing conclusion.

From Newtons 2nd Law:

$$\vec{F} = \frac{d\vec{p}}{dt} \qquad \ldots (3)$$

Integrating with-respect-to (wrt) time,

$$\vec{p} - \vec{p}_o = \int_{t_o}^{t} \vec{F}(t)\,dt \qquad \ldots (4)$$

Assuming system (i.e., shroud) at rest at $t = t_o$ implies $\vec{p}_o = \vec{o}$. Then

$$\vec{p} = \int_{t_o}^{t} F(t)\,dt \;, \quad (= \text{Impulse}) \qquad \ldots (5)$$

From Figure 1., the impulse is conservatively calculated by

$$\int_{t_o}^{t} F(t)\,dt < (240{,}000\ \text{lb}) \times (0.020\,\text{sec})$$

$$= 4{,}800\ \text{lb-sec} \qquad \ldots (6)$$

The momentum $\vec{p}$ is given by

$$\vec{p} = m\dot{x} = \frac{413{,}000}{386}\dot{x} = \left(1070\ \frac{\text{lb-sec}^2}{\text{in}}\right)\dot{x} \qquad \ldots (7)$$

Substitute (7) and (6) into (5),

$$1070\left(\frac{\text{lb-sec}^2}{\text{in}}\right)\dot{x} < 4800 \text{ lb-sec} \quad \ldots (8)$$

$\Rightarrow$

$$\dot{x} < 4800/1070 \text{ in/sec} = 4.49 \text{ in/sec.} \quad \ldots (9)$$

Then very conservatively assuming that the shroud had this upper bound velocity at the beginning of the acoustic loading, the shroud ~~[illegible]~~ lateral displacement at the end of the idealized rectangular impulse; i.e., after 0.020 seconds is

$$x < \dot{x} \times (0.020)$$
$$= (4.49) \times 0.02$$
$$= 0.090 \text{ in.} \quad \ldots (10)$$

Assumptions (1) & (2) were not used in the calculation. Hwang Choe 6/13/94

The actual lateral displacement is much less the conservative upper bound value given by (10). In addition to: (1) the assumed rectangular impulse, (2) the maximum velocity $\dot{x} = 4.49$ in/sec assumed to occur uniformily throughout the entire acoustic loading, and (3) the assumption of rigid body (actually particle) mechanics, the surface traction along the cracked weld surface as well as all ★ fluid drag forces and all restoring spring forces due to piping, etc. were neglected in the calculation. Only the acoustic loading was considered.

It can be concluded at this point that an upper bound on the shroud displacement relative to the RPV is well below 90 mils and that minimal benefi will be obtained by trying to more precisely quantify this higher order effect. However, based on the conservative, simplifying assumptions, it is expected that the upper bound displacement will be less than 20 mils.

★ Note: In displacement calculation, all those other force were ignored, but the restoring moment by the downward load was considered. Hwang Choe 6/13/94

Subject	Originator DK Henrie	Date 6/11/94
Number	Verifier	Date

SEISMIC SSE DISPLACEMENTS

The Quad Cities 1 & 2 primary structure seismic model was modified to account for a 360° through-wall crack of Weld H5. Two shroud configurations were analyzed to bound the H5 weld crack condition. The first configuration assumed that only the shroud shear could be transmitted through the cracked weld. Consequently, the shroud was pin-connected at the weld location.

In the second shroud configuration, it was assumed that neither the shroud shear nor the shroud moment could be transfered across the crack weld. Consequently, the shroud was roller connected in the horizontal direction at the H5 weld location in the second configuration.

Both shroud configurations resulted in model instability. In order to circumvent the corresponding analytical singularities in the liner time history analyses, the models were farther modified to include soft elastic links between the shroud and the RPV. In turn, two configurations each were selected for both the pin-connected and the roller-connected shroud configuration. In the first configuration, an elastic link was assumed between that shroud and the RPV at the top guide elevation only. In the second configuration, elastic links were assumed at both the top guide and core support plate elevations.

The stiffness of the shroud-to-RPV elastic links were initially selected low enough such that insignificant changes resulted in the eigendata set when the soft springs were added to the original (benchmark) primary structure model with no cracked welds. The elastic link stiffness were farther reduced to more realistically reflect the actual stiffness of connecting piping between the shroud and the RPV.

Subject		Originator D.K. Henrie	Date 6/11/94
Number		Verifier	Date

The modified primary structure models were subjected to the Quad Cities licensing basis free-field, seismic SSE acceleration time history; i.e., 1957 Golden Gate Park, S 80°E, normalized to 0.25g.

Conclusion. The maximum lateral displacement of the shroud relative to the RPV for the pin-connected shroud configuration model is 0.53" (Computer Run 2865V) and for the roller-connected shroud configuration model the maximum relative displacement is 0.68" (Computer Run 2866V)

FIGURE 1. Acoustic Load Resultant Time History

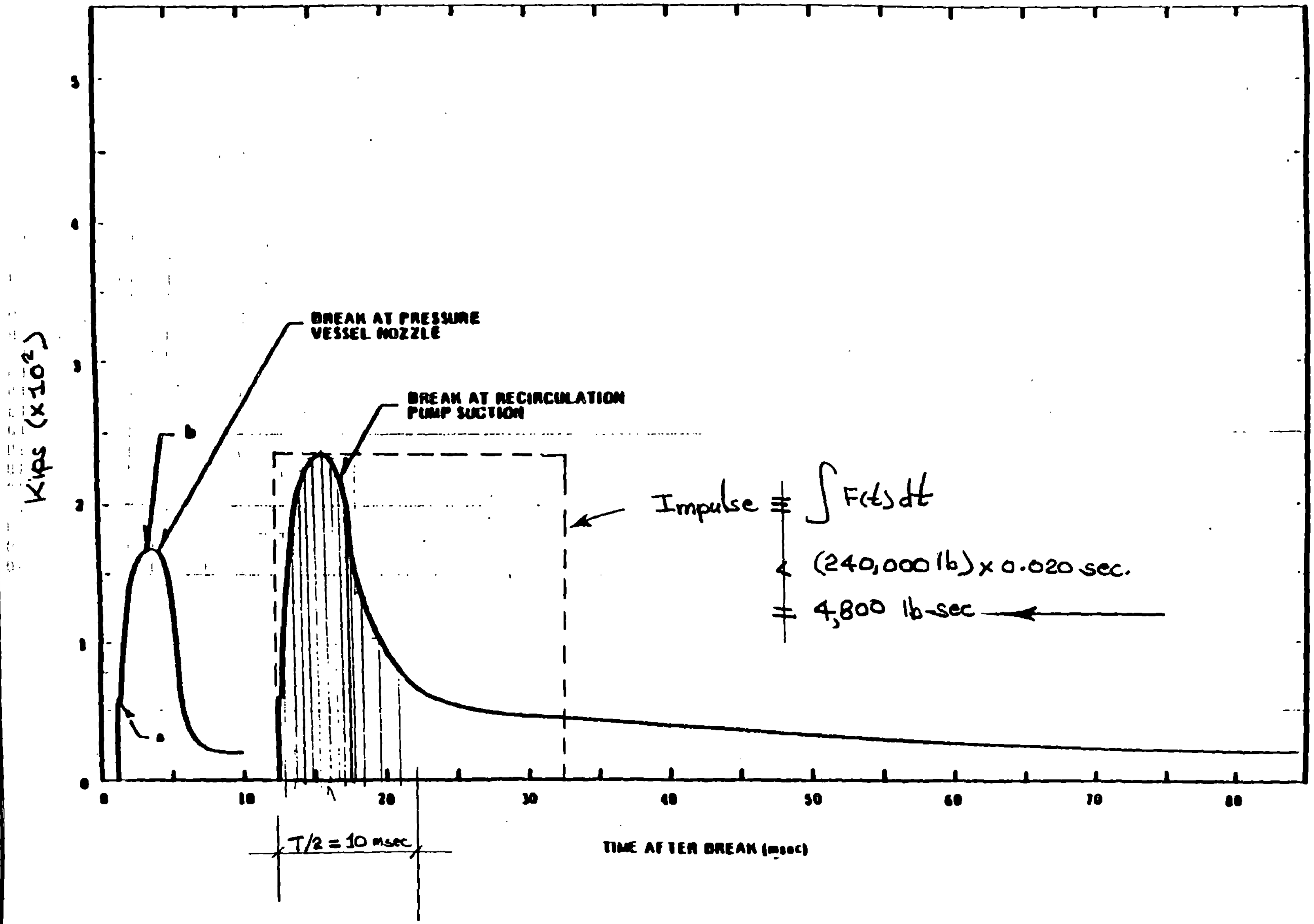

DRESDEN STATION
UNITS 2 & 3
REACTOR VESSEL SHROUD FORCE
FOLLOWING RECIRCULATION LINE BREAK

FIGURE 3.9-6

Peak values occur at damped natural frequencies!

$$\frac{\Omega}{\omega_d} = \frac{\Omega}{\omega\sqrt{1-\lambda^2}}$$

Then $\frac{\Omega}{\omega_d} = 1$

$$\Rightarrow \frac{\Omega}{\omega} = \sqrt{1-\lambda^2}$$

$\lambda \equiv \beta/\omega$

= FRACTION CRITICAL DAMPING

NOTE:

FIG. 2.18 GIVES THE FORCED PART; i.e., PARTICULAR SOLUTION, DLF. THUS THE RESPONSE IS AT THE DRIVING FREQUENCY Ω.

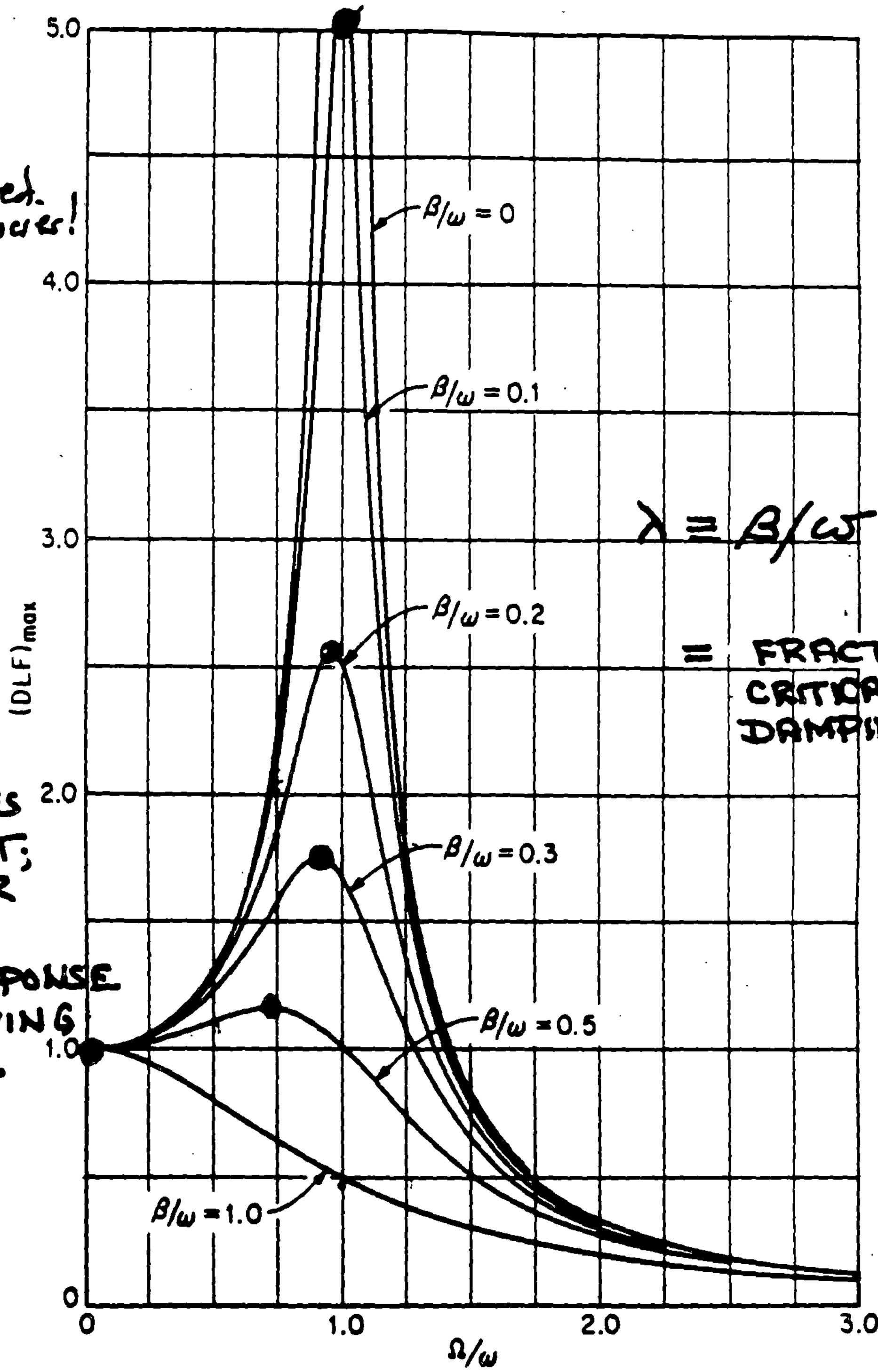

FIGURE 2.18 Maximum dynamic load factor for sinusoidal load, $F_1 \sin \Omega t$, damped systems.

FIGURE 2.

FIGURE 3.

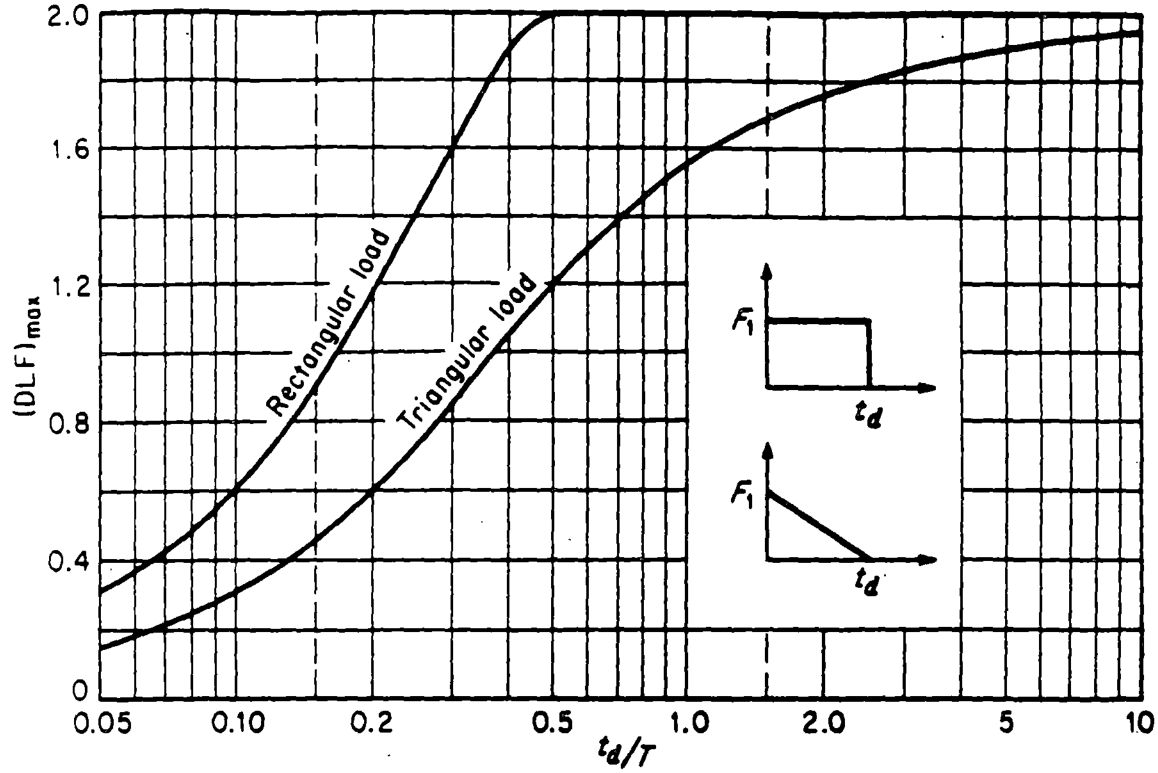

(DLF)max
Rectangular load
Triangular load
F1
td
td/T

(a)

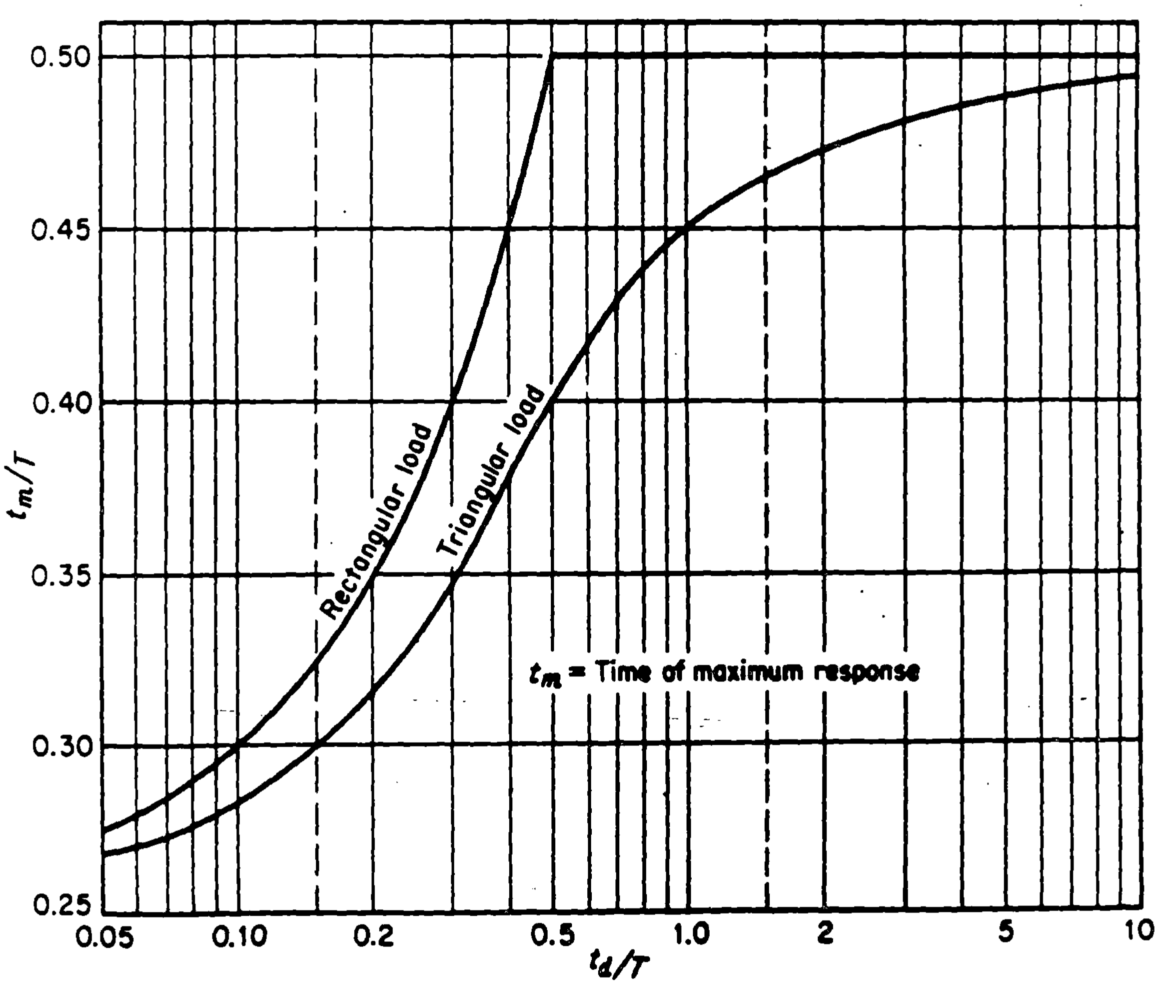

tm/T
Rectangular load
Triangular load
tm = Time of maximum response
td/T

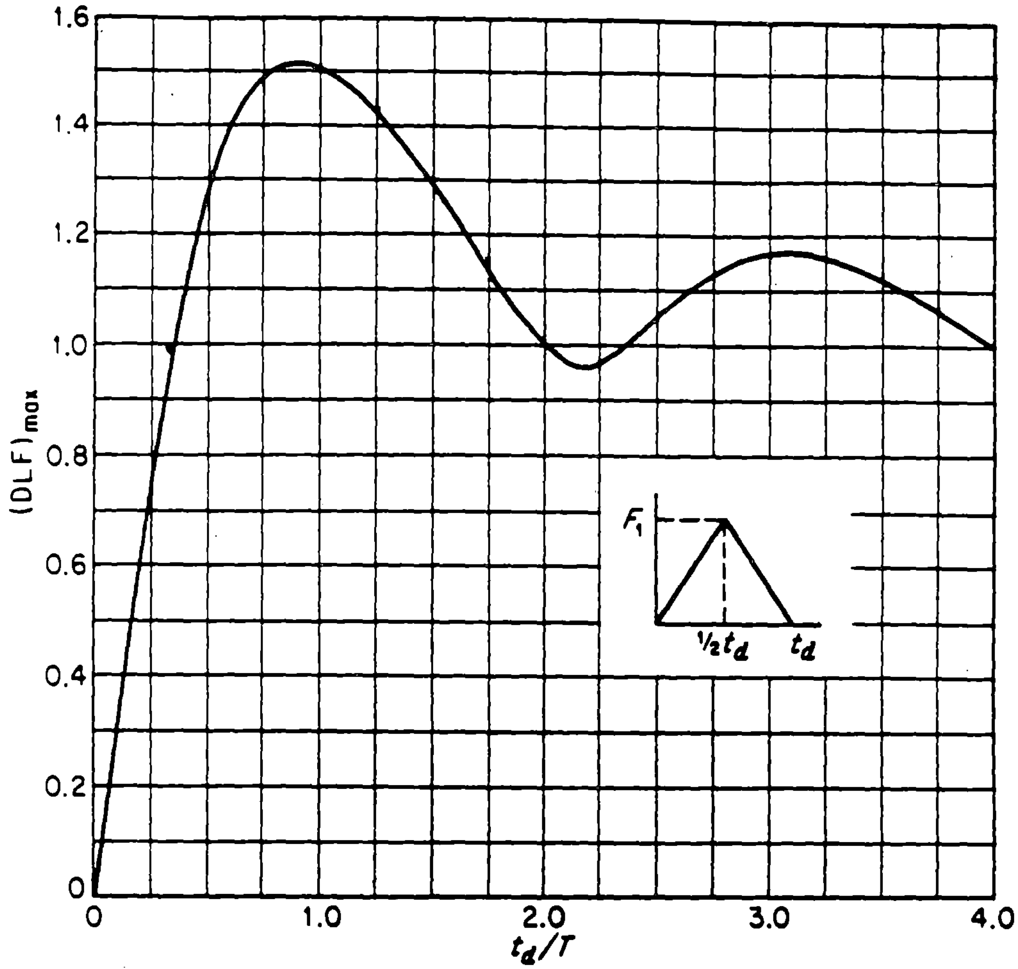

(a)

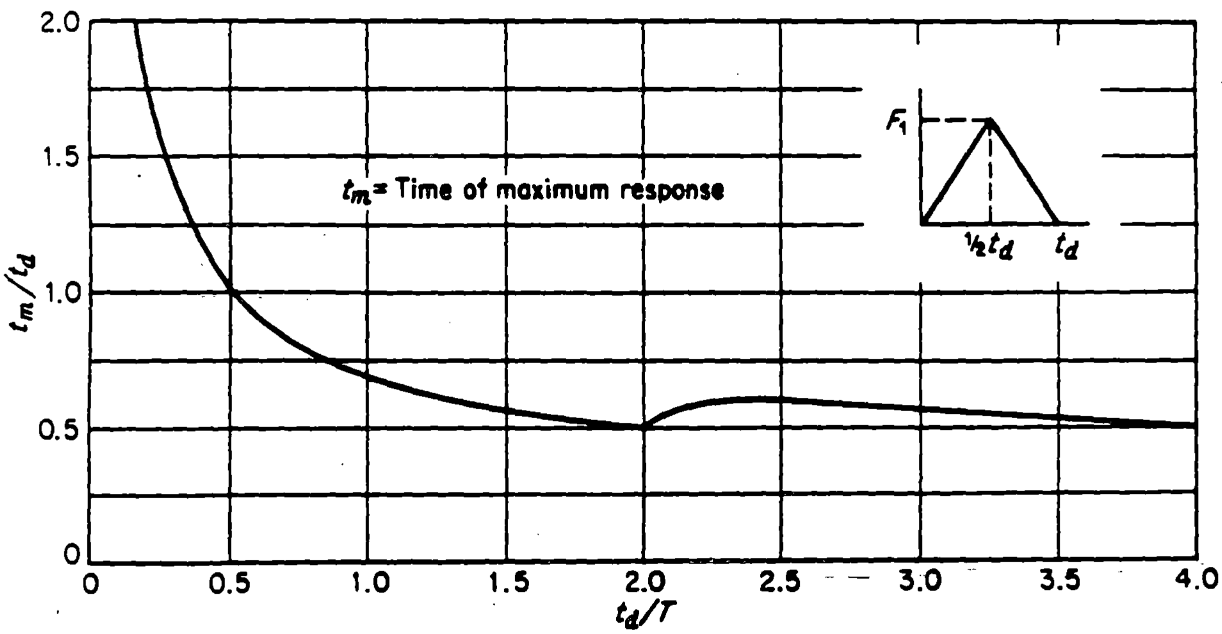

(b)

FIGURE 2.8 Maximum response of one-degree elastic systems (undamped) subjected to equilateral triangular load pulse.

TABLE 1.

CASE 1

$K_{s/s} = 0$

(Benchmark)

**** M O D A L D I S P L A C E M E N T S U M M A R Y T A B L E ****

MODE NUMBER	CIRCULAR FREQUENCY (RAD/TIME)	FREQUENCY (HERTZ)	PERIOD (TIME)	MAX MODAL AMPLITUDE	NODE NUMBER	DEG OF FREEDOM	MAX DYN DISPLACEMT	NODE NUMBER	DEG OF FREEDOM	MAX DYN ROTATION
1	1.8963E 01	3.0180E 00	3.3135E-01	1.9449E-01	29	1	3.9537E-02	19	5	1.8065E-05
2	2.5909E 01	4.1236E 00	2.4251E-01	1.3483E-01	24	1	8.4481E-02	24	5	1.0541E-02
3	2.6184E 01	4.1674E 00	2.3996E-01	1.6381E-01	18	1	4.6212E-02	19	5	5.5007E-03
4	3.4011E 01	5.4130E 00	1.8474E-01	7.6171E-01	38	1	8.0162E-02	24	5	1.8427E-03
5	3.9900E 01	6.3502E 00	1.5747E-01	5.0037E-01	38	1	5.1821E-02	17	5	4.3276E-03
6	4.2061E 01	6.6942E 00	1.4938E-01	1.1850E-01	11	1	3.2798E-02	17	5	5.9091E-03
7	5.5201E 01	8.7855E 00	1.1382E-01	4.8440E-02	30	1	1.2317E-02	17	5	1.0687E-04
8	6.2457E 01	9.9404E 00	1.0060E-01	5.5853E-03	11	1	7.0311E-04	17	5	1.1321E-04
9	7.6608E 01	1.2193E 01	8.2017E-02	3.5618E-03	40	1	1.1647E-03	24	5	3.4457E-07
10	8.9587E 01	1.4258E 01	7.0135E-02	1.7852E-02	1	1	3.9470E-03	24	5	1.9710E-04
11	9.6861E 01	1.5416E 01	6.4868E-02	3.1681E-02	1	1	1.3577E-03	11	5	7.0294E-05
12	1.0540E 02	1.6775E 01	5.9613E-02	2.6925E-04	21	1	7.4142E-05	20	5	1.1331E-05
13	1.1994E 02	1.9089E 01	5.2386E-02	4.0948E-05	19	1	1.3713E-05	18	5	5.6726E-06
14	1.2248E 02	1.9494E 01	5.1298E-02	1.6247E-03	21	1	1.1800E-04	20	5	1.4718E-05
15	1.3445E 02	2.1399E 01	4.6732E-02	1.3143E-03	21	1	1.0436E-03	20	5	1.1868E-04
16	1.3789E 02	2.1946E 01	4.5566E-02	3.0356E-04	39	1	1.1726E-04	11	5	4.8105E-07
17	1.3829E 02	2.2010E 01	4.5434E-02	2.5718E-04	11	1	1.2057E-04	11	5	1.9835E-05
18	1.5303E 02	2.4356E 01	4.1058E-02	8.6455E-03	21	1	5.9016E-04	24	5	1.2903E-04
19	1.7157E 02	2.7306E 01	3.6621E-02	9.9160E-05	23	1	5.0252E-05	24	5	2.6356E-05
20	1.8608E 02	2.9616E 01	3.3766E-02	3.1996E-04	31	1	1.7025E-04	24	5	5.7790E-07

TABLE 2.

**** M O D A L D I S P L A C E M E N T S U M M A R Y T A B L E ****

MODE MBER	CIRCULAR FREQUENCY (RAD/TIME)	FREQUENCY (HERTZ)	PERIOD (TIME)	MAX MODAL AMPLITUDE	NODE NUMBER	DEG OF FREEDOM	MAX DYN DISPLACEMT	NODE NUMBER	DEG OF FREEDOM	MAX DYN ROTATION
1	4.6289E-01	7.3671E-02	1.3574E 01	2.0813E-01	11	1	8.4700E-02	19	5	3.1530E-03
2	1.8963E 01	3.0180E 00	3.3135E-01	1.9447E-01	23	1	3.9532E-02	17	5	1.3841E-05
3	2.5928E 01	4.1266E 00	2.4233E-01	1.0803E-01	24	1	7.0556E-02	24	5	8.8180E-03
4	3.0956E 01	4.9268E 00	2.0297E-01	4.0632E-01	18	1	1.2131E-01	17	5	2.3162E-02
5	3.4159E 01	5.4366E 00	1.8394E-01	8.0811E-01	38	1	8.5816E-02	17	5	1.1780E-02
6	4.0087E 01	6.3801E 00	1.5674E-01	4.2656E-01	38	1	4.4231E-02	17	5	3.5226E-03
7	5.5201E 01	8.7854E 00	1.1382E-01	4.8427E-02	30	1	1.2311E-02	17	5	1.1748E-04
8	6.1774E 01	9.8316E 00	1.0171E-01	4.3202E-03	15	1	5.2869E-04	17	5	1.0706E-04
9	7.1421E 01	1.1367E 01	8.7974E-02	3.4139E-03	11	1	6.3966E-04	19	5	7.9477E-05
10	7.6608E 01	1.2193E 01	8.2017E-02	2.8427E-03	40	1	9.2955E-04	24	5	2.7444E-07
11	8.9596E 01	1.4260E 01	7.0128E-02	1.9230E-02	1	1	4.2654E-03	24	5	2.1332E-04
12	9.6861E 01	1.5416E 01	6.4868E-02	3.1006E-02	1	1	1.3385E-03	11	5	7.6208E-05
13	1.0588E 02	1.6851E 01	5.9343E-02	1.9649E-04	21	1	5.9658E-05	20	5	8.4309E-06
14	1.2068E 02	1.9207E 01	5.2064E-02	3.3044E-05	19	1	1.0815E-05	18	5	4.5364E-06
15	1.2248E 02	1.9494E 01	5.1298E-02	1.8217E-03	21	1	1.2960E-04	20	5	1.6328E-05
16	1.3485E 02	2.1462E 01	4.6594E-02	1.4224E-03	21	1	1.0964E-03	20	5	1.2960E-04
17	1.3789E 02	2.1946E 01	4.5566E-02	2.8654E-04	39	1	1.1070E-04	20	5	4.2231E-07
18	1.5302E 02	2.4354E 01	4.1061E-02	8.6461E-03	21	1	5.5250E-04	24	5	1.1966E-04
19	1.7079E 02	2.7182E 01	3.6789E-02	9.4143E-05	23	1	4.7045E-05	24	5	2.4676E-05
20	1.8607E 02	2.9614E 01	3.3768E-02	3.2690E-04	31	1	1.7341E-04	11	5	6.8776E-07

TABLE 3.

**** M O D A L D I S P L A C E M E N T S U M M A R Y T A B L E ****

MODE NUMBER	CIRCULAR FREQUENCY (RAD/TIME)	FREQUENCY (HERTZ)	PERIOD (TIME)	MAX MODAL AMPLITUDE	NODE NUMBER	DEG OF FREEDOM	MAX DYN DISPLACEMT	NODE NUMBER	DEG OF FREEDOM	MAX DYN ROTATION
1	4.5919E-01	7.3082E-02	1.3683E 01	1.8615E-01	11	1	7.9714E-02	11	5	3.1841E-03
2	8.5306E-01	1.3577E-01	7.3655E 00	1.4828E-01	61	1	5.7085E-02	11	5	3.4728E-03
3	1.8963E 01	3.0180E 00	3.3135E-01	2.1766E-01	29	1	4.4248E-02	17	5	1.5430E-05
4	2.5928E 01	4.1266E 00	2.4233E-01	9.0982E-02	24	1	5.9420E-02	24	5	7.4262E-03
5	3.1020E 01	4.9370E 00	2.0255E-01	5.6689E-01	18	1	1.6866E-01	17	5	3.2461E-02
6	3.4168E 01	5.4380E 00	1.8389E-01	7.3037E-01	38	1	7.7567E-02	17	5	1.1053E-02
7	4.0092E 01	6.3808E 00	1.5672E-01	5.1380E-01	38	1	5.3232E-02	17	5	4.3625E-03
8	5.5201E 01	8.7854E 00	1.1382E-01	4.2025E-02	30	1	1.0684E-02	17	5	1.0263E-04
9	6.1878E 01	9.8482E 00	1.0154E-01	4.7986E-03	11	1	6.4968E-04	17	5	1.1562E-04
10	7.6608E 01	1.2193E 01	8.2017E-02	2.8494E-03	40	1	9.3174E-04	24	5	2.9334E-07
11	8.1525E 01	1.2975E 01	7.7071E-02	8.3019E-03	15	1	1.4493E-03	19	5	2.4562E-04
12	9.0340E 01	1.4378E 01	6.9551E-02	1.8247E-02	1	1	4.2738E-03	18	5	2.8280E-04
13	9.6897E 01	1.5422E 01	6.4844E-02	2.9455E-02	1	1	1.5265E-03	18	5	1.0650E-04
14	1.0718E 02	1.7058E 01	5.8622E-02	9.9554E-05	21	1	3.5319E-05	20	5	4.5519E-06
15	1.2195E 02	1.9409E 01	5.1523E-02	1.5122E-05	19	1	4.8092E-06	18	5	2.0252E-06
16	1.2249E 02	1.9495E 01	5.1296E-02	2.1267E-03	21	1	1.2042E-04	18	5	2.5874E-05
17	1.3786E 02	2.1942E 01	4.5576E-02	9.1815E-04	39	1	3.2009E-04	20	5	3.6136E-05
18	1.3802E 02	2.1966E 01	4.5525E-02	1.2545E-03	21	1	8.4088E-04	20	5	1.0350E-04
19	1.5313E 02	2.4371E 01	4.1033E-02	7.9067E-03	21	1	6.9704E-04	24	5	1.5746E-04
20	1.7207E 02	2.7386E 01	3.6515E-02	1.0848E-04	23	1	5.4462E-05	24	5	2.8562E-05

Sheet 14 of 14

GE Nuclear Energy

Engineering Calculation Sheet

NUMBER Shroud Restoring / overturning Moment DATE
SUBJECT CECO SHROUD - H5 BY PBSHAH SHEET 1 OF 2

SHROUD OVERTURNING MOMENT CALCULATIONS

DRESDEN

FOR RECIRC BREAK. $\Delta P = 7 PSI$

FOR MAIN STEAM BREAK $\Delta P = 12 PSI$

AREA $= \pi (101.56)^2 = 32404 \ in^2$

$\therefore$ UPWARD FORCE IS

$= (7)(32404) = 227$ KIPS FOR RSB

$= (12)(32404) = 388.8$ KIPS FOR MSL

EFFECTIVE WT AT H5 = 306.8 KIPS

FOR RECIRC BREAK

NET VERT FORCE $= 306.8 - 227 = 79.8$ KIPS > 75 KIPS

RESTORING MOMENT $= 79.8 \times 101.56 = 8104.5$ in-KIPS

SEISMIC MOMENT $= 84$ in-KIPS.

GE Nuclear Energy — Engineering Calculation Sheet

NUMBER ____ DATE ____

SUBJECT CECO SHROUD - HS   BY PB/JAH   SHEET 2 OF 2

FOR MAIN STEAM BREAK

NET VERT FORCE = 306.8 - 388.8 = -82 KIP.

QUAD CITIES.

FOR RECIRC BREAK ΔP = 8 PSI

FOR MAIN STEAM BREAK ΔP = 20 PSI

UPWARD FORCE IS

= (8)(32404) = 259 KIPS FOR RSB

= (20)(32404) = 648 KIPS FOR MSB

EFFECTIVE VERT DOWNWARD FORCE = 296 KIPS

NET VERT FORCE = 296 - 259 = 37 KIPS - RSB

= 296 - 648 = -352 KIPS - MSB

FOR RECIRC RESTORING MOMENT

= (37)(101.56) = 3757 in-KIPS.

WHICH IS LESS THAN SEISMIC MOMENT OF [illegible] in-KIPS

Subject Acoustic Load | Originator H. Choe | Date
Number | Verifier | Date

Acoustic Load After Gillotine Break (Instantaneous) of Recirc Suction Line

- WhAM code is archived.
- Use the existing information to conservatively estimate the Force & Center of Force on the core shroud assembly above H5.
- Existing information
  - Total Integrated Force
  - Area to be applied
  - Circumferential pressure ($-\Delta p$) variation

Assumptions

1. Make least amount of circumferential propagation of decompression wave, and make, as much as possible, axial propagation. This makes

Subject	Originator	Date
Number	Verifier	Date

more pressure loads applied above H5 and also make the center of force as high as possible. Both of this assumption are conservative.

2. Use the Dresden USAR 3.9 load as a basis (Fig. 3.9-6)

3. Also use Grand Gulf RIPD information (383HA881) and BWR/6-238 (383HA880)

This info was only used as "INFO ONLY"

383HA881 - Fig. 6, § 8.2.3.1, 8.2.4.1

383HA880 - Fig. 7
§ 8.2.3.1, 8.2.4.1
Appendix A.

4. Also use Geometry Given in GE Drawing, 104R861.

Subject	Originator	Date
Number	Verifier	Date

Recirculation line

- cross sectional area, $\frac{\pi}{4}\left(\frac{25.154}{12}\right)^2 = 3.45 ft^2$
  $= 497 in^2$
  OD = 28.0
  ID = 25.154"

From UFSAR,

- Steady Force of 20,000 LBs @ Suction line, or toward the broken suction line
- Gran Gulf shows 25,000 LBs
- This force is below the H5 elevation

Elevations

- Recirc Line ℄ = $161\frac{1}{2}$
- H5 weld interface = $191\frac{1}{8}$
- JP Base plate (Top surface) ≅ $120\frac{1}{2}$
- H3 weld ~~interfaceline~~ = 355
- H6 weld interface ≅ $187\frac{1}{8}$
- L3 water level ≅ 512" + 10"
  Narrow range tap
- Top of shroud head ~ 446"

Subject | Originator | Date
Number | Verifier | Date

Now geometry shows that the decompression wave would be greatly reduced above top of shroud head because of the large area. Therefore one conservative way of ~~to~~ distributing the decompression wave is as follows:

constant Δp over the area

H = top of shroud head to JP base plate

W = area that fit the BWR-6/238 maximum area

$\therefore H = 406 - 120 = 286''$

$A = 27{,}000 \text{ in}^2$

$\rightarrow W = 94.4''$

This width is quite consistant with Appendix A, Fig A-1 of 383HA880 at 2.73 msec.

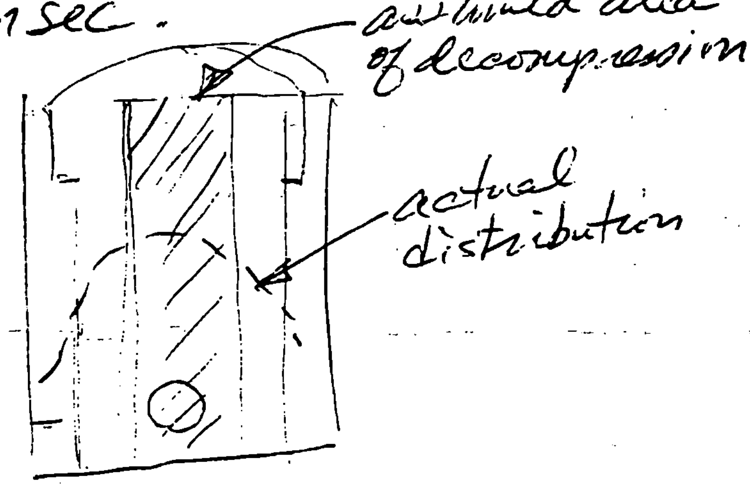

Subject | Originator | Date

Number | Verifier | Date

With this evaluation, the following conclusions are made:

1. The force applied to H5 weld and the shroud assembly above H5 weld is <75% of the Force calculated for the entire shroud. (*)

   A. If the load in UFSA of Dresden is used

   $$F = .75 * 233 \text{ Kips} = 175 \text{ Kips}$$

   B. If BWR-6/238 load is use (much smaller period)

   $$F = .75 * 645 \text{ Kips} = 484 \text{ Kips}$$

2. The center of the force is at $H = \frac{406+191}{2} = 298.5$

   This is lower than the center of mass because center of the mass would consider steam separators above the shroud head

moment arm

$$\boxed{\begin{aligned} l &= 298.5 - 191\tfrac{1}{8}\,(H5) \\ &= 107.375'' \end{aligned}}$$

(*) 75% was calculated by

$$\frac{406-191}{406-120} \cong .75 = \frac{\text{Distance (H5, Top)}}{\text{Distance (Base, Top)}}$$

Subject The motion due to | Originator H. Choe | Date
Number Acoustic Load | Verifier | Date

The following assumptions are made for this calculation

(1) The shroud assembly above H5 is considered as Rigid Body. In reality, some of the acoustic load would be used to deform the assembly and some to move the entire assembly. Therefore, this assumption is conservative (give bigger motion or displacement).

Also due to the irregular surface of the crack, a simple lateral motion is not likely. The irregular crack surface works like a mechanical bind and provides sufficient resisting force. The irregular surface exists both in radial and circumferential direction. Therefore most likely motion of the shroud is rotational (tipping) motion pivoted on one side of H5 weld.

Even for the rotational motion, there

Subject	Originator	Date
Number	Verifier	Date

would be substantial resisting force, but it has been assumed that rotational motion would not have any mechanical resisting force. (This is conservative)

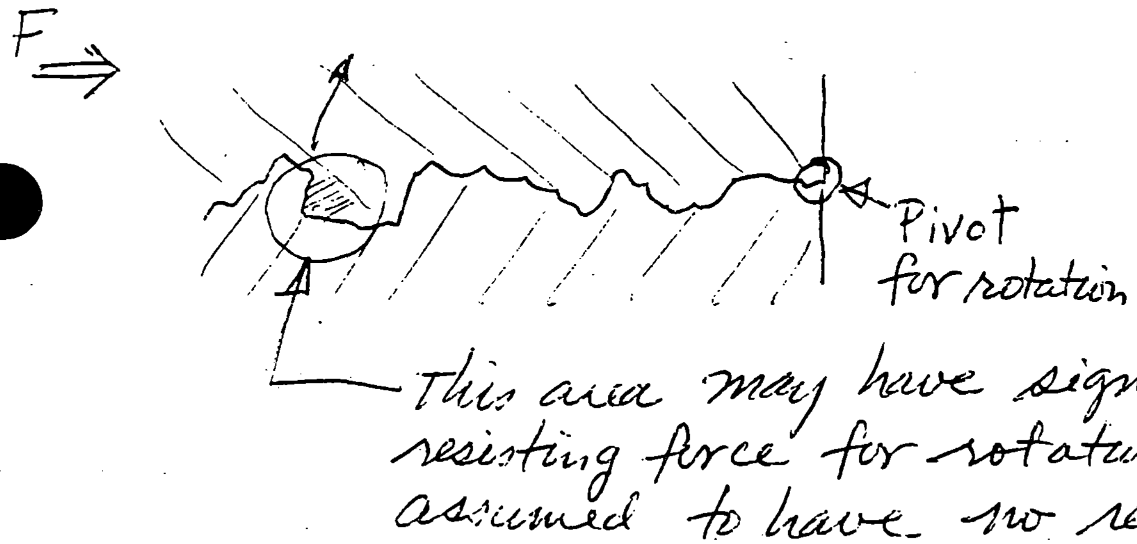

Equation of Motion for rotation can be written as

$$I \frac{d^2\theta}{dt^2} = g_c F(t) \cdot l - g_c M_r$$

where $I = M(R^2 + k^2)$

Mass

Distance Between Center of Mass and Pivot Point of Rotation

Radius of gyration

$F(t)$ = lateral force

Subject | Originator | Date

Number | Verifier | Date

l = moment arm for $F(t)$

M_r = restoring moment due to weight.

$M_r = F_N \cdot R_1$ { Larger than 75 Kips Force for Dresden
37 Kips Force for Quad Cities.

Both Plants have Radius $= 101.56$ inches
(R_1)

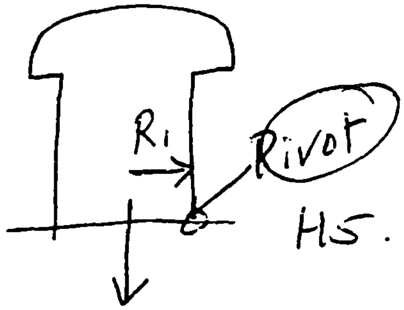

Net Force = { Weight
− $\Delta P \cdot A$
− Seismic Acceleration }

F_N = Net Force = 75 Kips
37 Kips

To maximize θ (tipping), "I" is minimized
Conservatively let $k=0$, R is calculated
as

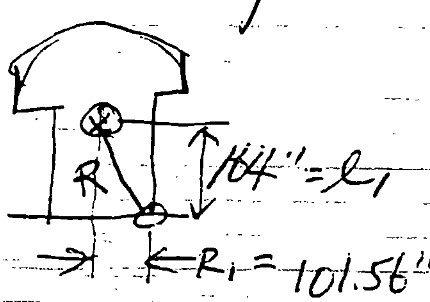

$$R = \sqrt{R_1^2 + l_1^2}$$
$$= \sqrt{(164)^2 + (101.56)^2}$$
$$= 193 \text{ inches}$$

Subject	Originator	Date
Number	Verifier	Date

$g_c = 386$ in/sec

$$\frac{d^2\theta}{dt^2} \leq \frac{g_c F(t) \cdot l}{M R^2} - \frac{g_c M r}{M R^2}$$

$$= 1.1088 \frac{F(t)}{M} - \frac{g_c F_N R_1}{M R^2}$$

$$= 1.1088 \frac{F(t)}{M} - 1.052 \frac{F_N}{M}$$

$$= 1.1088 \left(\frac{F(t) - 0.949 F_N}{M}\right)$$

@ $t=0$, $\theta = 0$, $\dot{\theta} = 0$

$$\therefore \theta = 1.1088 \int_0^t \int_0^t \left(\frac{F(t) - 0.949 F_N}{M}\right) (dt)^2$$

For Dresden $M = 413$ Kips
$F_N = 75$ Kips

$$\frac{0.949 \times 75}{413} = 0.1722$$

For Quad Cities $M = 413$ Kips
$F_N = 37$ Kips

$$\frac{0.949 \times 37}{413} = 0.0850$$

Subject	Originator	Date
Number	Verifier	Date

The integral for θ was done using QC/D impulse load as well as BWR 6/238 impulse load. Even though BWR 6/238 has much higher peak load, the rotational motion is much less due to the short duration, ~ 1.5 millisec, compared to ~ 5 millisec for QC/D.

$$D : \theta_{max} = 16.1 \times 10^{-6}$$

$$QC : \theta_{max} = 118.7 \times 10^{-6}$$

$$X_r = L * \theta = 164 * \theta_{max}$$

$$= 2.64 \times 10^{-3} \text{ in for Dresden}$$

$$= 19.5 \times 10^{-3} \text{ in for Quad Cities}$$

This calculation shows that the acoustic load does not make a large displacement because of the short duration in spite of the large magnitude of the maximum impulse force.

D2 TIPPING MOTION

Dresden UFSAR Data				
t (m sec)	F (kips)	a	v * E +3	theta * E +6
12.8	105	0.02048837	0	0
13.7	179	0.16949176	0.08549106	0.03847098
14.3	209	0.22989854	0.20530815	0.12571074
14.8	225	0.26211549	0.32831165	0.25911569
15.2	231	0.27419684	0.43557412	0.41189284
16.1	233	0.27822396	0.68416348	0.91577476
16.7	231	0.27419684	0.84988972	1.37599072
17	221	0.25406125	0.92912844	1.64284345
17.6	196	0.20372227	1.06646349	2.24152103
17.8	164	0.13928837	1.10076456	2.45824383
18.5	135	0.08089515	1.17782879	3.2557515
19.6	105	0.02048837	1.23358972	4.58203168
21.7	72	-0.04595909	1.20684547	7.14448863
24.4	57	-0.07616248	1.04198135	10.1804048
28.9	46	-0.09831163	0.6494146	13.9860457
35	43	-0.10435231	0.03128958	16.0621935
	a = 1.1088*(0.75*F/M-0.1722)			M = 413 kips
BWR-6/238 Data				
t (m sec)	F (kips)	a	v *E +3	theta *E+6
1.5	105	0.02048837	0	0
1.6	170	0.15136972	0.0085929	0.00042965
1.7	240	0.29231888	0.03077733	0.00239816
1.8	280	0.37286125	0.06403634	0.00713884
1.9	310	0.43326803	0.10434281	0.0155578
2	320	0.45340362	0.14867639	0.02820876
2.1	330	0.47353922	0.19502353	0.04539375
2.2	360	0.533946	0.24539779	0.06741482
2.3	390	0.59435278	0.30181273	0.09477535
2.4	440	0.69503074	0.3662819	0.12818008
2.5	530	0.87625108	0.444846	0.16873647
2.6	620	1.05747142	0.54153212	0.21805538
2.7	650	1.1178782	0.6502996	0.27764696
2.8	570	0.95679345	0.75403318	0.3478636
2.9	450	0.71516633	0.83763117	0.42744682
3	290	0.39299684	0.89303933	0.51398035
3.1	180	0.17150532	0.92126444	0.60469554
3.2	110	0.03055617	0.93136752	0.69732713

Quad Cities UFSAR Data				
t (m sec)	F (kips)	a	v * E +3	theta * E +6
12.65	60	0.02656556	0	0
12.8	105	0.11717573	0.0107806	0.00080854
13.7	179	0.26617912	0.18329028	0.08814044
14.3	209	0.3265859	0.36111978	0.25146346
14.8	225	0.35880285	0.53246697	0.47486014
15.2	231	0.3708842	0.67840438	0.71703441
16.1	233	0.37491132	1.01401237	1.47862195
16.7	231	0.3708842	1.23775102	2.15415097
17	221	0.35074861	1.34599595	2.54171301
17.6	196	0.30040963	1.54134342	3.40791482
17.8	164	0.23597573	1.59498195	3.72154736
18.5	135	0.17758251	1.73972734	4.88869561
19.6	105	0.11717573	1.90184437	6.89156005
21.7	72	0.05072827	2.07814357	11.0705474
24.4	57	0.02052488	2.17433532	16.8113939
28.9	46	-0.00162427	2.21686169	26.6915872
40	41	-0.01169207	2.14295601	50.8885754
50	34	-0.02578698	1.95556076	71.3811593
60	28	-0.03786834	1.63728415	89.3453838
70	24	-0.04592258	1.21832957	103.623452
80	21.6	-0.05075512	0.7349411	113.389806
90	20.8	-0.05236597	0.21933567	118.16119
100	20	-0.05397681	-0.31237822	117.695977
	a = 1.1088*(0.75*F/M-0.085)			M = 413 kips

8 88

BWR-6/238 Data		QC Case using BWR-6/238 data		
t (m sec)	F (kips)	a	v *E +3	theta *E+6
1.4	40	-0.01370563	0	0
1.5	105	0.11717573	0.00517351	0.00025868
1.6	170	0.24805708	0.02343515	0.00168911
1.7	240	0.38900624	0.05528831	0.00562528
1.8	280	0.46954861	0.09821605	0.0133005
1.9	310	0.52995539	0.14819125	0.02562086
2	320	0.55009098	0.20219357	0.04314011
2.1	330	0.57022658	0.25820945	0.06616026
2.2	360	0.63063336	0.31825245	0.09498335
2.3	390	0.69104014	0.38433612	0.13011278
2.4	440	0.7917181	0.45847403	0.17225329
2.5	530	0.97293844	0.54670686	0.22251233
2.6	620	1.15415878	0.65306172	0.28250076
2.7	650	1.21456556	0.77149794	0.35372875
2.8	570	1.05348081	0.88490026	0.43654865
2.9	450	0.81185369	0.97816698	0.52970202
3	290	0.4896842	1.04324388	0.63077256
3.1	180	0.26819268	1.08113772	0.73699164
3.2	110	0.12724353	1.10090953	0.846094
3.3	60	0.02656556	1.10859999	0.95656948
3.4	40	-0.01370563	1.10924298	1.06746163
10	35	-0.02377342	0.98556212	7.98031845
20	30	-0.03384122	0.69748889	16.3955735
30	25	-0.04390902	0.30873771	21.4267065
40	22	-0.04994969	-0.16055585	22.1676158
50	21	-0.05196325	-0.6701206	18.0142336
60	20	-0.05397681	-1.19982094	8.66452591

Attachemnt ME-1-4 Quad Cities Seismic Model

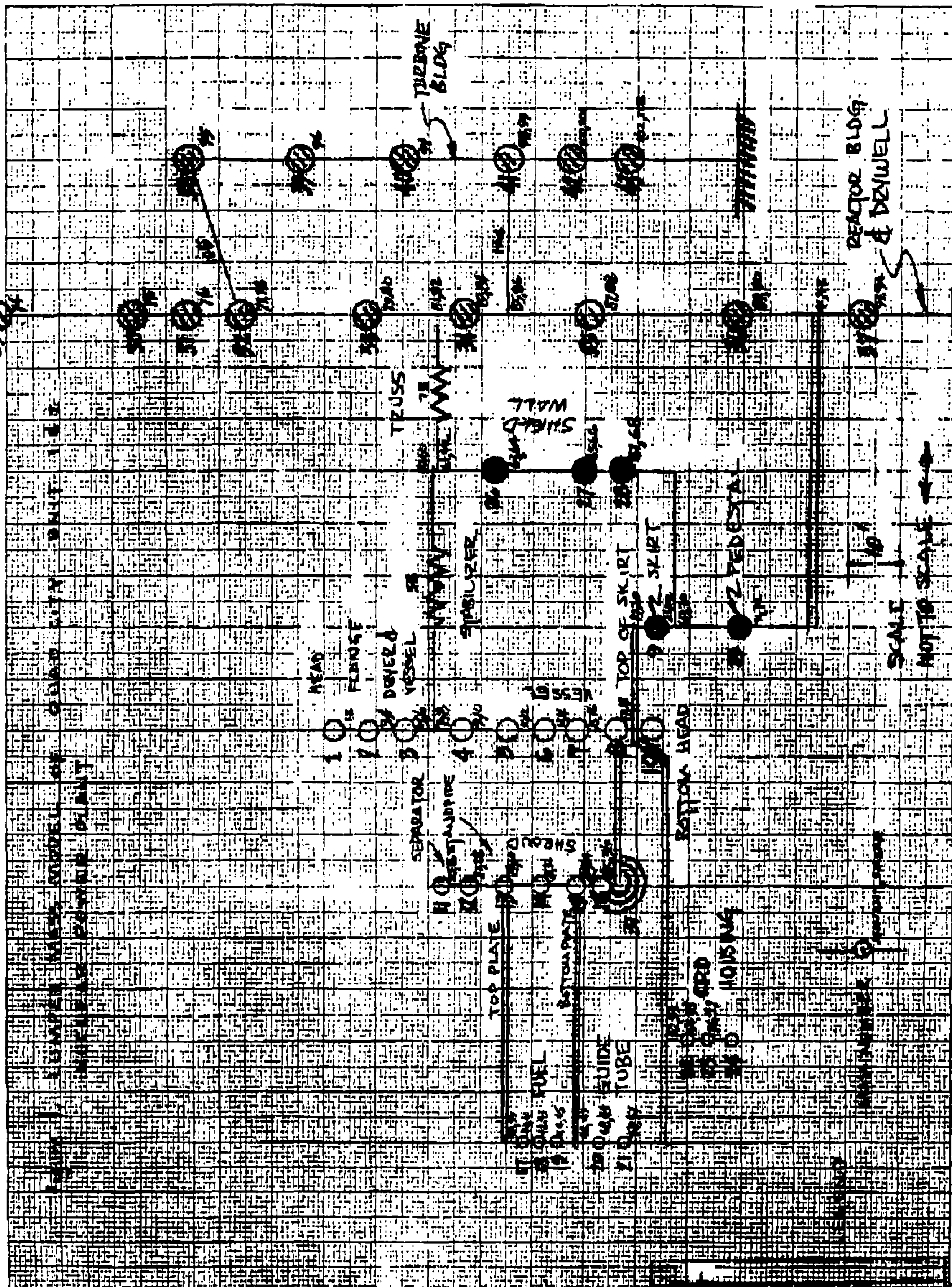

JAN 30 1970

257 HA 925

CONT ON SHEET 6 SH NO. 5

GE-NE-A00-05652-03, REV 1
DRF A00-05652 (15)
JUNE 1994

Attachment ME-1-5

Preliminary Safety Assessment of Core Shroud Indications for Cycle 14 Operation of Dresden Unit 2

Prepared by: H. Choe, Principle Engineer

Verified by: E. C. Eckert, Principle Engineer

Approved by: A. N. Baker, Project Manager

GE-NE Technical Services

IMPORTANT NOTICE REGARDING
CONTENTS OF THIS REPORT

TABLE OF CONTENTS

1.0 Introduction

Circumferential crack indications have been observed in the Dresden 3 core shroud assembly during the current refueling outage. The visual inspections performed have indicated that crack indications are found near the H3, H4, and H5 welds. The most severe indications are in the core support ring joined to the core shroud near the H5 weld and appear to be 360° circumferential cracking (Reference 1). Initial ultrasonic (UT) inspections performed near H5 weld has confirmed these indications. Reference 2 indicates that the UT inspections were done at six locations of the H5 area, using manually manipulated 60° and 70° probes. Reference 2 inspection is preliminary in nature in this sense. The concern addressed in this assessment is for potentially similar crack indications in the Dresden 2 core shroud because the design of the Dresden 2 reactor internals is identical to that of the Dresden 3 reactor internals. In that there is not adequate inspection data available pertaining to the condition of the welds in the shroud of Dresden 2, an engineering evaluation is sought by the Commonwealth Edison Company (CECo) to justify operation of Dresden 2 until planned shroud inspection will be done during the next refueling outage.

Preliminary safety assessment for the Dresden 2 core shroud in this report provides the engineering rationale for continued plant operation for the remainder of the current Dresden 2 fuel cycle. This preliminary safety assessment should be revised when the Dresden 2 core shroud is inspected during the next planned outage, and an updated safety assessment should be provided. The update of this report is not included in this contract.

This report uses the following approach. The Dresden 2 core shroud structural integrity is demonstrated with the assumption that crack indications are essentially identical at Dresden 2 and Dresden 3. The technical bases for this assumption and the differences at Dresden 2 are provided by comparing the plant water chemistry and operating histories between Dresden 2 and Dresden 3. This report also qualitatively addresses the potential situation during normal operation, anticipated operational events, and design basis accidents, if unexpected significant crack growth occurs during plant operation. This assessment describes the symptoms and consequences expected if the shroud has degraded to the point that through-wall cracking has occurred in the core support ring in the H5 weld area, which was the most extensively cracked area on the Dresden 3 shroud. A qualitative assessment is provided for other welds on the core shroud.

GE Rapid Information Communication Services Information Letter (RICSIL) 068 has been issued (Reference 3) to assist CECo and other utilities in the on-going evaluation of this situation. Previous communications about core shroud crack indications have included GE SIL 572 (Reference 4) and the US-NRC Information Notice 93-79.

2.0 Summary and Conclusions

The core shroud/core support ring cracking associated with the H5 weld at Dresden Unit 2, postulated to be similar to that observed at Dresden Unit 3, which was the most extensively cracked weld area in Dresden 3, does not represent a threat to the safe operation of Unit 2 for the remainder of the present cycle:

1. The combination of high ductility, high toughness and low stresses makes the shroud extremely flaw tolerant. Even for this situation with the indications of 360 degree circumferential cracking, crack depths of up to an average of 90% (2.7 inches) of the available material can be tolerated while maintaining the structural integrity for normal operation and postulated design basis accident conditions, including ASME Code safety factors. The available material considers the extra one inch of ligament provided by the weldment in addition to the two inch shroud wall thickness.

2. The maximum crack depth observed by ultrasonic examinations in Dresden 3 is approximately 1.55 inches, and is within the allowable crack depth of 2.7 inches. The plant water chemistry history indicates that Dresden 2 should be significantly better than Dresden 3. Even if the postulated cracking in Dresden 2 is equal to that in Dresden 3, Dresden 2 core shroud maintains the structural integrity for normal operation and postulated design basis accident conditions including the seismic load.

3. The realistic crack growth rate associated with the H5 weld area of the Dresden 2 core shroud was calculated by PLEDGE model, and is approximately 1/30 of that of the Dresden 3 core shroud because of hydrogen water chemistry implemented in Dresden 2, and is approximately 0.003 inch per year. With the realistic crack growth rate, the allowable crack depth is calculated not to be exceeded within one year if the maximum crack depth is 1.55 inches. Even using the bounding crack growth rate of 5 E-5 inch/hr (0.44 inch per year) for the BWR plant with normal water chemistry, it appears that the allowable crack depth is not expected to be exceeded within one year based on the assumptions made and the information provided by CECo. No BWR inspection to date has found through-wall cracking.

4. If the shroud assembly is postulated to have 360° through-wall crack, it would not lift because the weight of the core shroud above H5 is sufficient to hold the shroud in place. The leakage flow is small, is not detectable because the leakage flow temperature near H5 weld is almost the same as the downcomer annulus temperature, and does not impact plant operations.

5. In the unlikely occurrence of a design basis accident, safe reactor shutdown will be achieved, and no change in emergency core cooling function is anticipated, even with concurrent design basis earthquake.

3.0 Shroud and Top Guide Functions

The shroud support, shroud, core support, and top guide make up a stainless steel cylindrical assembly that provides lateral support for the core, vertical support for peripheral fuel bundles, and a partition between the core region and the downcomer annulus to separate the upward flow of coolant through the core from the downward recirculation flow. The shroud also provides (in conjunction with other components) a floodable region following a postulated recirculation line break. The shroud is not a primary pressure boundary component.

The top guide consists of a circular grid plate having square openings, lateral support and guidance for fuel assemblies. The majority of the fuel rests on fuel support castings that are supported by the control rod guide tubes. The fuel support castings are aligned by holes in the core support plate. The core support plate rests on the core support ring, which is welded to the shroud at the circumferential locations identified as H5 and H6.

4.0 Shroud Structural Evaluation

While the extent of the cracking that has been reported at Dresden 3 and assumed for Dresden 2 is not insignificant, there remains sufficient structural strength in the shroud to meet all of its design functions (Reference 5). This amount of cracking is considered to be a conservative estimate of the conditions at Dresden 2 as discussed in Section 5. The shroud is made of ductile material with high toughness properties even after accounting for any effects due to neutron fluence. The applied loading on the shroud is mainly from the differential pressure during normal operation, the transient differential pressure increase due to design basis accident loading, and design basis seismic loads. These loads are generally small and well within the remaining structural integrity of the shroud.

The applied loads during normal operation, anticipated operational events, and the transient differential pressure loading due to design basis accident are in the downward direction. The applied load is in the upward direction only when the main steam line break accident is assumed to occur simultaneously with a design basis earthquake. Reference 6 documents the design pressure drop loads of 7 psi on the upper part of the core shroud at normal, rated power conditions, and 12 psi during the main steam line break accident.

The combination of high ductility and low applied stresses make the shroud extremely flaw tolerant. It has been calculated that 360° circumferential cracking of greater than 90% of the 3.0 inch available material can be tolerated while maintaining the industry accepted ASME Code allowable safety factors based on limit load method for the H5 area (Reference 5). The available material considers the extra one inch of ligament provided by the weldment in addition to the two inch shroud wall thickness. The deepest observed cracking indication is 1.55 inches or 52% of the 3.0 inch available material at Dresden 3 (Reference 2).

The low stresses and high material ductility under relatively low neutron fluence level make unrealistic the postulation of the separation of the core shroud assembly at H5 weld area during the present cycle. The realistic crack growth rate under the Dresden 2 reactor water chemistry condition is very low, 0.003 inch per year, and discussed in the next section. With the realistic crack growth rate, the allowable crack depth is calculated not to be exceeded within one year if the maximum crack depth is 1.55 inches. Even using the upper bound crack growth rate of 5 E-5 inch/hr (0.44 inch per year) for the BWR plant with normal water chemistry, it appears that the allowable crack depth is not expected to be exceeded within one year based on the assumptions made and the information provided by CECo (References 1 and 2).

5.0 Comparison of Water Chemistry, Operating Histories, and Crack Growth Rates Between Dresden 2 and Dresden 3

5.1 Background

It is well documented that the BWR oxidizing environment is more than sufficient to provide the electrochemical driving force for intergranular stress corrosion cracking (IGSCC) of BWR structural materials. In BWR piping, a 200 ppb concentration of dissolved oxygen generates an electrochemical potential (ECP) for austenitic stainless steel of approximately +100 mV (SHE). The more oxidizing core of the BWR is characterized by a maximum measured austenitic stainless steel ECP of approximately +250 mV (SHE). Also, the conductivity of the BWR coolant is sufficiently high to allow this corrosion reaction to occur (References 3, 7, 8).

Over a decade of laboratory and in-reactor investigations have revealed that lowering the ECP of sensitized stainless steel to less than -230 mV(SHE) by injecting hydrogen gas into the BWR feedwater and reducing coolant conductivity to less than 0.3 µS/cm by better BWR water chemistry operational practices would mitigate IGSCC of BWR piping (Reference 7). For irradiation assisted stress corrosion cracking (IASCC) of non-thermally sensitized stainless steel, the threshold ECP is approximately -140 mV(SHE) (Reference 8). However, IASCC is not expected to be a significant factor in the area near H5. This process, hydrogen water chemistry (HWC), reduces the "corrosiveness" of the entire BWR coolant. The results of extensive testing have clearly demonstrated that HWC mitigates environmental cracking in numerous BWR structural materials and has no insuperable deleterious effect on materials (Reference 7).

Dresden-2 was the first domestic BWR to operate on HWC and has continuously operated on HWC since the middle of 1983. Dresden-3 is a non-HWC BWR. The level of hydrogen injected into Dresden-2 has ranged from 1.0 to 1.5 ppm (cycles 9 to 14) at approximately 90% availability. While this amount is not sufficiently high to completely protect reactor internals from IGSCC or IASCC, it still significantly retards crack propagation. Therefore, Dresden 2 should have a lower susceptibility to IGSCC than Dresden 3 and the crack growth rates for the existing defects should be also lower.

5.2 Crack Growth Rate

Figure 1 presents a schematic estimation of Dresden-2 and Dresden-3 crack growth rates as a function of conductivity using PLEDGE prediction model (Reference 9). This estimate considers the difference in ECP between Dresden 2 and Dresden 3. Crack growth rates based on actual conductivity averages for the first five cycles are compared to those based on the average conductivity for the last five cycles. The last five cycle average for conductivity has been less than 0.1 µS/cm, and the last five cycle average prediction is made at the conductivity value of 0.1 µS/cm, which is also the model limit. As noted in Figure 1, a reduction in crack growth rate by a factor of approximately 32 is obtained for the Dresden 2 H5 weld area because of the decrease in ECP.

The ECP of the H-5 stainless steel shroud location at Dresden-2 is estimated to be approximately -100 mV(SHE) based on ECP measurements at Quad Cities-2 (Reference 10), while at the non-HWC Dresden-3 the stainless steel at the same location is estimated to be characterized by an ECP of approximately +150 mV(SHE) (Reference 10).While the beneficial effect of HWC on crack growth rates at other weld locations can not be as well quantified, the process will have the effect of lowering crack growth rate compared to that achieved with normal water chemistry. Degrees of weld sensitization of 15 C/cm2 (no effects of irradiation) and a stress intensity of 20 ksi√in (no effects of irradiation relaxation) for H-5 are assumed to represent residual stress. This estimated

250 mV difference in stainless steel ECP is the main factor which reduces the crack growth rate (1.24E-5 vs. 3.92E-7 in/h [108 vs 3 mpy]).

It is clear that an increase in sulfate/conductivity results in an acceleration in crack initiation as measured by the constant extension rate test (CERT). The examination of Figure 1 shows that lower conductivity at Dresden 2 during the first 5 cycles (0.3 μS/cm) reduced the predicted crack growth rate by a factor of approximately 1.6 compared to Dresden 3 (0.4 μS/cm) at the same ECP of +150 mV(SHE). This high conductivity crack initiation and propagation acceleration factor is consistent with the relatively high incidence of IGSCC in creviced Alloy 600 shroud head bolts and Alloy X750 jet pump beam bolts at Dresden 3.

BWR water chemistry transients are reviewed with only limited data obtained after 1983. This reveals that although Dresden 2 has more documented transients than Dresden 3 all of the Dresden 2 transients are relatively minor and are not expected to alter the relative difference between Dresden 2 and Dresden 3 in this evaluation.

PLEDGE Model Prediction for Dresden 2/3 Sensitized Type 304 Crack Growth Rate

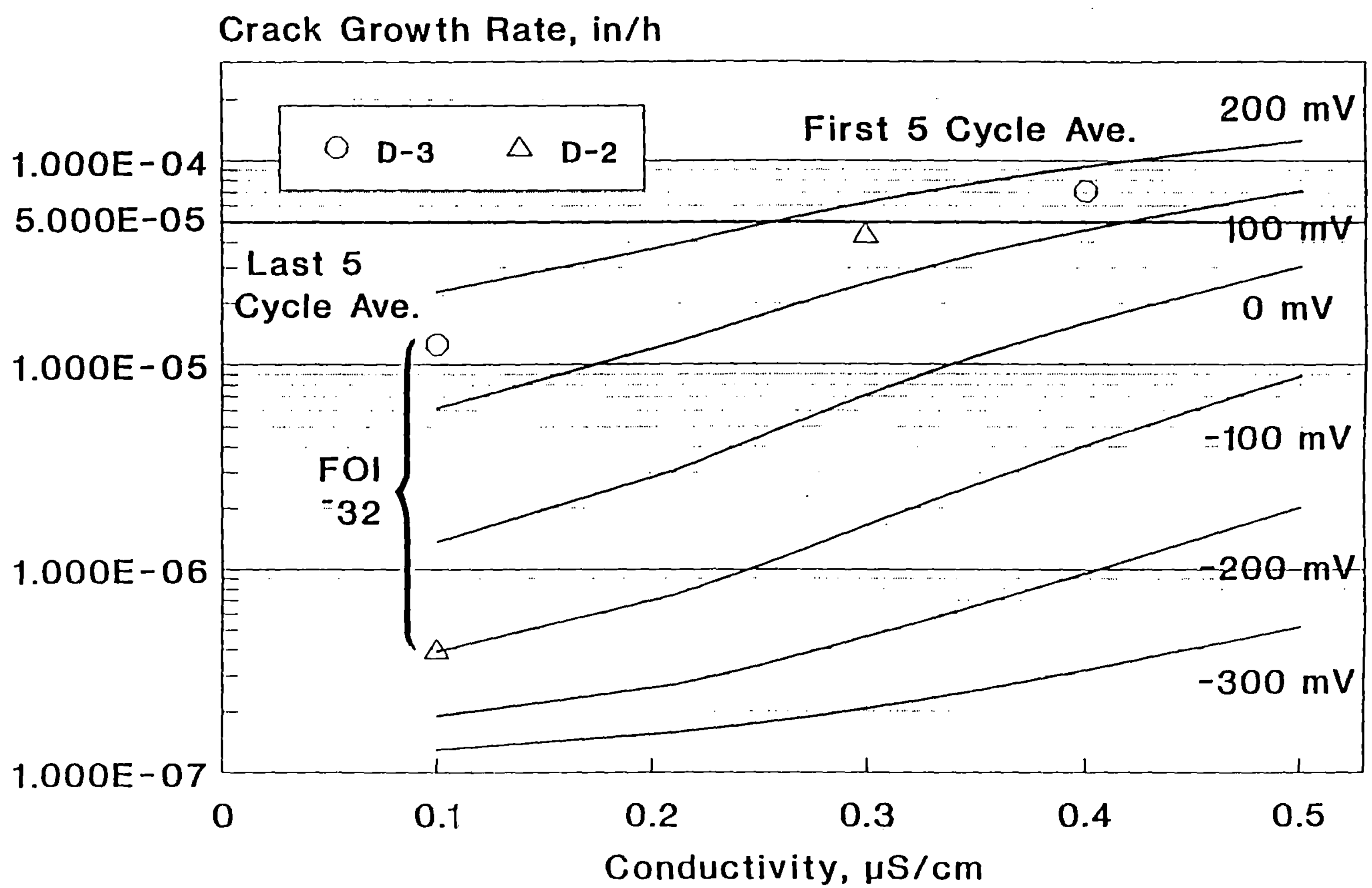

PLEDGE: 15 C/cm2, 20ksi√in

D23GR20C

Figure 1

PLEDGE MODEL Prediction Of Crack Growth Rate With Sensitized Type 304 Stainless Steel at H5 Weld Location for Dresden 2 and 3

GE-NE-A00-05652-03

6.0 Normal Operation

As discussed in the preceding sections, the postulation of significant through-wall cracking, leakage, or separation of the core shroud assembly at H5 weld area is extremely improbable. The more likely but still improbable scenario would be for some bypass flow to occur from the core bypass region to the reactor downcomer annulus.

Even if the postulated cracking or separation were to occur, the weight of the core shroud above H5 weld is sufficiently high to hold the core shroud assembly in place during all normal operating conditions. The postulated leakage would occur through a gap much less than 0.001 to 0.002 inch. The estimated leakage flow is less than 30 gpm, assuming that a 0.002 inch gap exists around the entire circumference at 7 psid differential pressure. Leakage flow of this magnitude has no consequence upon the plant operation. It also would not be detectable by the plant operator because the leakage flow is small and the leakage temperature at this location is the same as the downcomer temperature.

7.0 Anticipated Operational Events Related to Increased Shroud Head Pressure Loads

The previous sections demonstrate that cracks that grow through the shroud wall or cause complete separation of the shroud assembly at H5 area from the lower shroud are improbable. This section discusses anticipated operational occurrences that could increase shroud loads above those experienced during normal operation: pressure regulator failure - open, recirculation flow control failure - increasing to maximum flow, and inadvertent actuation of the Automatic Depressurization System. The normal operating pressure drop across the upper shroud is 7 psid (Reference 6).

7.1 Pressure Regulator Failure - Open

This postulated Safety Analysis Report (SAR) event involves a failure in the pressure controls such that the turbine control valves and the turbine bypass valves are opened as far as the Maximum Combined Flow Limiter (MCFL) allows. For the Dresden units, with a bypass capacity of 40% of rated steam flow, the worst case involves inadvertently increasing the steam flow to about 150% of rated. This would not happen because the steam flow limit is set at 105%. A depressurization and cooldown occurs which is isolated by Main Steamline Isolation Valve (MSIV) closure. This steam flow increase is small enough that the increased force on the shroud head (approximately 50% above the normal pressure drop) is less than the pressure differential of 12 psid due to the main steam line break (Reference 6). The weight of the core shroud above H5 weld is sufficiently high to hold the core shroud assembly in place at 12 psid load. Any leakage postulated may occur through a gap much less than 0.001 to 0.002 inch. The postulated leakage flow is approximately less than 40 gpm, with the assumption that a 0.002 inch gap exists around the entire circumference at 12 psid pressure differential. The leakage flow of this magnitude has no consequence for the plant operation.

7.2 Recirculation Flow Control Failure

This postulated event involves a recirculation control failure that causes both recirculation loops to increase to maximum flow. In this type of case, the pressure drop could change from a part-load condition to the high/maximum flow condition over a time period of several seconds, but it should not significantly exceed the pressure drop expected for normal full power, high core flow operating conditions (7 psid). Normal operating procedures are considered sufficient to minimize the consequences of this potential transient, and the force on the shroud head is within the inspected shroud capability (12 psid in Section 7.1).

7.3 Inadvertent Actuation of ADS

Inadvertent actuation of the Automatic Depressurization System (ADS) valves is another postulated event that could put an increased load on the upper shroud. The maximum steam flow and the depressurization rate are significantly smaller than for the postulated main steamline break, causing a short-term increase in steam flow of approximately 30% of rated steam flow. The increase in the shroud ΔP resulting from the opening of the ADS valves would occur over a period of about one second, spreading the effect of the change in load.

Inadvertent ADS is also a very low probability event; it is considered to be in the ASME Emergency category in the vessel thermal duty design. It has been used as the design basis Emergency event for the Dresden shroud. The effect of this event is bounded by Section 7.1.

8.0 Design Basis Accidents

Although the previous sections demonstrate that the probability of the postulated separation of the core shroud assembly at H5 weld area is extremely low, an accident occurring with a separated core shroud is addressed in this section.

The Main Steamline Break Accident imposes the largest potential lifting loads on the shroud head. Liquid breaks (e.g., recirculation line breaks) do not impose large pressure drops on the shroud head, and, in fact, the shroud pressure drop decreases from its initial value.

8.1 Main Steamline Break

The main steamline break inside primary containment is the postulated worst case because it results in the largest depressurization rate. During this SAR event, the reactor is rapidly depressurized as a result of a postulated instantaneous, double-ended break of the largest steamline. Thus a larger than normal pressure difference could develop across the shroud as fluid flow is drawn from the core region toward the break. For Dresden 2, the design basis pressure difference is 12 psid for the guillotine break of a main steam line (Reference 6).

The weight of the core shroud above H5 weld is sufficiently high to hold the core shroud assembly in place during the main steam line break, and the core shroud does not lift (Reference 5). The leakage may occur through a gap much less than 0.001 to 0.002 inch. The postulated leakage flow is approximately less than 40 gpm, with the assumption that a 0.002 inch gap exists around the entire circumference at 12 psid pressure differential. The leakage flow of this magnitude has no consequence for the emergency core cooling performance.

If the main steam line break occurs simultaneously with the design basis earthquake, and 360° complete through-wall crack is postulated, this added load might cause separation of the upper shroud assembly near the H5 indications, leading to an upward displacement of this structure and the associated top guide. The amount of lifting and the potential effect of these postulated occurrences on emergency operation are described below.

One of the key considerations of this postulated accident case is the ability of the control rods to insert before or during the postulated accident. Specifically, sufficient lifting of the top guide prior to control rod insertion could cause reorientation of the fuel bundles and thus impede the insertion of control rods.

The shroud head pressure drop characteristics calculated for the instantaneous, double-ended steamline break accident were evaluated for a typical BWR (Reference 11). The initial shroud head pressure drop loading is a result of the decompression wave which reduces system pressure overall, but would increase differential pressure across the shroud in the short term.

The pressure loading increase is short-lived (less than two seconds) and decreases to below normal steady state loads. Even if the remaining shroud ligament is small (see Section 4), the structural integrity of the shroud will remain intact for this postulated limiting event. If it is even further postulated that the initial load pulse causes the shroud to separate, the last part of the pressure loading could cause the shroud assembly to lift. The flow path created by any separation reduces the upward lifting forces. For this postulated scenario the core shroud assembly would not lift with the main stem line break alone, but would lift less than 2 inches if the main steam line break occurs simultaneously with the design basis earthquake.

Scram is initiated during the main steamline break (inside containment) accident by the high drywell pressure trip signal. Drywell pressure exceeds the setpoint almost instantaneously, so the only delays in the rod insertion come from the sensors, the Reactor Protection System, and rod motion. For the main steamline break outside containment, shroud loads are reduced, MSIV closure is initiated by high steam flow, and scram is initiated from the MSIV closure.

For either postulated steamline break scenario, the insertion of all control rods will occur within the required time. With the main steam line break alone, the core shroud assembly would not lift or move laterally, and no degradation of scram performance is expected. If the main steam line break occurs simultaneously with the design basis earthquake, the shroud assembly would lift less than 2 inches, and the lateral movement is limited to 2 inches by the clearance between the core shroud inner wall and the core support (Reference 12). Normal CRD alignment from the bottom end of the fuel bundles to CRD flange will be maintained and no binding within the CRD mechanisms is anticipated during a scram. However, during the design basis earthquake, the shroud assembly, if separated at H5, could shift laterally up to 2 inches. With the random displacement anticipated during seismic events, the CRD alignment in the core region would undergo intermittent periods of misalignment. Hence, the CRD scram speed would assume an oscillatory velocity profile, such as typically expected under seismic events. Minimal scram performance degradation is expected. Even under the worst condition, the control rods fully insert, and reactor shutdown would thus be achieved.

Movement of the upper shroud assembly (in the very unlikely case that it occurs) could affect the core spray system if it impacts the core spray line connection. The 2 inch lift can be easily accommodated by 1.69 inch vertical clearance in the core spray line brackets and the compliance in the core spray line itself (Reference 13). The coolant flow to the two core spray spargers is ensured. Therefore, no change is predicted in the emergency core cooling function.

The main steamline break has also been evaluated for radiological release consequences in the SAR. For a main steamline break inside of containment, the radiological consequences are bounded by the Loss of Coolant Accident. For the main steamline break outside of containment, the magnitude of the pressure loads that potentially could lead to separation of the upper shroud are less than that for breaks inside the containment, due to attenuation of the depressurization wave along the steamline. MSIV closure is initiated before any potentially increased radiological release outside containment from such a scenario could occur. The radiological consequences of this main steamline break scenario are thus still bounded by the plant SAR results.

8.2 Recirculation Line Break

For the design basis recirculation line break, the differential pressure across the upper shroud decreases from the initial value as the reactor depressurizes, upward forces are reduced, and thus there is no significant threat to core shroud integrity. With the shroud integrity maintained, a floodable core region is also preserved. Even if the entire circumference is postulated to be cracked as done in the previous sections, the shroud assembly does not lift, and the calculated leakage flow is very small compared to the emergency core cooling system flow capacity, and there is no significant decrease in coolant to the core. Therefore, the recirculation line break analysis results are unchanged.

9.0 Emergency Operator Actions

The Emergency Procedure Guidelines (EPGs) are the basis for plant specific Emergency Operating Procedures (EOPs). The EPGs are symptomatic in that they respond to detected symptoms and do not require diagnosis of the event by the operator. They address a very wide range of events, both less severe and more severe than the design basis accidents.

The worst postulated event discussed above could result in separation of the shroud assembly from the lower shroud, which has minimal impact to scram performance. Therefore, no further consideration is necessary for the impact of this postulated event on the EPGs.

The EPGs provide instructions for reactor pressure, water level, and power control, as well as control of key primary containment parameters. Actions specified in the EPGs for reactor power control are to (1) insert control rods using a variety of methods, and (2) initiate the Standby Liquid Control System (SLCS) before pool temperature increases to the allowable value (typically 110 F). EPG instructions are for water level to be controlled below the high water level setpoint; thus there would not be dilution of the liquid boron by flooding to the steamline elevation or loss of vessel inventory out the break in case SLCS injection were to occur.

Water level would be controlled after the postulated event because the break is high in the vessel and a large compliment of water injection systems would be available.

10.0 References

1. Telecons between Dave Rogowski and Dean Legler (CECo) and G. L. Stevens, Hwang Choe, Gene Eckert, and John Nash (GE), April 27 and 28,1994

2. Ultrasonic Examination of Dresden Unit #3 Shroud Weld # H5, CECo inspection report prepared by Brian F. Wilson, April 27, 1994

3. GE Rapid Information Communication Services Information Letter (RICSIL) 068, Update on Core Shroud Cracking, April 8, 1994.

4. GE Services Information Letter (SIL) 572, Revision 1, Core Shroud Cracks, October 4, 1993.

5. Limit Load Analysis on Allowable Crack Depth, Dresden 3 Shroud Circ Flaw at H5, GE Design Record File, DRF-137-0010-7, Report Number GE-NE-523-05-0194. This reference shows also the core shroud cumulative weights, and effective weights for OBE and DBE at various elevations of core shroud.

6. Updated Final Safety Analysis Report, Dresden 2 and Dresden 3, Tables 3.9-19, and 3.9-20, and Figure 3.9-5

7. B. M. Gordon et al, "Hydrogen Water Chemistry for BWRs-Materials Behavior-Final Report," EPRI TR-100304, Palo Alto, CA, February 1992.

8. M. E. Indig et al, "Investigation of the Protection Potential Against IASCC," paper #71 presented at Corrosion 92, NACE, Nashville, April 1992.

9. F. P. Ford et al, "Prediction and Control of Stress Corrosion Cracking in the Sensitized Stainless Steel/Water System," paper 352 presented at Corrosion 85, Boston, MA, NACE, March 1985

10. M. E. Indig, "Quad Cities-2 Hydrogen Ramping Test," February 21, 1994 (Draft)

11. Letter dated November 9,1994, from L. A. England to US NRC, "BWROG Safety Assessment - BWR Shroud Crack Indications"

12. GE drawings, 105E1415C, 706E873, 104R861

13. Calculation of Stress in the Core Spray Riser Pipe Due to a Lift of 1.5" in the Shroud, and Same for 3.0" Lift, GE Design Record File, DRF-137-0010-7, Report Number GE-NE-523-05-0194.

Lateral Loads on the Core Shroud During LOCA Due to Non-symmetric Depressurization In the Downcomer Annulus

This load is due to an instantaneous break of the recirculation suction line. Such a load is unrealistic in the sense that it takes a finite time for the break to occur, at least 100 milliseconds. However, a hypothetical instantaneous break is considered as the source of a bounding load. The asymmetric load is caused by the fact that the sound wave takes finite time to travel from the broken suction line side to the unbroken suction line side of the annulus. The duration of the load is extremely short, about 5 milliseconds, as shown in Figure 3.9-6 of the UFSAR (Reference 6). The accoustic load has a stronger effect on the lower portion of the shroud, including the H5 weld area (near the recirculation line suction nozzle). This load has little effect on the upper shroud areas (e.g., near H2 and H3).

Three areas that the accoustic load could impact are examined: allowable crack length, allowable crack depth, and lateral motion of the shroud assembly during a recirculation line break. Short duration loads of this type do not lead to any significant deformation and are generally not included in the analysis of the allowable flaw sizes. Pressure associated with the main steam line break exceeds that of the recirculation line suction break. Thus even with any effects of the acoustic loads from the recirculation line suction break, the main steam line break still bounds. Therefore, The allowable crack depth is still bounded by the combination of the main stream line break with the design basis earthquake. The lateral motion of the shroud assembly is limited to a very small magnitude due to the short duration of the accoustic load. In conclusion, this load does not affect the evaluations performed for the H5 weld area.

Prepared by: Hwang Choe 5/4/94
H. Choe

Verified by: E. C. Eckert 5/4/94
E. C. Eckert

ENGINEERING ANALYSIS VERIFICATION COVER SHEET

(Reference EOP 42-6.00, Rev. 4, and EOP 25-6.00, Rev. 1)

DRF No./Section: A00-05652-15 sh. 1 of 1

Subject: Preliminary Safety Assessment of Core Shroud Indications for Cycle 14 operation of Dresden Unit 2

1 **VERIFICATION REQUIREMENTS** Designated Verifier E.C. Eckert

1A **APPLICATION.** (System/Project/Program) Dresden 2, remainder of cycle 14.

1B **METHOD OF VERIFICATION.** Checking, Alternate Calc., Indiv. Design Review, Team Design Review, Test (circle as needed); Other (describe)

1C **SCOPE.** Identify what is to be verified (e.g., level of detail).
verify by method specified in 1B that the 1E output have been correctly prepared using 1D inputs, and that the 1E outputs are adequate and reasonable for 1A application.

1D **INPUTS.** Identify any GE and external interfaces and requirements, assumptions, input documents, test, analyses, reasons for changes.
DRF A00-05652-15, Hand calculations & References

1E **OUTPUTS.** Identify output document(s) or analysis results to be verified.
DRF A00-05652-15, Report No. GE-NE-A00-05652-03

1F Responsible Engineer: Hwang Choe Date 5/2/94 Comp. 523

2 **INDEPENDENT VERIFICATION** See attached 4 pages of comments.

2A **VERIFICATION STATEMENT.** The method and scope of verification are appropriate and the same as stated in 1B and 1C. The inputs are appropriate and are the same as identified in 1D. All comments and technical issues are resolved. The verification establishes that the analysis output identified in 1E is correct and is adequate for its intended application as identified in 1A.
Comments incorporated in evaluation. See DRF markup notes

2B Independent Verifier: E C Eckert Date 5/2/94 Comp. 208

3 **APPROVAL OF VERIFICATION**

3A **MANAGER'S APPROVAL.** All design requirements have been identified and all technical issues are adequately resolved. The verification described in the above sections 1 and 2 is sufficient to issue/apply the analysis results.

3B Resp. Manager or Delegate: S Ranganath Date 5/2/94 Comp 523
S. Ranganath

4A Are there attached sheets for 1A, 1B, 1C, 1D, 1E, 2A, 3A (circle as applicable)?

Rev. 0 (7/22/91)

GE Nuclear Energy
Engineering Calculation Sheet

Dresden 2, Core Shroud

Sheet 1 of

Subject	Lift Calc + Leakage	Originator	H. Choe	Date	4/30/99
Number	calc	Verifier	E.C. Eckert	Date	5/1/99

Not Req'd for Assessment Report ECE 5/1/99 ECE 5/1/99

- Calculate how much gap is needed at H5 to leak 100% of Bypass flow (~10% of Total Flow)

$$\dot{m}_{core} = 98 \times 10^6 \text{ LB/hr}$$

$$\dot{m}_{stm} = 8.6 \times 10^6 \text{ LB/hr}$$

$$X_0 = \frac{\dot{m}_{stm}}{\dot{m}_{core}} = 8.78\%$$

(Bypass) $\dot{m}_2 = 0.1 \times \dot{m}_{core} = 9.8 \times 10^6 \text{ LB/hr}$

ECE 5/1/99 Core inlet enthalpy = 522.5 Btu/lb

@ 521.8 @ 528°F
526.8 @ 532°F → @ 528.56°F

$V_f = 0.02114$

$$X_1 = \frac{8.6}{(98-9.8)} = 9.75\%$$

✓ ECE 5/1/99

(Flow to Stm Sep) ECE 5/1/99

$\dot{m}_1 = 98 \times 0.9 \times 10^6$ LB/hr $= 88.2 \times 10^6$ LB/hr

@ 1000 psia

$v_0 = x_0 v_g + (1 - x_0) v_f = v_f + x_0 v_{fg}$

$= 0.02159 + 0.0878 * 0.42436$

$= 0.0588488$

$v_1 = v_f + x_1 v_{fg} = 0.02159 + 0.0975 * 0.42436$

$= 0.062965$

$\Delta P_0 = C_1 v_0 \dot{m}_{core}^2 = 7.0$ psi or 9 psi to 12 psi

$\Delta P = C_1 v_1 m_1^2$

$\therefore \Delta P = \Delta P_0 * \dfrac{v_1 m_1^2}{v_0 \dot{m}_{core}^2}$

$= \underbrace{\Delta P_0}_{7\,psi} * \underbrace{\dfrac{0.062965}{0.0588488} * (0.9)^2}_{0.8666571}$

$= 6.067$ psi

ECE 5/1/99

$\Delta P_o =$ 7 psi 9 psi 12 psi

$\Delta P =$ 6.067 psi 7.80 psi 10.40 psi

EJE 5/1/94

(1) $\Delta P_o = 7$ psi (normal operating condition)

$$\Delta P = \frac{K}{v_2}\frac{V^2}{2g_c} = 6.067 \text{ psi}$$

Typical Gap, $K \simeq 1.0$ to 1.5 use 1.4

$$V = \sqrt{\frac{2 g_c v_2 \Delta P}{K}}, \quad v_2 = v_f @ 528.56°F$$

$$= \sqrt{\frac{2 \times 32.2 \times 0.02114 \times 6.067 \times 144}{1.4}}$$

$$= 29.15 \text{ ft/sec}$$

EJE 5/1/94

$$\cancel{\frac{LB_f}{ft^2}} \; \cancel{\frac{ft^2}{LB_m}} \cancel{\frac{LB_f}{LB}}$$

$$\dot m_2 = \rho_2 A V = \frac{1}{v_2} \pi D t V$$

$$= 9.8 \times 10^6 \text{ LB/hr} = 2722.2 \frac{LB}{sec}$$

EJE 5/1/94

Subject | Originator | Date

Number | Verifier E C Eckert | Date 5/1/94

$D = 203.12'' = 16.927\ ft$

$t = v_2 \cdot m_2 / (\pi D V)$

$= 0.02114 \times 2722.2 / (\pi \times 16.927 \times 29.1$

$= 0.0371252\ ft$

$= 0.4455\ inch$

Gap required to leak 100% bypass flow is not very high

(2) $\Delta P_0 = 9$ or 12 psi

$V \propto \sqrt{P_0}$

$\therefore$ m_2 will increase by $\sqrt{P_0}$ ratio at the same gap.

Since the m_1 will be increased by $\sqrt{P_0}$ ratio also, Approximately the same gap size is needed as for $\Delta P_0 = 7$ psi o Comparison of liquid leak thru H5 and Homogeneous 2φ leak thru H5 @ 10% leak

pp 1-4 calculates

$$\Delta P = 6.067 \text{ psi} \quad @ \quad \Delta P_0 = 7.0 \text{ psi}$$

for single phase water leak

If this were homogeneous leak for $t = 0.4455$ inch

$$\frac{\Delta P_h}{\Delta P_0} = \frac{1}{(1+ax)^2}$$

see PB DRF section for this formula

$$a = \sqrt{\frac{C_1}{C_2'}}$$

$$\Delta P_0 = C_1 v_0 \dot{m}_{core}^2$$

$$C_1 = \frac{7.0 \text{ psi}}{0.0588488 \times (98 \times 10^6)^2}$$

$$\frac{\frac{LBf}{in^2}}{\frac{ft^3}{\cancel{LBm}}\left(\frac{LBm}{hr}\right)^2} = \frac{LBf \cdot hr^2}{ft^3\, in^2\, LBm}$$

$$C_2' = \frac{K_2}{2g_c(\pi D)^2}\,\frac{144}{3600^2}$$

$$= \frac{1.4 \times 144 \times}{2 \times 32.2 \times (203.12 \times \pi)^2 (360}$$

$$\frac{in^2/ft^2 \quad ft/in}{\frac{LBm \cdot ft}{\cancel{sec^2} \cdot LBf} \times in^2 \times \left(\frac{sec}{hr}\right)^2}$$

$$= \frac{LBf \cdot \cancel{sec} \cdot hr^2}{LBm \cdot ft^3}$$

Subject | Originator | Date
Number | Verifier G.C. Eckert | Date 3/1/94

$\frac{C_1}{C_2'}$ has unit of $\left(\frac{1}{in^2}\right)$,

and

$$\frac{C_1}{C_2'} = \frac{\dfrac{7.0}{0.0588488 * (98\times10^6)^2}}{\dfrac{1.4 \times 144}{2\times32.2 \times (203.12 * \pi)^2 (3600)^2}}$$

$$= \frac{7.0 \times 2\times32.2 \times (203.12 * \pi)^2 \times (3600)^2}{1.4\times144\times0.0588488 \times (98\times10^6)^2}$$

$$= 0.02088 \ \frac{1}{in^2}$$ ✓ GCE 3/1/94

$$a = \sqrt{\frac{C_1}{C_2'}} = 0.1445 \ \frac{1}{in}$$ ✓

$$X = t = 0.4455 \text{ inch}$$

$$\therefore ax = 0.064373$$ ✓

GCE 3/1/94

$$\therefore \frac{1}{(1+ax)^2} = 0.8827$$ ✓

$$\therefore \Delta P_h = 7 * 0.8827 = 6.18 \text{ psi}$$ ✓

GE Nuclear Energy
Engineering Calculation Sheet

Subject | Originator | Date
Number | Verifier E C Eckert | Date 5/1/94

Comparison of

$\Delta p = 6.067$ (calculated by assuming 10% single phase water leak)

and

$\Delta P_h = 6.18$ psi (calculated by assuming two phase homogeneous leak)

Therefore for the calculation of the dynamic behavior, using the homogeneous flow leak would be a good approximation. When gap is bigger than $X > 0.4455$ inch, two phase flow will ~~also~~ leak.

When homogeneous leak is assumed, even though ΔP & dynamic behaviors are similar the actual leakage flow would be different. In the above case

$$\Delta P = C_2 \rho_2^{-1} m_2^2$$

$$\Delta P_h = C_2 \rho_0^{-1} m_{2h}^2$$

$$\frac{m_{2h}^2}{\rho_0} \frac{\rho_f}{m_2^2} = \frac{\Delta P_h}{\Delta P}$$

$$\therefore m_{2h}^2 = m_2^2 \frac{\Delta P_h}{\Delta P} \frac{\rho_o}{\rho_f}$$

$$= m_2^2 \frac{\Delta P_h}{\Delta P} \frac{v_f}{v_o} = m_2^2 \frac{6.18}{6.067} * \frac{0.02114}{0.05848}$$

$$\therefore m_{2h} = 0.605\, m_2$$

Therefore, 2ϕ leak is only 60% of the single phase leak

EGE 5/1/94

Subject | Originator | Date

Number | Verifier E. C. Eckert | Date 5/1/94

Condition for maximum lift,

$$\frac{B}{1+ax} = 1$$

$$\therefore X_{max} = \frac{B-1}{a}$$ (see PB DRF Section for this formula)

$a = 0.1445$ inch

$$B = \frac{g_c A \Delta P_o}{M_s g}$$

Ref. 5. ECE 5/1/94

For ~~H5~~ H5 Weld, $M_s = 413.74$ KIP

	El	Effective mass	Cummulative Wt
(H4) El	266.375	259.06 kip	?
	208.01		405.62 kip
(H5)	191.125	334.48	
	147.53		434.59

$$H5 \text{ mass} = 405.62 + \frac{(34.59-5.62)}{(208.01-147.53)}(208.01-191.12)$$

$$= 413.74 \text{ kip}$$

GE Nuclear Energy
Engineering Calculation Sheet

Subject

Number | Originator | Sheet 10 of | Date

Verifier E.C. Eckert | Date 5/1/94

$$A = \frac{\pi}{4} D^2 = \frac{\pi}{4} \times (203.12)^2 = 32,403.75 \text{ in}^2$$

B values

B

$\Delta p = 7$ psi $\quad B = \frac{7 \times 32,403.75}{413.74 (10^3)} = 0.548$

ECE 5/1/94

$\Delta p = 12$ psi $\quad B = 0.94$

The effects of Drag force, Momentum, Buoyancy Force, Hydrodynamic mass are small, and canceles most of their effects each other

No lift up to 12.77 psi of pressure drop

Given

GE Nuclear Energy
Engineering Calculation Sheet

Sheet 11 of

Subject	Originator	Date
Number	Verifier E. C. Eckert	Date 5/1/94

Assume DBE

$W @ H5 = 306.76$ From Ref 5. ✓ EC 5/1/94

@ $\Delta P_o = 12$ psi

$$B = \frac{12 \times 32{,}403.75}{306{,}760} = 1.27$$

$$X_{max} = \frac{1.27 - 1}{0.1445} = 1.85''$$

1.69" slack
.25" Thermal Exp
1.44" clearance

Assume OBE

$$B = \frac{12 \times 32{,}403.75}{334{,}480} = 1.1625$$

Ref. 5 EC 5/1/94

$X_{max} = 1.13''$

can be accommodated by the slack in the Core Spray line bracket

Leakage Flow at the bottom H5 Weld assuming 360° crack through the wall

- Assume the gap is less than 0.1 inch during LOCA for long term cooling

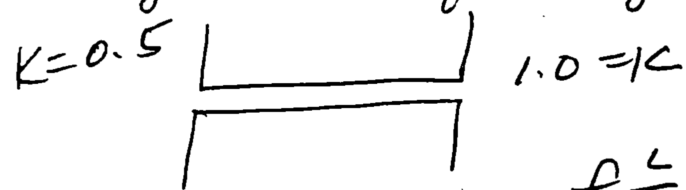

$$f\frac{L}{D} = 0.02 * \frac{2}{0.1} = 0.4$$

Total $\Sigma K = 1.9$

Water height = 12.5 ft

$$\rho g h + K\frac{\rho V^2}{2} = \text{const}$$

$$\therefore \quad V = \sqrt{\frac{2gh}{K}} = \sqrt{\frac{32.2 \times 2 \times 12.5}{1.9}}$$

$$= 20.6 \text{ ft/sec}$$

$$Q = AV = \pi D t V = \pi \times \frac{203.12}{12} \times \frac{0.1}{12} \times 20.6$$

$$= 9.12 \text{ ft}^3/\text{sec} \checkmark$$

$$= 4094 \text{ gpm}$$

✓ EE 3/1/94

Two core sprays available
4500 gpm × 2 = 9000 gpm

Even with 0.1 inch gap, there will be sufficient coolant available for the core cooling. Because of the small lift or no lift, practically

For the gap of 0.002 inch during Normal op.

$f\frac{L}{D} = 0.02 \times \frac{2.0}{0.002} = 20 \quad \Sigma K = 1.5 + 20 = 21.5$

$\Delta p = 7.0\, psi = \Sigma K \frac{\rho V^2}{2g_c}, \quad V = \sqrt{\frac{2g_c \Delta P}{\rho \Sigma K}}$

$\therefore V = \sqrt{\frac{2 \times 32.2 \times 7 \times 144}{46 \times 21.5}} = 8.1\ ft/sec$

$Q = AV = \pi D t = \pi \times \frac{203.12}{12} \times \frac{2 \times 10^{-3}}{12} \times 8.1 = 7.18 \times 10^{-2}\ ft^3/s$

$= 32\ gpm$

VC
EC
5/1/94

If the gap is 0.001 inch, $\Sigma K = 41.5$
$V = 5.83\ ft/sec$
$Q = 11.6\ gpm$

Actual friction factor for crack path would be much higher than 0.02 due to ① Rough surfaces, propably jagged ② relatively low Re number. Therefore,
$Q < 30\ gpm$ with 0.002 inch gap.

ULTRASONIC EXAMINATION OF DRESDEN UNIT #3 SHROUD WELD # H5

Ref. 2

On 4-26 & 27-94 a ultrasonic examination was performed on six areas of the H5 Shroud weld to confirm and depth size a probable crack indication detected visually, during the under water examination. Commonwealth Edison Procedure NDT-C-41, Rev. 2 was used as a guide line for this examination. Although this procedure is applicable it has not been qualified for remote manual under water ultrasonic sizing as was done during this examination.

A 70° dual R-L Probe focused at .300" deep was used to confirm the presents of the crack and a 60° dual R-L Probe focused at 1.0" deep was used to better determine the crack depth.

RESULTS:

The visual crack like indication was confirmed to be a crack at the six locations around the shroud weld. The crack was also suspected of being deeper than .500" with the 70° probe. The crack depth was sized with the 60° probe at the same six locations and it's depth varied from .95" to 1.55". Refer to the ultrasonic sizing data sheets for more specific information.

To determine more exactly the crack depth and if it is deeper than 1.55" a properly focused 45° dual R-L probe should be used on a automatic remote scanner.

Brian J Wilson
CECo. Chief Level III
4-27-94

Post-it™ brand fax transmittal memo 7671 | # of pages ▸ 27

To HWANG CHOE	From D LEGLER
Co. GE	Co. CECO
Dept.	Phone # DRESDEN 2276
Fax # 408-925-1150	Fax #

Ref(5)

DRF-137-0010-7

GENE-523-05-0194

2/24/1994 - 12:19:17

TITLE: Dresden 3 Shroud Circ Flaw at H5, Limit Load

FLOW STRESS FACTOR ON SM = 3.000

PM = .000 PM + PB = .036 SAFETY FACTOR = 2.800
FLOW STRESS FACTOR = 3.000
PM = .004 PM + PB = .076 SAFETY FACTOR = 1.400
FLOW STRESS FACTOR = 3.000

SAFETY FACTOR = 2.800		SAFETY FACTOR = 1.400	
LENGTH	DEPTH	LENGTH	DEPTH
.760	1.000	.751	1.000
.800	.992	.800	.991
.850	.987	.850	.985
.900	.984	.900	.983
.950	.983	.950	.982
1.000	.983	1.000	.982
.000	.000	.000	.000
.000	.000	.000	.000
.000	.000	.000	.000
.000	.000	.000	.000
.000	.000	.000	.000
.000	.000	.000	.000
.000	.000	.000	.000
.000	.000	.000	.000
.000	.000	.000	.000
.000	.000	.000	.000
.000	.000	.000	.000
.000	.000	.000	.000
.000	.000	.000	.000
.000	.000	.000	.000
.000	.000	.000	.000

Ref. 5

Purpose: Determine the bending stresses in the shroud due to the seismic load

Reference: See DRF Reference List.

Discussion: The relative elevations for the dynamic loads were taken from Ref. 1. The section modulus Z was calculated at each weld location. Linear interpolation was used to determine the moments for each weld; the corresponding weld elevations were determined from Refs. 3b, 3c, 3e, and 3f. The bending stresses were calculated for OBE and DBE conditions using standard strength of materials equations (stress = M/Z).

The maximum seismic moments for the shroud summarized below in Table 2 are taken from Reference 1. The DBE (SSE) loads in Table 2 are two times the OBE loads, from Ref. 1.

Table 1 below shows the seismic loads applied to each weld for OBE and DBE conditions.

TABLE 1 SEISMIC LOADS AND STRESSES FOR EACH WELD LOCATION

Weld Designation	Elev. (in)	Outside Radius (in)	Inside Radius (in)	Thick. (in)	Section Modulus (in^3)	OBE Moment (in-kips)	DBE Moment (in-kips)	OBE Pb (ksi)	DBE Pb (ksi)	Effective Wt. (kip) OBE	Effective Wt. (kip) DBE	NOT USED Shear (kips) OBE
H1	391.375	110.00	108.00	2.00	7.47E+04	3.24E+03	6.48E+03	0.04	0.09	177.77	163.04	25
H2	357.875	110.00	108.00	2.00	7.47E+04	6.78E+03	1.36E+04	0.09	0.18	201.10	184.43	186
H3	355.375	103.56	101.56	2.00	6.61E+04	7.22E+03	1.44E+04	0.11	0.22	202.24	185.48	186
H4	266.375	103.56	101.56	2.00	6.61E+04	2.34E+04	4.67E+04	0.35	0.71	259.06	237.59	193
H5	191.125	103.56	101.56	2.00	6.61E+04	4.01E+04	8.02E+04	0.61	1.21	334.48	306.76	327
H6	187.125	100.50	98.50	2.00	6.22E+04	4.14E+04	8.28E+04	0.67	1.33	336.02	308.18	327
H7	131.500	100.50	98.50	2.00	6.22E+04	6.03E+04	1.21E+05	0.97	1.94	351.36	322.24	366
H8	120.531	100.50	98.50	2.00	6.22E+04	6.43E+04	1.29E+05	1.03	2.07	351.36	322.24	366

TABLE 2 REFERENCE 1 LOADS

Elevation from VB (in)	Node #	Cumulative Wt. (kip)	Effective Wt. (kip) OBE	Effective Wt. (kip) DBE	Moment (in-kips) OBE	Moment (in-kips) DBE	NOT USED Shear (kips) OBE
463.49	12	133.87	108.23	99.27	1.44E+03	2.87E+03	25
375.53	13	238.78	193.05	177.05	3.64E+03	7.28E+03	186
288.77	14	287.73	232.62	213.35	1.91E+04	3.81E+04	193
208.01	15	405.62	327.94	300.76	3.46E+04	6.91E+04	327
147.53	16	434.59	351.36	322.24	5.43E+04	1.09E+05	366
120.53	*	434.59	351.36	322.24	6.43E+04	1.29E+05	366

* Shroud Support Plate

OBE to DBE Factor: 2

Vertical Acceleration (g's) OBE	Vertical Acceleration (g's) DBE	Density (lb/in^3) Steel	Density (lb/in^3) Water
0.067	0.134	0.290	0.036

Buoyancy: subtract weight of water displaced
= metal wt. * water density/metal density
Effective Wt = Cum. Wt. * (1-Dens. Ratio-Vert. Acc.)
stainless steel density from Y1002A002 rev. 4

CIRCUMFERENTIAL FLAW

Dimensions for Welds H3 to H5

Out dia. = Do	207.125 inches	In Dia = Di	203.125 inches	from GE 718E861
Out radius = Ro	103.56 inches	In Radius = Ri	101.56 inches	Shroud, Spec Control
thick = t	2.0 inches	Area = A	1288.84 in²	

Above the Core Plate, Limit Load Analysis

		H3	H4	H5		
Normal & Upset:	Shroud Head Press. (psi)	7.0	7.0	7.0		From Dresden UFSAR, Tables 3.9-18,19,20
	Sig(p) = P*Ri/2*t (ksi) =	0.178	0.178	0.178		
	Wt. & Vert. Seis (ksi) =	-0.157	-0.201	-0.260		
	Total Membrane Stress (ksi) =	0.021	-0.023	-0.082	= Pm	Use Zero if negative
	Upset Bending Stress (ksi) =	0.109	0.353	0.606	= Pb	From Seismic Load Table
	Sm (ksi) = 16.9					
	Pm/Sm =	0.001	-0.001	-0.005		
	(Pm+Pb)/Sm =	0.006	0.021	0.036		
	Safety Factor =	2.8	2.8	2.8		
Faulted:	Shroud Head Press. (psi)	12.0	12.0	12.0		From Dresden UFSAR, Tables 3.9-18,19,20
	Sig(p) = P*Ri/2*t (ksi) =	0.305	0.305	0.305		
	Wt. & Vert. Seis (ksi) =	-0.144	-0.184	-0.238		
	Total Membrane Stress (ksi) =	0.161	0.120	0.067	= Pm	Use Zero if negative
	Faulted Bending Stress (ksi) =	0.218	0.707	1.213	= Pb	From Seismic Load Table
	Pm/Sm =	0.010	0.007	0.004		
	(Pm+Pb)/Sm =	0.022	0.049	0.076		
	Safety Factor =	1.4	1.4	1.4		
Allow. Flaw Length:	fraction of circumference from 1CRITFLA run	0.827	0.784	0.751		
	(using mean radius) * 2*pi*Rm (in) =	532.9	505.2	484.0		
	Allowable Flaw Length/4 (in) =	133.23	126.31	120.99		
	Limiting Case:	Faulted	Faulted	Faulted		

Above the Core Plate, LEFM

			H4	H5	
Normal & Upset:	Total Sig = Pm+Pb (ksi) =		0.353	0.606	
Faulted:	Total Sig = Pm+Pb (ksi) =		0.827	1.279	
Governing Case:	3.16	x Norm/Upset =	1.117	1.916	
	1.4	x Faulted =	1.158	1.791	
		Limiting Case:	Faulted	Upset	
	Allowable Flaw =		489	326	from spreadsheet DR3SHRDN.XLS

Ref. 6

In summary, the design of the TAP supports is adequate for the loads, load combinations, and acceptance criteria limits specified in NUREG-0661[5] and substantiates the piping analysis results.

3.9.4 Control Rod Drive Systems

The design of the CRD system is discussed in Section 4.6. Control rod drive materials are addressed in Section 4.5.

3.9.5 Reactor Pressure Vessel Internals

The following sections provide descriptions of the physical layout of the reactor pressure vessel internals (Section 3.9.5.1), of loading conditions applicable to their structural and functional integrity (Section 3.9.5.2), and of their design evaluation (Section 3.9.5.3). Design of the control rods is described in Section 4.6. Information on the reactor internals materials is provided in Section 4.5.2.

3.9.5.1 Design Arrangements

In addition to the fuel and control rods, reactor vessel internals include the following components:

A. Shroud,

B. Baffle plate (shroud support plate),

C. Baffle plate supports,

D. Fuel support piece,

E. Control rod guide tubes,

F. Core top grid,

G. Core bottom grid,

H. Jet pumps,

I. Feedwater sparger,

J. Core spray spargers,

K. Standby liquid control system sparger,

L. Steam separator assembly,

M. Steam dryer assembly, and

N. Incore nuclear instrumentation tubes.

The shroud is a stainless steel cylinder which surrounds the reactor core and provides a barrier to separate the upward flow of coolant through the reactor core from the downward recirculation flow. Bolted on top of the shroud is the steam separator assembly which forms the top of the core discharge plenum. This provides a mixing chamber before the steam-water mixture enters the steam separator. Refer to Figure 3.9-4 for the reactor vessel cut away isometric for illustration of parts arrangement.

The recirculation outlet and inlet plenum are separated by the baffle plate joining the bottom of the shroud to the vessel wall. The jet pump diffuser sits on and is welded to the baffle plate, making the jet pump diffuser section an integral part of the baffle plate.

The baffle plate and inner rim are made of Inconel to allow for welding to the ferritic base metal of the reactor vessel. The bottom of the shroud is welded on top of the rim, which provides for the differential expansion between the ferritic, Inconel, and stainless steel components. Inconel legs welded at intervals around the baffle plate support it from the vessel bottom head.

The baffle plate supports carry all the vertical weight of the shroud, steam separator and dryer assembly, top and bottom core grids, peripheral fuel assemblies, core plugs not carried on guide tubes, and jet pump components carried on the shroud. In addition, the supports must withstand the differential pressures of normal operations and blowdown accidents (either upward or downward), and for the vertical and horizontal thrust of the seismic design.

The reactor fuel supports are the 4-lobed, Type 304 stainless steel fuel support pieces mounted on top of the control rod guide tubes. Each support piece holds four fuel assemblies and is designed to hold the orifice plates used for core flow distribution. There are two types of orifices, one for peripheral assemblies and one for nonperipheral assemblies. The control rods pass through slots in the center of the support piece. Each fuel support piece is removed to take out the control rod with attached velocity limiter.

The control rod guide tubes extend up from the control rod drive housing through holes in the core bottom grid. Each tube is designed as a lateral guide for the control rod and as the vertical support for the fuel support piece which holds the four fuel assemblies surrounding the control rod. The guide tubes are fabricated from stainless steel with 0.165-inch nominal and 0.134-inch minimum wall thickness which results in a safety factor of 4 during the maximum applied loading. This maximum loading occurs at the end of control rod insertion so that even if the tube were to buckle the control rod would remain inserted. The bottom of the guide tube is inserted and locked into a sleeve in the control rod drive housing.

The core top grid appears as a series of beams at right angles forming square openings, each for four fuel assemblies. The grid provides lateral support and guidance for the assemblies. Holes in the beams are provided to receive the top hooks of the temporary control curtains, which are then prevented from unhooking by the adjacent fuel assemblies. The top grid is attached to the reactor core shroud.

The core bottom grid consists of a perforated stainless steel plate supported on a grid beam structure, which is in turn supported on the reactor core shroud. The fuel support pieces are held laterally in the grid openings. Sixteen fuel assemblies or core plugs at the periphery of the core, which are not adjacent to control rods, are directly supported by the bottom grid. Proper orificing for coolant flow is provided in the grid for these 16 assemblies. Smaller perforations in the core plate provide guidance for the incore neutron monitor guide tubes, between fuel assembly locations.

The 20 jet pumps are of stainless steel construction and consist of a driving nozzle, suction inlet, throat or mixing section, and diffuser. The jet pumps are arranged in two symmetric groups around the reactor core shroud in the downcomer annulus. Each of the 10 supply lines from the recirculation pumps supply high-pressure water to a pair of jet pumps. Each supply line is welded to a nozzle on the outside of the reactor vessel. On the inside of the vessel a stainless steel riser pipe terminates at the pair of jets. The riser is held in position by support arms welded to the vessel wall.

The jet nozzle, contoured inlet, and throat are joined together as a removable unit, clamped to the top piece of the riser by nut-locking system. The joint between the throat and the diffuser is a slip fit. The throat section is supported by a clamp ring attached to the riser.

The jet pump diffuser is a gradual conical section changing to a straight cylindrical section and flange at the lower end. The diffuser is inserted up through the hole in the baffle plate, and is supported by brackets from the vessel wall. A water seal is formed by a preloaded Belleville washer between the diffuser flange and the baffle plate and by a bellows seal welded at the top to the diffuser and down to the baffle plate.

The hydraulic and operational effects of the jet pump design are discussed in Section 5.4.1.

Feedwater sparger integrity is discussed in Section II.3.2 of Amendment No. 5 for the Dresden Unit 3 Plant Design and Analysis Report,[11] which also includes a discussion of the core spray sparger integrity. The following paragraphs, however, cover some of the features unique to the feedwater sparger.

Four feedwater spargers are utilized in the reactor. Each sparger is approximately 70 inches in length and mounted to the inside reactor vessel surface. The thermal sleeve is attached to the sparger midpoint; however, the sleeve is not welded to the vessel nozzle. Therefore the feedwater sparger is removable. The spargers are mounted in the vessel at one elevation to distribute the feedwater in a symmetric pattern about the vessel axis. Vibration consideration for feedwater spargers is the same as that discussed on page II.3.3-10 Amendment No. 5 for the Dresden Unit 3 Plant Design and Analysis Report.[11] Each sparger is supported by the thermal sleeve and a bracket mounted to each end of the sparger.

The feedwater nozzle inner bore, the thermal sleeves, and the feedwater spargers were modified (January 1981 on Unit 2 and January 1982 on Unit 3). This modification consisted of removing (by machining) clad from the feedwater nozzle, boring the inside diameter of the safe-end to accommodate the new feedwater sparger seal surfaces and finally installing the new design sparger. The modified thermal sleeve is a double seal/triple thermal sleeve which gives a dual seal.

interference fit (piston ring type). The four new stainless steel feedwater spargers now have nozzles instead of the conventional drilled round holes which were subject to cracking.

The new sparger/thermal sleeve design will extend the service life of the feedwater nozzles and will limit the number of mandatory in-vessel dye penetrant examinations in the future. This modification is in compliance with NUREG-0619[12] which required a "final fix."

The reactor has two 100%-capacity core spray spargers. Each sparger is in two halves to allow for thermal expansion and is supported by slip-fit brackets welded just below the top of the core shroud. Each half receives spray water from one of a pair of supply lines routed in the reactor vessel to accommodate differential movement between the shroud and the vessel. The supply line pair for each system terminates at a common vessel nozzle. The sparger distribution nozzles are pointed radially inward and downward at a slight angle to achieve specified distribution pattern.

The standby liquid control system sparger is a perforated pipe attached inside the bottom end of the core shroud. It discharges the sodium pentaborate solution into the cooling water which then rises upward through the reactor fuel.

The steam separator assembly consists of the core top plenum head into which are welded an array of standpipes, with a steam separator attached to the top of each standpipe. The assembly is bolted on top of the core shroud by long bolts which permit removal for refueling operations. The assembly is guided into place by vertical guide tracks on the inside of the reactor vessel and by locating pins on top of the shroud.

The fixed centrifugal-type steam separators have no moving parts. In each separator, the steam-water mixture rising through the standpipe passes vanes which impart a spin to establish a vortex which separates the steam from the water. The steam exits from the top of the separator and rises up to the dryers. The separated water exits from under the separator cap and returns to the trays among the standpipes, which drain into the downcomer annulus.

The steam dryer assembly is bolted on brackets on the inside of the reactor vessel wall below the steam outlet nozzle. A skirt extends down from the dryer assembly into the water to form a seal between the wet steam plenum below the dryers and the dry steam flowing out the top and down to the steam nozzles. Moisture is removed by impinging on the dryer vanes and flows down through collecting troughs and tubes to the water trays above the downcomer annulus. The vertical tracks inside the reactor vessel are also used to guide the dryer assembly into position.

There are 53 incore nuclear instrumentation guide tubes extending up through the bottom of the reactor vessel to the core top grid.

The guide tubes are inserted into the reactor through housings that are attached to the bottom head of the reactor vessel and extend down to the same level as the drive housing flanges.

Twelve of the tubes are closed at the top end and are designed for the same pressure as the reactor vessel to prevent leakage of reactor water. Four of these 12 tubes are for the source range monitor detectors and 8 for the intermediate range monitor detectors.

The other 41 each contain 4 local power range monitor (LPRM) incore detector strings and a guide tube for the traversing incore probe. Each of the 41 stainless steel tubes is approximately 1 inch in diameter, is open at the top for water cooling, and has a pressure seal at the bottom where the coaxial cables leave the reactor.

3.9.5.2 Loading Conditions

The reactor internals are designed mechanically to:

1. Provide an adequate distribution of coolant flow within the reactor, and

2. Maintain structural integrity during normal operations, seismic disturbances, and design basis accident conditions.

The specific design requirements for each internal component may vary due to differences in material, and location. Each component must be able to withstand the combined loadings from differential pressures and temperature, dead weight, fluid movement, control rod motion, seismic acceleration, and vibration. Allowable stresses as defined by the ASME Code will not be exceeded. Allowances must be made for thermal expansion, corrosion, and crud buildup.

The reactor core structural components are designed to accommodate the loadings applied during normal operation and maneuvering transients. Deflections are limited so that the normal functioning of the components under these conditions will not be impaired. Where deflections are not the limiting factor, ASME Section III is used as a guide to determine limiting stress intensities and cyclic loadings for the core internal structure.

The loading conditions which occur during excursions or loss-of-coolant accidents have been examined. The reactor core shroud, shroud support, and jet pump body, which comprise the inner vessel around the core within the reactor vessel, are designed to maintain a reflooding capability following a design basis loss-of-coolant accident. Reflooding the reactor core to the top of the jet pump inlets will provide adequate cooling of the fuel.

The design of the jet pump parts takes into account the pressure loading both in normal and accident conditions and the reactions at the supporting brackets due to differential thermal expansion of the pump and reactor primary vessel.

The reactor internals are designed to preclude failure which would result in any part being discharged through the main steam line, in the event of a steam line break, which might block a main steam line isolation valve.

The structural components which guide the control rods are analyzed to determine the loadings which would occur in a design basis loss-of-coolant accident. The reactor core structural components are designed so that deformations produced by accident loading will not prevent insertion of the control rods.

Pressure differentials, jet reactions, and earthquake loadings have been considered in the analysis of the feedwater sparger. These stresses were all within the requirements of ASME Section III for Class A Vessels. The sparger was analyzed assuming the thermal sleeve is welded into the nozzle. The resultant bracket loads were then given to the vessel manufacturer so that properly sized vessels brackets could be sized to meet the Section III criteria.

3.9.5.3 Design Bases

This section presents the details of key evaluations performed for the reactor vessel internals. A discussion of the jet pump assembly and its relationship to the vessel and to the other reactor internal components during steady-state and transient operation is included in the jet pump topical report APED-5460.[13] Section 4.3.2.2 of the report describes the stress analysis that was performed to demonstrate the adequacy of the structural design of the jet pump assembly and the core shroud during operation of the emergency core cooling system, which is the condition of maximum stress for the jet pump core shroud assemblies.

The reactor internals which must maintain their functional integrity to assure safe shutdown following the various postulated accidents are the following:

A. Reactivity Control Systems

   1. Control Rod and Control Rod Drive Systems

      a. Fuel channel-core support complex.

      b. Control rod control assemblies.

   2. Stand-by Liquid Control

B. Emergency Core Cooling Systems

   1. LPCI System

      a. Core shroud and baffle, relative to the ability to maintain water level in the core.

      b. Jet pump structure relative to the ability to introduce and maintain a water level in the core.

   2. HPCI System; with components corresponding to those above.

   3. Core Spray System

      a. Core spray piping and sparger in the reactor pressure vessel.

      b. Arrangement of the core support complex, relative to its ability to accept water from the core spray.

Based on analyses of the reactor internals during both normal and accident conditions, it was determined that stresses in the individual components are limiting, except in the following areas where deformation is the controlling parameter:

A. Deflection of the fuel channels under accident pressure conditions is limited to an amount substantially less than that which would prevent control rod drive insertion. The maximum frictional force exerted on the fuel channel by the control rod (as a result of interference), during a design basis accident, is less than 100 pounds. The minimum force exerted by the control rod drive on a control blade is 3000 pounds. Therefore, control blades can be fully inserted against the forces of fuel channel deflection under the most severe accident conditions. Under the above control rod insert conditions, the fuel bundles which weigh about 700 pounds will not be lifted due to the resisting insertion forces of 100 pounds friction from the deflection of its members.

B. Horizontal deflection of the control rod drive housings is limited to a value which through test has been demonstrated not to impede control rod insertion.

C. Deflection of the core plate and lower grid assembly is limited under normal operation to preclude taking up vertical clearance between the core plate and control rod guide tubes so that the core bypass leakage flow can be predicted. This results in stresses that are below yield even during accident conditions. The maximum deflection of the core plate under accident conditions is limited to 0.125 inches, which represents a considerable factor of safety below the deflection at which the core plate and guide tube could come into contact.

The maximum value of primary stress in reactor internal components generally results from the large pressure difference created when either the recirculation line or the steam line are completely severed. A discussion of these two accidents is given in Sections 3.9.5.3.1.2 and 3.9.5.3.1.3, respectively.

The sensitive point within the reactor pressure vessel which is most affected by operation of the emergency core cooling systems (HPCI and LPCI) is in the area of the jet pump to baffle plate joint. The stress and fatigue evaluation of this location is discussed in Section 3.9.5.3.2.

3.9.5.3.1 Pressure Loadings

Values of calculated pressure difference versus design pressure capability for major reactor internal components are included in Tables 3.9-18 and 3.9-19 to show the margin of safety that exists below ASME Section III limits. The margin of safety for these components which actually exist, based upon the GE Atomic Power Equipment Department (APED) design criteria for reactor internals, is equal to or greater than the margin specified in the tables. The loading combinations, and stress and deformation limits for reactor internal components are also discussed in these criteria.

3.9.5.3.1.1 Thermal-Hydraulic Model

In this section, the internal pressure forces which would be imposed across the internal reactor components during rapid depressurizations associated with pipe breaks are discussed in detail.

Internal reactor pressure forces are calculated for two postulated break conditions, a steam line rupture and recirculation line rupture. The steam line break is assumed to be a guillotine line severance which is located upstream of the flow limiter. This break gives the maximum break steam flow and maximum pressure forces. The conclusion of the event is complete blowdown to the drywell. The recirculation line break is assumed to be a guillotine line severance at the pressure vessel outlet. This places the break in the downcomer and the conclusion of this event is again to have a complete blowdown to the drywell. In both cases, reflooding of the reactor is accomplished by the emergency core cooling system. The break is assumed, in each case, to occur while the plant is operating at 2527 MWt with 98 x 10^6 lb/hr core recirculation flow.

When calculating internal pressure loading due to a blowdown accident, an analytical model is employed in which the pressure vessel is divided into five major chambers or nodes. Each node is connected to adjoining nodes by a flow resistance as shown in Figure 3.9-5. The five nodes are: (1) subcooled lower plenum, (2) saturated core, (3) saturated upper plenum, (4) saturated mixing plenum, and (5) saturated steam dome.

The lower plenum to core resistance includes the inlet orifice, acceleration, local, and flow losses to the core midplane. The core to upper plenum resistance consists of the remaining core local losses and flow losses. The separator resistance is between the upper plenum and mixing plenum and steam dome. In the recirculation line break, one additional resistance is included — the resistance between the downcomer and the lower plenum through the open jet pumps of the broken line. Jet pumps are described in Section 5.4.1.

Referring to Figure 3.9-5, the pressure forces acting on major components are as shown in Table 3.9-20:

The two design basis breaks will be discussed individually.

3.9.5.3.1.2 Recirculation Line Rupture

The instantaneous recirculation line rupture (double-ended) causes high flowrate from the downcomer and plenum regions. Initially, supercritical flow (high-single-phase flow) exists in the blowdown lines prior to flashing of the water. After bubbles form in the lines, two-phase critical flow is established and the blowdown rate is reduced from the supercritical flow value. No credit is taken for friction losses in the broken line.

Although the flowrate from the downcomer is high, the pressure change rate in the mixing plenum is only about 20 psi/s assuming no turbine control valve action to maintain pressure. Because large amounts of saturated water are present in the mixing plenum, the depressurization rate is low due to the accompanying flashing.

Large pressure forces due to depressurization of the subcooled lower plenum do not develop in the BWR plant. The principle reason in this case is that, in the event of a line break, the subcooled lower plenum does not discharge directly to the atmosphere. Instead, it discharges to the downcomer region through the inoperative jet pump diffusers, and the downcomer pressure is maintained by compression of the steam above the mixing plenum.

Thus, large pressure forces cannot develop across the diffusers and shroud support because the inoperative jet pump diffusers are open between the downcomer and lower plenum. Even though the lower plenum is subcooled, its depressurization rate is limited by the downcomer and mixing plenum depressurization rate. The fact that some water flows through the jet pump nozzles to the atmosphere is not serious since the flow will be critical or "choked" in the nozzles, and the total nozzle area is only 15% of a 28-inch OD recirculation line.

Results of the recirculation line break are given in Table 3.9-18 and compared to component capabilities. The upper shroud, lower shroud, and shroud support are of interest with respect to the emergency core cooling system. The guide tubes and core plate are necessary for scram capability.

The calculated maximum pressure differential across the core for the recirculation line break does not increase above that at rated conditions, (i.e., 18 psi upward); well below the 45-psi pressure differential required for fuel bundle lifting.

The calculated maximum pressure differential across the fuel channel would be approximately 9 psi outward (initial value) for the recirculation line break. Core inlet flow decreases to about 40% of rated flow resulting in a decrease in channel box pressure level. Since the channel deflection is no more than that occurring during normal operation, control rod interference cannot occur.

If the mechanism by which the fluid is actually accelerated to its maximum flowrate is specifically to be considered, then the effect of the actual break opening time must be included since this is a significant factor in the acceleration phenomenon. Following a sudden recirculation line break, about 7 — 75 milliseconds is required to accelerate the fluid to its maximum flow depending on the actual pipe length from the vessel to the break. Since the actual break opening time is expected to be 100 milliseconds or longer, a relatively gradual fluid acceleration will occur and the resulting asymmetric loads are low. Therefore, the loads discussed above are the maximum loads to be expected following a sudden complete pipe line break.

Pipe rupture studies such as those performed at GE and Battelle Memorial Institute investigating fracture mechanics provide some insight into the mechanism of break enlargement. Although no specific data is available which would quantitatively define break opening times to be expected for large systems, it is clear from these studies that large amounts of energy are required to cause sudden enlargement of an existing flow into a through-wall crack and subsequently into a large break which would allow unobstructed blowdown flow.

Since a finite time is required for this energy to be supplied by the fluid system to the crack location, the postulated large break cannot occur instantaneously. Furthermore, the studies have shown that an existing part-through wall flaw which is as much as 2 feet long would propagate through the wall and cause a detectable leak without propagating into the postulated large break. Therefore, it is expected that at least 100 milliseconds would be realistically required for a crack to propagate into a large break.

As discussed above, large asymmetric loads are not expected for a realistic break opening time. However, a hypothetical case has been analyzed in which the break opening was conservatively assumed to be instantaneous. It is assumed that the fluid pressure at the break drops instantaneously from rated pressure to saturation pressure and generates a step change in pressure which propagates toward the vessel. The analysis was performed for a break just outside the pressure vessel nozzle.

Analytical results showed that for this worst case, the peak load on the shroud is about 170,000 pounds (Point b, Figure 3.9-6) and is about 5 milliseconds in duration. Thereafter, the load decreases to 20,000 lbs at 8 milliseconds, which corresponds to a steady blowdown flow loading.

Stresses were calculated in the shroud for two asymmetric loading conditions. The first case considered a small load, approximately 60,000 pounds (Point a, Figure 3.9-6), acting over a small area of the shroud (approximately equal to the recirculation pipe cross-section). A conservative magnification factor of 2 was applied to the force to account for the dynamic effect of sudden application of the load. Local stresses in the vicinity of the applied load were calculated using the methods of Bijilaard for radial loads acting on cylindrical shells. The calculated stresses were elastic and were well within the limits of ASME Section III which was used as a guide for the design of reactor internals. The second case considered the effects of a large load (approximately 233,000 pounds) acting over a large area of the shroud (approximately 21,600 square inches). The conservative magnification factor of 2 was again applied. The effect of the large laterally applied load is to produce an overturning moment which acts on a shroud; however, the resultant overturning moment is no larger than that produced by the design or operational basis earthquake and the concomitant stresses are quite acceptable.

3.9.5.3.1.3 Steam Line Rupture

Following the instantaneous, double-ended, steam line rupture, critical flow is established in each broken line. Since the break is postulated to be upstream of the flow restrictor, the break area is the sum of one open steam line area plus one steam flow restrictor area. As shown in Figure 3.9-7, this break causes the system to depressurize at about 35 psi/s, during initial steam blowdown. About 4 seconds later the depressurization rate is reduced to about zero when the two-phase mixture at about 7 % quality enters the steam line. In comparison, for a steam line break downstream of a flow limiter the initial depressurization rate is 25 psi/s as reported in Section 15.6.4.6.

The design break is assumed to have a constant break area of 2.33 square feet. Actually the effective break area will diminish with time since the isolation valves are closing in one end of the break. When the isolation valves have been closed, the effective break area is reduced to only one steam line.

Rapid decompression of the subcooled lower plenum does not occur because the decompression rate is limited by the saturated upper core regions.

The initial pressure differential increase across the separators and shroud support is caused by the momentum effects associated with the accelerating flow into the depressurizing mixing plenum. The increased loadings at approximately 2 seconds are the result of saturating the previously subcooled lower plenum inventory. The high exit mass flowrate is associated with this phenomenon.

Flashing will decrease as the inventory becomes depleted. As this occurs the loadings across the various internal components will be reduced. Subsequently, no means exist for sustaining large differentials between any of the vessel regions and all pressure differentials drop to low values. For this reason the curves have not been extended beyond 10 seconds.

The shroud loads discussed above are the maximum loads that will occur following a main steam line break. The asymmetric load due to steam line break is small due to the compressible effects of steam and the large expansion as the wave enters the pressure vessel, and does not alter the design basis loads. Because steam is highly compressible, it is not possible to transmit a rarefaction shock similar to the one that can be transmitted in water even for an instantaneous break. In the event of a sudden complete steam line break, the linear gradient is such that the sonic velocity at the back of the wave (low-pressure) is much less than at the front of the wave (high-pressure). Therefore, even if the break is hypothetically assumed to be instantaneous, the compressible effects of the steam prevent the transmission of a shock wave.

Compressibility effects will also limit the amplitude of the linear rarefaction wave that would be transmitted into the pressure vessel. This is because steam is highly compressible and as the ramped rarefaction wave begins to expand into the pressure vessel, a relatively small decrease in pressure would result in a rapid increase in particle velocity which would quickly establish steady flow at the break. This has the effect of limiting the amplitude of the rarefaction wave that can be transmitted into the vessel.

Based on one dimensional plane wave theory, the amplitude of this ramped rarefaction wave would be further decreased by expanding to the cross-sectional area of the vessel. Since this low-amplitude plane wave would be propagating axially down the vessel, the asymmetric load on the shroud would be small and does not alter the design basis loads for the shroud.

The maximum vessel internal loading has been evaluated without any consideration of the rise in coolant level that would occur after a steam line break. This level rise would in fact cause two-phase blowdown from the vessel and thus reduce the depressurization rate and the time when the maximum loadings would occur. It is also assumed that the recirculation pumps remain at full speed through the transient. Since they help to sustain interregion pressure differentials this is a pessimistic assumption. Similarly the assumption of continued injection of full feedwater flow is conservative since it would contribute to the depressurization rate and thus maximize the internals loadings.

Besides the internal forces, there are two other concerns related to the postulated steam line break accident. The first is the possibility of lifting fuel bundles due to the transient pressure differentials imposed across the core. The second is the degree of interference that might exist between the control rods and the channel walls because the channel walls deflect outward under the pressure differentials existing at the time the blades are being inserted. Both of these concerns are alleviated because of the following conditions.

The calculated maximum pressure differential across the core would be considerably less than the 45-psi value required to lift fuel bundles. In fact, as shown by Curve 1 of Figure 3.9-8 it is only slightly over rated differential pressure. These calculations were based on the assumptions of continued feedwater flow, zero steam line resistance and constant break area which all tend to increase the depressurization rate and, therefore, cause the lower plenum to flash prematurely. Even if any bundles did lift, the bundle would only lift an inch or two before relief action would occur at the nose piece and the pressure drop across the core would be rapidly reduced.

The maximum pressure differential tending to bulge the channel outward was calculated to be approximately 12 psi. Test data from a similar type fuel channel indicated that the deflections followed the elastic equation at room temperatures for stresses greater than 2 times the yield stress.

Therefore, based on this experimental factor and the corresponding yield stresses at operating temperatures the best estimate would be that a pressure differential of approximately 25 psi could be applied to the channel without causing the sides to deflect sufficiently to bind the control rods.

Even if it were possible for the channel walls to make contact with the control rods, the deflection is not sufficient to cause permanent distortion, and the channel springs back when the transient pressure decreases. Furthermore, the blades could be inserted even if the channel did pinch the blade. Calculations were performed assuming that a 20-psi transient peak pressure difference existed as a steady-state force on the entire channel. The net normal force acting on each of the control blade rollers was then calculated. Assuming only sliding could take place and using a coefficient of friction of unity the total upward force required to force the walls apart was only 440 pounds per blade.

The control rod drive mechanism is characterized by high forces when scrammed. At zero reactor pressure a drive develops a force of 6000 pounds tending to insert the rod, using the energy stored in the accumulator. The effect of the accumulator decreases as reactor pressure increases, but is approximately 3000 pounds at a reactor pressure of 1000 psi at the beginning of the scram stroke, well in excess of the 440 pounds calculated above. The drive is also scrammed by reactor pressure alone, the force exerted from this energy source being approximately 1100 pounds. Thus, there is no question that the drives are capable of inserting the blades.

Another study was based on a statistical evaluation of the manufacturing tolerances considering three-point contact. The results of this study indicate that even with outward pressure differences of 25-psi adequate clearance for the control rod movement would remain. Furthermore the signal to insert the control rods would occur within approximately 1 second after the accident and the rods would be inserted before the peak pressure difference across the channel could occur.

Therefore, it is concluded that the pressure difference across the core is not sufficiently high to lift the bundles; that the control rods will be fully inserted before the maximum pressure differences across the channels occur; and that the calculated maximum pressure difference across the channel would not be sufficient to pinch the control blade.

The control rod guide tube dimensions and tube design were derived to provide flexural stability during normal operation and collapse resistance during blowdown accident conditions; the differential pressure which would result from these conditions are tabulated in Table 3.9-18. Based upon a yield stress of 17,300 psi, the minimum collapse pressure is 54 psi of pressure differential across the guide tube.

When the earthquake design reactions of 0.4 g horizontal and 0.08 g vertical (greater than design earthquake [OBE] ground acceleration of 0.1 g horizontal and 0.067 g vertical) are combined with the pressure differential of 32 psi across the lower shroud, the maximum resulting general primary membrane stress in the shroud support legs is 15,200 psi. The ASME Code allowable stress is 23,300 psi for this category of loading.

3.9.5.3.2 Thermal Shock Effects on Core Internals

High-stress or strain points have been analyzed on the internals structure during the LPCI thermal shock transient. Three specific locations are summarized and shown on Figure 3.9-9:

1. Baffle plate ligament strains,
2. Shroud-to-baffle discontinuity strains, and
3. Inside-shroud highest irradiation zone.

The baffle plate peak ligament strain analysis results in a peak strain range of 6.5%. This strain range, while higher than the 5.0% strain range permitted in ASME Section III for 10 cycles of loading, corresponds to about 6 allowable cycles of an extended type ASME Section III curve which would apply to fewer loading cycles than 10. Figure 3.9-10 illustrates both the ASME Section III curve and the basic material curves from which it was established (with the safety factor of 2 on strain or 20 on cycles whichever is more conservative). It is seen that extension of the ASME Section III curve represents a similar criteria to that used in ASME Section III but applied to fewer cycles of loading than 10. For this 304 stainless steel material, a 10% peak strain range would correspond to 1 allowable cycle of loading. It is emphasized that even 10% strain level for single cycle loading represents a very conservative suggested limit because this has a large safety margin below the point at which even minor cracking would be expected to begin. Since the conditions which lead to the calculated peak strain range of 6.5% are not expected to occur even once during the entire reactor lifetime, the strain is considered quite tolerable.

The result of the baffle to shroud analysis for strain is as follows:

Amplitude of alternating stress	180,000 psi
Allowable ASME Section III cycles	220
Maximum strain range	1.34%

The shroud receives the maximum irradiation at the inside surface opposite the midpoint of the core where the total integrated neutron flux at end of life is 2.7 x 10^{20} nvt (greater than 1 MeV). The maximum thermal shock stress in this region is 155,700 psi or 0.57% strain. All reactor internal structural members located in high-flux regions, including the shroud, are constructed of 304 stainless steel which does not suffer from irradiation embrittlement. It does experience hardening and an apparent loss in uniform elongation but its reduction in area is not changed. Since the reduction in area is the property which relates to tolerable local strain, it can be concluded that irradiation can generally be ignored. However, even on the basis of changes in the total elongation, one would conclude that this material at 2.7 x 10^{20} nvt integrated flux would be capable of about 15 — 20% elongation.

The strain range of 0.57% was calculated at the midpoint of the shroud which is the zone of highest neutron irradiation. The value of 0.57% strain range was determined by dividing the calculated stress range of 155,700 psi (peak surface stress) by the modulus of elasticity for Type 304 stainless steel which was assumed to be 27.5 x 10^6 psi. The calculated strain range of 0.57% represents a considerable margin of safety below measured values of percent reduction in area (which is the property that relates to tolerable local strain) for annealed Type 304 stainless steel irradiated to 1 x 10^{21} nvt (greater than 1 MeV). The value of percent reduction in area for Type 304 stainless steel reported in Reference 14 is a minimum of approximately 38% for a temperature of 550°F and neutron flux of 1 x 10^{21} nvt (greater than 1 MeV) and in Reference 15 a reduction in area of 52.5% is reported for a temperature of 750°F and neutron flux of 6.9 x 10^{21} nvt (greater than 1 MeV). At lower values of temperature or neutron flux, the percent reduction in area is generally even higher. Therefore, thermal shock effects on the shroud at the point of highest irradiation level will not jeopardize the proper functioning of the shroud following the design basis accident (DBA).

3.9.5.3.3 Thermal Shock Effects on Reactor Vessel Components

Several high stress points on the reactor vessel have been analyzed approximately and conservatively to determine the effects of LPCI cold water injection. The points examined are as follows:

1. Recirculation inlet nozzle,
2. Midcore inside of vessel, and
3. Control rod drive penetration.

The results on the recirculation nozzle are as follows:

	Sleeve	Nozzle
Amplitude of alternating stress	595,000 psi	215,000 psi
Allowable ASME Section III cycles	12	130
Maximum strain range	4.5%	1.6%

The results at midcore inside of vessel are 67,500 psi peak stress. More than 1000 such cycles would be imposed under ASME Section III fatigue criteria. The total maximum vessel irradiation (greater than 1 MeV) at this point has been found to be 2.4×10^{17} nvt which is below the threshold level of any nil ductility temperature (NDT) shift for the vessel material. Therefore, irradiation effects can be ignored at all locations on the vessel.

The results on the control rod drive penetration are:

Amplitude of alternating stress	560,000 psi
Allowable ASME Section III cycles	14
Maximum strain range	3.7%

3.9.5.3.4 Seismic Loading

A dynamic analysis was performed which determined the seismic responses of the Dresden Unit 2 reactor internals. The methods, approximations, and computer programs used in this analysis are detailed in a report by GE Atomic Power Equipment Department.(16)

The nuclear steam supply system of Dresden Unit 2 was modeled with lumped mass configurations. The internals model included the following components: shroud. CRD housing, top guide and core plate, fuel, guide tubes, separators, dryer, and vessel head in addition to the flanges, vessel skirt, standpipes, pedestal, shield wall. building, foundation, and the vessel itself. Not included in the mathematical model were light components such as jet pumps, incore guide tube and housing, spargers and their supply headers. Representative damping values used were reinforced concrete structure, 5%; reinforced or prestressed concrete primary containment structure, 2%; vessel and skirt, 1%; shroud, 1%; fuel, 7%; guide tubes, 1%; and control rod drive, 1%.

The maximum seismic shears and moments of reactor internals due to their respective SSEs were determined. These were used to determine the adequacy of the component design.

3.9.6 Inservice Testing of Pumps and Valves

Presently, inservice testing (IST) of pumps and valves is governed by the Third 10-Year Interval IST Program which will remain in effect through February 28, 2002. The IST program was developed in response to the requirements of 10 CFR 50.55a.

In accordance with 10 CFR 50.55a, IST programs are updated at 10-year intervals to incorporate the provisions of newer editions of ASME Section XI. Specifically, the regulation requires that IST program revisions meet the requirements (to the extent practical) of the latest ASME Code edition and addenda incorporated by reference in Paragraph (b) of 10 CFR 50.55a 12 months prior to the start of the 10-year inspection interval. The current IST program is based upon the requirements of the 1986 Edition of Section XI, consistent with the requirements of 10 CFR 50.55a.

The construction permits for Dresden Units 2 and 3 were issued on January 10, 1966, and October 14, 1966, respectively. At that time the ASME Code covered only nuclear reactor vessels and associated piping up to and including the first isolation or check valve. Piping, pumps, and valves were built primarily to the Power Piping Code rules of USAS B31.1. Consequently, the Dresden IST program contains no ASME Code Class 1, 2, or 3 designed systems. The system classifications used as a basis for the IST program are based on the requirements given in 10 CFR 50.55a(g) and Regulatory Guide 1.26, and were developed for the sole purpose of assigning the appropriate IST requirements. Components within the reactor coolant pressure boundary (RCPB), as defined in 10 CFR 50.2, are designated as Inservice Inspection (ISI) Class 1 while other safety-related components are designated as ISI Class 2 and 3 in accordance with the guidelines of Regulatory Guide 1.26. Pursuant to 10 CFR 50.55a(a)(1), IST requirements of Section XI of the ASME Code are then assigned to these components, within the constraints of existing plant design.

The extent of the Class 1, 2, and 3 designations for systems or portions of systems subject to the IST requirements are identified on the Dresden Piping and Instrumentation Diagrams (P&ID). In accordance with Regulatory Guide 1.26, the IST boundaries on the P&ID are limited to safety-related systems which contain water, steam, or radioactive materials.

Inservice inspection and testing of the reactor coolant pressure boundary is addressed in Section 5.2.4. Table 5.2-3 provides a listing of the ISI classification for various plant systems. Inservice inspection for Class 2 and 3 components is discussed in Section 6.6. Preservice inspection and testing of pumps and valves is discussed in Chapter 14.

3.9.6.1 Inservice Testing of Pumps

The inservice testing program for ISI Class 1, 2, and 3 pumps meets the requirements for Subsection IWP of Section XI of the ASME Code, 1986 Edition. Where these requirements were determined to be impractical, specific requests for relief have been approved by the NRC.

The IST program establishes the requirements for inservice testing to assess the operational readiness of certain centrifugal and positive displacement pumps used in nuclear power plants. The pumps covered are those that are provided with an emergency power source, which are required in shutting down the reactor to the cold shutdown condition, maintaining the cold shutdown condition, or mitigating the consequences of an accident. In addition to ISI Class 1, 2, and 3 pumps, some safety-related pumps and some nonsafety-related pumps have been included in the IST program at the request of the NRC.

3.9.6.2 Inservice Testing of Valves

The IST program for ISI Class 1, 2 and 3 valves meets the requirements of Subsection IWV of Section XI of the ASME Code, 1986 Edition. Where these requirements were determined to be impractical, specific requests for relief have been approved by the NRC.

The IST program establishes the requirements for IST to assess the operational readiness of certain valves and pressure relief devices (and their actuating and position indicating systems). The valves covered are those which are required to perform a specific function in shutting down the reactor to the cold shutdown condition, in maintaining the cold shutdown condition, or in mitigating the consequences of an accident. The pressure relief devices covered are those for protecting systems, or portions of systems, which are required to perform a specific function in maintaining the cold shutdown condition, or in mitigating the consequences of an accident. In addition to ISI Class 1, 2, and 3 valves, some safety-related valves and some nonsafety-related valves have been included in the IST program at the request of the NRC.

3.9.7 References

1. General Electric Company Report SASR 87-36, "Thermal Cycle Counting Procedure for Dresden Units 2 and 3 and Quad Cities Units 1 and 2", July 1987.

2. General Electric Company Report SASR 89-111, "Tabulation of Thermal Cycles for Dresden Nuclear Power Stations Units 2 and 3, "Rev. 2, November, 1990.

3. V.R. Wetzel, C.S. Duckwald, and M.A. Head, "Vibration Analysis and Testing of Reactor Internals," APED-5453, April, 1967.

4. J.E. Corr and E. Kiss, "Flow-Induced Vibration for Light Water Reactors," GEAP-22274, DOE/ET/34209-32, March 1983.

5. "Mark I Containment Long-Term Program," Safety Evaluation Report, USNRC, NUREG-0661, July 1980; Supplement 1, August 1982.

6. "Mark I Containment Program Structural Acceptance Criteria Plant Unique Analysis Applications Guide," Task Number 3.1.3, Mark I Owners Group, General Electric Company, NEDO-24583, Revision 1, July 1979.

7. United States Nuclear Regulatory Commission Inspection and Enforcement Bulletin 79-14 July 2, 1979 Issue with Supplements of August 15, 1979 and September 7, 1979.

8. Impell Corporation, Report No. 01-0590-1275, Revision O, "Dresden Unit 2 Summary Report of IE 79-14 Evaluations, Plant Accessible Piping Excluding Safe-Shutdown Scope, March 1984"; Report No. 01-0590-1274, Revision O, "Dresden Unit 3 Summary Report of IE 79-14 Evaluations, Plant Accessible Piping Excluding Safe-Shutdown Scope, April 1984"; Report No. 04-0590-0023, Revision 2, "Dresden Unit 2 Summary Report of IE 79-14 Evaluations, Inaccessible Piping"; Report 01-0590-1281, Revision 1, "Dresden Unit 3 Summary Report of IE 79-14 Evaluations, Inaccessible Piping," March 1984.

9. "Mark I Containment Program Load Definition Report," General Electric Company, NEDO-21888, Revision 2, November 1981.

10. "Mark I Containment Program Augmented Class 2/3 Fatigue Evaluation Method and Results for Typical Torus Attached and SRV Piping Systems," MPR Associates, Inc., MPR-751, November 1982.

11. Dresden Unit 3 Plant Design and Analysis Report, Amendment No. 5, Description and Evaluation of Dresden Unit 3 Emergency Core Cooling Provisions, July 26, 1966.

12. "BWR Feedwater Nozzle and Control Rod Drive Return Line Nozzle Cracking," NUREG-0619, November 1980.

13. "Design and Performance of G.E. BWR Jet Pumps," General Electric Company, APED-5460, September 1968.

14. "The Effects of Radiation on Structural Materials," ASTM Special Technical Publication No. 426, ASTM, Philadelphia, Pa., 1966, pages 278-327.

15. L.A. Waldman and M. Doumas, "Fatigue and Burst Tests on Irradiated In-Pile Stainless Steel Pressure Tubes," Nuclear Applications, Vol. 1, October 1965.

16. "Seismic Analysis of Reactor Internals for the Dresden II Plant," General Electric Company Atomic Power Equipment Department, December 1968.

Table 3.9-1

SUMMARY OF DESIGN BASIS, PREDICTED, AND ALLOWABLE THERMAL CYCLES FOR THE REACTOR PRESSURE VESSEL

Cycle Description	Units 2 and 3 Original Design Basis Allowable(1)	Unit 2 Cycle Prediction Year 40(2)	Unit 3 Cycle Prediction Year 40(2)	Units 2 and 3 New Design Basis Allowable(3)
Plant cooldown(4)	119	293	263	293
Plant heatup(4)	120	297	266	298
Safety relief valve blowdown(4)	1	3	0	5
Reduction of power for plant shutdown(4)	119	158	111	159
Turbine roll with feedwater injection(4)	120	154	107	160
Head spray injection(4)	119	15	23	119
Loss of feedwater heaters — full(4)	80	9	11	114
Loss of feedwater heaters — partial(4)	80	16	41	80
Loss of feedwater flow(4)	80	10	12	80
Scram(4)	200	248	242	294
Turbine Trip(4)	40	78	73	NA(6)
Batch feedwater addition during hot standby or plant cooldown(4)	595	40	72	122
Reduced power operation, 75%—100%	NA	NA	NA	10,000(5)
Reduced power operation, 50%—75%	NA	NA	NA	2,000(5)
Vessel pressure test to 1250 psig	NA	NA	NA	130

Table 3.9-1 (Continued)

SUMMARY OF DESIGN BASIS, PREDICTED, AND ALLOWABLE THERMAL CYCLES FOR THE REACTOR PRESSURE VESSEL

Cycle Description	Units 2 and 3 Original Design Basis Allowable[1]	Unit 2 Cycle Prediction Year 40[2]	Unit 3 Cycle Prediction Year 40[2]	Units 2 and 3 New Design Basis Allowable[3]
Improper start of shutdown recirculation loop	NA	NA	NA	10
Sudden start of recirculation loop	NA	NA	NA	10
Overpressure up to 1250 psig	NA	NA	NA	1
Overpressure up to 1375 psig	NA	NA	NA	1
Bolt-up	NA	NA	NA	123
Unbolt	NA	NA	NA	123

Notes:

1. Original cycles formed the original basis for Dresden design. These were the originally analyzed values.

2. Predicted cycles for each unit are based upon extrapolating actual counted cycles through October 1989 over the full 40 year plant life and are thus predictions of the actual cycles that each unit will experience.

3. New design basis allowables provide new basis for Dresden design and envelop the predicted cycles for both units.

4. Cycles reviewed by General Electric (GE).

5. There is no impact on vessel fatigue from reduced power operation cycles. These cycles are counted as a means of tracking the impact of economic generation control (EGC) on rapid thermal cycling fatigue.

6. Turbine trip cycles are counted as either Loss of Feedwater Heater events or scram events, so an allowable is not applicable.

Table 3.9-2

REACTOR PRESSURE VESSEL INTERNALS
VIBRATION MEASUREMENTS LOCATION AND DIRECTION

		Quantity		
		Cold Flow Tests	Power Operation Tests	Type
1.	Four Control Rod Guide Tubes Measure axial strain in center of span, 129" level, at 2 points 90° apart (±45°).	4		SG
2.	Four Incore Guide Tubes Measure axial strain at approximately 167" level, for 2 points 90° apart (±45°).	4		SG
3.	Four Fuel Channels Measure axial strain at 2 levels, 288" and 327", in the center of the 2 faces adjacent to the control rod for each fuel channel.	8	4[1]	SG
4.	Core Plate Measure acceleration in three directions vertical and horizontal at 0° and 90°. Mount triaxial array of sensors of temporary fuel nozzle plugs near the center of the core.	3		A
5.	Shroud Measure the horizontal displacement of the shroud at the flange, 385" level, at the four locations 8°, 98°, 188° and 278°. (Tangential motion of shroud OD preferred.)	4	4	D
6.	Separators Measure the horizontal displacement of the separator assembly at the 557" level by measuring the relative displacement of the outer ring with respect to the vessel wall at 8°, 188°, and 278°. (Tangential motion of the ring preferred.)	4	4	D

Table 3.9-2 (Continued)

REACTOR PRESSURE VESSEL INTERNALS
VIBRATION MEASUREMENTS LOCATION AND DIRECTION

		Quantity		
		Cold Flow Tests	Power Operation Tests	Type
7.	Recirculation Loops	6[2]		A
	Measure the horizontal motions of the following sections in the recirculation loops. The motion is to be measured in directions radial and tangential to the pressure vessel.			
a.	Suction line at -64" level	12[2]		M[2]
b.	Pump body at -252" level	12[2]		M[2]
c.	Top of pump motor at -84" level	12[2]		M[2]
d.	Inlet manifolds at 3 azimuth locations each and also including vertical direction.	12[2]		M[2]
8.	Jet Pumps			
	Measure the horizontal relative displacement at the following locations:			
a.	Top of riser pipe to pressure vessel at ±45° directions in pipe (referenced to vessel radial)	2		D or SG
b.	Top of jet pump throat to pressure vessel wall. Make measurements on both pumps in the pair attached to riser in a. above	2		D
c.	Across slip joint between throat and diffuser at ±45° directions (referenced to vessel radial). Make measurements on both pumps as in the pair of b. above	4		D
d.	Top of diffuser to pressure vessel at ±45° directions in diffuser. On same diffuser as c. above	4		D
e.	One sensor on each of 5 (1 riser for 2 pumps) assemblies.	5	2[1]	D

Table 3.9-2 (Continued)

REACTOR PRESSURE VESSEL INTERNALS
VIBRATION MEASUREMENTS LOCATION AND DIRECTION

	Quantity		
	Cold Flow Tests	Power Operation Tests	Type
9. Differential Pressures (Dynamic 0 — 100 Hz)			
Measure the differential pressures at the following locations:			
a. Across the jet pump mounting ring, 123" level	1	1	
b. Across the core plate by using a spare fuel nozzle plug, 207" level	1		
c. Across the shroud head, 416" level	1	1	

SG = strain gauge
A = accelerometer
D = linear differential transducers

Notes:

1. The measurement points used were selected after a study of the cold-flow test results. They were the most active gauges on the two channels.

2. The 12 points here are locations that were by covered by a manual survey using a portable vibration meter "M." The six points shown are selected locations from the manual surveys and were displayed on the chart recorder.

Table 3.9-18

RPV INTERNALS PRESSURE DIFFERENTIAL
DUE TO RECIRCULATION LINE RUPTURE

Major Component	Maximum dP (psi)	Design Capability dP (psi)[1]
Shroud Support[2]	25 (initial)	100
Guide Tube	17 (initial)	68
Lower Shroud[2]	25 (initial)	185
Upper Shroud[2]	7 (initial)	185
Core Plate	17 (initial)	50
Shroud Head Assembly	9	25

JCS
7/1/94

Notes:

1. This is the pressure differential consistent with ASME Code allowable stresses. For primary loading, considerably higher differentials can be sustained before failure.

2. Core cooling dependent.

Table 3.9-19

RPV INTERNALS PRESSURE DIFFERENTIAL DUE TO STEAM LINE BREAK

Major Component	Maximum ΔP (psi)	Design Capability ΔP (psi)[1]
Shroud Support	30	100
Guide Tube	20	68
Lower Shroud	30	185
Upper Shroud	12	185
Core Plate	20	50
Shroud Head Assembly	12	25

5/1/94

Notes:

1. Capability within ASME Code allowable stresses. For primary loading, considerably higher differentials can be sustained before failure.

Table 3.9-20

RPV INTERNALS PRESSURE FORCES

Major Component	Pressure Force	Initial Value (psi)
Shroud Support	P_1-P_4	25
Guide Tube	P_1-P_3	17
Core Plate	P_1-P_3	17
Lower Shroud	P_1-P_4	25
Upper Shroud	P_3-P_4	7
Shroud Head Assembly	P_3-P_4	7
Jet Pump Diffuser	P_1-P_4	25

Notes:

1. Refer to Figure 3.9-5 (BWR Internal Configuration) for location of pressure nodes.

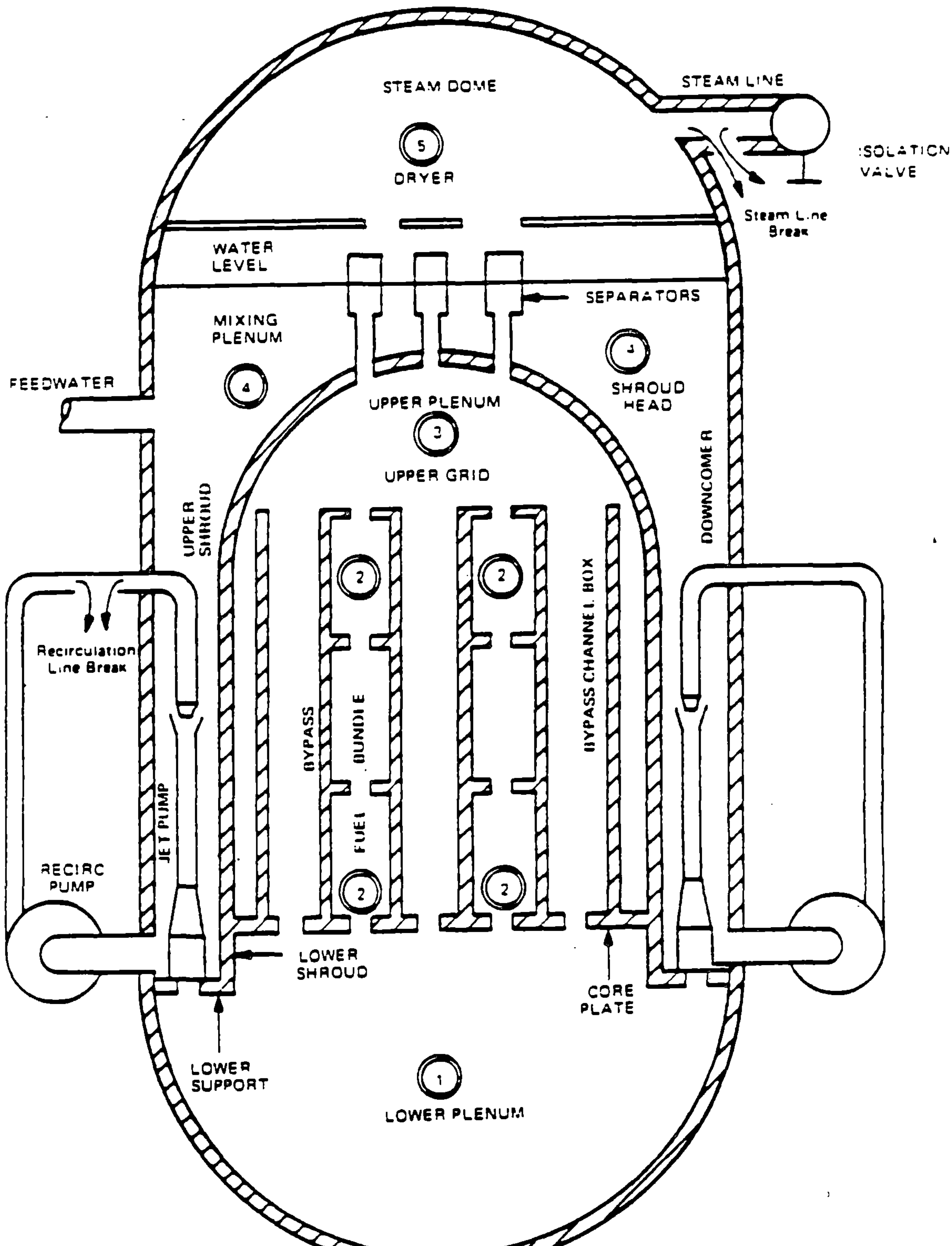

DRESDEN STATION UNITS 2 & 3
BWR INTERNAL CONFIGURATION WITH JET PUMP
FIGURE 3.9-5

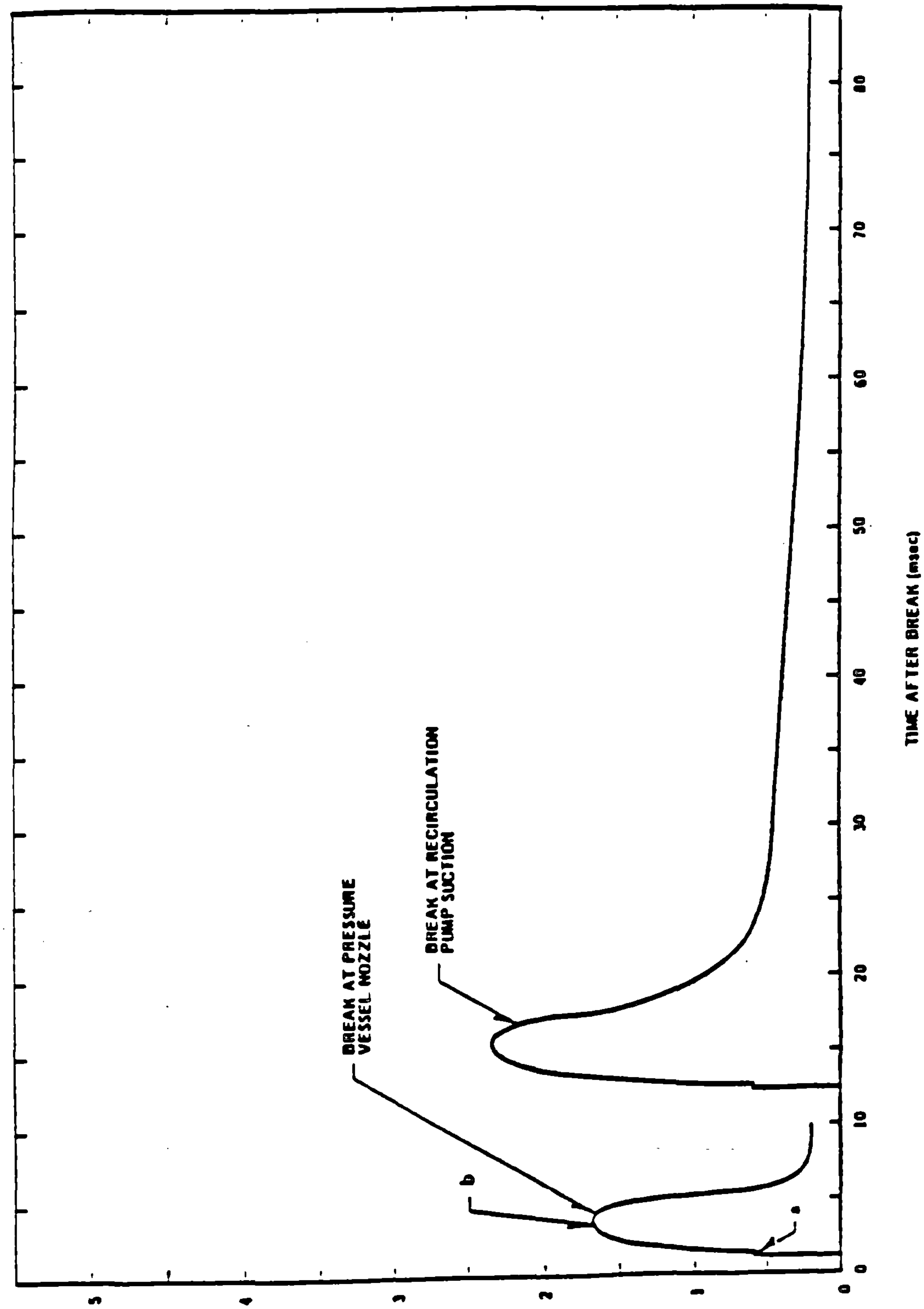

DRESDEN STATION
UNITS 2 & 3

REACTOR VESSEL SHROUD FORCE FOLLOWING RECIRCULATION LINE BREAK

FIGURE 3.9-6

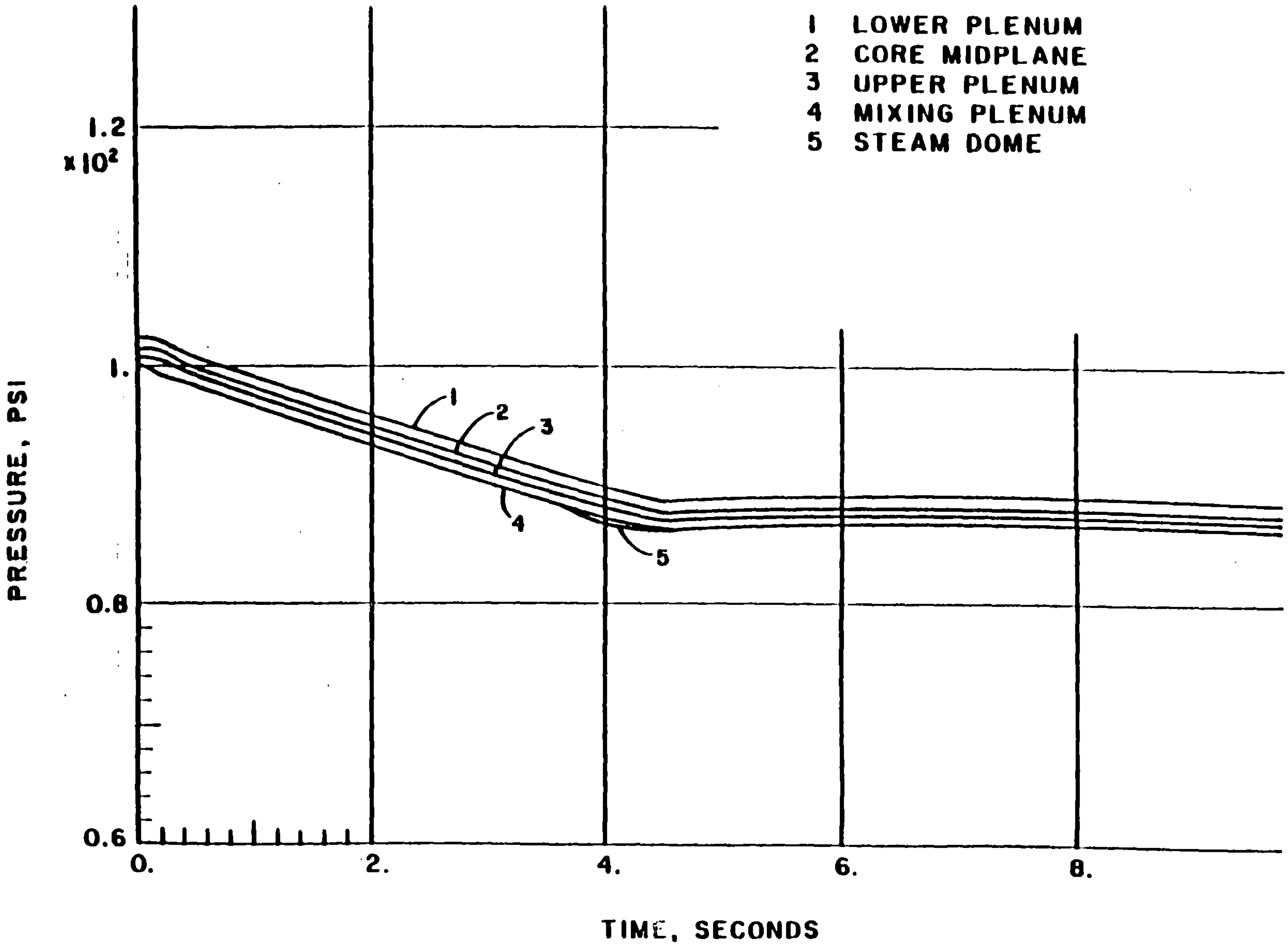

DRESDEN STATION
UNITS 2 & 3
BLOWDOWN TRANSIENT REACTOR PRESSURE FROM 2527 MWt
FIGURE 3.9-7

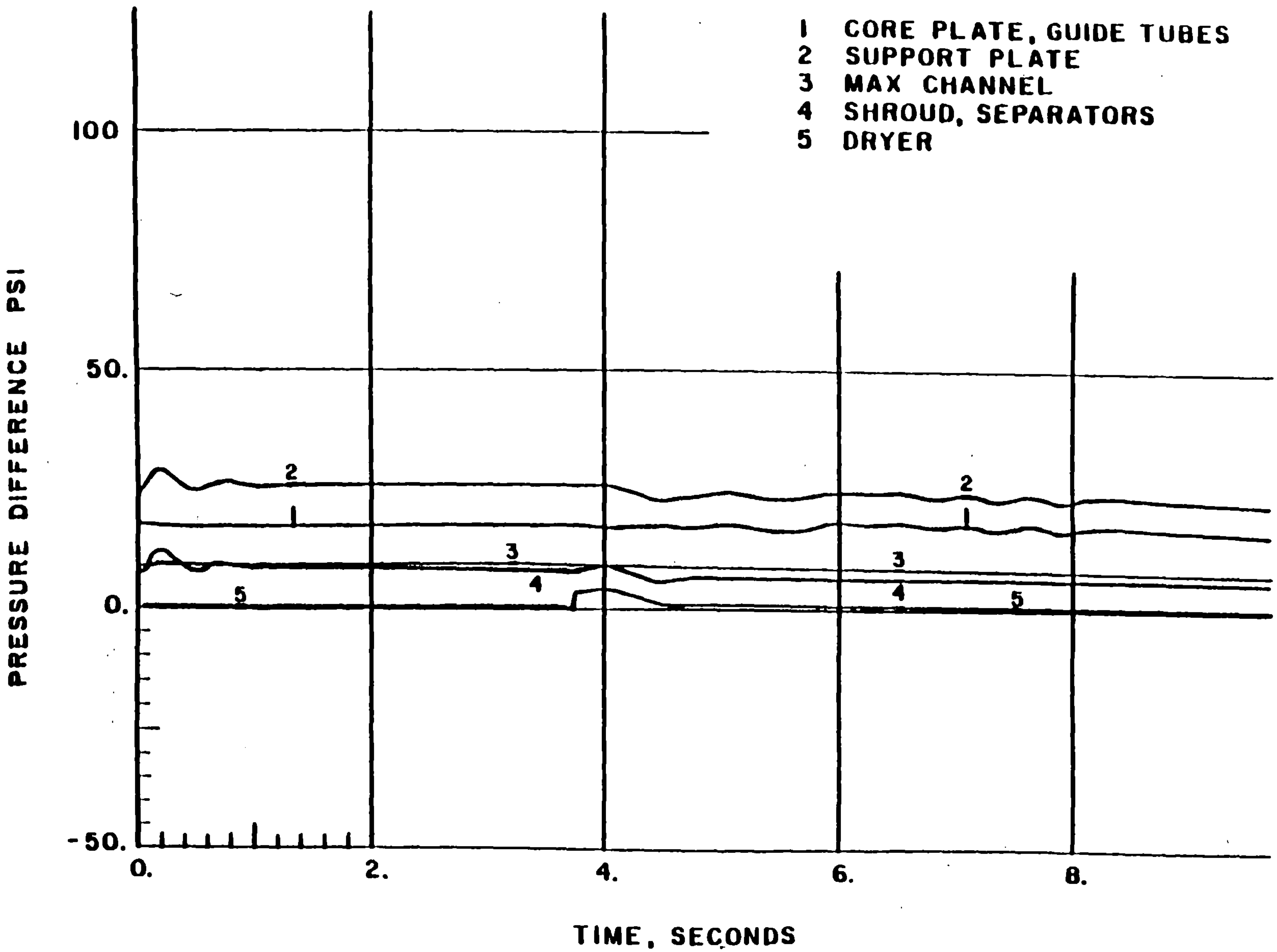

DRESDEN STATION
UNITS 2 & 3

BLOWDOWN TRANSIENT REACTOR
DIFFERENTIAL PRESSURE FROM 2527 MWt

FIGURE 3.9-8

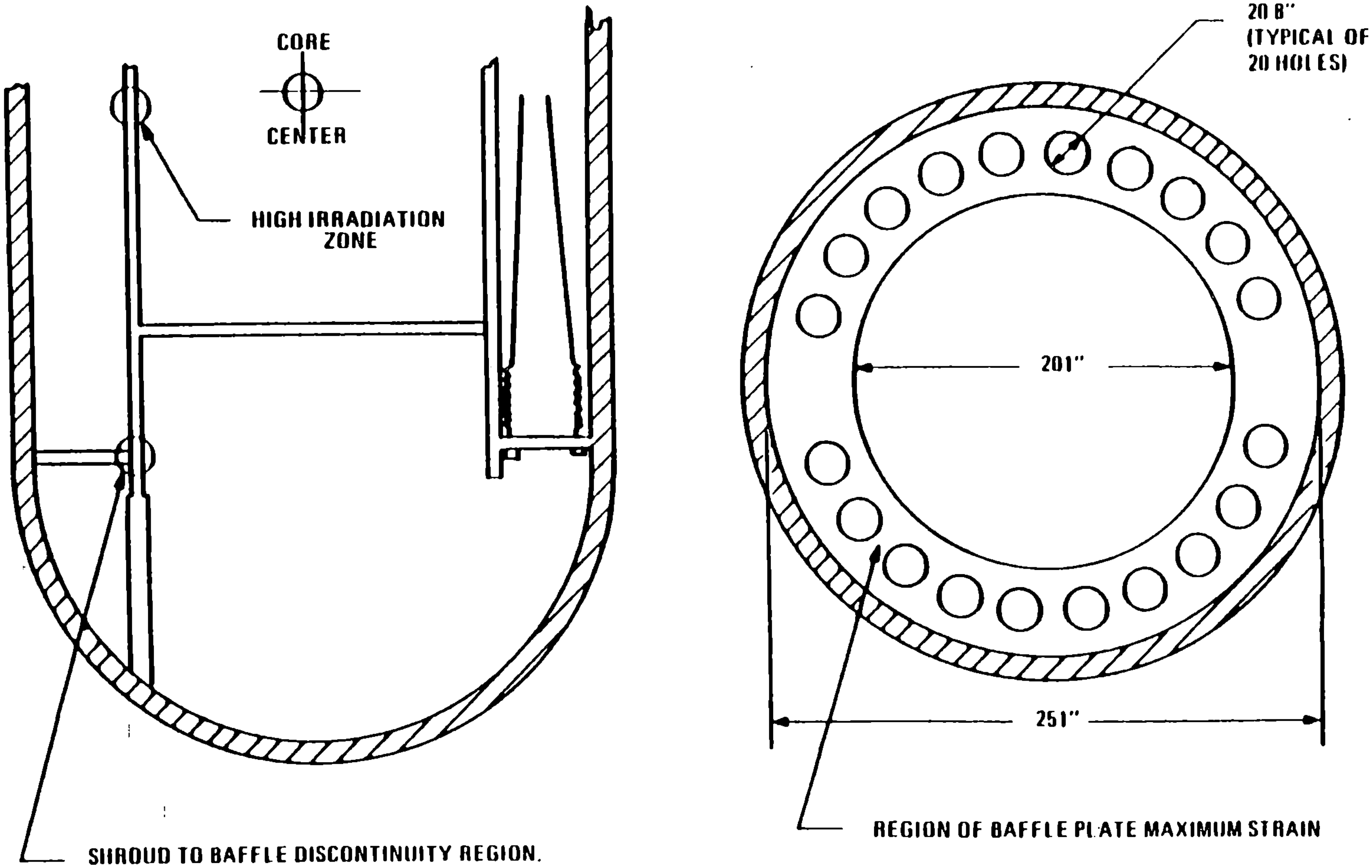

DRESDEN STATION
UNITS 2 & 3
REACTOR INTERNAL BAFFLE PLATE
LIGAMENT STRAIN STUDY

FIGURE 3.9-9

SAFETY ASSESSMENT

BWR SHROUD CRACK INDICATIONS

Prepared for the BWR Owners' Group
by GE - Nuclear Energy

H. Choe
L. B. Claassen
E. C. Eckert
M. L. Herrera
J. S. Post
G. L. Sozzi
G. B. Stramback
W. A. Zarbis

Executive Summary

This document provides information to address for all Boiling Water Reactors the safety significance of the circumferential crack indications in the heat-affected zone of the top guide support ring weld of the core shroud assembly. The report concludes that the observed phenomenon does not represent a threat to the safe operation of the plant.

The shroud provides a partition between the core region and the downcomer annulus to separate the upward flow of core coolant from the downward recirculation flow. The shroud is not a primary pressure boundary component.

The shroud is made of ductile material with high toughness properties even after accounting for any effects due to neutron fluence, while the applied loads on the shroud are generally small. The combination of ductility and low stresses makes the shroud extremely flaw tolerant.

Assuming 360 degree circumferential cracking, and utilizing ASME Code safety factors, crack depths of up to an average of 90% of the shroud thickness can be tolerated while maintaining the structural integrity for normal operation and postulated accident conditions (the worst observed crack indications are an average of about 60% of the shroud thickness). Even with only 10% thickness remaining, the ASME Code safety margins are maintained.

Should significant through-wall cracking occur, it would be detected during normal operation using existing instrumentation and normal plant shutdown could be initiated. Even under very conservative assumptions, safe reactor shutdown is achieved automatically and adequate core cooling is provided, with manual backup available using the existing Emergency Operating Procedures.

Acknowledgment

This report is the result of the collaborative efforts of the BWR Owners' Group and GE - Nuclear Energy. The valuable input received from the BWR Owners' Group utility members is worth noting.

1.0 Introduction

Circumferential and axial crack indications have been reported at various locations in the core shroud assembly of a BWR/4 located in the US. The circumferential crack indications located in the inside surface in the heat-affected zone of the top guide support ring horizontal weld (referred to as the H3 weld) are of the most interest because they appear to extend 360 degrees around the circumference of the shroud. GE Services Information Letter 572, Revision 1 has been issued to assist utilities in their individual evaluation of this situation. The USNRC has also issued Information Notice 93-79.

This document provides information for all Boiling Water Reactors (BWRs) to address the safety significance of the concerns related to crack indications of the H3 weld. A generic shroud cracking evaluation procedure, which will describe the process for performing detailed plant-specific evaluations of the shroud, is being prepared under the sponsorship of the BWR Owners' Group.

2.0 Summary and Conclusions

Crack indications near the H3 weld do not represent a threat to the safe operation of a plant:

1. The combination of ductile material and low stresses makes the shroud extremely flaw tolerant. Assuming 360 degree circumferential cracking, and utilizing ASME Code safety factors, crack depths of up to an average of 90% of the shroud thickness can be tolerated while maintaining the structural integrity for normal operation and postulated accident conditions (the worst observed crack indications are an average of about 60% of the shroud thickness). Even with only 10% thickness remaining, the ASME Code safety margins are maintained.

2. The probability of postulated separation of the top guide assembly from the shroud is negligible. A more likely but still improbable scenario would be that the crack grows through the shroud and allows some flow to be bypassed from the core to the downcomer. If it is postulated that the average crack depth is greater than 90% and significant leakage flow occurs, it would be detected during normal operation using available instrumentation. The operator would initiate a normal shutdown.

3. In the unlikely occurrence of a design basis accident or seismic condition with undetected 360 degree circumferential cracking up to an average of greater than 90% of the shroud thickness, but with the top guide assembly still attached to the shroud, safe reactor shutdown is achieved and adequate core cooling is available. In the unlikely scenario that the shroud mechanical integrity is severely distorted such that complete control rod insertion does not occur, current Emergency Operating Procedures adequately direct the operator to use the Standby Liquid Control System to shut down the reactor, and to maintain other aspects of safe shutdown.

3.0 Shroud and Top Guide Functions

The shroud support and shroud make up a stainless steel cylindrical assembly that provides a partition between the core region and the downcomer annulus to separate the upward flow of coolant through the core from the downward recirculation flow. The shroud also provides (in conjunction with other components) a floodable region following a postulated recirculation line break. The shroud is not a primary pressure boundary component.

The top guide consists of a circular grid plate with square openings secured to the bottom of the top guide cylinder. Each opening provides lateral support and guidance for four fuel assemblies or, in the case of peripheral fuel, less than four fuel assemblies.

4.0 Shroud Structural Evaluation

Crack indications have been observed in various locations of the shroud. The circumferential crack indications located in the inside surface of the heat-affected zone for the top guide support ring horizontal weld are of the most potential significance because they appear to extend 360 degrees around the circumference of the shroud. The vertical welds in the top guide support ring are relatively short (on the order of a couple of inches) compared to the length of the horizontal weld and therefore are not of concern.

4.1 Characteristics of the Crack Indications

While the extent of the crack indications that have been reported at the BWR/4 plant is significant, there remains sufficient structural strength in the components to meet their intended function. Testing demonstrates that the shroud and support ring are made of ductile material with high toughness properties even after accounting for any effects due to neutron fluence. The applied loading on the shroud is mainly from the differential pressure during normal operation and the transient differential pressure increase due to design basis accident loading and design basis seismic loads. The applied load during normal, high power (>~ 80%) operation is in the upward direction. The accident and seismic loads are generally small relative to the Code allowable loads and well within the remaining structural integrity of the shroud.

The combination of high ductility and low applied stresses makes the shroud extremely flaw tolerant. In fact, it can be shown that through-wall cracking of over 50% of the shroud circumference can be tolerated while maintaining normal ASME Code allowable design safety factors. Typical allowable flaw sizes range from 75 - 110 inches for each 90 degree sector of the shroud (the length of a 90 degree sector is plant-specific but typically about 150 inches). If 360 degree circumferential cracking is postulated, an allowable flaw size of up to an average of 90% of the thickness can be tolerated with sufficient remaining industry-accepted Code margins. Even if the crack depth is greater than 90% of the shroud thickness (up to the "critical flaw size", with no additional safety factor), the full design basis and seismic loads can be accommodated.

4.2 Potential for Further Structural Degradation

Even if relatively deep cracks occur, it is important to consider the nonuniformity of the crack growth around the circumference. Because of differences in sensitization, fluence, cold work and weld residual stresses around the circumference, uniform crack growth at different crack locations is not expected. This means that any further crack growth will not be uniform and the growth rate will be higher at some locations than others. Even if the growth continues until it is through-wall, this would only occur at selected locations (similar to the leak before break scenario in piping). Under the core internal pressure load, this would lead to a crack opening and leakage from the core. Leakage due to significant cracking will relieve the differential pressure loading and retard the subsequent crack growth rate. While the exact amount of leakage is difficult to predict, the fact remains that if leakage occurs (especially when the remaining ligament is small) it will eventually lead to detection as described in Section 5.0.

In summary, the low stresses and high material ductility make postulation of a 360 degree crack leading to separation of the top guide assembly from the shroud extremely unrealistic.

5.0 Normal Operation

As discussed in the preceding section, the postulated separation of the top guide assembly from the shroud is an extremely low probability event. A more likely but still improbable scenario would be for the crack to create some flow from the core region to the downcomer.

If separation of the top guide and shroud assembly did occur during normal operation, the upward displacement of the top guide and shroud assembly would be less than a few inches, and the core assembly and fuel bundle orientation would be held intact. Moreover, flow through the resulting gap would be detected during normal operation by the reactor operator using available instrumentation for monitoring reactor performance, as described below.

If the crack and leakage occurred on one side of the shroud only, the indications would be asymmetrical which would facilitate detection. The process computer calculations of power/flow operating conditions would not match expected conditions. Additionally, for example, differences will develop in the relationships between recirculation drive flow to core flow and in power level relative to the core flow. If the leakage flow is large enough, those plants with recirculation loop cavitation monitoring instruments will indicate low subcooling of recirculation loop fluid, while all plants should indicate higher than normal recirculation loop temperature(s).

After detecting such an anomaly, a normal shutdown would be initiated until the cause of the anomaly is found and corrected.

Analogous situations have previously been observed in BWRs. In 1984, a plant began startup with shroud head bolts improperly engaged, resulting in bypass flow paths similar to those that would result from through-wall cracking of the shroud. A similar situation also occurred at a different plant in 1991. In both cases, anomalies such as those described above were detected and the operators shut the plant down.

6.0 Anticipated Operational Events Related to Increased Shroud Head Pressure Loads

The previous sections demonstrate that postulated cracks that grow through the shroud wall or cause complete separation of the top guide from the shroud are improbable, but should either occur it would be detectable during normal operation. Assuming there are no indications of shroud leakage, this section discusses anticipated operational occurrences that could increase shroud loads above those experienced during normal operation: pressure regulator failure - open, recirculation flow control failure - increasing to maximum flow, and inadvertent actuation of the Automatic Depressurization System (ADS).

6.1 Pressure Regulator Failure - Open

This postulated Safety Analysis Report (SAR) event involves a failure in the pressure controls such that the turbine control valves and the turbine bypass valves are opened as far as the maximum combined steam flow limit allows. For units with standard bypass capacity (about 25% of rated steam flow), the worst case involves inadvertently increasing the steam flow to about 130% of rated. This is also true for units with larger bypass capacity if the steam flow limit is set at 130% or less. A depressurization and cooldown occurs which is isolated by Main Steamline Isolation Valve (MSIV) closure. This steam flow increase is small enough that the increased force on the shroud head (about 50% above the normal pressure drop) is within the load capability of the shroud as discussed in Section 4.0.

6.2 Recirculation Flow Control Failure

This postulated event involves a recirculation control failure that causes all recirculation loops to increase to maximum flow. In this type of case, the pressure drop could change from a part-load condition to the high/maximum flow condition over a time period of about 30 seconds, but it should not significantly exceed the pressure drop expected for normal full power, high core flow operating conditions. Normal operating procedures are considered sufficient to minimize the consequences of this potential transient, and the force on the shroud head is within the shroud capability as discussed in Section 4.0.

6.3 Inadvertent Actuation of ADS

Inadvertent actuation of the ADS valves is another postulated event that could put an increased load on the upper shroud. The maximum steam flow and the depressurization rate are significantly smaller than for the postulated main steamline break, causing a short-term increase in steam flow of about 50% of rated steam flow (plant dependent). The increase in the shroud ΔP resulting from the opening of the ADS valves would occur over a period of about one second, spreading the effect of the change in load. This is also a very low probability event; it is considered to be in the ASME Emergency category in the vessel thermal duty design. The effect of this event is also within the shroud capability as discussed in Section 4.0.

7.0 Design Basis Accidents

Sections 4.0 and 5.0 demonstrate that cracks that might grow through the shroud wall or cause complete separation of the top guide from the shroud are highly improbable, but should either occur it would be detectable during normal operation. Although the combined probability of an accident occurring when a severe (360 degree circumferential crack of uniform depth greater than 90% of the shroud thickness) undetected crack exists is thus very low, such a postulated event is addressed in this section.

The Main Steamline Break Accident imposes the largest potential lifting loads on the shroud head. Liquid breaks (e.g., recirculation line breaks) do not impose large pressure drops on the shroud head, and in fact the shroud pressure drop decreases from its initial value.

7.1 Main Steamline Break

The main steamline break inside primary containment is the postulated worst case because it results in the largest depressurization rate. During this SAR event, the reactor is rapidly depressurized as a result of a postulated instantaneous, double-ended break of the largest steamline. Thus a larger than normal pressure difference could develop across the shroud as fluid flow is drawn from the core region toward the break. If a sufficient ΔP is developed across the top guide support ring weld (H3) area, and sufficient cracking exists, it is postulated that this added differential pressure might cause separation of the shroud leading to an upward displacement of this structure and the associated top guide. The amount of lifting and the potential effect of these postulated occurrences on emergency operation are described below.

One of the key considerations of this postulated accident case is the ability of the control rods to insert before or during the postulated accident. Specifically, sufficient lifting of the top guide prior to control rod insertion could cause reorientation of the fuel bundles and thus the potential to impede the insertion of control rods.

The shroud head pressure drop characteristics calculated for the instantaneous, double-ended steamline break accident were evaluated for a typical BWR. The initial shroud head pressure drop loading is a result of the depressurization of the steam dome region which reduces system pressure overall, but which increases differential pressure across the shroud in the short term. This pressure loading increase is short-lived (less than two seconds) and decreases to below normal steady state loads. Even if the remaining shroud ligament is enough so that significant cracking is undetected, but the ligament is less than an average of 10% (see Section 4.2), the structural integrity of the shroud will remain intact for this postulated limiting event plus seismic loads. If it is even further postulated that the initial load pulse causes the shroud to separate, the last part of the pressure loading could cause the top guide assembly to lift. The flow path created by any separation reduces the upward lifting forces. For this postulated scenario the top guide assembly would remain engaged with the fuel channels.

Scram is initiated during the main steamline break (inside containment) accident by the high drywell pressure trip signal. Drywell pressure exceeds the setpoint almost instantaneously, so the only delays in the rod insertion come from the sensors, the Reactor Protection System, and rod motion. For the main steamline break accident outside containment, shroud loads are reduced, MSIV closure is initiated by high steam flow, and scram is initiated from the MSIV closure.

For either postulated steamline break scenario, the insertion of all control rods will occur. Even if the first loading pulse causes the upper shroud assembly to break free, control rod motion will be started before the upper shroud assembly and top guide lift significantly. It is likely that the top guide will remain engaged with the tops of the fuel bundles. Any control rods that are partially inserted as part of normal operation are already in position to initiate shutdown. Insertion of fully withdrawn control rods to 5% of full stroke will occur by 0.9 second, early enough for the control rods to be moving up between the bundles before any significant lifting of the top guide could take place. The remainder of the insertion will occur because the fuel will remain properly oriented. Reactor shutdown would thus be complete with all drives inserted.

In the very unlikely case that scram may not be complete, the Standby Liquid Control System is available to provide shutdown capability, as discussed in Section 8.0.

Movement of the upper shroud assembly (in the very unlikely case that it occurs) could affect the core spray system if it impacts the core spray line connections. If this were to occur, core spray flow sufficient to provide long term cooling would still be expected. Any one Emergency Core Cooling System (ECCS) pump is sufficient to provide adequate makeup and maintain reactor water level.

The main steamline break has also been evaluated for radiological release consequences in the SAR. For a main steamline break inside of containment, the radiological consequences are bounded by the recirculation line break Loss of Coolant Accident. For the main steamline break outside of containment, the magnitude of the pressure loads that potentially could lead to separation of the upper shroud are less than that for breaks inside the containment, due to attenuation of the depressurization wave along the steamline. Therefore, separation and disengagement of the fuel from the top guide is even more unlikely. Nevertheless, if it is further postulated that the top guide assembly is lifted and then is repositioned on the fuel assemblies, there is a potential to mechanically damage some of the fuel cladding leading to some fission product release within the core. However, assuming closure of the MSIVs within the time permitted by Technical Specifications (typically three to five seconds), this scenario results in MSIV closure before a potential release outside containment from such an improbable scenario could occur. The radiological consequences of this very conservative main steamline break scenario are thus still bounded by the plant SAR results.

7.2 Recirculation Line Break

For the design basis recirculation line break, the differential pressure across the upper shroud decreases from the initial value as the reactor depressurizes, upward forces are reduced, and thus there is no significant threat to core shroud integrity. With the shroud integrity maintained, a floodable core region is also preserved. Therefore, the recirculation line break analysis results are unchanged.

8.0 Operator Actions

The Emergency Procedure Guidelines (EPGs) are the basis for plant specific Emergency Operating Procedures (EOPs). The EPGs are symptomatic in that they respond to detected symptoms and do not require diagnosis of the event by the operator. They address a very wide range of events, both less severe and more severe than the design basis accidents.

The worst postulated event discussed above could result in separation and potential disengagement of the top guide from the fuel channels, which is further postulated to prevent a full scram. This event (a large steamline break with failure to completely insert the control rods) is beyond the design basis of the plant. Nonetheless, it is adequately addressed by EOPs.

The EPGs provide instructions for reactor pressure, water level, and power control, as well as control of key primary containment parameters. Actions specified in the EPGs for reactor power control are to (1) insert control rods using a variety of methods, and (2) initiate the Standby Liquid Control System (SLCS) before pool temperature increases to the allowable value (typically 110 °F). The postulated event would clearly lead to SLCS injection within a very few minutes, resulting in safe shutdown. EPG instructions are for water level to be controlled below the high water level setpoint; thus, there would not be dilution of the liquid boron by flooding to the steamline elevation or loss of vessel inventory out the break.

Water level would be controlled after the postulated event because the break is high in the vessel and a large complement of water injection systems would be available. Separation of the shroud above the top of the fuel channels would not prevent maintaining the core in a flooded condition.

Even if the core spray delivery system were damaged by the shroud or top guide displacement, some core spray flow would be expected. Any one ECCS pump would be sufficient to provide adequate makeup. For some plants, SLCS injection occurs through the High Pressure Core Spray system. For these plants, boron injection would still occur through the spray flow even if the system flow path was changed by the shroud or top guide displacement.

Calculation of Stress in the Core Spray Riser Pipe Due to a lift of 1.5" in the Shroud

+ 1.44" in the CS line bracket (Total lift of 2.94")

Lift =	1.5	in
2R*theta=	71.0	in
2R sin(theta)=	69.5	in
theta/sin(theta)=	1.022	

R	theta	theta/sin(theta)	2R*theta	2R sin(theta)
99.4	0.357	1.022	71.0	69.5

delta = R(1-cos(theta))= 6.3 in

for 6"SCH 40S per Reference 1	pipe ID =	6.065	in	Pipe Dimensions from Mark's Handbook, 8th Edition, Page 8-158
	pipe t =	0.280	in	
	pipe OD =	6.625	in	
	I = Inertia	450.27	in^4	Moment of Inertia = pi/4 (Ro^4-Ri^4)
for 304 SS @ 70°F	E =	2.58E+07	psi	89 ASME Code
	l =	71.0	in	Reference 1 - shorter length is conservative
	a = l/2 =	35.5	in	

W = delta*3EI(l+2a)^2/(-2(l-a)^2*a^3) = -3.9E+07 lbs — Equation from Roark's, 6th Edition, Page 101, Reference no. 1d.

M =2Wa^2/l^3 = -275,049 in-lb

Stress = Mc/I = **-2,023** psi

Reference 1: GE Drawing # 919D906, Rev. 3, "Core Spray Line, Purchase Part," GE - APED, San Jose, CA.

Ref (12)

Calculation of Stress in the Core Spray Riser Pipe Due to a lift of 3.0" in the Shroud +1.44" in the CS line bracket (Total lift of 4.44")

Lift =	3.0 in	
2R*theta=	71.0 in	
2R sin(theta)=	68.0 in	Lenght - lift
theta/sin(theta)=	1.044	

R	theta	theta/sin(theta)	2R*theta	2R sin(theta)
70.3	0.505	1.044	71.0	68.0

	delta = R(1-cos(theta))=	8.8 in	
for 6"SCH 40S per Reference 1	pipe ID =	6.065 in	Pipe Dimensions from Mark's Handbook, 8th Edition, Page 8-158
	pipe t =	0.280 in	
	pipe OD =	6.625 in	
	I = Inertia	450.27 in^4	Moment of Inertia = pi/4 (Ro^4-Ri^4)
for 304 SS @ 70°F	E =	2.58E+07 psi	'89 ASME Code
	l =	71.0 in	Reference 1 - shorter length is conservative
	a = l/2 =	35.5 in	
	W = delta*3EI(l+2a)^2/(-2(l-a)^2*a^3) =	-5.5E+07 lbs	Equation from Roark's, 6th Edition, Page 101, Reference no. 1d.
	M =2Wa^2/l^3 =	-385,118 in-lb	
	Stress = Mc/I =	**-2,833 psi**	

Reference 1: GE Drawing # 919D906, Rev. 3, "Core Spray Line, Purchase Part," GE - APED, San Jose, CA.

April 30, 1994

Input from Ed Gibo

To: H. Choe

From: E. Y. Gibo

Subject: Assessment of CRD Scrammability Due to Dresden Shroud Crack

The following contains my assessment of the CRD scrammability performance in the event of a shroud failure. Per your input, the shroud cracks observed at Dresden is at the bottom end (near the core plate), the allowable displacement is less 2 inches and no lifting occurs during the LOCA events.

Discussion

The significant shroud cracks observed at Dresden have been at the at the lower end, in the vicinity of the core plate. Analysis indicates that a completely circumferential cracked shroud would not lift and no vertical or lateral displacement is anticipated during a LOCA event. Therefore, the proper CRD driveline alignment would be maintained and the scram performance would not be degraded.

During a seismic event, a completely circumferential cracked shroud may lift. Since the lower end of the shroud is in close proximity of the jet pump diffusers, the allowable lateral displacement is limited. Since the core plate is attached to the RPV support cylinder, the fuel supports are maintained in their proper alignment. Normal CRD driveline alignment from the bottom end of the fuel bundles to CRD flange will be maintained and no binding within the CRD mechanisms is anticipated during a scram. However, during a seismic event, the severed shroud assembly may tilt. If the shroud assembly assumes the tilting mode within the confines of the lateral displacement, it is likely that it will be only momentary before the shroud uprights itself. With the subsequent random displacement, the CRD driveline alignment in the core region would undergo periods of misalignment. Hence, the CRD scram speed would assume an oscillatory velocity profile, such as typically anticipated during seismic events. Minimal scram performance degradation is expected under most siesmic events. Under the worst case condition, the control rods is likely to fully insert in less than 7 seconds and reactor shutdown would thus be completed.

Justification for Continued Operation of Dresden-2

1.0 Introduction

Recent inspections at Dresden-3 have revealed 360° cracking in the H-6A region of the core shroud. Dresden-3 will require a full structural repair prior to restart. The concern now is for similar cracking of Dresden-3's sister plant, Dresden-2, i.e., should Dresden-2 be prematurely shutdown prior to the next scheduled outage for an inspection of this same location. As will be documented below, a premature shutdown of Dresden-2 is not technically warranted.

2.0 Justification for Continued Operation

2.1 Electrochemical Potential

It is well documented that the BWR oxidizing environment is more than sufficient to provide the electrochemical driving force for intergranular stress corrosion cracking (IGSCC) of BWR structural materials. In the BWR piping, the ~200 ppb concentration of dissolved oxygen generates an electrochemical potential (ECP) for austenitic stainless steel of ~+100 mV (SHE). The more oxidizing core of the BWR is characterized by an austenitic stainless steel ECP of ~+250 mV (SHE). Also, the conductivity of the BWR coolant is sufficiently high to allow this corrosion reaction to occur.

Over a decade of laboratory and in-reactor investigations have revealed that lowering the ECP of sensitized stainless steel to <-230 mV(SHE) by injecting hydrogen gas into the BWR feedwater and reducing coolant conductivity to <0.3 µS/cm by better BWR water chemistry operational practices would mitigate IGSCC of BWR piping (1). For irradiation stress corrosion cracking (IASCC) of non-thermally sensitized stainless steel, the threshold ECP is ~-140 mV(SHE) (2). Since this process, hydrogen water chemistry (HWC), reduces the "corrosiveness" of the entire BWR coolant, it is considered a "blanket" IGSCC mitigation technique. The results of extensive testing have clearly demonstrated that HWC mitigates environmental cracking in numerous BWR structural materials and has no insuperable materials deleterious effects (1).

Dresden-2 was the first domestic BWR to operate on HWC and has continuously operated on HWC since the middle of 1983. Dresden-3 is a non-HWC BWR. Although the level of hydrogen injected into Dresden-2 ranges from 1.0 to 1.5 ppm (cycles 9 - 14) at ~90% availability (3) is not sufficiently high to completely protect reactor internals from IGSCC or IASCC, it still significantly retards crack propagation. For example, based on ECP measurements at Quad Cities-2 (4), the ECP of the H-6A stainless steel shroud location at Dresden-2 is estimated to be ~-100 mV(SHE) while at the non-HWC Dresden-3 the stainless steel at the same location is estimated to be characterized by an ECP of ~+150 mV(SHE) (4). Assuming identical water qualities of 0.1 μS/cm conductivity, degrees of weld sensitization of 15 C/cm^2 (no effects of irradiation) and a stress intensity of 20 ksi$\sqrt{in}$ (no effects of irradiation) for H-6A, this estimated 250 mV difference in stainless steel ECP results in a factor of ~32 (1.24E-5 vs. 3.92E-7 in/h [108 vs 3 mpy]) decrease in crack growth rate as calculated by the GE PLEDGE IGSCC model (5). Therefore, **all other factors being equal**, any H-6A crack at Dresden-2 would be propagating ~32 times slower than any H-6A crack at Dresden-3 and thus would be significantly shallower even though Dresden-2 has been operating slightly longer than Dresden-3 (April 1970 vs. July 1971).

2.2 Conductivity

An example of the effects of conductivity (sulfate) on crack initiation in uncreviced material is presented in Figure 1 (6-9). It is clear that an increase in sulfate/conductivity results in an acceleration in crack initiation as measured by the constant extension rate test (CERT). A specific example of an acceleration in crack propagation rate (creviced) with sulfate is shown in Figure 2. Figure 2 displays June 1986 Peach Bottom 3 on-line crack monitoring data for sensitized Type 304 stainless steel. The results clearly illustrate the change in crack growth observed after two closely linked water chemistry transients of 4-5 μS/cm, i.e., increases in water conductivity due to intrusions of demineralizer resin material (10). This figure demonstrates the dramatic increase in crack growth rate (2X) with conductivity. Similar on-line crack monitoring results with sulfate have also been documented in the laboratory. Other anions such as chloride, carbonate, etc. have similar kinetic effects on IGSCC initiation and propagation (11-12).

This high conductivity crack initiation and propagation acceleration factor is consistent with the relatively high incidence of IGSCC in creviced Alloy 600 shroud head bolts and access hole covers. Additional documentation on the strong correlation of IGSCC susceptibility with actual BWR plant water chemistry history for creviced BWR components has been published (13).

Based on available data, over the first five cycles of operation Dresden-2 (actually cycles 3 through 7, no information for the first two cycles) and Dresden-3 (cycles 1 through 5) have an average mean conductivity of 0.299 and 0.399 μS/cm, respectively, i.e., Dresden-3's initial average cycle mean conductivity is 0.1 μS/cm higher than Dresden-2's. The average cycle mean conductivity for Dresden-2 (cycles 3 through 14) and Dresden-3 (cycles 1 through 13) are 0.195 and 0.270 μS/cm, respectively. This conductivity comparison clearly suggests that even if no credit is taken for Dresden-2's lower ECP, Dresden-2's lower average mean conductivity would result in a lower crack propagation rate. At a non-HWC environment of ~+150 mV(SHE), a GE PLEDGE model calculation shows a decrease in crack propagation rate of ~1.8 (3.59E-5 vs. 2.04E-5 in/h [314 vs 179 mpy]).

Table 1 presents a summary of BWR water chemistry transients with only limited data obtained after 1983. The table reveals that although Dresden-2 has more documented transients than Dresden-3, all of the Dresden transients are relatively minor and are not expected to alter the relative any of the above evaluations.

2.3 Hydrogen Water Chemistry

Finally, the synergistic effect of conductivity and ECP (HWC) on Dresden-2 and Dresden-3 crack propagation will be compared using the GE PLEDGE model. Figure 3 presents a schematic estimation of Dresden-2 and Dresden-3 crack growth rates as a function of conductivity using PLEDGE. Crack growth rates based on actual conductivity averages for the first five cycles as discussed in Section 2.2 were compared to those averages for the last five cycles (0.1 μS/cm model limit). The ECPs were graphically estimated between 0 and 100 mV(SHE). As noted in Figure 3, a synergistic factor of approximately 32x decrease in crack growth rate is obtained with the unit's decrease in ECP.

3.0 Summary

The above discussion clearly indicates that although the Dresden 2 HWC coolant does not mitigate IGSCC and IASCC of its reactor internals, its long term significantly lower ECP values retard crack propagation by an estimated factor of approximately 30. This lower ECP effect suggests that any defect in the Dresden-2 H-6A weld would be propagating slowly (~3 mpy) and would be significantly shallower as compared to the defects identified in Dresden 3. Dresden-2's H-6A shallow defects and slow growth allows continued operation to the next outage.

4.0 References

1. B. M. Gordon et al, "Hydrogen Water Chemistry for BWRs-Materials Behavior-Final Report," EPRI TR-100304, Palo Alto, CA, February 1992.

2. M. E. Indig et al, "Investigation of the Protection Potential Against IASCC," paper #71 presented at Corrosion 92, NACE, Nashville, April 1992.

3. NRC Meeting with BWROG/GE/EPRI, Rockville, MD, October 10, 1989.

4. M. E. Indig, "Quad Cities-2 Hydrogen Ramping Test," February 21, 1994 (Draft).

5. F. P. Ford et al, "Prediction and Control of Stress Corrosion Cracking in the Sensitized Stainless Steel/Water System," paper 352 presented at Corrosion 85, Boston, MA, NACE, March 1985.

6. W. J. Shack, et al, "Environmentally Assisted Cracking in Light Water Reactors: Semiannual Report April - September 1985," NUREG/CR-4667, ANL-86-31, June 1986.

7. W. J. Shack, et al, "Environmentally Assisted Cracking in Light Water Reactors: Annual Report October 1983 - September 1984," NUREG/CR-4287, ANL-85-33, June 1985.

8. L. G. Ljungberg, D. Cubicciotti and M. Trolle, "Effects of Impurities on the IGSCC of Stainless Steel in High Temperature Water," Corrosion, Vol. 44, No. 2, February 1988.

9. W. E. Ruther, W. K. Soppet and T. F. Kassner, "Effect of Temperature and Ionic Impurities at Very Low Concentrations on Stress Corrosion Cracking of Type 304 Stainless Steel," paper 102 presented at Corrosion 85, Boston, MA, NACE, March 1985, published in Corrosion, Vol. 44, No. 11, November 1988.

10. D. A. Hale and C. G. Diehl, "Real Time Monitoring of Environmental Crack Growth in BWRs", paper 455 presented at Corrosion 88, St. Louis, MO, NACE, March 1988.

11. R. B. Davis and M. E. Indig, "The Effect of Aqueous Impurities on the Stress Corrosion Cracking of Austenitic Stainless Steel in High Temperature Water," paper 128 presented at Corrosion 83, Anaheim, CA, NACE, April 1983.

12. P. L. Andresen, "A Mechanism for the Effects of Ionic Impurities on SCC of Austenitic Iron and Nickel Base Alloys in High Temperature Water," paper 101 presented at Corrosion 85, Boston, MA, NACE, March 1985

13. K. S. Brown and G. M. Gordon, "Effects of BWR Coolant Chemistry on the Propensity for IGSCC Initiation and Growth in Creviced Reactor Internals Components," paper presented at the Third Int. Symp. of Environmental Degradation of Materials in Nuclear Power Systems-Water Reactors, Traverse City, MI, August 1987, published in proceedings of same, TMS-AIME, Warrendale, PA, 1988.

SEVERE TRANSIENTS IN BWRS

04/29/94

RANK	PLANT	MAX COND. uS/cm	pH, min/ max	MAX Cl, ppb	MAX SO4, ppb	POWER LEVEL	DATE yr-mo-d	COMMENTS	REFERENCE	DATA PT
1	AH	182.0	10.6	12000	10000	P	931225	TURBINE BLADE THROUGH CONDENSER, CIRC INTRUSION	BAM QC 6956167	100
2	AG	95.0	4.5	100		P	780307	COND DEMIN RESIN BLEEDTHROUGH	PC&RT 82LDA01	35
3	AG	88.0				P	800802	CONDENSATE DEMIN RESIN INTRUSION	EPRI NP 4134	46
4	AL	84.0	3.2	14500		P	720901	CONDENSER LEAK, DEMIN DEPLETED	PC&RT 82LDA01	6
5	ND	72.0		560		P	660820		PC&RT 82LDA01	1
6	AG	70.0	4.6	198		P	771116	CRUD & CONDENSATE DEMIN RESIN INTRUSION	PC&RT 82LDA01	30
7	N	54.0	3.8			P	740804	RESIN BEAD INTRUSION *	NEDE 13405	13
8	AB	40.5	3.9			P	740608	AIR/AIR RESIN MIXTURE INJECTED INTO Rx FROM RWCU	PC&RT 82LDA01	11
9	N	33.0	4.0			P	740426	RESIN BEAD INTRUSION *	NEDE 13405	10
10	AC	30.0				P	710903	HIGH CONDUCTIVITY WATER IN CST	PC&RT 82LDA01	3
11	ND	28.5				P	661130		PC&RT 82LDA01	2
12	B	25.6	4.1	50		P	770601	RESIN INTRUSION	PC&RT 82LDA01	28
13	B	25.0		2500		p	810412	CONDENSER LEAK	PMET 81-688-45	52
14	J	23.6				P	800205	POSSIBLE CONDENSATE DEMIN RESIN INTRUSION	EPRI NP 4134	80
15	ND	23.0		3000		P	790407	LEAKAGE OF COOLING WATER INTO RPV VIA CORE SPRAY	PC&RT 82LDA01	42
16	W	23.0		30		P	730406	AIR INJECTED INTO Rx FROM RWCU	PC&RT 82LDA01	7
17	AG	22.0				P	771212	COND DEMIN RESIN INTRUSION	PC&RT 82LDA01	32
18	K	21.0	4.6	2500		P	820428	TRICHLOROETHANE VIA CST FROM RADWASTE VIA DRAIN	PC&RT 82LDA01	53
19	AG	20.0	4.5			p	821004	POSSIBLE CONDENSATE DEMIN RESIN INTRUSION	EPRI NP 4134	94
[illegible]	F	17.0				P	801001	CONDENSER TUBE LEAKS	PC&RT 82LDA01	49
[illegible]	C	14.0				P	750605	RWCU OUT OF SERVICE	PC&RT 82LDA01	20
[illegible]	T	13.8	4.7	100		P	781110	ORGANIC INTRUSION VIA CONDENSATE, DECON DETER/OILS	PC&RT 82LDA01	39
[illegible]	AB	13.5				P	740925	HIGH COND WATER	PC&RT 82LDA01	14
24	AB	13.0		100		P	800428	UNKNOWN (LONG SHUTDOWN)	EPRI NP 4134	81
25	T	12.1				P	780225	RWCU RESIN INTRUSION	PC&RT 82LDA01	34
26	Q	12.0				P	750702	CONDENSER TUBE LEAK	PC&RT 82LDA01	21
27	O	12.0	4.8	50		P	761025	RWCU RESIN TRAP, RWCU INOPERABLE	PC&RT 82LDA01	25
28	T	11.8				P	800812	ORGANIC INTRUSION	EPRI NP 4134	82
29	Q	11.5	4.8	60		P	750127	RWCU RESIN INTRUSION	PC&RT 82LDA01	17
30	AB	11.3	4.7			p	830106	POSSIBLE CONDENSATE DEMIN RESIN INTRUSION	EPRI NP 4134	95
31	B	10.8	4.5	50		P	750601	RESIN FROM FLUFFING CONDENSATE DF/D	PC&RT 82LDA01	19
32	AG	10.6	4.5	100		P	730507	RWCU RESIN INTRUSION	PC&RT 82LDA01	8
33	AG	10.0				p	820818	RWCU RESIN INTRUSION	EPRI NP 4134	92
34	Q	10.0				P	741208	CONDENSER LEAK	PC&RT 82LDA01	15
35	DRESDEN 2	9.2	7.4	57		P	780211	CONDENSATE DEMIN RESIN INTRUSION	EPRI NP 4134	74
36	B	8.2	4.3	50		P	751210	WASHOUT OF IMPURITIES FROM TURBINE	EPRI NP 4134	63
37	B	8.0	5.0	500		P	790516		PMET 81-688-45	44
38	B	7.5				p	810411	RWCU RESIN INTRUSION	EPRI NP 4134	86
39	C	7.1		100		P	811010	DECOMPOSITION OF RADWASTE RESINS DUE TO HOT WATER	EPRI NP 4134	89
40	C	6.5				P	810210	CAUSTIC INTRUSION VIA CONDENSATE STORAGE	EPRI NP 4134	84
41	K	6.2	4.8	20		P	741118	SUSPECTED RESIN INTRUSION	EPRI NP 4134	57
42	O	5.8	4.5	50		P	730812	SUSPECTED RESIN INTRUSION	EPRI NP 4134	54
43	AA	5.6				P	700123	RESIN INTRUSION WHEN C/D RETURNED TO SERVICE	JMS QC 930717	98
44	B	5.4	4.7	50		P	751218	PROBABLE RWCU RESIN INTRUSION	EPRI NP 4134	64
[illegible]	B	5.1				p	810220	ORGANIC INTRUSION VIA RADWASTE	EPRI NP 4134	85
[illegible]	DRESDEN 2	5.1		68		P	770727	CONDENSATE DEMIN RESIN INTRUSION, ANION RICH	EPRI NP 4134	70
47	O	5.1	4.8	50		P	760806	CONDENSATE DEMIN RESIN INTRUSION	EPRI NP 4134	67

SEVERE TRANSIENTS IN BWRS

04/29/94

RANK	PLANT	MAX COND. uS/cm	pH, min/ max	MAX Cl, ppb	MAX SO4, ppb	POWER LEVEL	DATE yr-mo-d	COMMENTS	REFERENCE	DATA PT
48	C	5.0		100		P	750309	POSSIBLE CONDENSATE DEMIN RESIN INTRUSION	EPRI NP 4134	79
49	Q	4.9	4.9	50		P	760522	SUSPECTED RESIN INTRUSION	EPRI NP 4134	66
50	T	4.5	5.0	50		P	781227	ORGANIC INTRUSION VIA CONDENSATE SYSTEM	EPRI NP 4134	77
51	Q	4.3	4.9	48		P	760221	SUSPECTED RESIN INTRUSION	EPRI NP 4134	65
52	K	4.1	5.1	80		P	741015	RWCU RESIN INTRUSION	EPRI NP 4134	56
53	C	3.3	5.2	38		P	750309	POSSIBLE RESIN INTRUSION	EPRI NP 4134	59
54	AL	3.3	5.4	50		P	770126	IMPROPER RINSE OF CONDENSATE DEMIN	EPRI NP 4134	68
55	S	3.2	4.7	495		P	780131	RESIN INTRUSION	EPRI NP 4134	73
56	B	3.2				p	810715	RWCU RESIN INTRUSION	EPRI NP 4134	88
57	DRESDEN 2	3.0	5.6	96		P	750902	SUSPECTED RESIN INTRUSION	EPRI NP 4134	61
58	B	2.9	5.4	50		P	751126	PROBABLE RWCU RESIN INTRUSION	EPRI NP 4134	62
59	T	2.8	5.2	65		P	770912	IMPROPER RINSE OF CONDENSATE DEMIN	EPRI NP 4134	71
60	B	2.7	7.6			P	750626	RESIN INTRUSION	EPRI NP 4134	60
61	T	2.3				P	800824	ORGANIC INTRUSION	EPRI NP 4134	83
62	T	2.2	5.5	50		P	790108	SUSPECTED ORGANICS IN CONDENSATE STORAGE	EPRI NP 4134	78
63	Y	1.8	5.4	355		P	781208	CONDENSATE DEMIN RESIN INTRUSION	EPRI NP 4134	76
64	DRESDEN 2	1.4	8.1	38		P	780112	CONDENSATE DEMIN RESIN INTRUSION	EPRI NP 4134	72
65	AC	1.4	5.6	83		P	741125	VALVING ERROR DURING RESIN TRANSFER	EPRI NP 4134	58
[illegible]	AJ	1.4				P	750906	SUSPECTED FLOC/FILTER AID/SURFACT FROM RAD WASTE	JMS QC 930717	99
[illegible]	DRESDEN 2	1.1	8.8	72		P	780511	CONDENSATE DEMIN RESIN INTRUSION	EPRI NP 4134	75
[illegible]	Q	1.1	5.6	30		P	770225	SUSPECTED RESIN INTRUSION	EPRI NP 4134	69
[illegible]	P	1.0				P	810622	OIL INTRUSION INTO HOTWELL	EPRI NP 4134	87
[illegible]	W	1.0				P	811030	GYLCOL INTRUSION VIA RADWASTE	EPRI NP 4134	90
71	B			540		P	780129		PC&RT 82LDA01	33
72	B			1200		P	760708	CONDENSATE SYSTEM MOMENTARILY BYPASSED	PC&RT 82LDA01	24
73	AS			725		P	711113	HIGH FEEDWATER CONDUCTIVITY	PC&RT 82LDA01	4
74	DRESDEN 3			600		P	750103	RWCU OUT OF SERVICE	PC&RT 82LDA01	16
75	B	641.0	3.5	87000		S	790426	COOLING WATER INGRESS FROM RHR, RPV H2O TO HOTWELL	PC&RT 82LDA01	43
76	B	423.0	3.2			S	740801	ACID INTO RPV FROM DEMIN STORAGE TANK	PC&RT 82LDA01	12
77	DRESDEN 2	140.0				S	760519		PC&RT 82LDA01	22
78	T	45.9	3.8	244		S	761103	TORUS WATER PUMPED INTO RPV PRIOR TO STARTUP	PC&RT 82LDA01	26
79	B	13.3		1800		S	760520		PC&RT 82LDA01	23
80	A	13.0				S	780801	LEAK IN RHR HEAT EXCHANGER	PC&RT 82LDA01	36
81	B	12.9				S	770917	RWCU OUT OF SERVICE	PC&RT 82LDA01	29
82	T	12.1				S	800815		PC&RT 82LDA01	47
83	AL	11.6				S	730603	RWCU OUT OF SERVICE	PC&RT 82LDA01	9
84	B	11.2				S	800822		PC&RT 82LDA01	48
85	O	11.2				S	801219		PC&RT 82LDA01	51
86	F	10.5				S	820427	POSSIBLE ORGANIC INTRUSION	EPRI NP 4134	91
87	B	10.5	5.6	140		S	780923	RWCU RESIN INTRUSION	EPRI NP 4134	37
88	DRESDEN 2	10.3				S	750405	RWCU OUT OF SERVICE	PC&RT 82LDA01	18
89	AS	10.0		730		S	720604	DEPLETED RWCU DEMIN	PC&RT 82LDA01	5
90	Q	5.0	5.5	60		S	740829	CONDENSATE DEMIN RESIN INTRUSION	EPRI NP 4134	55
91	AX	4.5	5.2	220		S	830505	ORGANIC INTRUSION VIA RADWASTE	EPRI NP 4134	97
[illegible]	B	4.2	5.3	600		S	781110	ORGANIC INTRUSION VIA CONDENSATE, DECON DETER/OILS	PC&RT 82LDA01	38
[illegible]	AY	1.7			232	S	940423	RESIN INTRUSION DURING RESTART		
94	AP	1.0				S	820900	GYLCOL INTRUSION VIA RADWASTE	EPRI NP 4134	93

SEVERE TRANSIENTS IN BWRS

04/29/94

RANK	PLANT	MAX COND. uS/cm	pH, min/ max	MAX Cl, ppb	MAX SO4, ppb	POWER LEVEL	DATE yr-mo-d	COMMENTS	REFERENCE	DATA PT
95	B			800		S	771206	RWCU OUT OF SERVICE	PC&RT 82LDA01	31
96	AC			683		S	770309		PC&RT 82LDA01	27
97	T			1200		S	790316	CONDENSER LEAK, CONDENSATE DEPLETED, CI INTO CST	PC&RT 82LDA01	40
98	F			700		S	800305		PC&RT 82LDA01	45
99	T			1300		S	790329	CONDENSER LEAK, CONDENSATE BYPASSED, RWCU OUT	PC&RT 82LDA01	41
100	K					S	830213	GYLCOL INTO RADWASTE, DETECTED PRIOR TO COND STOR	EPRI NP 4134	96
101	O			500		S	801017		PC&RT 82LDA01	50

NOTE: BWRS RANKED IN THE FOLLOWING ORDER:

1. POWER (P) OR SHUTDOWN (S)
2. CONDUCTIVITY

OTHER NOTES: * = RESIN BEADS PROVIDE LONG TERM LOW pH

Sulfate IGSCC Initiation Acceleration
Sensitized Type 304 SS

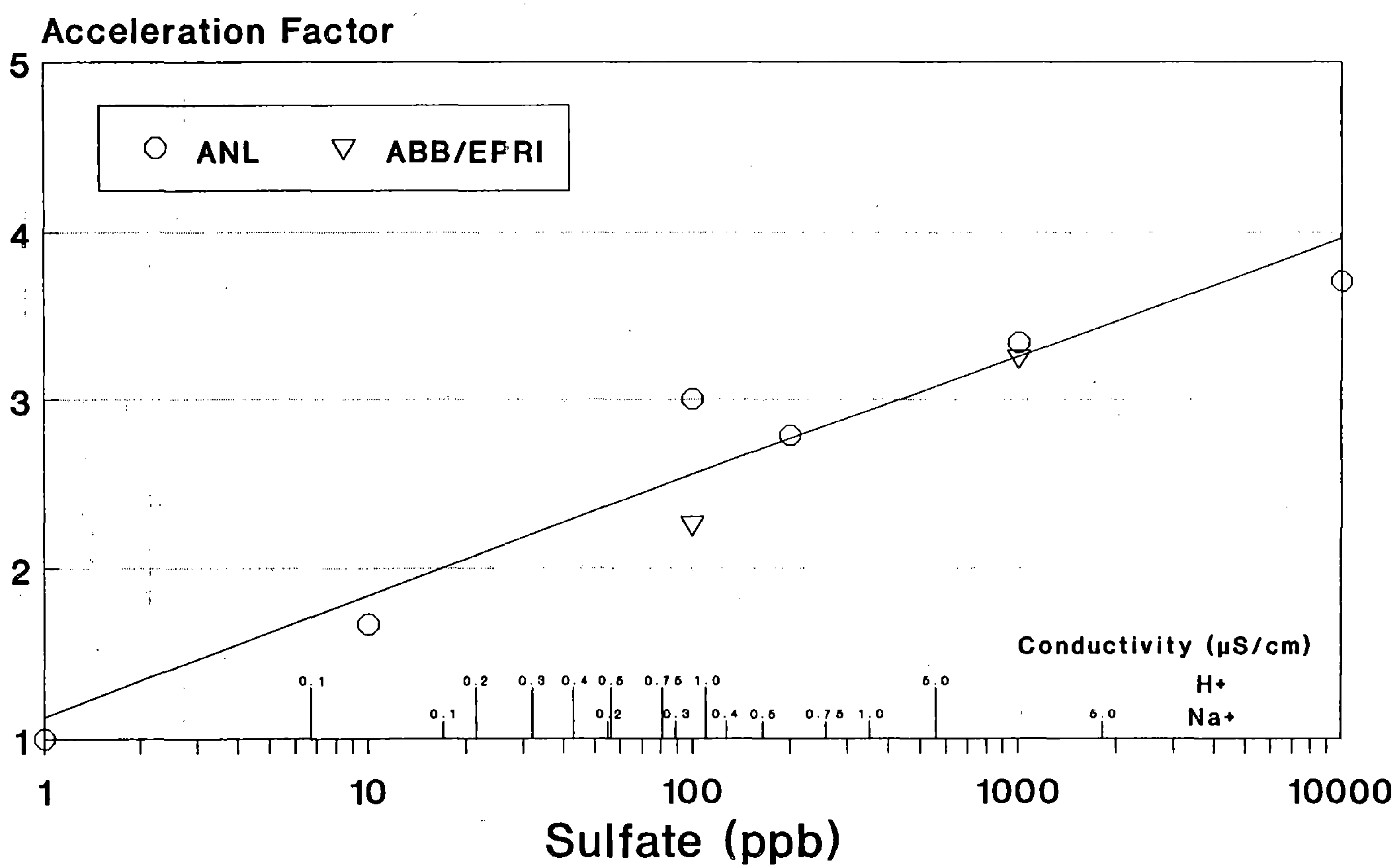

Crack initiation data based on CERT

SO4WCON

Response to Water Chemistry Transient
BWR Resin Intrusion in NWC

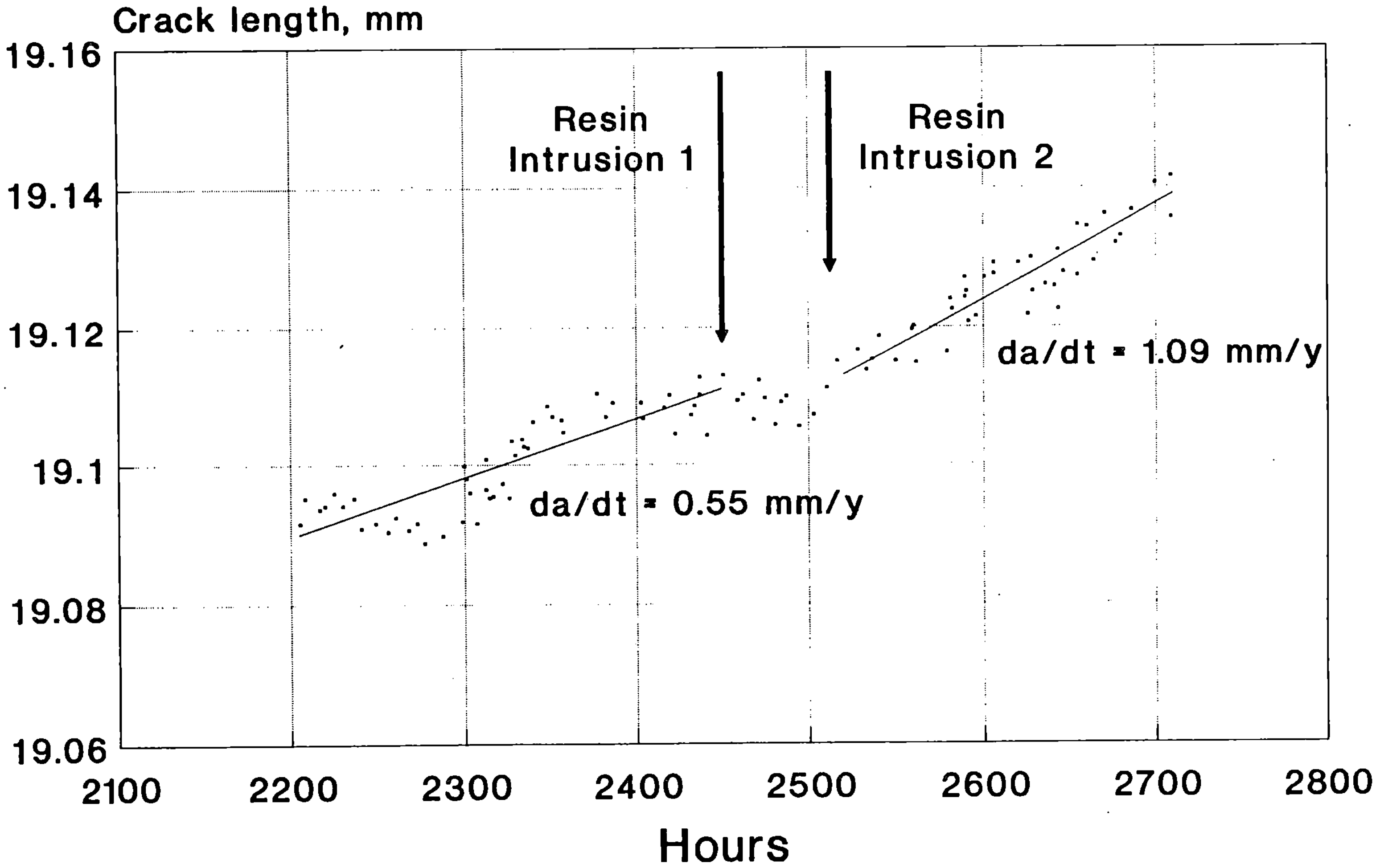

RESNTRAN

PLEDGE Model Prediction for Dresden 2/3 Sensitized Type 304 Crack Growth Rate

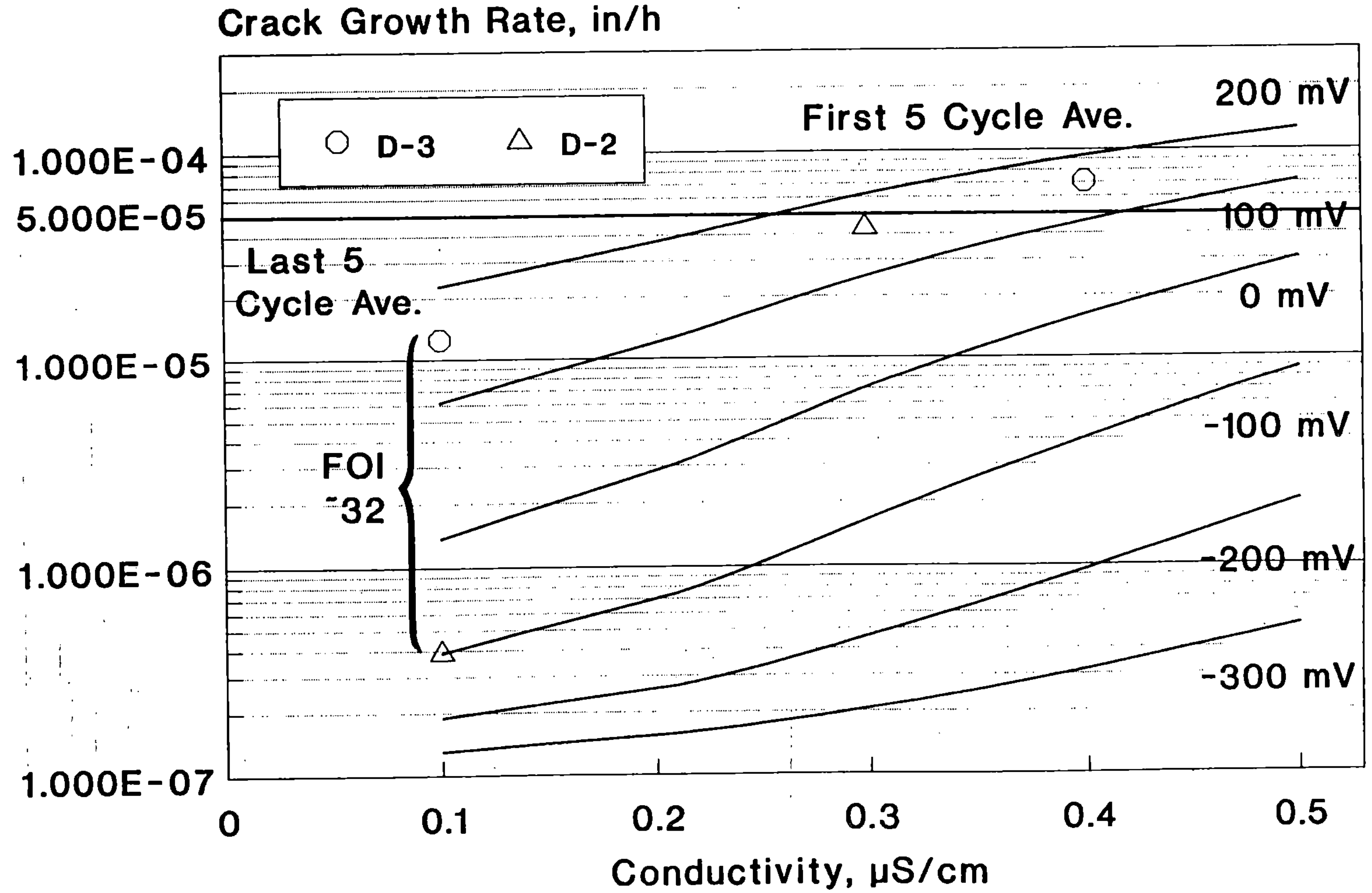

PLEDGE: 15 C/cm2, 20ksi√in

D23GR20C

GENE-NE-A00-05652-04
Revision 2 (Non Proprietary Version)
DRF A00-05652 (16)
JUNE 1994

Attachment ME-1-6

Safety Assessment of Core Shroud Indications for Cycle 13 Operation of Quad Cities Unit 2

Prepared by: ____________________
D. K. Rao, Senior Engineer

Verified by: ____________________
H. Choe, Principal Engineer

Approved by: ____________________
S. Ranganath, Manager,
Engineering and Licensing
Consulting Services

GE-NE Technical Services
GE Nuclear Energy
San Jose, California

PROPRIETARY INFORMATION NOTICE

This document contains proprietary information of the General Electric Company (GE) and is furnished to Commonwealth Edison Company (CECo) in confidence solely for the purpose or purposes stated in the transmittal letter. No other use, direct or indirect, of the document or the information it contains is authorized. CECo shall not publish or otherwise disclose it or the information to others without written consent of GE.

IMPORTANT NOTICE REGARDING CONTENTS OF THIS REPORT

The only undertakings of the General Electric Company (GE) respecting information in this document are contained in the contract between Commonwealth Edison Company (CECo) and GE for this work, and nothing contained in this document shall be construed as changing the contract. The use of this information by anyone other than CECo, or for any purpose other than that for which it is intended, is not authorized; and with respect to such unauthorized use, GE makes no representation or warranty, and assumes no liability as to the completeness, accuracy, or usefulness of the information contained in this document, or that its use may not infringe privately owned rights.

1. Introduction

Circumferential and axial crack indications have been reported at various locations in the core shroud assemblies of BWRs. GE Services Information Letter 572, Revision 1 (SIL-572), has been issued to assist utilities in their individual evaluation of this situation. SIL -572 recommends that shroud inspection be performed at the next scheduled refueling outage. The USNRC issued Information Notice 93-79 on this subject. Based on these recommendations, a shroud inspection was performed at Quad Cities Unit 1 during the current refueling outage.

The inspection indicated the presence of circumferential cracks in the Quad Cities Unit 1 (QC1) core shroud assembly. The concern addressed in this assessment is for potentially similar crack indications in the Quad Cities Unit 2 (QC2) core shroud because the design of the QC2 reactor internals is identical to that of the QC1 reactor internals. The visual inspections performed have shown the presence of cracks near the H3, H4, H5 and H6 welds for QC1. Because there is not adequate inspection data available pertaining to the condition of the welds in the shroud of QC2, an engineering evaluation is sought by the Commonwealth Edison Company (CECo) to determine if operation of QC2 can be justified until shroud inspection can be done during the next planned outage (Reference 1). The region near the H5 weld showed random indications of cracks in all areas inspected for QC1. The most severe indications are in the core support ring joined to the core shroud near the H5 weld and appear to be 360° circumferential cracking. Therefore, UT inspections were done at six locations of the H5 area using 60° dual R-L transmitters (Reference 2). The results used in this report are based on the current inspections and the following discussion is based on the results of the current inspections. If future inspections indicate that potentially larger cracks could exist, this assessment will have to be reviewed and amended appropriately.

The preliminary safety assessment for the QC2 core shroud in this report provides the engineering rationale for continued plant operation for the remainder of the current QC2 fuel cycle. This safety assessment is preliminary in that it should be revised when the QC2 core shroud is inspected during the next planned outage and an updated safety assessment should be prepared when inspection results for QC2 become available.

This report uses the following approach. The QC2 core shroud structural integrity is demonstrated with the assumption that crack indications are essentially identical at QC1 and QC2. The technical bases for this assumption are provided by comparing the plant water chemistry and operating histories between QC1 and QC2. This report also qualitatively addresses the potential situation during normal operation, anticipated operational events, and design basis accidents, if unexpected significant crack growth occurs during plant operation. This assessment describes the symptoms and consequences expected if the shroud has degraded to the point that through-wall cracking has occurred in the core support ring in the H5 weld area, which was the most extensively cracked area on the QC1 shroud. A qualitative assessment is provided for other welds on the core shroud. Similar crack indications have been found during inspections at the Dresden 3 plant and a similar assessment was done to support continued operation of the Dresden 2 plant until its next planned outage. The approach used in this assessment to justify continued operation of QC2 is similar.

GE Rapid Information Communication Services Information Letter (RICSIL) 068 has been issued (Reference 3) to assist CECo and other utilities in the on-going evaluation of this situation. Previous communications about core shroud crack indications have included GE SIL 572 (Reference 4) and US-NRC Information Notice 93-79. Reference 4 states that current understanding of the root cause for shroud cracks is Intergranular Stress Corrosion Cracking with apparent propagation by Irradiation Assisted Stress Corrosion Cracking.

2. Summary and Conclusions

The core shroud/core support ring cracking associated with the H5 weld at QC2 does not represent a threat to the safe operation of QC2 for the remainder of the present cycle. The cracking is postulated to be similar to that observed for the H5 weld at QC1, which was the most extensively cracked weld area in QC1.

1. The combination of high ductility, high toughness and low stresses makes the shroud extremely flaw tolerant. Even for this situation with the indications of 360 degree circumferential cracking, crack depths of 96% (2.88 inches) of the available material can be tolerated while maintaining the structural integrity for normal operation and postulated design basis accident conditions, including ASME Code safety factors. The available material considers the extra one inch of ligament provided by the weldment in addition to the two inch shroud wall thickness. The weld detail is shown in Figure 1.

2. The maximum crack depth observed by ultrasonic examinations in QC1 is approximately 1.24 inches, and is within the allowable crack depth of 2.88 inches. The postulated cracking in QC2 is equal to that in QC1 and the QC2 core shroud maintains the structural integrity for normal operation and anticipated plant transients.

3. The crack growth rates associated with the H5 weld area for the QC1 and QC2 will be similar. This is based on the similar water chemistry histories and average conductivities for both QC1 and QC2. Even discounting Hydrogen Water Chemistry (HWC) benefits that QC1 and QC2 have had since 1990, and using the bounding crack growth rate of 5E-5 inch/hr (0.44 inch/year), as established in the BWROG Core Shroud Evaluation report for normal water chemistry, the crack depth is not expected to exceed the allowable crack depth in one year.

4. The weight of the core shroud above H5 is sufficient to hold the shroud in place even if the shroud assembly is postulated to have a 360° through-wall crack at the H5 weld, both under normal operating conditions and during anticipated plant transients. The shroud would not lift. Since the crack size is on the order of mils, any leakage flow through the crack is small and would not impact plant operations.

5. An evaluation of the design basis accident coupled with a seismic condition has been done with the shroud assembly postulated to have a 360° through-wall crack at the H5 weld. The evaluation was done to investigate the possibility of shroud movement. For recirculation line breaks, no shroud lifting occurs. Adequate long term cooling of the core will be maintained throughout the postulated event. For steamline breaks, shroud lifting is limited. Even if the shroud lifting causes the core spray line to fail, core spray water is delivered to

the reactor vessel and adequate long term cooling of the core will be maintained throughout the postulated event. For both the recirculation and main steam line break events, safe reactor shutdown capability and long term core coolability is maintained. This conclusion is applicable to both QC1 and QC2.

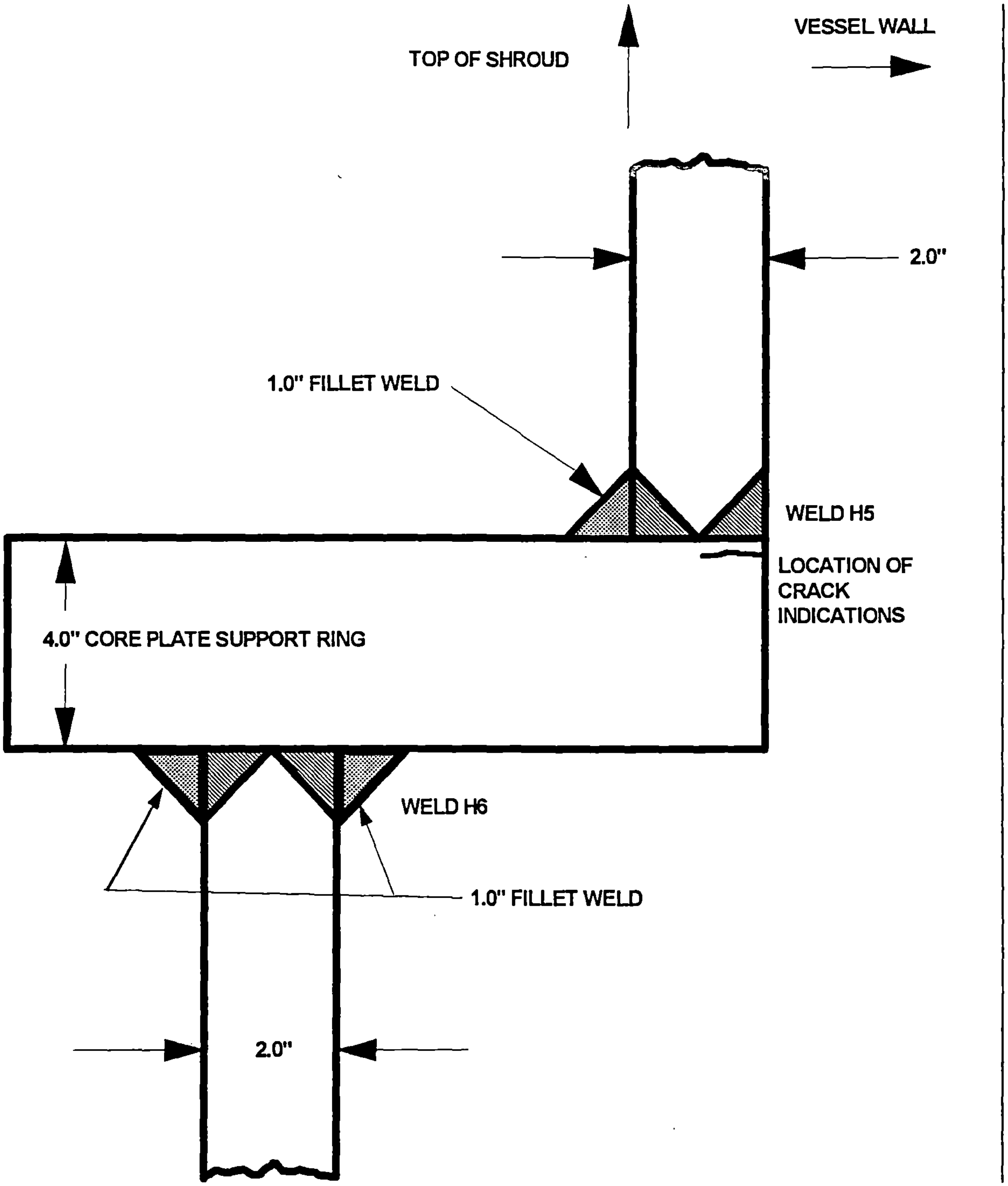

Figure 1 Shroud Weld Detail

3. Shroud Support, Shroud, and Top Guide Functions

The shroud support, shroud, core support, and top guide make up a stainless steel cylindrical assembly that provides lateral support for the core, vertical support for peripheral fuel bundles, and a partition between the core region and the downcomer annulus to separate the upward flow of coolant through the core from the downward recirculation flow. The shroud also provides (in conjunction with other components) a floodable region following a postulated recirculation line break. The shroud is not a primary pressure boundary component.

The top guide consists of a circular grid plate having square openings, lateral support and guidance for fuel assemblies. The core support plate consists of a circular plate with openings and provides lateral support for the control rod guide tubes. The core support plate also provides vertical support for peripheral fuel assemblies. The majority of the fuel rests on fuel support castings that are supported by the control rod guide tubes. The fuel support castings are aligned by holes in the core support plate. The core support plate rests on the core support ring, which is welded to the shroud at the circumferential locations identified as H5 and H6.

4. Shroud Structural Evaluation

4.1 Shroud Loading Considerations

While the extent of the cracking reported at QC1 and assumed for QC2 is not insignificant, there remains sufficient structural strength in the shroud to meet all of its design functions (Reference 5). The shroud is made of ductile material with high toughness properties even after accounting for any effects due to neutron fluence. The applied loading on the shroud is mainly from the differential pressure during normal operation, the transient differential pressure increase due to design basis accident loading, design basis seismic loads, and non-symmetric acoustic loads during the recirculation suction line break. These loads are generally small and well within the remaining structural integrity of the shroud.

The applied loads during normal operation, anticipated operational events, and the recirculation line break accident are in the downward direction. The applied load is in the upward direction when the main steam line break accident is assumed to occur alone or simultaneously with a safe shutdown earthquake (SSE). Reference 6 documents the design pressure drop loads of 8 psi on the upper part of the core shroud at normal, rated power conditions and 20 psi during the main steam line break accident.

The combination of high ductility and low applied stresses make the shroud extremely flaw tolerant. It has been calculated that 360° circumferential cracking of greater than 96% of the 3.0 inch available material can be tolerated while maintaining the industry accepted ASME Code allowable safety factors based on limit load method for the H5 area (Reference 16). The analysis that determines the 96% criterion conservatively ignores the available material of the extra one inch of ligament provided by the weldment in addition to the two inch shroud wall thickness. The deepest observed cracking indication is 1.24 inches or less than 42% of the 3.0 inch available material at QC1 (Reference 2).

Lateral loads on the core shroud due to an instantaneous break of the recirculation suction line and non-symmetric depressurization of the downcomer annulus are considered to be unrealistic in that it takes finite time (about 100 milliseconds) for the break to occur (Section 3.9.5.3.1.2 of the Quad Cities UFSAR). The asymmetric load is due to the time it takes for the pressure wave to travel from the broken suction line to the unbroken suction line. This duration is extremely short (about 5 milliseconds, as shown in Figure 3.9-12 of the Quad Cities UFSAR). This acoustic load affects the lower portion of the shroud (near H5) rather than the upper shroud (H2 and H3). Three areas that the acoustic load could affect are allowable crack length, crack depth, and lateral motion of the shroud assembly. Short duration loads of this type do not lead to significant deformation and are not included in the analysis of flaw sizes. The pressures due to the Main Steamline Break exceed those due to the Recirculation Line Break.

Thus, from the standpoint of total loads, the steamline break with Safe Shutdown Earthquake is limiting. Lateral movement for the Main Steamline Break with SSE and the tipping motion of the shroud pivoted on one side of the H5 weld crack area during the Recirculation Suction Line Break are estimated to be less than 3/4 inch and the shroud would then return to its vertical position (Reference 19).

The low stresses and high material ductility under relatively low neutron fluence level ($3X10^{16}$ n/cm^2, Reference 16) make unrealistic the postulation of the separation of the core shroud assembly at H5 weld area during the present cycle based on the assumptions made and the information provided by CECo (References 1 and 2).

4.2 Water Chemistry Considerations

The BWR oxidizing environment can provide the electrochemical driving force for intergranular stress corrosion cracking (IGSCC) of BWR structural materials. Also, the conductivity of the BWR coolant is sufficiently high to allow this corrosion reaction to occur (References 3, 7, and 8).

The crack growth rate depends on the water chemistry and the conductivity of reactor water. Both QC1 and QC2 have been operated on Hydrogen Water Chemistry (HWC) continuously since the third quarter of 1990. The levels of hydrogen injected into both QC1 and QC2 have ranged from 1.4 to 1.5 ppm in the feedwater line with a corresponding concentration in the reactor vessel of approximately 180 ppb (Reference 9). The HWC system was available for approximately 57% (for QC1) and 44% (for QC2) of the time the reactor was above 20% power. While this duration and availability is not high enough to protect reactor internals from IGSCC or IASCC, it could retard crack propagation. A comparison of conductivity measurements for QC2 and QC1 shows that the average conductivities through Cycle 12 for QC1 and QC2 are 0.257 µS/cm and 0.258 µS/cm, respectively (Reference 10). QC1 has been operated for one more cycle than QC2 with the number of hours of reactor critical being 151,487 hours for QC1 and 146,195 hours for QC2. Thus, the total hours above 200 F ("hot operational hours") are greater for QC1. In view of the similar conductivities and water chemistry histories, both QC1 and QC2 should have similar susceptibilities to IGSCC.

Based on the information for QC1 inspection findings provided by CECo (i.e., the deepest crack indication for QC1 is 1.2 inches), and conservatively using the bounding crack growth rate of 5E-5 inch/hr (0.44 inch/year), as stated in Reference 20 for normal water chemistry BWRs, the crack depth would be 1.64 inches in one year. Since QC2 is scheduled to be inspected in less than one year, the calculated crack depth is within the allowable crack depth of 2.7 inches.

5. Normal Operation

As discussed in the preceding sections, the postulation of significant through-wall cracking, leakage, or separation of the core shroud assembly at H5 weld area is extremely improbable. The more likely, but still improbable scenario, would be for some bypass flow to occur from the core bypass region to the reactor downcomer annulus.

Even if the postulated cracking or separation were to occur, the weight of the core shroud above H5 weld is sufficiently high to hold the core shroud assembly in place during all normal operating conditions. The postulated leakage would occur through a gap much less than 0.001 to 0.002 inch. The estimated leakage flow is less than 35 gpm, assuming that a 0.002 inch gap exists around the entire circumference at 8 psid differential pressure. Leakage flow of this magnitude has no consequence on plant operation. It also would not be detectable by the plant operator because the leakage flow is small and the leakage temperature at this location is the same as the downcomer temperature.

6. Anticipated Operational Events

The previous sections demonstrate that cracks that grow through the shroud wall or cause complete separation of the shroud assembly at H5 area from the lower shroud are improbable. This section discusses anticipated operational occurrences that could increase shroud loads above those experienced during normal operation. The transients associated with such an occurrence are those that tend to depressurize the reactor vessel and those that increase core flow. The transients evaluated are: Pressure Regulator Failure - open, Recirculation Flow Control Failure - Increasing to Maximum Flow, and Inadvertent Actuation of the Automatic Depressurization System. The normal operating pressure drop across the upper shroud is 8 psid (Reference 6).

6.1 Pressure Regulator Failure - Open

This postulated Safety Analysis Report (SAR) event involves a failure in the pressure controls such that the turbine control valves and the turbine bypass valves are opened as far as the Maximum Combined Flow Limiter (MCFL) allows. For both QC1 and QC2, the bypass capacity is 40% of rated steam flow, the worst case involves inadvertently increasing the steam flow. The steam flow increase would be limited by the Maximum Combined Flow Limiter (MCFL) to 105% (Reference 17). A depressurization and cooldown occurs, followed by Main Steamline Isolation Valve (MSIV) closure. The steam flow increase is small enough that the increased force on the shroud head is offset by the weight of the core shroud above the H5 weld. Any leakage postulated may occur through a gap much less than 0.001 to 0.002 inch. Even if it is assumed that a momentary 20 psid pressure differential exists and that a 0.002 inch gap exists around the entire circumference, the postulated leakage flow is less than 60 gpm. A realistic flow, corresponding to a pressure differential of 10 psid, is less than 40 gpm. Leakage flows of this magnitude have no adverse consequences on plant operation.

6.2 Recirculation Flow Control Failure - Maximum Flow

This postulated event involves a recirculation control failure that causes both recirculation loops to increase to maximum flow. For this event, the pressure drop could change from a part-load condition to the high/maximum flow condition over a time period of several seconds, but it should not significantly exceed the pressure drop expected for normal full power, high core flow operating conditions (8 psid). Normal operating procedures are considered sufficient to minimize the consequences of this potential transient.

6.3 Actuation of ADS

Inadvertent actuation of the Automatic Depressurization System (ADS) valves is another postulated event that could put an increased load on the upper shroud. The maximum steam flow and the depressurization rate occur over a period of about one second, spreading the effect of the change in load. There is a short-term increase in steam flow to approximately 130% of rated steam flow. The increase in the shroud ΔP resulting from the opening of the ADS valves is not expected to cause lifting of the shroud. Furthermore, inadvertent ADS is a very low probability event; it is classified in the ASME Emergency category.

7. Design Basis Accidents

Although the previous sections demonstrate that the probability of the postulated separation of the core shroud assembly at H5 weld area is extremely low, an accident occurring with a separated core shroud is addressed in this section.

The Main Steamline Break Accident imposes the largest potential lifting loads on the shroud head. Liquid breaks (up to and including the recirculation line break) do not impose significant pressure drops on the shroud head.

7.1 Main Steamline Break

The main steamline break inside primary containment is the postulated worst case because it results in the largest depressurization rate. During this SAR event, the reactor is rapidly depressurized as a result of a postulated instantaneous, double-ended break of the largest steamline. Thus, a larger than normal pressure difference could develop across the shroud as fluid flow is drawn from the core region toward the break. For QC2, the design basis pressure difference is 20 psid for the guillotine break of a main steam line (Reference 6).

The weight of the core shroud above H5 weld (Reference 5) is not high enough to hold the core shroud assembly in place during the main steam line break, and if the presence of the shroud ligament is totally neglected, the core shroud could lift momentarily by up to 4 inches while the reactor vessel is depressurizing. If the main steam line break occurs simultaneously with the safe shutdown earthquake (SSE), and 360° complete through-wall crack is postulated, the core shroud could lift momentarily by up to 8 inches while the reactor vessel is depressurizing. The estimated displacement is less for the OBE than for the SSE and is not discussed further. Since the break is in the main steamline, the core is capable of being reflooded up to and above two-third core height.

One of the key considerations of this postulated accident case is the ability of the control rods to insert before or during the postulated accident. Specifically, sufficient lifting of the top guide prior to control rod insertion could cause reorientation of the fuel bundles and thus impede the insertion of control rods.

The shroud head pressure drop characteristics calculated for the instantaneous, double-ended steamline break accident were evaluated generically (Reference 11). The conclusions, as described below, are applicable to QC2. The initial shroud head pressure drop loading is a result of the decompression wave which reduces system pressure overall, but would increase differential pressure across the shroud in the short term. The pressure loading increase is short-lived (less than two seconds) and decreases to below normal steady state loads. If it is even further postulated that the initial load pulse causes the shroud to separate, the last part of the pressure loading could cause the shroud assembly to lift. The flow path created by any separation reduces the upward lifting forces.

Scram is initiated during the main steamline break (inside containment) accident by the high drywell pressure trip signal. Drywell pressure exceeds the setpoint almost instantaneously, so the only delays in the rod insertion come from the sensors, the Reactor Protection System, and rod motion. For the main steamline break outside containment, shroud loads are lower, MSIV closure is initiated by high steam flow, and scram is initiated from the MSIV closure.

For all of the postulated steamline break scenarios, the insertion of all control rods will occur. Even if the first loading pulse causes the upper shroud assembly to break free, control rod motion will commence before the upper shroud assembly and top guide lift significantly. It is likely that the top guide will remain engaged with the tops of the fuel bundles. Any control rods that are partially inserted as part of the normal operation are already in position to initiate shutdown. Insertion of fully withdrawn control rods will occur by 0.9 second to 5% full stroke, which is early enough for the control rods to be moving up between the bundles before any significant lifting of the top guide can take place. The shroud assembly, if separated at H5, could shift laterally up to 3/4 inch (Reference 19). With the random displacement anticipated during seismic events, the CRD alignment in the core region would undergo intermittent periods of misalignment. Minimal scram performance degradation is expected. Even with 8 inches of lift during the main steam line break concurrent with the SSE, the fuel bundles and the top guide will stay engaged because the height of the top guide is approximately 14 inches (Reference 12) and an 8 inch lift retains the fuel bundles within the top guide. Friction between the fuel bundles and top guide is not high and the fuel bundles will slide against the top guide and stay within it. Control rod insertion will occur because the fuel will remain properly oriented. Reactor shutdown would thus be complete with all drives inserted. Even under the worst scenario discussed above, the control rods would fully insert and reactor shutdown would thus be achieved. In the very unlikely case that scram is not completed, the SLCS is available to provide shutdown capability.

Movement of the upper shroud assembly could affect the performance of the core spray system if it impacts the core spray line connection. If the lifting of the core shroud causes the core spray sparger or the riser to deflect, the coolant flow to the core from the core spray spargers could be affected. However, significant margins exist in the LOCA analysis results for QC1 and QC2 (Reference 13, Table 5-3) even if a large deflection, resulting in a condition up to and including the failure of the core spray sparger or riser should occur. The core spray crack analysis (Reference 14) has shown that the core spray line crack is approximately 120° of the piping circumference. The effect of a deflection would tend to open the crack and allow water from the core spray system to enter the downcomer and thence to the core region. Such a condition would not prevent the entry of core spray system water into the reactor vessel. Therefore, even if the LPCI should fail to deliver water to the reactor vessel (Reference 15), the core spray water would be available and adequate long-term cooling would be available.

The main steamline break has also been evaluated for radiological release consequences in the SAR. For a main steamline break inside containment, the radiological consequences are bounded by the Loss of Coolant Accident. For the main steamline break outside containment, the magnitude of the pressure loads that potentially could lead to separation of the upper shroud are less than that for breaks inside the containment, due to attenuation of the depressurization wave along the steamline. MSIV closure is initiated before any potentially increased radiological release outside containment from such a scenario could occur. The radiological consequences of this main steamline break scenario are thus still bounded by the plant SAR results.

7.2 Recirculation Line Break

For the design basis recirculation line break combined with the SSE, the differential pressure across the upper shroud does not increase from the initial value as the reactor depressurizes, upward forces are reduced, and thus there is no significant threat to core shroud integrity in the vertical direction. The effect of lateral loads due to acoustic phenomena does not cause the shroud to move (see Section 4). Lateral movement due to tipping motion of the shroud does not exceed 3/4 inch and the shroud would then return to the vertical position. As described in Section 7.1, reactor shutdown would thus be complete with all drives inserted.

With the shroud integrity maintained, a floodable core region is also preserved. Even if the entire circumference is postulated to be cracked as done in the previous sections, the shroud assembly does not lift. The calculated leakage flow is very small compared to the emergency core cooling system flow capacity and there is no significant decrease in coolant to the core. Therefore, the recirculation line break analysis results are unchanged.

8. Emergency Operator Actions

The Quad Cities-specific Emergency Procedures (QGAs) are symptomatic in that they respond to detected symptoms and do not require diagnosis of the event by the operator. They address a wide range of events, both less severe and more severe than the design basis accidents.

The worst postulated event discussed above could result in separation of the shroud assembly from the lower shroud. However, this has minimal impact to scram performance because no disengagement of the fuel bundles from the top guide occurs. Therefore, no further consideration is necessary for the impact of this postulated event on the QGAs.

The QGAs provide instructions for reactor pressure, water level, and power control, as well as control of key primary containment parameters. Actions specified in the QGAs for reactor power control are to (1) insert control rods using a variety of methods, and (2) initiate the Standby Liquid Control System (SLCS) before pool temperature increases to the allowable value of 110 F (Reference 18). QGA instructions are for water level to be controlled below the high water level setpoint; thus there would not be dilution of the liquid boron by flooding to the steamline elevation or loss of vessel inventory out the break in case SLCS injection were to occur.

Water level would be controlled after the postulated event because the most challenging break is high in the vessel and water injection systems would be available to provide core cooling.

9. References

1. Telecon between Dilip Rao (GE) and Bob Walsh (CECo) May 4, 1994

2. Letter form M.D.Lyster (CECo), to W.D.Russell (NRC), dated 6/6/94. "Response to NRC Request for Additional Information Concerning Core Shroud Cracking at Dresden Units 2 & 3 and Quad Cities Units 1 & 2."

3. GE Rapid Information Communication Services Information Letter (RICSIL) 068, Revision 2, Update on Core Shroud Cracking, May 6, 1994.

4. GE Services Information Letter (SIL) 572, Revision 1, Core Shroud Cracks, October 4, 1993.

5. Evaluation and Screening Criteria for the Quad Cities 1 and 2 Shrouds, Dresden 3 Shroud Circ Flaw at H5, GE Design Record File, DRF-137-0010-7, Report Number GE-NE-523-02-0194..

6. Fax, Bob Walsh (CECo) to Dilip Rao (GE), Received May 5, 1994. (Includes Pages from Updated Final Safety Analysis Report, Quad Cities Units 1 and 2, Tables 3.9-19 and 3.9-20).

7. B. M. Gordon et al, "Hydrogen Water Chemistry for BWRs-Materials Behavior- Final Report," EPRI TR-100304, Palo Alto, CA, February 1992.

8. M. E. Indig et al, "Investigation of the Protection Potential Against IASCC," Paper #71 presented at Corrosion 92, NACE, Nashville, April 1992.

9. Telecon, Dilip Rao (GE) and Tracy Finnegan (CECo), May 5, 1994.

10. Internal Communication, Barry Gordon/Dilip Rao (GE), May 5, 1994.

11. Letter dated November 9,1993, from L. A. England to US NRC, "BWROG Safety Assessment - BWR Shroud Crack Indications"

12. GE drawings, 718E861 and 104R921

13. NEDC-31345P, "Quad Cities Nuclear Power Station Units 1 & 2 SAFER/GESTR LOCA Analysis," General Electric Company, June 1987.

14. GENE-523-A80-0594, "Core Spray Crack Analysis for Quad Cities Units 1 & 2."

15. Quad Cities Station UFSAR, Copy 40, Section 7.3.1.2.1.2, "Single Failure Criterion (IEEE 279, paragraph 4.2)."

16. GENE-523-A79-0594, "Evaluation of the Indications Found at the H5 Weld Location in the Quad Cities Unit 1 Shroud."

17. Fax, Mark Uhrich, CECo, to Dilip Rao, GE, dated 6/1/94, "Comments on Safety Assessment."

18. QGA 200, Torus Temperature Control Methods.

19. GENE-A00-05652-03, Supplement 3, Revision 1, "Preliminary Safety Assessment of Core Shroud Indications for Cycle 14 Operation of Dresden Unit 2."

20. GE-NE-523-148-1193, April 1994, "BWR Core Shroud Evaluation."

Hand Calculations

1. Leakage Flows
2. Shroud Δp during AOOs
3. Lift Forces during MSLB with and w/o earthquakes

Prep: DKR
Verif: ECE

A00-05652
Sect. 16

1. Basis for Leakage Flows at 7 psid & 20 psid

From Section 15 of DRF A00-05652

0.001 inch gap => 11.6 gpm @ 7 psid
0.002 inch gap => 32 gpm @ 7 psid

Since $Q \propto \sqrt{\Delta p}$

The corresponding values @ 20 psid.

$11.6\sqrt{20/7}$ = 19.6 gpm (0.001")

$32\sqrt{20/7}$ = 54.1 gpm (0.002")

Use 60 gpm for MSLB (momentary)

Note: the normal condition Δp @ QC is 8 psi (not 7 psi).

The normal operation flows are

$11.6\sqrt{8/7}$ = 12.4 gpm (0.001")

$32\sqrt{8/7}$ = 34.2 gpm (0.002")

(Use 35 gpm)

Ref: DKR

Verif: ECS

2. ΔP changes during AOOs with Decreasing RPV Pressure

Pressure Regulator Failure – Open:

The maximum flow is limited to 110% by the MCFL.

The new Δp is given by

$$\frac{\Delta p}{8} = \left(\frac{110}{100}\right)^2 = 9.6 \text{ psi.}$$

$$\text{Leakage flow} = 32\sqrt{\frac{9.6}{7}} = 37.5 \quad (0.002'')$$

(Use 40 gpm)

ADS Actuation

The maximum flow is limited to 130% (see Ref. 6 and Dresden Assessment)

$$\Delta p = 8\left(\frac{130}{100}\right)^2 = 13.5 \text{ psi.}$$

The Dresden assessment also shows that lift is incipient at 12.77 psi

At 125%, $\Delta p = 8(125/100)^2 = 12.5$ psi.

126% $\Delta p =$ 12.7 psi

127% $\Delta p =$ 12.9 psi

An better estimate (see following page) shows 128.4%

Prep: DKR

Verif ECE

The actual SC1&2 RV & S/RV data is:
[ZEER Sec 5.2.2.1, 5.2.2.4]
- 4 RVs, each 558,990 lb/hr @ 1120 psig
- 1 S/RV 598,900 lb/hr @ 1080 psig

The actual flows (nominal) at normal RP/pressure (1005 psia) are

$$4 * \frac{558,990}{0.9} * \frac{(1005-14.7)}{1120} + \frac{598,900}{0.9} \frac{(1005-14.7)}{1080(1.03)}$$

$$= 2,784,320 \text{ lb/hr} \quad (2.784 \times 10^6 \text{ lb/hr})$$

Added to steam flow of 9.8×10^6 lb/hr,

$$\frac{9.8+2.784}{9.8} = 1.284$$

128.4%.

The $\Delta p = 8\left(\frac{128.4}{100}\right)^2 = 13.18$ psid

Since the ADS actuation is not an instantaneous Δp, but occurs with finite time, the calculated Δp is a bounding value and realistically, the Δp will not adversely affect the shroud Δp limit of 12.77 psi

Prep: DKR

Verif: ECE

3. Lift Forces for Main Steam Line Break

From A00-05352, Sec. 15, (Dresden)

Condition for Max. Lift:

$X = \frac{B-1}{a}$; $a = 0.1545$ (inch)

(See following Page for calculation of a)

$B = \frac{g_c}{g} \frac{(A \, \Delta P)}{M_s}$

Comparison of Masses between Dresden and QC in DRF-137-0010-7 shows M_s, A are same.

Thus B is ratioed:

For Dresden, $\Delta p = 7$, $B = 0.548$

$\Delta p = 12$ $B = 0.94$

@ $\Delta p = 20$, $B = \frac{20}{12} * 0.94 = 1.567$

1. Break Only $\Big\}$ $X_1 = \frac{1.567-1}{0.1545} = 3.67$ inches. (Only Break Loads)

2. Break (SSE) $\Big\}$ $M = 296,000$ lb (DRF-137-0010-7)

$B = \frac{20 \times 32403.75}{296,000} = 2.183$

$X_2 = \frac{2.183-1}{0.1545} = 7.696$ inches.

Prep: DKR

Verif: ECE

Lift Forces ~~fuel~~ MSLB with [illegible]

3. Break + OBE $\qquad M = 329{,}000 \text{ lb}$

$$B = \frac{20 * 32{,}403.75}{329{,}000}$$

$$= 1.9698$$

$$X = \frac{1.9698 - 1}{0.1545} = 6.28 \text{ inches.}$$

Displacements are positive for

MSLB: 3.67 inches (Use 3.7 inches)

MSLB+OBE: 6.28 inches (Use 6.3 inches)

MSLB+SSE: 7.696 inches (Use 7.7 inches)

—— x ——

Calculation of "a": $\quad a = \sqrt{C_1 / C_2'}$

$$C_1 = \frac{\Delta p}{v_0 \dot{m}_{core}^2} \; ; \qquad C_2' = \frac{K}{2g_c (\pi D)^2} * \frac{144}{3600^2}$$

Since only Δp is changed from 7 psid to 8 psid. between Dresden and QC (See following pages)

$$C_1/C_2')_{QC} = C_1/C_2')_{Dresden} * 8/7$$

$$C_1/C_2')_{Dresden} = 0.1445^2 \; ; \qquad C_1/C_2')_{QC} = 0.1445^2 * 8/7$$

$$a = 0.1445\sqrt{8/7} = 0.1545$$

ITEM NO.	PLANT IDENTITY	PROJ CODE	1 TURBINE MFG		2 TURBINE BY-PASS CAPACTY (%)		3 STEAM FLOW AT WARRNTD (MLB/H)		4 STEAM FLOW AT T-G RTD (MLB/H)		5 STEAM FLOW AT T-G DSN (MLB/H)		6 RTD SEC STEAM FLOW (MLB/H)		7 NO OF PRESS REG		8 PRIMARY PRESS REG TYPE		9 BACKUP PRESS REG TYPE		10 DOME PRESS AT RTD (PSIG)	
1	DRESDEN 1	EB1	GE		100+		1.405		1.57		1.405		1.35				MPR		MPR		1000	
2	HUMBOLDT BAY 3	ED1	GE		100+		0.59				0.59		N/A				MPR		MPR		1135	
3	GARIGLIANO	AB1	ANSALDO		128		1.544		1.544	D	1.544		0.476				MPR		MPR		972	D
4	BIG ROCK POINT	EJ1	GE		100+		0.606		0.945		0.606		0				MPR		MPR		1350	
5	KRB-A	AD1	AEG	S	100+	S	2.25	S	2.25	S	2.25	S	0.99		3	S	ASKANIA	S	ASKANIA	S	1000	S
6	TARAPUR 1	BE1	GE		100+		1.9		1.9		1.9		0.792		3	S	EPR		MPR		1000	
7	TARAPUR 2	BE2	GE		100+		1.9		1.9		1.9		0.792		3	S	EPR		MPR		1000	D
8	DODEWAARDE	AE1	STORK	S	100+		0.512	S	0.512	S	0.64	S	N/A		3	S	ASKANIA	S	ASKANIA	S	1020	S
9	NINE MILE POINT 1	EA1	GE	S	40	S	6.0	S	7.0		7.3	S	N/A	S	2	S	EPR	S	MPR	S	1030	D
10	OYSTER CREEK 1	EN1	GE		45		5.9		6.9		7.3		N/A		2		EPR		MPR		1020	D
11	DRESDEN 2	EB2	GE		40		8.6	D	9.3		9.8		N/A		2		EHC		EHC		1000	D
12	DRESDEN 3	EB3	GE		40		8.6	D	9.3		9.8		N/A		2		EHC		EHC		1000	D
13	MILLSTONE 1	EH1	GE		100+		6.74	D	7.6	D	8.0	D	N/A		2	S	EPR		MPR		1035	D
14	TSURUGA	BK1			15		3.8		4.3	D	4.3	D	N/A		2		EPR		MPR		1000	D
15	NUCLENOR	BH1	GE	S	15		4.7		5.5		5.5		N/A		2	S	EPR		MPR		1000	D
16	MONTICELLO	EK1	GE		15		5.9		6.4		6.8		N/A		2		EPR		MPR		1008	D
17	QUAD CITIES 1	EE1	GE		40		8.6		9.3		9.8		N/A		2	S	EHC		EHC		1005	D
18	QUAD CITIES 2	EE2	GE		40		8.6		9.3		9.8		N/A		2	2	EHC		EHC		1005	D
19	FUKUSHIMA 1	BP1			100+		4.7		5.5	D	5.6		N/A		2		EPR		MPR		1005	D
20	BROWNS FERRY 1	ER1	GE	S	30	D	13.33	D	13.33	D	14.05	D	N/A	S	2	D	EHC	D	EHC	S	1005	D
21	BROWNS FERRY 2	ER2	GE	S	30	D	13.33	D	13.36	D	14.05	D	N/A	S	2	D	EHC	D	EHC	S	1005	D
22	BROWNS FERRY 3	ER3	GE	S	30		13.33	D	13,422	D	14.05	D	N/A	S	2	S	EHC	S	EHC	S	1005	D
23	VERMONT YANKEE	HB1	GE	S	105	D	6.43	D	6.43	D	6.75	D	N/A	S	2	S	EPR		MPR		1005	D
24	PEACH BOTTOM 2	HE2	GE		30	D	13.4	D	13.4	D	14.0	D	N/A		2	D	EHC	D	EHC		1005	D
25	PEACH BOTTOM 3	HE3	GE	S	30	D	13.4	D	13.4	D	14.0	D	N/A	S	2	D	EHC	D	EHC	S	1005	D
26	KKM	BN1	BBC		105	D	3.86	D	4.071	D	4.152	D	N/A				HYD(BBC		HYD(BBC		1005	D
27	FITZPATRICK 1	EP1	GE		30	D	10.47	D	10.47	D	10.96	D	N/A		2		EHC		EHC		1005	D
28	SHOREHAM	KS1	GE	A	30	D	10.47	D	10.47	D	10.96	D	N/A		2	A	EHC		EHC		1005	D
29	COOPER	HP1	WEST		26		9.55	D	9.55	D	10.04	D	N/A		2		DHC		DHC		1005	D
30	PILGRIM	HK1	GE		26		7.60	D	7.60	D	7.98	D	N/A		2	S	EPR		MPR		1035	D
31	FUKUSHIMA 2	BR1	GE		30	D	9.8		9.767	D	10.3		N/A		2		EHC		EHC		1005	D
32	HATCH 1	HT1	GE		30	D	10.03	D	10.03	D	10.96	D	N/A		2		EHC		EHC		1005	D
33	HATCH 2	HT2	GE		25		10.47	D	10.47	D	10.96	D	N/A		2		EHC		EHC		1005	D
34	BRUNSWICK 2	KB1	GE	A	100+		10.47	D	10.47	D	10.96	D	N/A		2		EHC		EHC		1005	D
35	BRUNSWICK 1	KB2	GE		30	D	10.47	D	10.47	D	10.96	D	N/A		2		EHC		EHC		1005	D
36	DUANE ARNOLD	KE1	GE	S	30	D	6.84	D	6.84	D	7.16	D	N/A		2	S	EHC		EHC		1005	D
37	ENRICO FERMI 2	KH1	ENGLISH				14.16	D	14.16	D	14.86	D	N/A		2						1005	D
38	LIMERICK 1	HH1	GE	S	25	S	14.16	D	14.16	D	14.86	D	N/A		2		EHC		EHC		1005	D
39	LIMERICK 2	HH2	GE				14.16	D	14.16	D	14.86	D	N/A		2		EHC		EHC		1005	D
40	HOPE CREEK 1	KT1	GE				14.16	D	14.16	D	14.86	D	N/A		2		EHC		EHC		1005	D

ITEM NO.	PLANT IDENTITY	PROJ CODE	1 RPV ID (IN)		2 RPV MFG		3 RPV CODE SECT (ASME)		4 RPV HEAD CLAD (Y/N)		5 CORE PLATE HOLES (NO/DIA		6 FW SPARGER DESIGN	7 FUEL CHANNEL THICK (MILS)		8 FUEL CHANNEL FAB METHOD		9 CORE RECIRC FLOW (MLB/H)		10 NO OF RECIRC LOOPS	
1	DRESDEN 1	EB1	146		NYSHIP						0/0		HIDRUM	60				26		5	
2	HUMBOLDT BAY 3	ED1	120		CE				YES		0/0			60		S		13.8		0	
3	GARIGLIANO	AB1	141		TERNI						0/0		HIDRUM	80		S		22.0	D	2	
4	BIG ROCK POINT	EJ1	106		CE						0/0		HIDRUM	100				12.0		2	
5	KRB-A	AD1	146	S	RUHRSTL	S	1&862		YES	S	0/0		HIDRUM	60	S	S	S	30	S	3	S
6	TARAPUR 1	BE1	144		CE		1	S	YES	S	0/0		S	60		S	S	23.0		2	
7	TARAPUR 2	BE2	144		CE		1	S	YES	S	0/0		S	60		S	S	29.2	D	2	
8	DODEWAARDE	AE1	110	S	RDM	S	3	S	YES	S	0/0			60	S	S	S	9.92	S	0	
9	NINE MILE POINT 1	EA1	213	S	CE	S	1/8		YES	S	0/0	S	RIF	80	S	S	S	67.5	D	5	S
10	OYSTER CREEK 1	EN1	213		CE		1/8		YES		0/0		RIF	80		S		61.0	D	5	S
11	DRESDEN 2	EB2	251	D	B&W		3		YES		0/0		RIF	80	D	S		98.0	D	2	D
12	DRESDEN 3	EB3	251	D	B&W		3		YES		0/0		RIF	80	D	F		98.0	D	2	D
13	MILLSTONE 1	EH1	224	D	CE		3		YES		0/0		RIF	80	D	S		69.0	D	2	D
14	TSURUGA	BK1	171		HITACHI		1/8		YES		0/0		S	80		S		39.0	D	3	
15	NUCLENOR	BH1	188	S	RDM	S	3	S	YES	S	0/0	S	S	80	S	S		48.0	D	2	S
16	MONTICELLO	EK1	205		CBI		3		YES		0/0		SPR	80		F		57.6	D	2	
17	QUAD CITIES 1	EE1	251		B&W		3		YES		0/0		RIF	80	D	F		98.0	D	2	D
18	QUAD CITIES 2	EE2	251		B&W/CBI		3		YES		0/0		DPR	80	D	F		98.0	D	2	D
19	FUKUSHIMA 1	BP1	188		IHI		3		YES		0/0		DPR	80		F		48.0	D	2	
20	BROWNS FERRY 1	ER1	251	D	B&W	S	3	S	NO	S	129/1.0		TTS	100	D	F		102.5	D	2	D
21	BROWNS FERRY 2	ER2	251	D	B&W/IHI	S	3	S	NO	S	129/1.0		TTS	100	D	F	S	102.5	D	2	D
22	BROWNS FERRY 3	ER3	251		B&W/IHI	S	3	S	NO	S	129/1.0		TTS	80	D	F	S	102.5	D	2	
23	VERMONT YANKEE	HB1	205		CBI	S	3	S	YES	S	58/1.0		RIF	80	D	F		48.0	D	2	D
24	PEACH BOTTOM 2	HE2	251	D	B&W/CBI		3		NO		129/1.0		TTS	100	D	F		102.5	D	2	D
25	PEACH BOTTOM 3	HE3	251	D	B&W/CBI	S	3	S	NO	S	129/1.0		TTS	100	D	F		102.5	D	2	D
26	KKM	BN1	158	D	SULZRDM		3		NO		37/1.0		S	80		F		29.7	D	2	D
27	FITZPATRICK 1	EP1	218	S	CE		3		NO		77/1.0		TTS	100	D	F		77.0	D	2	D
28	SHOREHAM	KS1	218	S	CE	A	3		NO	A			TTS	100	D	F		77.0	D	2	
29	COOPER	HP1	218		CE		3		NO		88/1.0		TTS	80		F		73.5	D	2	
30	PILGRIM	HK1	224		CE		3		YES		104/1.0		RIF	80		F		69.0	D	2	
31	FUKUSHIMA 2	BR1	218		TOSHIHI		3		NO		88/1.0		S	80		F		73.5	D	2	D
32	HATCH 1	HT1	218		CE		3		NO		96/1.0		TTS	100	D	F		78.5	D	2	D
33	HATCH 2	HT2	218		CE		3		NO				W	100		F		77.0	D	2	D
34	BRUNSWICK 2	KB1	218		CBI		3		NO		77/1.0		RIF	80		F		77.0	D	2	D
35	BRUNSWICK 1	KB2	218		CBI		3		NO		77/1.0		W	100	D	F		77.0	D	2	
36	DUANE ARNOLD	KE1	183		CBI	S	3	S	NO	S	49/1.0		RIF	80	D	F	S	49.0	D	2	
37	ENRICO FERMI 2	KH1	251	D	CE		3						TTS	100	D	F		100.0	D	2	D
38	LIMERICK 1	HH1	251	D	CBI	S	3	S					TTS	100		F		100.0	D	2	D
39	LIMERICK 2	HH2	251	D	CBI		3						TTS	100		F		100.0	D	2	D
40	HOPE CREEK 1	KT1	251	D	HITACHI		3						TTS	100		F		100.0	D	2	D

Subject | Originator | Date

Number | Verifier E. C. Eckert | Date 5/1/94

Condition for maximum lift,

$$\frac{B}{1+ax} = 1$$

$$\therefore X_{max} = \frac{B-1}{a}$$ (see PB DRF Section for this formula)

$a = 0.1445$ inch

$$B = \frac{g_c A \Delta P_o}{M_s g}$$

Ref. 5. ✓ EC 5/1/94

same for g_c

For H5 weld, $M_s = 413.74$ KIP

	El	Effective mass	Cummulative Wt
(H4) El	266.375	259.06 kip	?
	208.01		405.62 kip
(H5)	191.125	334.48	
	147.53		434.59

$$H5 \text{ mass} = 405.62 + \frac{(34.59 - 5.62)}{(208.01 - 147.53)}(208.01 - 191.12$$

$= 413.74$ KiP

GE Nuclear Energy
Engineering Calculation Sheet

Subject	Originator	Date
Number	Verifier E.C. Eckert	Date 5/1/94

$$A = \frac{\pi}{4} D^2 = \frac{\pi}{4} \times (203.12)^2 = 32,403.75 \text{ in}^2$$

<u>B values</u> <u>B</u>

$\Delta p = 7$ psi $\quad B = \dfrac{7 \times 32,403.75}{413.74\,(10^3)} = 0.548$

ECE 5/1/94

$\Delta p = 12$ psi $\quad B = 0.94$

The effects of Drag force, Momentum, Buoyancy Force, Hydrodynamic mass are small, and canceles most of their effects each other.

No lift up to 12.77 psi of pressure drop.

Gives B = 1

ECE 5/1/94

Subject | Originator | Date

Number | Verifier E. C. Eckert | Date 5/1/94

Assume DBE

296 for QC2 — From Ref 5. ✓ EC 5/1/94

W @ H5 = 306.76

@ $\Delta P_0 = 12$ psi

$$B = \frac{12 \times 32,403.75}{306,760} = 1.27$$

$$X_{max} = \frac{1.27 - 1}{0.1445} = 1.85''$$

1.69" slack
.25" Thermal Exp
1.44" clearance

Assume OBE

$$B = \frac{12 \times 32,403.75}{334,480} = 1.1625$$

329,100 / 16 for QC2 — Ref. 5a EC 5/1/94

$$X_{max} = 1.13''$$

Can be accommodated by the slack in the Core Spray line bracket

Reference 1

Telecon D.K. Rao (GE) and Bob Walsh (CECo)

@ 1 pm on 5/4/94 (309) 654-2241 (x2198)
Fax (x2265)

Subject: Quad Cities Unit 2 Shroud Cracking.

Summary of Discussion:

1. Schedule: Critical to get assessment by 5/6/94
CECo will work on it over weekend to
give to NRC on 5/9/94.

2. Required Inputs: (@ 3 pm, by voice mail)

Dilip Rao requested the following by voice mail

- Examination Report of Welds for Quad Cities 1.
  (Location of Cracks,
  Depth of Cracks.)
- Are shrouds identical for Unit 1 & 2
- Hydrogen Injection Data (% availability, concentration)
- Conductivity Data (average values)
- FSAR chapter 15
  - Bypass capability
  - MCPL Setting
  - No of ADS Valves
- Radiological Consequences of MSLB-IC, MSLB-OC, LOCA

3. The assessment is required to continue Quad Cities Unit 2 operation. A comparative evaluation will be done between Units 1 and 2. The results of Unit 1 inspection are still coming in.

Reference 2 (a)

Telecon D.K. Rao, H. Choe (GE), Tom Sfory, John Dawn (CECo @ San Jose), Bob Walsh (CECo).

8:30 am 5/5/94.

<u>Subject</u>: Quad Cities 2 Shroud Cracking

<u>Summary of Conversation</u>:

1. Visual Inspections are complete at QC1.
   360° crack at H5.
   Max depth 1.2" for 6 area examined by UT.

2. Unit 1 has run longer than Unit 2.
   (Followup phone call Bob Walsh / Dilip Rao gave 151,487 hours for QC1 and 146,195 hours) QC2.

3. Hydrogen Injection Information will be given later

4. QC1/QC2 shrouds are Identical

5. Conductivity data is available from Barry Gordon @ GE.

6. FSAR data has been sent by Fax to D. Rao

7. Radiological consequences for Dresden and Quad Cities sites are similar.

8. 40% Bypass Capability, 110% MCFL setting for QC1 & QC2.

Reference 2(b)

(309) 6~~4~~ 2241 x2198 - Bob
x2994 - Mark

Telecon 5/6/94: D.K. Rao / H. Choe (GE) and
Bob Walsh, Mark Ulrich (CECo), John Dawr, Tom Spry.

Subject: QC2 Evaluation Status:

Summary of Discussion:

1. Crack Depth of 1.2 inches, as reported by CECo shows margin to calculated value. (2.7 inch) that is allowable. Visuals are complete, UT will be done on tracker and complete next week

2. Please provide GE with details of Report.
   - Which welds were inspected
   - which show flaws
   - Which are significant

3. Crack growth rates are not expected to cause to exceed calculated value, if starting from 1.2 inches reported by CECo.

4. Water Chemistry Issues:
   - Hydrogen effects are only implemented in short term QC2 ~~QC2~~ is non bounding. 57% + 44% (1.5ppm) But GE position is to treat as Normal Water chem.
   - Conductivity is Comparable. (0.257 QC1 vs 0.258 QC2 μS/cm)

5. Crack leakage flows are small (<60 gpm)

6. Transients not likely to be problem.

7. Accidents
   - In progress.

QC2: Jan '95 (Next Outage.) Now in Cycle 13.

Reference 2 b)

Page 2

- QC2 will be in refueling outage in January '95
  (Now QC2 is in Cycle 13)
- Visual Inspections are complete
- UT done for H5 with 60° dual R-L
  Transducer at Six Locations
  Deepest was 1.2 inches
  45° examination was not done
  (Following Pages are a follow-up fax)
- Report should address:
  - All welds inspected and their findings
  - 2/3 core height (or more is attainable)
    (Post LOCA / MSLB)
  - Lateral Loads
  - ISGCC is primary mode

Reference 2b Pg. 3

TO: Pelip Rao

From: Mark D. Uhrich
(309)654-2241 #2994

Subject: Shroud Welds

Here is the information you requested at the 1030A meeting on the results of the vessel inspections.

Please contact me if you require any more information.

Post-it™ brand fax transmittal memo 7671 | # of pages ▸ 3

To Felip Rao	From Mark D. Uhrich
Co. GE	Co. CeCo
Dept. (408) 925-1071	Phone # (309)654-2241 #2994
Fax # (408) 925-1496	Fax # 2265

May 3, 1994

QUAD CITIES UNIT 1
SHROUD INSPECTION STATUS

WELD #	SURFACE	AREA EXAMINED	INSPECTION RESULTS	QUALIFICATION STATUS
H1	O.D.	INSPECTED 4 AREAS (~12" EACH)	CECo LEVEL III REVIEW PENDING	Weld will be re-inspected
H2	O.D.	INSPECTED 4 AREAS (~12" EACH)	CECo LEVEL III REVIEW PENDING	Weld will be re-inspected
H3	I.D.	100% (638")	TOTAL OF 134" OF INDICATIONS (21% OF LENGTH) (WORST FLAW 45" IN LENGTH)	EVALUATION IN PROGRESS
H3	O.D.	0° - 80° (142")	NO INDICATIONS FOUND	QUALIFIED INSPECTED 100% OF WELD O.D. IDENTIFIED AS NO INDICATIONS FOUND ON I.D. TO VERIFY BOTH I.D. AND O.D HAVE NO INDICATIONS
		85° - 90° (9")	NO INDICATIONS FOUND	
		92° - 160° (121")	NO INDICATIONS FOUND	
		167° - 170° (5")	NO INDICATIONS FOUND	
		175° - 180° (9")	NO INDICATIONS FOUND	
		215° - 240° (44")	NO INDICATIONS FOUND	
		260° - 0° (177")	NO INDICATIONS FOUND	
H4	O.D.	INSPECTED 4 AREAS (~22" EACH)	NO INDICATIONS FOUND	Need to re-inspect 2 areas
H4	I.D.	INSPECTED 4 AREAS (~22" EACH)	2 MINOR (1/2") INDICATIONS	QUALIFIED ~~I.D. & O.D. CORRESPOND~~
H5	O.D.	INSPECTED 8 AREAS (~200" TOTAL)	RANDOM INDICATIONS FOUND IN ALL AREAS INSPECTED (LOCATED BELOW H5 IN RING)	EVALUATION IN PROGRESS
H6	O.D.	INSPECTED 6 AREAS (~16" EACH)	2 MINOR (1/2" & 2") INDICATIONS	Need to re-inspect 2 locations
H7	O.D.	INSPECTED 8 AREAS (~130" TOTAL)	NO INDICATIONS FOUND	QUALIFIED ~~PENDING REVIEW~~

Reference 26

Page 4

Virgil

We ultrasonically examined the H5 Shroud weld with a 60 dual R-L Transducer a six locations and the following crack depths were obtained:

356° = .70" deep

315° = .90" deep

230° = 1.10" deep

175° = 1.10" deep

135° = 1.00" deep

90° = 1.20" deep

We never performed a 45° examination due to problems and we had problems with the 60° exam. I will complete a report in the morning.

Brian J. Wilson
CECo Level III
5-1-94

DRF-137-0010-7

GENE-523-02-0194

Evaluation and Screening Criteria for the Quad Cities 1

Reference 5

Verification of Methods & Results

GE Nuclear Energy

Engineering Services Verification Cover Sheet
(Reference EOP 25-6.00) *Sheet 4 of __*

DRF NO./SECTION DRF-137-0010-7, GE-NE-523-02-0194
Subject: Evaluation and Screening Criteria for the Quad Cities 1 and 2 Shrouds

1 VERIFICATION REQUIREMENT Designated Verifier H. S. Mehta

1A APPLICATION. (System/Project/Program) Charge # 1EETT

Shroud/ Quad Cities 1 and 2 / Fracture Mechanics Analysis

1B METHOD OF VERIFICATION. Checking, Alternate Calc. Indiv. Design Review, Team Design Review, Test (circle as needed); Other (describe)

Individual Design Review

1C SCOPE. (Identify what is to be verified; e.g., level of detail).

Please verify that the latest customer-requested changes to the methods, calculations, and report of the analysis are reasonable and correct, and that the analysis and report apply to both units.

1D INPUTS. (Identify any GE and external interfaces and requirements, assumptions, input documents, test analyses, reasons for changes).

See references in report GENE-523-02-0194 and DRF Reference Sheet.

1E OUTPUTS. (Identify output document(s) or analysis results to be verified).

Report GENE-523-02-0194 and the associated DRF.

1F Responsible Engineer W F Weitze Date 3-15-94 Comp. 523
W. F. Weitze

2 INDEPENDENT VERIFICATION

Comments: No Yes (See Attached)

2A VERIFICATION STATEMENT: The method and scope of verification as stated in 1B and 1C are appropriate. The inputs as identified in 1D. All comments and technical issues are resolved. The verification establishes that the output identified in 1E is correct and is adequate for its intended application as identified in 1A.

2B Independent Verifier H S Mehta Date 3/16/94 Comp. 523
H. S. Mehta

3 APPROVAL OF VERIFICATION

3A MANAGER'S APPROVAL: All design requirements have been identified and all technical issues are adequately resolved. The verification described in the above Sections 1 and 2 is sufficient to issue/apply the results.

3B Resp. Manager: [signature] for Date 3/22/94 Comp. 521
or Delegate S. Ranganath

4A Are there attached sheets for 1A, 1B, 1C, 1D, 1E, 2A, 3A? (circle as applicable)

SD-056B(1/92)

CIRCUMFERENTIAL FLAW

Dimensions for Welds H3 to H5

Out dia. = Do	207.125	inches	In Dia = Di	203.125	inches	from GE 718E861 Shroud, Spec Control
Out radius = Ro	103.56	inches	In Radius = Ri	101.56	inches	
thick = t	2.0	inches	Area = A	1288.84	in^2	

Above the Core Plate, Limit Load Analysis

		H3	H4	H5		
Normal & Upset:	Shroud Head Press. (psi)	8.0	8.0	8.0		from QC 1&2 UFSAR, Table 3.9-19
	Sig(p) = P*Ri/2*t (ksi) =	0.203	0.203	0.203		
	Wt. & Vert. Seis (ksi) =	-0.154	-0.198	-0.255		
	Total Membrane Stress (ksi) =	0.049	0.005	-0.052	= Pm	Use Zero if negative
	Upset Bending Stress (ksi) =	0.187	0.651	1.169	= Pb	From Seismic Load Table
	Sm (ksi) = 16.9					
	Pm/Sm =	0.003	0.000	-0.003		
	(Pm+Pb)/Sm =	0.014	0.039	0.069		
	Safety Factor =	2.8	2.8	2.8		
Faulted:	Shroud Head Press. (psi)	20.0	20.0	20.0		from QC 1&2 UFSAR, Table 3.9-19
	Sig(p) = P*Ri/2*t (ksi) =	0.508	0.508	0.508		
	Wt. & Vert. Seis (ksi) =	-0.139	-0.178	-0.230		
	Total Membrane Stress (ksi) =	0.369	0.330	0.278	= Pm	Use Zero if negative
	Faulted Bending Stress (ksi) =	0.374	1.303	2.337	= Pb	From Seismic Load Table
	Pm/Sm =	0.022	0.020	0.016		
	(Pm+Pb)/Sm =	0.044	0.097	0.155		
	Safety Factor =	1.4	1.4	1.4		
Allow. Flaw Length:	fraction of circumference from 1CRITFLA run	0.778	0.724	0.681		
	(using mean radius) * 2*pi*Rm (in) =	501.4	466.6	438.8		
	Allowable Flaw Length/4 (in) =	125.34	116.64	109.71		
	Limiting Case:	Faulted	Faulted	Faulted		

Above the Core Plate, LEFM

		H4	H5	
Normal & Upset:	Total Sig = Pm+Pb (ksi) =	0.657	1.169	
Faulted:	Total Sig = Pm+Pb (ksi) =	1.633	2.615	
Governing Case:	3.16 x Norm/Upset =	2.075	3.693	
	1.4 x Faulted =	2.286	3.661	
	Limiting Case:	Faulted	Upset	
	Allowable Flaw =	281	183	from spreadsheet QC1SHRDN.XLS

Purpose: Determine the bending stresses in the shroud due to the seismic load

Reference: See DRF Reference List.

Discussion: The relative elevations for the dynamic loads were taken from Ref. 1. The section modulus Z was calculated at each weld location. Linear interpolation was used to determine the moments for each weld; the corresponding weld elevations were determined from Refs. 3b, 3c, 3e, and 3f. The bending stresses were calculated for OBE and DBE conditions using standard strength of materials equations (stress = M/Z).

The maximum seismic moments for the shroud summarized below in Table 2 are taken from Reference 1. The DBE (SSE) loads in Table 2 are two times the OBE loads, from Ref. 1.

Table 1 below shows the seismic loads applied to each weld for OBE and DBE conditions.

TABLE 1 SEISMIC LOADS AND STRESSES FOR EACH WELD LOCATION

Weld Designation	Elev. (in)	Outside Radius (in)	Inside Radius (in)	Thick. (in)	Section Modulus (in^3)	OBE Moment (in-kips)	DBE Moment (in-kips)	OBE Pb (ksi)	DBE Pb (ksi)	Effective Wt. (kip) OBE	Effective Wt. (kip) DBE	NOT USED Shear (kips) OBE
H1	391.375	110.00	108.00	2.00	7.47E+04	5.19E+03	1.04E+04	0.07	0.14	174.91	157.32	43
H2	357.875	110.00	108.00	2.00	7.47E+04	1.16E+04	2.31E+04	0.15	0.31	197.87	177.87	338
H3	355.375	103.56	101.56	2.00	6.61E+04	1.24E+04	2.47E+04	0.19	0.37	198.99	178.98	338
H4	266.375	103.56	101.56	2.00	6.61E+04	4.31E+04	8.61E+04	0.65	1.30	254.89	229.28	415
H5	191.125	103.56	101.56	2.00	6.61E+04	7.72E+04	1.54E+05	1.17	2.34	329.10	296.00	604
H6	187.125	100.50	98.50	2.00	6.22E+04	7.96E+04	1.59E+05	1.28	2.56	330.62	297.37	604
H7	131.500	100.50	98.50	2.00	6.22E+04	1.13E+05	2.26E+05	1.82	3.63	345.71	310.94	592
H8	120.531	100.50	98.50	2.00	6.22E+04	1.19E+05	2.39E+05	1.92	3.84	345.71	310.94	592

TABLE 2 REFERENCE 1 LOADS

Elevation from VB (in)	Node #	Cumulative Wt. (kip)	Effective Wt. (kip) OBE	Effective Wt. (kip) DBE	Moment (in-kips) OBE	Moment (in-kips) DBE	NOT USED Shear (kips) OBE
463.49	12	133.87	106.49	95.78	2.13E+03	4.26E+03	43
375.53	13	238.78	189.94	170.84	5.86E+03	1.17E+04	338
288.77	14	287.73	228.88	205.87	3.38E+04	6.77E+04	415
208.01	15	405.62	322.66	290.21	6.71E+04	1.34E+05	604
147.53	16	434.59	345.71	310.94	1.03E+05	2.07E+05	604 ~~592~~
120.53	*	434.59	345.71	310.94	1.19E+05	2.39E+05	592

* Shroud Support Plate

OBE to DBE Factor: 2

Vertical Acceleration (g's) OBE	Vertical Acceleration (g's) DBE	Density (lb/in^3) Steel	Density (lb/in^3) Water
0.08	0.16	0.290	0.036

Buoyancy: subtract weight of water displaced
= metal wt. * water density/metal density
Effective Wt = Cum. Wt. * (1-Dens. Ratio-Vert. Acc.)
Stainless steel density from Y1002A002 rev. 4

WGW
3-16-94

3/09/1994 - 10:47:18

TITLE: Quad Cities 1 Shroud Circ Flaw At H5, Limit Load

FLOW STRESS FACTOR ON SM = 3.000

PM = .000 PM + PB = .069 SAFETY FACTOR = 2.800
FLOW STRESS FACTOR = 3.000
PM = .016 PM + PB = .155 SAFETY FACTOR = 1.400
FLOW STRESS FACTOR = 3.000

SAFETY FACTOR = 2.800		SAFETY FACTOR = 1.400	
LENGTH	DEPTH	LENGTH	DEPTH
.698	1.000	.681	1.000
.700	.999	.700	.992
.750	.985	.750	.978
.800	.976	.800	.969
.850	.971	.850	.964
.900	.969	.900	.962
.950	.968	.950	.961
1.000	.968	1.000	.961
.000	.000	.000	.000
.000	.000	.000	.000
.000	.000	.000	.000
.000	.000	.000	.000
.000	.000	.000	.000
.000	.000	.000	.000
.000	.000	.000	.000
.000	.000	.000	.000
.000	.000	.000	.000
.000	.000	.000	.000
.000	.000	.000	.000
.000	.000	.000	.000
.000	.000	.000	.000

All [illegible]

Reference 6

To D. Rao

1. The shrouds on the Quad Cities units are identical.
2. Attached Table
3. Bypass Valve Capacity — Reference UFSAR Figure 10.1
   MCF 110% — No reference found
   Peak Steam Flow w/ADS — Not found, same as Dresden
4. This is about 30 pages. Are you sure you need it? Does Dresden's give you the info you need?
5. GE has information from package that was put together to evaluate the susceptibility of the shroud.

If you need additional info I need specifics on what info you are looking for for Hydrogen Water Chemistry and Conductivity.

Post-it™ brand fax transmittal memo 7671		# of pages ▸	
To	D RAO	From	B-WALSH
Co.	GE	Co.	CECO
Dept.	408 925-1071	Phone #	2198
Fax #	408 925 ~~1077~~ 1990	Fax #	2265

May 3, 1994

QUAD CITIES UNIT 1
SHROUD INSPECTION STATUS

WELD #	SURFACE	AREA EXAMINED	INSPECTION RESULTS	QUALIFICATION STATUS
H1	O.D.	INSPECTED 4 AREAS (~12" EACH)	CECo LEVEL III REVIEW PENDING	Weld will be re-inspected
H2	O.D.	INSPECTED 4 AREAS (~12" EACH)	CECo LEVEL III REVIEW PENDING	Weld will be re-inspected
H3	I.D.	100% (638")	TOTAL OF 134" OF INDICATIONS (21% OF LENGTH) (WORST FLAW 45" IN LENGTH)	EVALUATION IN PROGRESS
H3	O.D.	0° - 80° (142")	NO INDICATIONS FOUND	INSPECTED 100% OF WELD O.D. IDENTIFIED AS NO INDICATIONS FOUND ON I.D. TO VERIFY BOTH I.D. AND O.D HAVE NO INDICATIONS
		85° - 90° (9")	NO INDICATIONS FOUND	
		92° - 160° (121")	NO INDICATIONS FOUND	
		167° - 170° (5")	NO INDICATIONS FOUND	
		175° - 180° (9")	NO INDICATIONS FOUND	
		215° - 240° (44")	NO INDICATIONS FOUND	
		260° - 0° (177")	NO INDICATIONS FOUND	
H4	O.D.	INSPECTED 4 AREAS (~22" EACH)	NO INDICATIONS FOUND	Need to re-inspect 2 areas
H4	I.D.	INSPECTED 4 AREAS (~22" EACH)	2 MINOR (1/2") INDICATIONS	I.D. & O.D. CORRESPOND
H5	O.D.	INSPECTED 8 AREAS (~200" TOTAL)	RANDOM INDICATIONS FOUND IN ALL AREAS INSPECTED (LOCATED BELOW H5 IN RING)	EVALUATION IN PROGRESS
H6	O.D.	INSPECTED 6 AREAS (~16" EACH)	2 MINOR (1/2" & 2") INDICATIONS	Need to re-inspect 2 locations
H7	O.D.	INSPECTED 8 AREAS (~130" TOTAL)	NO INDICATIONS FOUND	QUALIFIED PENDING REVIEW

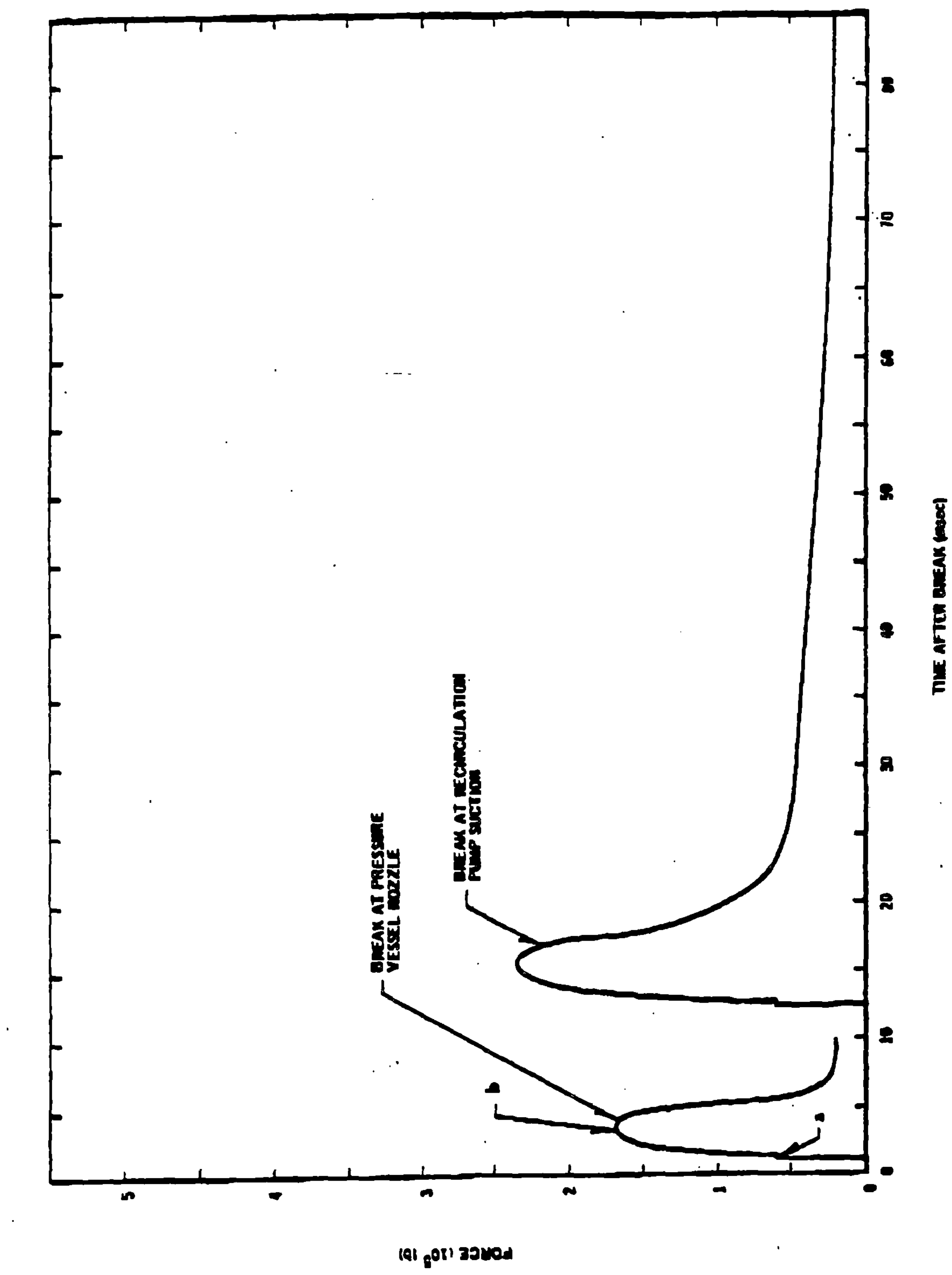

QUAD CITIES STATION
UNITS 1 & 2

REACTOR VESSEL SHROUD FORCE FOLLOWING RECIRCULATION LINE BREAK

FIGURE 3.9-12

Table 3.9-19

REACTOR INTERNAL PRESSURE DIFFERENTIALS

Component	Δ P At Turbine-Generator Design Power	Maximum Δ P Following A Steam Line Break	Maximum Δ P Following a Recirculation Line Break
Shroud support	25	43	25
Guide tube	17	30	17
Core plate	17	30	17
Lower shroud	25	43	25
Upper shroud	8	20	8
Shroud head	8	20	8
Dryers	2	4[Note 1]	2
Channel box	9	16	9

Notes:

1. Evaluated from the outside steam-line break described in Chapter 15.

Table 3.9-20

PRESSURE FORCES ACTING ON MAJOR REACTOR INTERNAL COMPONENTS

Major Component	Pressure Force[Note 1]
Shroud support	P_1-P_4
Guide tube	P_1-P_3
Core plate	P_1-P_3
Lower shroud	P_1-P_4
Upper shroud	P_1-P_4
Shroud head	P_3-P_4
Jet pump diffuser	P_1-P_4

Notes:

1. Refer to Figure 4.1-2; subscripts refer to model nodes shown on Figure 3.9-7.

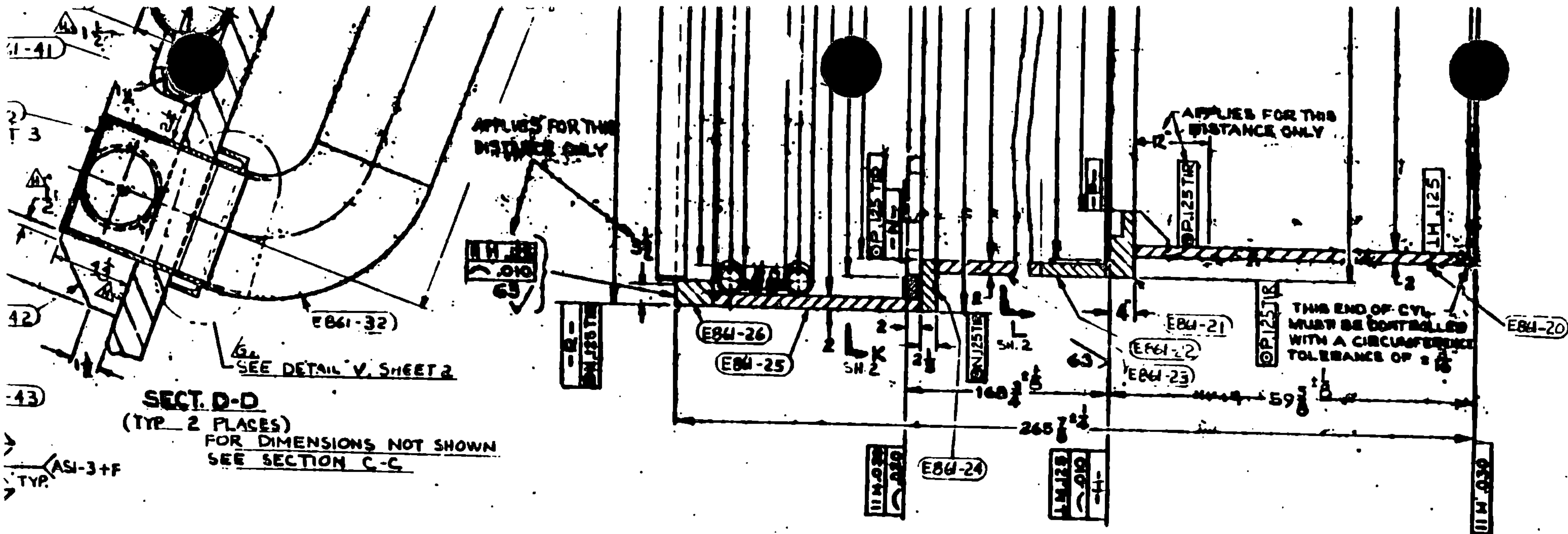

SECT. D-D
(TYP 2 PLACES)
FOR DIMENSIONS NOT SHOWN SEE SECTION C-C

SECT. A-A

CERTIFIED FOR CONSTRUCTION
FOR WILLAMETTE IRON AND STEEL COMPANY

NOTES:

1. APPROXIMATE WEIGHT: 114,200 LBS.
2. FOR SUPPLEMENTARY INFORMATION SEE G.E. APED SPEC. 21A3319.
3. ℄ M IS DETERMINED AS LINE BETWEEN CENTERS OF "N" & "P" DIAMETERS.
4. THE ALIGNMENT OF SECTIONS AT EDGES TO BE WELDED MUST NOT EXCEED A MAX. OFFSET OF 1/8" NOR CAUSE A REDUCTION IN THE THICKNESS OF EITHER SECTION.

NOTES (CONT)

5. REFER TO SEPARATE MATERIAL LIST FOR MATERIAL SPECIFICATION & CERTIFICATION
6. BREAK SHARP EDGES
7. WELDING PER WISCO W-001 & PROCEDURES.
8. WELD INSPECTION PER WISCO QC-660510-NDT-1 & -NDT-2.
9. CLEANING PER WISCO QC-660510-C-1.
10. LUBRICATE THREADS PER WISCO QC-660510-L-1
11. FOR FAB. OF SPARGER PIPES EB61-2 & EB61-10 SEE SHEET 3.

CERTIFIED by VENDOR
APPROVED
FOR GENERAL ELECTRIC

GENERAL ELECTRIC CO.
S.O. 680353

EB61-1 SHROUD

MAT'L LIST SH. 9, 10 & 11

REFERENCE DRAWINGS	G.E. C° DWG. 718E861
FOR CONTRACT	G E C° P.O. NO. 205-H0187
TITLE	GENERAL ELECTRIC C° APED - SAN JOSE CORE STRUCTURE QUAD CITIES 1 & 2 SHROUD
	WILLAMETTE IRON & STEEL COMPANY
SALES ORDER NO.	660510
DWG. NO.	EB61 SH. 1 OF 4
REV.	J

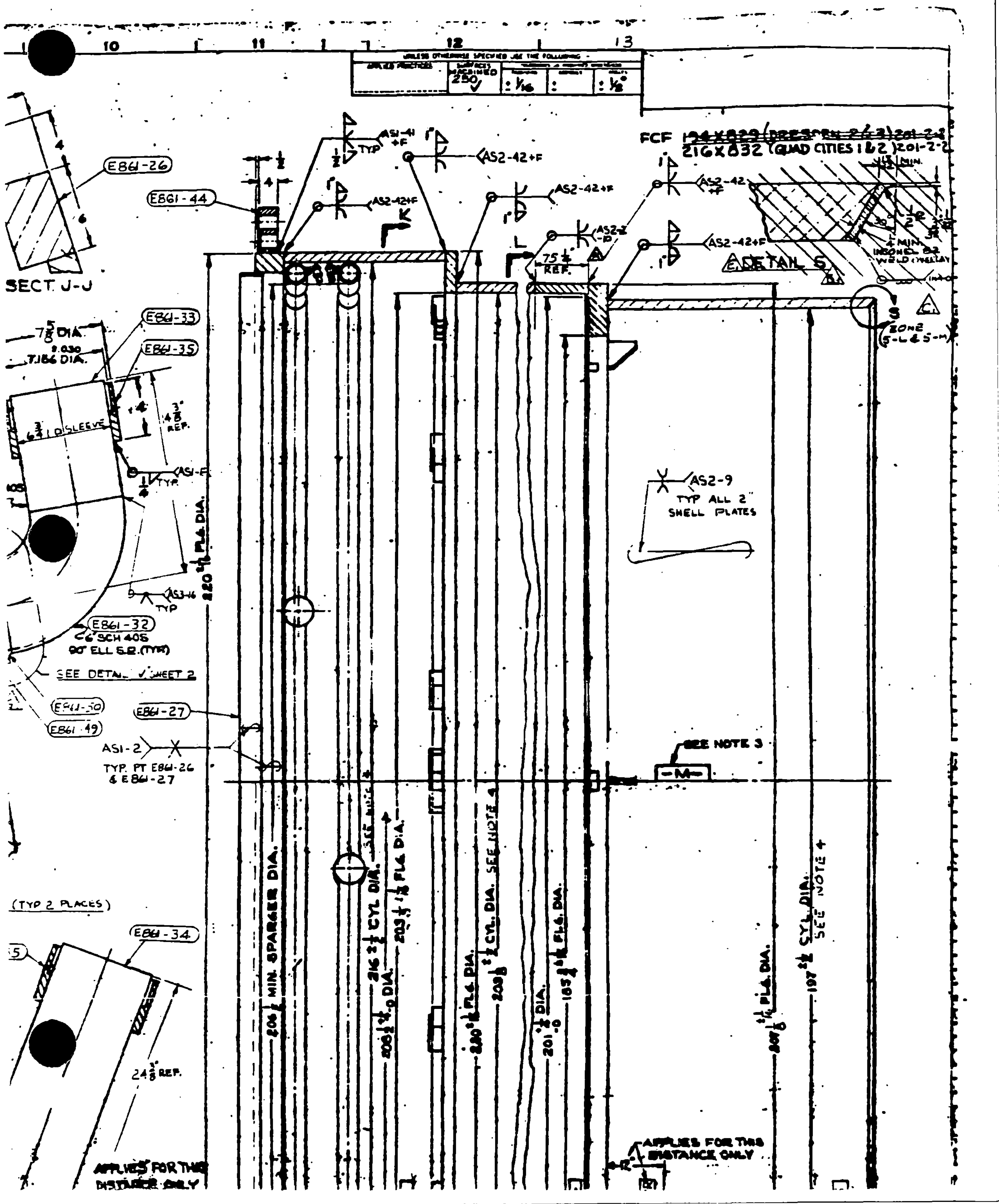

FCF 216X832 (QUAD CITIES 1 & 2) 201-2-2
DETAIL S
SECT. J-J
E861-26
E861-44
E861-33
E861-35
E861-32
E861-27
E861-49
E861-34
AS2-42+F
AS2-9
TYP ALL 2" SHELL PLATES
SEE NOTE 3
SEE DETAIL V SHEET 2
6" SCH 40S 90° ELL S.R. (TYP)
ASI-2
TYP. PT E861-26 & E861-27
(TYP 2 PLACES)
APPLIES FOR THIS DISTANCE ONLY
206 MIN. SPARGER DIA.
220 FLG. DIA.
SEE NOTE 4

Ref. 13.

ECE 3/6/94

NEDC-31345P

June 1987

GENERAL ELECTRIC COMPANY

QUAD CITIES NUCLEAR POWER STATION UNITS 1 & 2

SAFER/GESTR - LOCA

LOSS-OF-COOLANT ACCIDENT ANALYSIS

T. C. Hoang
D. G. Hoover
D. C. Serell
P. E. Elliott

Approved: L D Noble

L. D. Noble, Manager
Reload Nuclear Engineering-1

Approved: WL Zaman for

J. S. Charnley, Manager
Reload Fuel Licensing

NUCLEAR ENERGY BUSINESS OPERATIONS • GENERAL ELECTRIC COMPANY
SAN JOSE, CALIFORNIA 95125

GENERAL ELECTRIC

GENERAL ELECTRIC COMPANY

IMPORTANT NOTICE REGARDING CONTENTS OF THIS REPORT

Please Read Carefully

The only undertakings of the General Electric Company respecting information in this document are contained in the contract between CECo and General Electric Company for this report, and nothing contained in this document shall be construed as changing the contract. The use of this information by anyone other than CECo or for any purpose other than that for which it is intended, is not authorized; and with respect to any unauthorized use, General Electric Company makes no representation or warranty, and assumes no liability as to the completeness, accuracy, or usefulness of the information contained in this document.

Table 4-1

SIGNIFICANT INPUT PARAMETERS USED IN THE QUAD CITIES 1 & 2 LOCA ANALYSIS

A. Plant Parameters

	Nominal	Appendix K
Core Thermal Power (MWTH)	2511	2561
Vessel Steam Output (lbm/hr)	9.759×10^6	9.954×10^6
Corresponding Power (%)	100	102
Vessel Steam Dome Pressure (psia)	1020	1020
Maximum Recirc Line Break Area (ft^2)	4.26	4.26

B. Fuel Parameters

	P8x8R/BP8x8R	GE8x8EB
PLHGR (kW/ft) - Appendix K	13.4x1.02	14.4x1.02
Initial MCPR - Appendix K	1.20/1.02	1.20/1.02
- Nominal	1.22	1.22
Axial Peaking Factor	1.4	1.4
Number of Fueled Rods per Bundle	62	60/62

C. Emergency Core Cooling System Parameters

Low Pressure Coolant Injection (LPCI) System

Vessel Pressure at Which Flow May Commence (psig)	325
Minimum Rated Flow at Vessel Pressure (psig)	20
for two pumps (gpm) into one loop	9000

[a]Represents the limiting operating condition resulting in the maximum calculated PCT at anytime in the fuel lifetime.

Table 4-1 (Continued)

Initiating Signals and Setpoints	
Low Water Level [feet above Top of Active Fuel (TAF)]	7
or	
High Drywell Pressure (psig)	2.5
Maximum Allowable Time Delay from Initiating Signal to Pump at Rated Speed (sec)	25
Injection Valve Stroke Time (sec)	25
Maximum Vessel Pressure at Which LPCI Injection Valve Can Open (psig)	325
Recirc Discharge Valve Closure	
Closure Pressure Permissive For Loop Selection (psig) (For Single- or No-Loop Operation)	900
Time Delay for Loop Selection	3
Maximum Discharge Valve Stroke Time (sec)	45
Minimum Break Size for which Loop Selection Logic Assumed to Select Unbroken Loop (ft^2)	0.1
<u>Low Pressure Core Spray (LPCS) System</u>	
Vessel Pressure at Which Flow May Commence (psig)	325
Minimum Rated Flow at Vessel Pressure (psig) for One Loop (gpm)	90 4500
Initiating Signals and Setpoints	
Low Water Level (feet above TAF)	7
or	
High Drywell Pressure (psig)	2.5
Maximum Allowed (Runout) Flow (gpm)	5650
Maximum Allowable Delay Time from Initiating Signal to Pump at Rated Speed (sec)	28
Injection Valve Stroke Time (sec)	15
Maximum Vessel Pressure at Which LPCS Injection Valve Can Open (psig)	325

Simplified Equ

$$M \frac{d^2x}{dt^2} = g_c \Delta P \cdot A - Mg$$

- conservative
- integrated

$$\Delta P = \frac{\Delta P_0}{(1+ax)^2} \leftarrow \text{no lift}$$

$$\frac{d^2x}{dt^2} = \frac{g_c B}{(1+ax)^2} - g$$

@ $t=0$, $x=0$, $\dot{x}=0$

Multiply $2\frac{dx}{dx}$

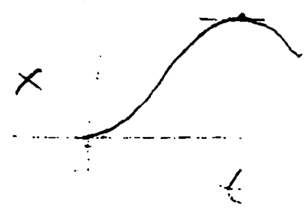

$$2\frac{dx}{dt} \cdot \frac{d}{dt}\left(\frac{dx}{dt}\right) = \frac{g_c B}{(1+ax)^2}\frac{dx}{dt} - g\frac{dx}{dt}$$

$$(\dot{x})^2 = 2gx\left[\frac{B}{1+ax} - 1\right]$$

X_{max} occurs at $\dot{x}=0$

$$\frac{B}{1+ax_{max}} = 1$$

$$X_{max} = \frac{B-1}{a}$$

$$\frac{1}{(1+ax)^2} = \frac{\Delta P}{\Delta P_0}$$

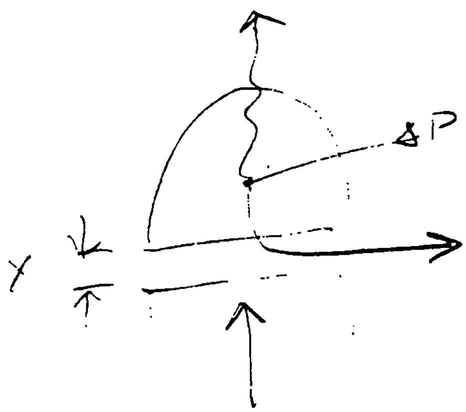

$$\dot{m}_T = \dot{m}_s + \dot{m}_L$$

$$\dot{m}_L = (\pi D \cdot x)\, \rho_\phi \frac{K V^2}{2 g_c}$$

$$\dot{m}_s = \sqrt{\frac{\Delta P}{\Delta P_0}}\, \dot{m}_T$$

$$\Delta P_0 = C\, \dot{m}_T^2 \qquad \dot{m}_s = R_s\, \Delta P$$

$$\Delta P = C\, \dot{m}_s^2 \qquad \dot{m}_L = R_L\, \Delta P$$

$$a = \frac{R_s}{R_L}\, x$$

$$ax = \frac{R_s}{R_L}$$

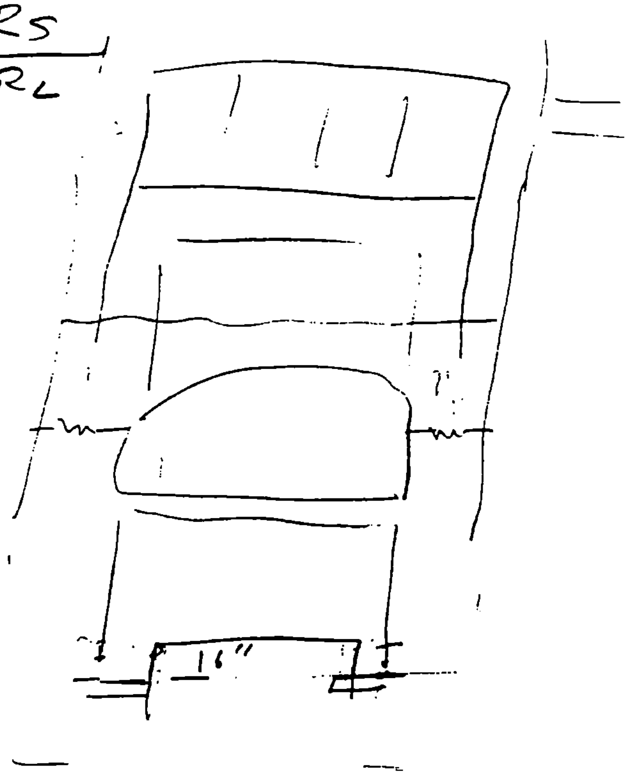

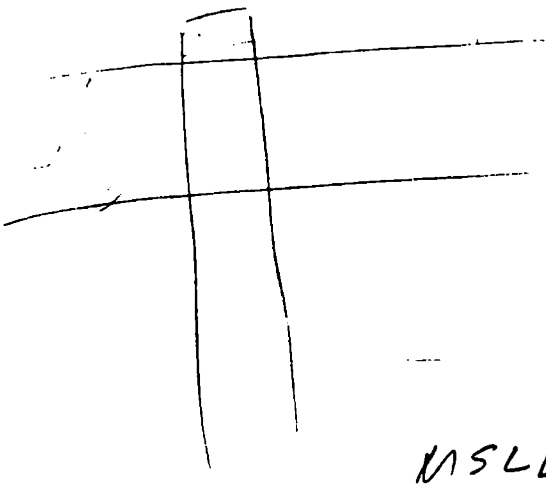

MSLB ~ 4"
SSE+MSLB ~ 8"

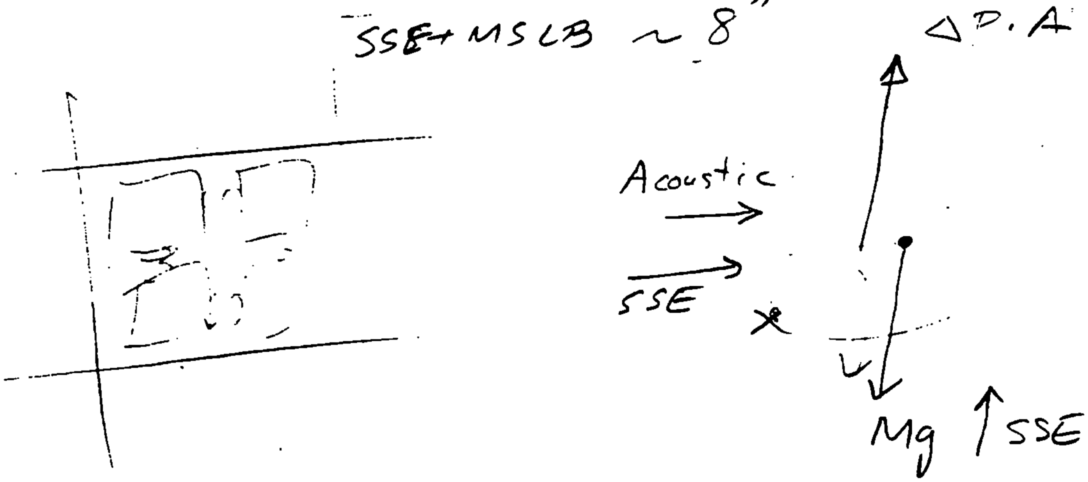

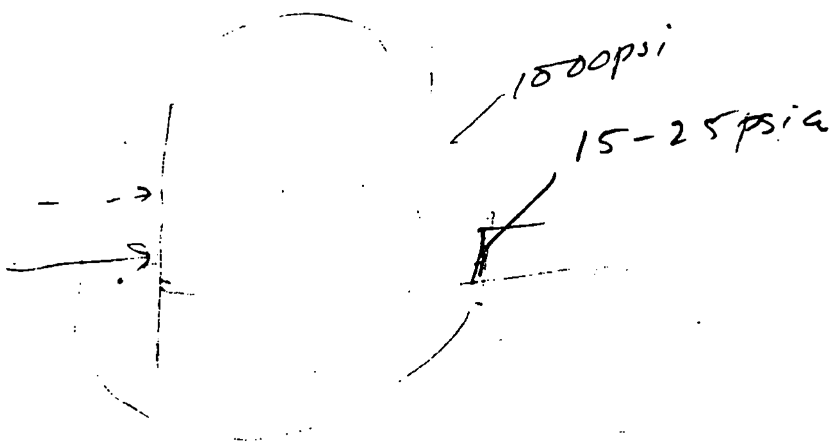

Code limits for the nuclear process barrier. Turbine trips from lower initial power levels decrease in severity to the point where scram may even be avoided within the bypass capacity if auxiliary power is available from an external source.

14.5.1.4 Bypass Valves Failure Following Turbine Trip, High Power

This event is included to illustrate that single failure could prevent the turbine bypass valves from opening in conjunction with a turbine trip.

14.5.1.5 Bypass Valves Failure Following Turbine Trip, Low Power

This abnormal operational transient is of interest because turbine stop valve closure and turbine control valve fast closure scrams are automatically bypassed when the reactor power level is low. Turbine first-stage pressure is used to initiate this bypass at 154 psig. The highest power level for which these scrams remain bypassed is about 30 percent of rated power. Figure 14.5-3 graphically shows the transient starting with the recirculation pumps at about 20 percent speed producing 40 percent core flow at 31 percent rated power. Reactor scram is initiated at about 3.0 seconds by high vessel pressure. No bypass flow is assumed; however, the relief valves partially open to relieve the pressure transient. The peak pressure at the safety/relief valves is 7
well below the ASME Code limits. Since pressure remains below 1375 psig at the bottom of the vessel, no damage occurs to the nuclear process system barrier. No fuel damage occurs since peak heat flux is significantly lower than rated conditions.

14.5.1.6 Main Steam Line Isolation Valve Closure

Automatic circuitry or operator action can initiate closure of the main steam isolation valves. Position switches on the valves provide reactor scram if valve(s) in three or more main steam lines are less than 90 percent open and reactor pressure is greater than 1,055 psig or the mode switch is in the Run position. However, Protection System logic does permit the test closure of one valve without initiating scram from the position switches. Inadvertent closure of one or all of the isolation valves from reactor scrammed conditions (such as Operating States C or E) will produce no significant transient. Closures during plant heatup (Operating State D) will be less severe than the maximum power cases (maximum stored and decay heat) which follow.

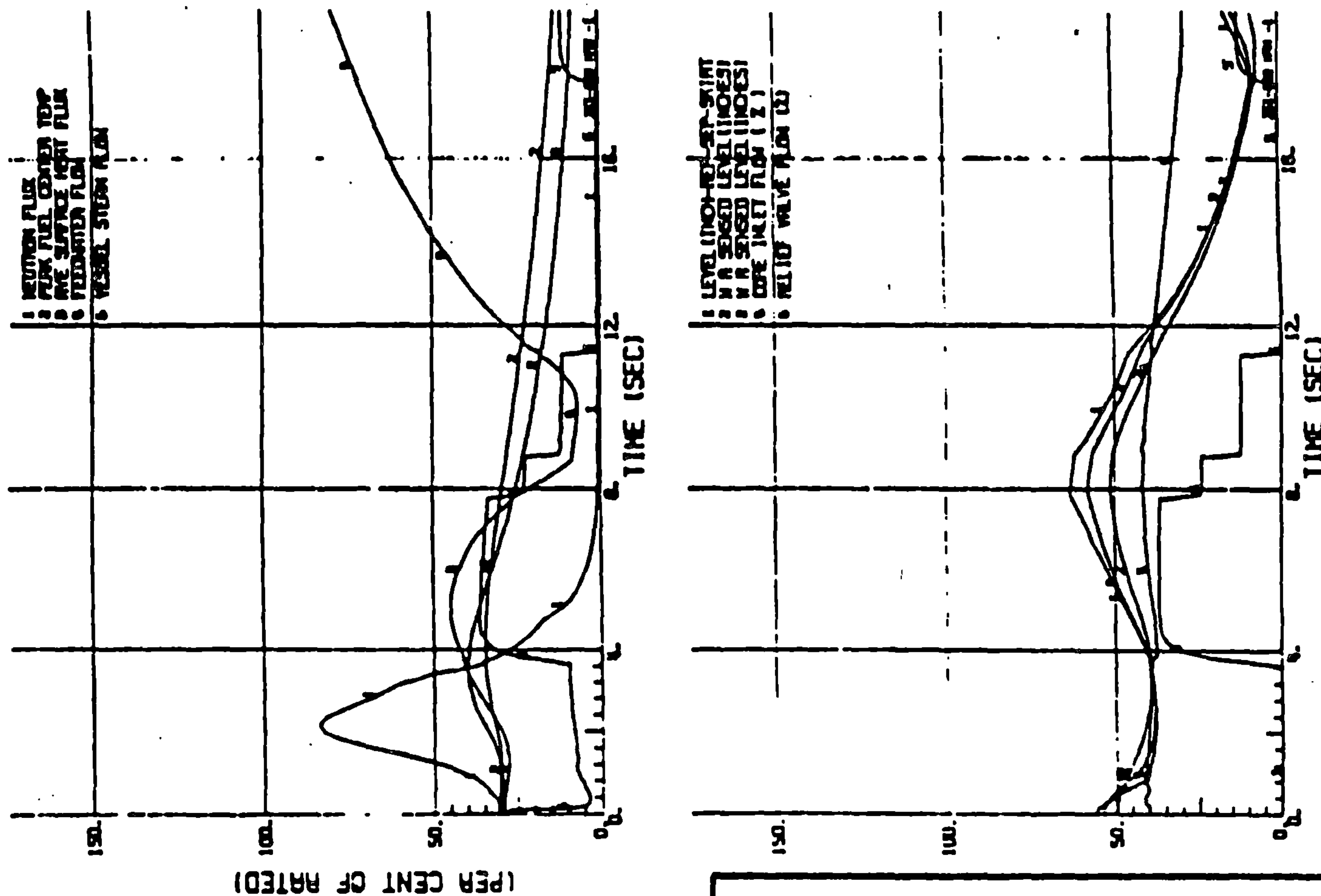

AMENDMENT 7

BROWNS FERRY NUCLEAR PLANT
FINAL SAFETY ANALYSIS REPORT

Transient Results, Turbine Trip from Low Power without Bypass
FIGURE 14.5-3

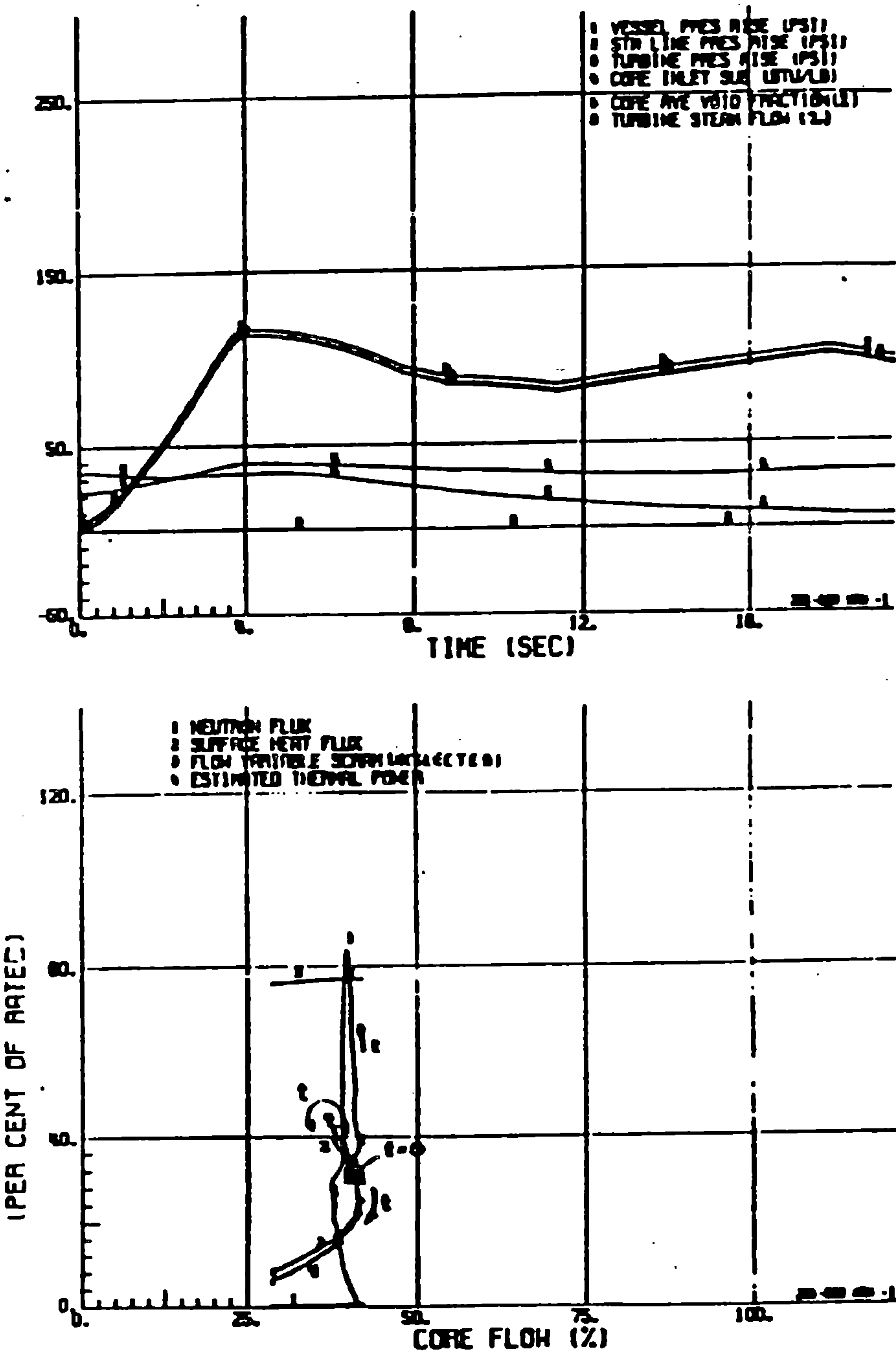
VESSEL PRES RISE (PSI)
STM LINE PRES RISE (PSI)
TURBINE PRES RISE (PSI)
CORE INLET SUB (BTU/LB)
CORE AVE VOID FRACTION(%)
TURBINE STEAM FLOW (%)
250.
150.
50.
-50.
0.
4.
8.
12.
16.
TIME (SEC)
NEUTRON FLUX
SURFACE HEAT FLUX
ESTIMATED THERMAL POWER
120.
80.
40.
0
25.
50.
75.
100.
CORE FLOW (%)
(PER CENT OF RATED)

BFNP

GE Nuclear Energy

General Electric Company
175 Curtner Avenue,
San Jose, CA 95125

May 17, 1994
JNL-03-94
DRF A00-05652 (17)

TO: J. Tanaka
GETSCO

FROM: J. N. Loomis

SUBJECT: Scram Bypass Setting for Turbine Stop Valve and Control Valve Fast Closure

CC: F. Leone
J. Pansch
S. Ranganath

Question

Item 3 of the Reference 1 memo states that

"RPT design specification 22A4699, rev. 1, sec. 3.5, states that "the RPT system shall be operable above the power set point for the turbine valve closure and control valve fast closure scram bypass." RPS design specification data sht. 22A3066-AL, rev. 2, sht. 20, sec. 4.2.17.7. had indicated that the bypass setting for turbine stop valve and control valve fast closure scram bypass is turbine first stage pressure less than 205 psig (30% of equivalent reactor power)."

JAPC requested to know whether in the last sentence of Item 3 of Reference 1, should it be 30% of reactor power or 30% of turbine output power?

Background

At low thermal power levels, the margins to fuel thermal-hydraulic limits are large and the immediate scram on turbine stop valve (TSV) or control valve (TCV) fast closure is not necessary. Therefore, to increase plant availability, an automatic power dependent, low power bypass of these scrams has been provided. This bypass is controlled by the turbine first stage steam pressure and bypasses the two scrams on TCV fast closure and TSV closure when the first stage pressure is below the setpoint.

Reply to Question

The scram bypass setpoint is based on core thermal power, as clarified in Reference 2. The scram bypass setpoint for Tokai-2 (Reference 3) is based on core thermal power less than or equal to 30% of rated, which is 5% above the bypass capacity. The basis of the thermal core power level for scram bypass can vary from plant to plant, but is generally bypass capacity plus 5%, which for Tokai-2 would be 30%. It has been shown that for Browns Ferry, a typical BWR/4/5 plant like Tokai-2, a T/G trip with bypass failure from an initial power level of 30% has adequate protection from other trips (e.g., vessel pressure and neutron flux) (Reference 4).

GENE Memo JNL-03-94 (Continued)

References

1. "Tokai-2 - RPS," General Electric Nuclear Energy memo from R.W. Skrotsky (GENE) to J. J. Peterson (GETSCO), July 31, 1978.
2. "Erroneous Scram Bypass Setpoint," General Electric Nuclear Energy Service Information Letter (SIL) Number 423, May 31, 1985.
3. RPS Design Specification data sheet 22A3066-AL, rev. 2, sht. 20, sec. 4.2.17.7
4. Browns Ferry Nuclear Plant Updated Final Safety Analysis Report, Volume 7, Section 14.5

Please let me know if you have any questions or need additional information.

J. N. Loomis

E. C. Eckert

J. N. Loomis
Engineering and Licensing Consulting Services Projects
(408) 925-1792

Verified by : E. C. Eckert
Plant Upgrade Projects
(408) 925-1198

TO: S. CHIANG
J. PANSCH

FROM: F. LEONE

SUBJECT: REACTOR POWER OR TURBINE OUTPUT POWER QUESTION.

REFERENCE: (1) RWS-78-406 (7/31/78)
ATTACHED

JAPC NEEDS RESPONSE TO FOLLOWING QUESTION BY 5/18/94 JAPAN TIME.
(END OF DAY 5/17, TODAY U.S. TIME)

* SEND RESPONSE TO J. TANAKA AT TSURUGA SITE.
84 525 - 4033

" QUESTION: IN LAST SENTENCE OF ITEM 3 OF REF (1) WHICH IS ATTACHED SHOULD IT BE 30% OF REACTOR POWER OR 30% OF TURBINE OUTPUT POWER? "

YOUR RESPONSE MUST INCLUDE RATIONALE, JUSTIFICATION AND SUPPORTING DATA.

I'M NOT SURE WHO CAN ANSWER THIS QUESTION. MAYBE W. DAVIS OR L. YOUNGBORG IN MARKLEIN ORGANIZATION BASED ON LSE LIST DATED 3/11/94 THAT S. CHIANG HAS COPY OF.

F. Leone

GETSCO 田中 監

JAPC

2/3

GENERAL ELECTRIC

NUCLEAR ENERGY

PROJECTS DIVISION

GENERAL ELECTRIC COMPANY, 175 CURTNER AVE., SAN JOSE, CALIFORNIA 95125

cc: R. V. Hallner
J. Y. Fujitani
R. J. Hunter
K. Otaka
J. P. Sluka
file: 10.C.72 w/a

NES78-406

RECEIVED
AUG 7 1978
TOKAI

TMS-17169
8/9/78

July 31, 1978

J. J. Petersen
GE Technical Services Co., Inc.
Ibaraki-ken, Japan

SUBJECT: Tokai 2 - RPS

REFERENCE: 1. TMS-16393, May 1, 1978.
2. EI-0554, February 20, 1978.
3. TMS-17071, July 27, 1978.

The following is a response to item per item of Reference 2:

1. In order to prevent the possibility of tripping two pumps on a single component failure and to increase recirc system availability, the manual trip for RPT function was deleted. Manual trips are available for RPT breakers 3A/4B and 4A/3B and this is presently shown in sht. 3, rev. 3 of 761E791-HF.

2. The wiring scheme as shown on recirc system elementary diagram 761E791-HF, sht. 2B, rev. 3, intend to minimize electrical separation problems by having the electrical power from RPS to trip RPT breakers CB 3A/3B and 4A/4B the same as that of the recirc system logic power. Since 125 Vdc Bus A and Bus B can only originate from battery A/B source. Please compare the electrical scheme of 761E791-HF, sht. 2, rev. 1, to that of sht. 2B, rev. 3.

3. RPT design specification 22A4699, rev. 1, sec. 3.5, states that "the RPT system shall be operable above the power set point for the turbine valve closure and control valve fast closure scram bypass." RPS design specification data sht. 22A3066-AL, rev. 2, sht. 20, sec. 4.2.17.7, had indicated that the bypass setting for turbine stop valve and control valve fast closure scram bypass is turbine first stage pressure less than 205 psig (30% of equivalent reactor power).

4. We felt strongly that a ten second time delay is sufficient time to allow an operator to turn the RPS mode switch from refuel to shutdown position, and furthermore, the timer can be adjusted to a maximum of

Tk-II Main Stop Valve Closure
Control Valve Fast Closure } Scram Bypass setpoint 205psig (30% of equivalent reactor power) first stage pressure

の根拠?

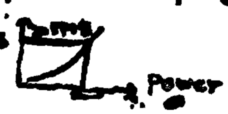

3/3

GENERAL ELECTRIC

J. J. Peterson
July 31, 1978
Page 2

fifteen seconds delay if ten seconds is not sufficient. We disagree that a single timer failure would prevent a shutdown scram when the mode switch is on its way to the shutdown position. We decline JAPC proposal in changing the contacts in the mode switch in place of the current timing circuit, since the mode switch is a class 1E component and it has already been qualified as such.

Please have Tokai 2 site electrical engineer initiate an FDDR to replace existing neon bulb with EI16.

We appreciate your information regarding type CR2940 scram reset switch problem, and I have informed C&I engineer D. V. Thorne accordingly. Please have Tokai 2 site electrical engineer check contacts 9-10, 11-12, 13-14 and 15-16 while moving the switch from reset to normal position to insure the contact is making and breaking properly.

All current GE BWR-5 designs use shorting link in the RPS system, and GE Engineering does not intend to modify the present circuit design.

8. Attached is a copy of Fukushima 6 FDDR BV1-JU for the turbine control valve fast closure scram setting change from 850 psig to 600 psig. The attached FDDR further states GE Engineering's final disposition, and this change is also being applied to Tokai 2. We believe this should clarify our position on the C72-N005 A-D set point change as requested by Ref. 3.

Best Regards,

R. W. Skrotsky
Principal Project Engineer
Tokai 2 Project

ATW78-85/jm
A78-1681
A78-2247

Attachment: FDDR BV1-JU

0532

GE Nuclear Energy

Structural Mechanics Projects
175 Curtner Avenue M/C 747
San Jose, CA 95125
Phone: (408) 925-3863
FAX: (408) 925-1150

DRF 137-0010-7
GENE-523-A95-0694
June 20, 1994

cc: S. Ranganath
G. Stevens

TO: Dave Rogowski
Commonwealth Edison Company
Dresden Nuclear Power Station
6500 N. Dresden Road
Morris, Illinois 60450

SUBJECT: Dresden and Quad Cities Shroud Buckling Assessment

This letter provides results for evaluating the consequences of a postulated main steam line guillotine break event concerning buckling of the shroud support legs and the shroud cylinder.

For the results presented below, it is assumed that the shroud support legs take the full dynamic load resulting from a shroud lift (above the H5 weld) and subsequent drop caused by a Main Steam Line Break (MSLB).

1. <u>Shroud Buckling for Dresden</u>

a) Effect on Shroud Support Legs

For a postulated MSLB, the portion of the shroud above the H5 weld will not lift. Thus buckling is not an issue.

For a postulated MSLB with a Safe Shutdown Earthquake (SSE), the shroud above the H5 weld may lift and drop, causing a stress on the shroud support legs of 14 ksi. This stress is within the elastic limit, and the overall load is well below the elastic buckling load. Therefore the postulated drop will not cause buckling to occur.

b) Effect on Shroud

For a postulated MSLB with an SSE, the shroud above the H5 weld may lift and drop, causing an average stress on the shroud of 2.1 ksi. This is judged to be well below any value at which buckling would be an issue.

c) Effect on Vessel

The effects of the vessel head drop and shroud head drop are covered by the heavy load drop analysis (NUREG 0612). It is judged that the shroud drop is covered by the same analysis.

2. Shroud Buckling for Quad Cities

a) Effect on Shroud Support Legs

For a postulated MSLB, the shroud above the H5 weld may lift and drop, causing a stress on the shroud support legs of 23.3 ksi. This stress is within the elastic limit, and the overall load is well below the elastic buckling load. Thus the postulated drop will not cause buckling to occur.

For a postulated MSLB with an SSE, the shroud above the H5 weld may lift and drop, causing a stress on the shroud support legs of 45 ksi. This potentially exceeds the inelastic buckling load. As a result, local buckling cannot be ruled out. However, considering the short-duration impulse loading, the probability of buckling is judged to be low.

b) Effect on Shroud

For a postulated MSLB, the shroud above the H5 weld may lift and drop, causing a stress on the shroud of 4.8 ksi. This is judged to be well below any value at which buckling would be an issue.

For a postulated MSLB with an SSE, the shroud above the H5 weld may lift and drop, causing a stress on the shroud of 9.1 ksi. This is judged to be well below any value at which buckling would be an issue.

c) Effect on Vessel

The effects of the vessel head drop and shroud head drop are covered by the heavy load drop analysis (NUREG 0612). It is judged that the shroud drop is covered by the same analysis.

If the loading is taken by fewer than the full complement of shroud support legs, some local buckling could occur. An evaluation was performed to address this scenario. The evaluation assumed that the impact loading as a result of shroud lift will be distributed equally to all shroud support legs (i.e., the shroud impacts over the entire 360-degree circumference). This assumption was made based on the following:

(1) The amount of rotational tip experienced by the shroud during lift is small (approximately 0.75"). Therefore, the ability of the shroud to rotate and land on one side is significantly hampered.

(2) Even if the shroud were to rotate and impact entirely on one side, it is expected that the resulting impact load will be distributed throughout the remaining lower shroud before it reaches the shroud support legs.

If shroud tipping is assumed, the 0.75" horizontal movement associated with the tipping at the top guide elevation causes approximately 0.75" of vertical lift on one side of the shroud compared to the other side at the H5 weld elevation. Therefore, the maximum possible deformation of the remaining lower shroud is 0.75" on one side before 360-degree contact is made with the "lifted" portion of the shroud. This amount of deformation, when transferred to the core support plate, causes minimal lateral motion (calculated to be approximately 1 mil) of the core support plate. Prior testing has been performed which showed that the control rods can be inserted with as much as 0.25" lateral displacement of the core plate. As a result, the ability to insert control rods will not be affected by such a scenario.

Regards,

Steven Hlavaty

Steven T. Hlavaty, Engineer
Structural Mechanics Projects
GE Nuclear Energy

Dresden/Quad Cities Shroud Support Legs Buckling Evaluation

Purpose: The purpose of this analysis is to evaluate the consequences of a postulated main steam line guillotine break event concerning buckling of the shroud support legs and the shroud cylinder for Dresden and Quad Cities, assuming a 360 degree crack exists in the shroud H5 weld.

For this analysis, it is assumed that the shroud support legs take the full dynamic load and that the load is distributed equally to all of the shroud support legs.

The following calculations are included:

- Given the maximum height (taken from previous calculations) that the shroud above the H5 weld lifts during a MSLB (with and without a Safe Shutdown Earthquake), determine the velocity of the shroud when it drops and impacts the static portion of the shroud (Dresden and Quad Cities)

- Given the impact velocity of the shroud (calculated above), determine the impact force (and stress) on the shroud support legs and shroud cylinder (Dresden and Quad Cities)

- Determine the smallest elastic buckling load for the shroud support legs (Dresden and Quad Cities)

- Determine the elastic limit for the shroud support legs.

Maximum Shroud Impact Velocity Derivation

Subject	Dresden / Quad Cities Shroud	Originator	STH	Date	6/3/94
Number		Verifier		Date	

Maximum Velocity Derivation

$$M \frac{dx^2}{dt^2} = g_c \frac{A_1 \Delta P_0}{(1+ax)^2} - gM$$

(Ref: Discussion with Hwang Choe)

Simplified ODE for shroud lift and drop due to ΔP during Main Steam Line Break.

(eqn. 1) $$\frac{dx^2}{dt^2} - \frac{g_c B}{(1+ax)^2} = -g$$

$$\left(B \equiv \frac{A_1 \Delta P_0}{M}\right)$$

Multiply each side by $2\dot{x}$:

$$2\dot{x}\left(\frac{d\dot{x}}{dt}\right) - \frac{g_c B}{(1+ax)^2}\left(2\frac{dx}{dt}\right) = -2g\frac{dx}{dt}$$

Multiply each side by dt:

$$2\dot{x}\, d(\dot{x}) - \frac{2g_c B}{(1+ax)^2}\, dx = -2g\, dx$$

Integrate. The result is:

$$(\dot{x})^2 = 2gx\left[\frac{B^{g_c/g}}{1+ax} - 1\right] + C_1$$

BC: $\dot{x}=0$ at $x=0 \Rightarrow C_1 = 0$.

Check integration by taking derivative of above equation:

$$2\dot{x}\ddot{x} = -2g\dot{x} + 2g B^{g_c/g}\left[\frac{(\dot{x})(1+ax) - x(a\dot{x})}{(1+ax)^2}\right]$$

$$(2\dot{x})\ddot{x} = (2\dot{x})(-g) + (2\dot{x})\, B g_c \left[\frac{1+ax-ax}{(1+ax)^2}\right]$$

$$\ddot{x} = -g + \frac{B g_c}{(1+ax)^2}$$

(same as eqn. 1 above, so equation is correct.)

Subject: Dresden/Quad Cities Shroud | Originator: STH | Date: 6/3/94
Number: | Verifier: | Date:

Maximum Velocity Derivation (continued)

$$\Rightarrow (\dot{x})^2 = 2gx\left[\frac{B^{g_c/g}}{1+ax} - 1\right].$$

V_{max} occurs at $\frac{d^2x}{dt^2} = 0$. $(\dot{x}_{max} = V_{max})$

$$\Rightarrow \frac{-g_c B}{(1+ax)^2} = -g$$

$$(1+ax) = \sqrt{B^{g_c/g}}$$

$$x = \frac{\sqrt{B^{g_c/g}} - 1}{a} \longrightarrow$$ V_{max} occurs at this value of x.

$$\Rightarrow (\dot{x}_{max})^2 = 2g\left[\frac{\sqrt{B^{g_c/g}}-1}{a}\right]\left[\frac{B^{g_c/g}}{1+a\left(\frac{\sqrt{B^{g_c/g}}-1}{a}\right)} - 1\right]$$

$$(\dot{x}_{max})^2 = \frac{2g}{a}\left(\sqrt{B^{g_c/g}}-1\right)\left(\sqrt{B^{g_c/g}}-1\right)$$

$$(\dot{x}_{max})^2 = \frac{2g}{a}\left(\sqrt{B^{g_c/g}}-1\right)^2$$

Expression for maximum shroud velocity. This is used to obtain the initial condition for the second-order ODE (spring-mass) even though this maximum velocity is actually reached before the shroud impact occurs. The actual impact velocity is less than this maximum (conservative).

Subject	Dresden Shroud	Originator	STH	Date	6/6/94
Number		Verifier		Date	

$\dot{X}_{max}$ Calculation for Dresden:

$$(\dot{X}_{max})^2 = \frac{2g}{a}\left(\sqrt{B\,g_c/g} - 1\right)^2$$

$a = 0.1445$ 1/inch for Dresden

$g = 32.2$ ft/s²

$g_c = 32.2 \frac{lbm\ ft}{lbf\ s^2}$

$A_1 = \frac{\pi}{4} D^2 = \frac{\pi}{4}(203.12\,in)^2$

Ref: "Preliminary Safety Assessment of Core Shroud Indications for Cycle 14 operation of Dresden Unit 2"

$\Delta P_0 = 12$ psid (for Dresden during guillotine break of main steam line)

$M = 413.7 \times 10^3$ lbm → cumulative weight above H5 weld
$M = 306.76 \times 10^3$ lbm → during DBE

Ref: Table taken from Dresden Screening Criteria report.

$$B = \frac{A_1 \Delta P_0}{M}$$

IF $B < 1$ => no shroud lift

With no SSE

$M = 413.7 \times 10^3$ lbm

=> $B = 0.94 < 1$

=> No lift.

With SSE

$M = 306.76 \times 10^3$ lbm

=> $B = 1.268$

$\frac{\sqrt{B g_c/g} - 1}{a}$ ... = 0.87 in

With no SSE

$\dot{X}_{max} = 0$ (no shroud lift)

With SSE

$$(\dot{X}_{max})^2 = \frac{2(32.2\ ft/s)}{(0.1445\ 1/in)(12\,in/ft)}\left[\sqrt{(1.268)\frac{32.2\ \frac{lbm\,ft}{lbf\,s^2}}{32.2\ ft/s^2}} - 1\right]^2$$

$\dot{X}_{max} = 0.768$ ft/s (For MSLB with SSE)

Could ... results ...

Subject	Quad Cities Shroud	Originator	JTH	Date	6/6/94
Number		Verifier		Date	

$\dot{X}_{max}$ Calculation for Quad Cities:

$$(\dot{X}_{max})^2 = \frac{2g}{a}\left[\sqrt{B^{g_c/g}} - 1\right]^2$$

$a = 0.1545$ 1/inch for QC

$g = 32.2\ ft/s^2$

$g_c = 32.2\ \frac{lbm\ ft}{lbf\ s^2}$

$A_1 = \frac{\pi}{4}D^2 = \frac{\pi}{4}(203.12\ in)^2$ → Ref: "Safety Assessment of Core Shroud Indications for Cycle 13 Operation of Quad Cities Unit 2"

$\Delta P_0 = 20$ psid (for QC during guillotine break of main steam line)

$M = 413.7 \times 10^3$ lbm (moving mass above H5 weld) → Cumulative wt.
$M = 296.0 \times 10^3$ lbm (interp) during DBE (above H5 weld)
} Table from Quad Cities Screening Criteria report.

$$B = \frac{A_1 \Delta P_0}{M}$$ IF $B < 1$ => No shroud lift.

With no SSE	With SSE
$M = 413.7 \times 10^3$ lbm	$M = 296.0$ lbm
=> $B = 1.567\ \frac{lbf}{lbm}$	$B = 2.189\ \frac{lbf}{lbm}$

With no SSE

$$(\dot{X}_{max})^2 = \frac{2(32.2\ ft/s)}{(.1545\ 1/in)(12\ in/ft)}\left[\sqrt{\left(1.567\ \frac{lbf}{lbm}\right)^{\frac{32.2\ \frac{lbm\ ft}{lbf\ s^2}}{32.2\ ft/s^2}}} - 1\right]^2$$

$\dot{X}_{max} = 1.484\ ft/s$ (For MSLB with no SSE)

With SSE

$$(\dot{X})^2_{max} = \frac{2(32.2)}{(.1545)(12)}\left[\sqrt{(2.189)^{\frac{32.2}{32.2}}} - 1\right]^2$$

$\dot{X}_{max} = 2.83\ ft/s$ (For MSLB with SSE)

Subject	Originator	Date
Number	Verifier	Date

Identifiable — Structure, System, Component • Purpose

Impact

Solution Outline

Given the shroud impact velocity, evaluate the maximum deflection (and force) on the shroud support legs.

Subject: Dresden / Quad Cities | Originator: STH | Date: 6/14/94

Number: | Verifier: | Date:

SOLUTION OUTLINE

Given: Mass m_1 is dropped from h (maximum shroud lift height). The resulting impact velocity is v (ft/s)

(m_1 = cumulative mass above shroud H5 weld).

Note: a static mass m_2 also exists above the shroud support legs.

Assume linear momentum is conserved and determine the average velocity of the entire mass $M = m_1 + m_2$ (after the collision between the dynamic and static masses):

$$m_1 v = (m_1 + m_2) \forall = M \forall$$

$$\forall = \frac{m_1}{m_1 + m_2} v$$

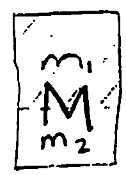

(Note: $\forall$ is the initial velocity for the Initial Value Problem).

Before:

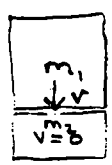

After:

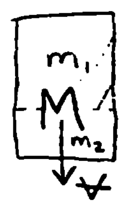

$$\underset{\text{momentum before}}{m_1 v_I} = \underset{\text{momentum after}}{\cancel{(m_1+m_2)\forall}}$$

GE Nuclear Energy
Engineering Calculation Sheet

Subject	Dresden / Quad Cities	Originator	STH	Date	6/14/94
Number		Verifier		Date	

SOLUTION OUTLINE (continued)
Initial Value Problem

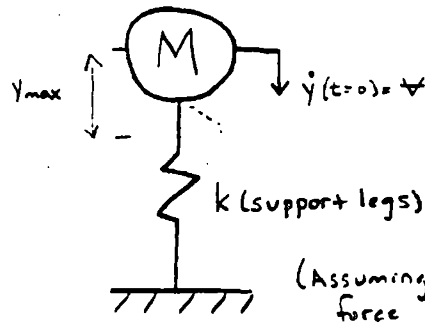

k (support legs) $= \sum \frac{AE}{L}$ for each support leg.
(Assuming that all of the force goes to the support legs).

$$M\ddot{y} + c\dot{y} + ky = F(t) = 0$$

M (lbm)
$\ddot{y}$ (in/s²)
c (lbm/s)
$\dot{y}$ (in/s)
k (lbm/s²)
y (in)
} UNITS

I.C. 1) $y(t=0)=0$ (no deflection)
2) $\dot{y}(t=0)=\forall$ (initial velocity of entire mass M)

$$c = \lambda\sqrt{4kM} = 2\lambda\sqrt{kM}$$

λ = damping factor → obtain from FSAR

Need to solve this second-order ODE and find y_{max}. Then $F_{max} = k y_{max}$.

Solution of ODE: Assume $y = e^{\alpha t}$:

$$M\alpha^2 e^{\alpha t} + c\alpha e^{\alpha t} + k e^{\alpha t} = 0$$

$\Rightarrow$ $M\alpha^2 + c\alpha + k = 0$ for $e^{\alpha t} \neq 0$ (nontrivial solution)

$$\alpha^2 + \frac{c}{M}\alpha + \frac{k}{M} = 0$$

$$\alpha = \frac{-\frac{c}{M} \pm \sqrt{\frac{c^2}{M^2} - \frac{4k}{M}}}{2}$$ → evaluate to obtain general solution. Then apply Initial Conditions.

Subject	Originator	Date
Dresden Evaluation	STH	6/14/94
Number	**Verifier**	**Date**

Main Steam Line Break With SSE

The worst-case scenario for Dresden is a Main Steam Line guillotine break with an SSE. For these conditions, the shroud may lift to a height of 1.87" ≈ 1.9" (Ref. "Preliminary Safety Assessment of Core Shroud Indications for Cycle 14 Operation of Dresden Unit 2"). From this, it has been determined that the maximum velocity of mass m_1 (the entire mass above H5 weld) is 0.77 ft/s (see attached calculations). Using this velocity (even though this maximum velocity actually occurs slightly before the point of impact):

$$m_1 v = M V \quad \Rightarrow \quad V = \frac{m_1}{M} v$$

$m_1 = 413.7 \times 10^3$ lbm (interpolated from Dresden Screening criteria data for mass above H5 weld)

$v = 0.77$ ft/s

$M = m_1 + m_{\text{region between shroud support legs and H5 weld}} = m_1 + m_2$

height of extra region ≈ 191.125 in − $\underset{\text{approx.}}{106\text{ in}}$ = 85.125 in

m_{extra} ≈ ratio of $\frac{\text{extra height}}{\text{shroud height}}$ * m_{shroud} (between 191.125 in and 391.375 in),
413.7×10³ lbm   219.9×10³ lbm

Could ...
results ...

Subject: Dresden Evaluation | Originator: STH | Date: 6/14/94
Number: | Verifier: | Date:

MSLB With SSE (continued)

assumed same value as Quad Cities plant

$$m_{extra} = \frac{85.125\,in}{(391.375\,in - 191.125\,in)}(413.7\times10^3\,lbm - 219.9\times10^3\,lbm) = 82.4\times10^3\,lbm$$

$$\Rightarrow M = 413.7\times10^3\,lbm + 82.4\times10^3\,lbm = 496.1\times10^3\,lbm$$

$$\Rightarrow V = \frac{413.7}{496.1}(0.77\,ft/s) = \underline{7.71\,in/s}$$

$$K_{TOTAL} = \underbrace{\sum \frac{AE}{L}}_{\text{of shroud support legs}} = \underbrace{4\left(\frac{AE}{L}\right)_{\text{small leg}} + 2\left(\frac{AE}{L}\right)_{\text{large leg}}}_{\text{6 total legs}} = \frac{E}{L}(4A_{small} + 2A_{large})$$

Assumed this value for SB-168. (Actual value is 28.85×10^6 psi at 550°F. Ref: 1986 ASME Boiler Pressure Vessel Code)

$$K_{TOTAL} = \frac{28.35\times10^6\,psi}{56.375\,in}\left[4(10.125\,in \times 2.3125\,in) + 2(20.21875\,in \times 2.3125\,in)\right]$$

$$K_{TOTAL} = 9.412\times10^7\,\frac{lbf}{in}\cdot\frac{32.2\,lbm\,\cancel{ft}}{\cancel{lbf}\,s^2}\cdot\frac{12\,in}{\cancel{ft}} = \underline{3.64\times10^{10}\,lbm/s^2}$$

for shroud (from FSAR Table 3.7-1)

$$C = 2\lambda\sqrt{KM} = 2(0.02)\sqrt{(3.64\times10^{10}\,\tfrac{lbm}{s^2})(496.1\times10^3\,lbm)}$$

$$\underline{C = 5.373\times10^6\,lbm/s}$$

TABLE I-6.0
MODULI OF ELASTICITY E OF MATERIALS FOR GIVEN TEMPERATURES

Material	Modulus of Elasticity E = Value Given × 10^6 psi, for Temp. °F of										
	−325	−200	−100	70	200	300	400	500	600	700	800
Ferrous Materials											
Carbon steels with C ≤ 0.30%	31.4	30.8	30.2	29.5	28.8	28.3	27.7	27.3	26.7	25.5	24.2
Carbon steels with C > 0.30%	31.2	30.6	30.0	29.3	28.6	28.1	27.5	27.1	26.5	25.3	24.0
Carbon–molybdenum steels	31.1	30.5	29.9	29.2	28.5	28.0	27.4	27.0	26.4	25.3	23.9
Nickel steels	29.6	29.1	28.5	27.8	27.1	26.7	26.1	25.7	25.2	24.6	23.0
Chrome–molybdenum steels											
½–2 Cr	31.6	31.0	30.4	29.7	29.0	28.5	27.9	27.5	26.9	26.3	25.5
2¼–3 Cr	32.6	32.0	31.4	30.6	29.8	29.4	28.8	28.3	27.7	27.1	26.3
5–9 Cr	32.9	32.3	31.7	30.9	30.1	29.7	29.0	28.6	28.0	27.3	26.1
Straight chromium steels	31.2	30.7	30.1	29.2	28.5	27.9	27.3	26.7	26.1	25.6	24.7
Austenitic, precipitation hardened, and other high alloy steels	30.3	29.7	29.1	28.3	27.6	27.0	26.5	25.8	25.3	24.8	24.1
Nonferrous Materials											
High Nickel Alloys										550°F operation	
N02200 (200) N02201 (201)	32.1	31.5	30.9	30.0	29.3	28.8	28.5	28.1	27.8	27.3	26.7
N04400 (400) N04405 (405)	27.8	27.3	26.8	26.0	25.4	25.0	24.7	24.3	24.1	23.7	23.1
N07750 (750)	33.2	32.6	31.9	31.0	30.2	29.8	29.5	29.0	28.7	28.2	27.6
N07718 (718)	31.0	30.5	29.9	29.0	28.3	27.8	27.6	27.1	26.8	26.4	25.8
N06002 (X)	30.5	29.9	29.4	28.5	27.8	27.4	27.1	26.6	26.4	25.9	25.4
Inconel 600 N06600 (600)	33.2	32.6	31.9	31.0	30.2	29.9	29.5	29.0	28.7	28.2	27.6
N06625 (625)	32.1	31.5	30.9	30.0	29.3	28.8	28.5	28.1	27.8	27.3	26.7
N08020 (20Cb–3)	30.0	29.4	28.8	28.0	27.3	26.9	26.6	26.2	25.9	25.5	24.9
N08800 (800) N08810 (800H)	30.5	29.9	29.4	28.5	27.8	27.4	27.1	26.6	26.4	25.9	25.4
N08825 (825)	30.0	29.4	28.8	28.0	27.3	26.9	26.6	26.2	25.9	25.5	24.9
N10001 (B)	33.3	32.7	32.0	31.1	30.3	29.9	29.5	29.1	28.8	28.3	27.7
N10665 (B-2)	33.6	33.0	32.3	31.4	30.6	30.1	29.8	29.3	29.0	28.6	27.9
N10276 (C-276)	31.9	31.7	30.7	29.8	29.1	28.6	28.3	27.9	27.6	27.1	26.5
Aluminum and Aluminum Alloys											
A03560 (356) A95083 (5083) A95086 (5086) A95456 (5456)	11.4	11.1	10.8	10.3	9.8	9.5	9.0	8.1	...	...	...

Ref: 1986 ASME Boiler and Pressure Vessel Code

Table 3.7-1

DAMPING FACTORS FOR STRONG VIBRATIONS WITHIN THE ELASTIC LIMIT

Item	Percentage of Critical Damping	
Reinforced Concrete Structures	5.0	
Steel Frame Structures	2.0	$\lambda = 0.02$
Welded Assemblies	1.0	
Bolted and Riveted Assemblies	2.0	
Vital Piping Systems	0.5	

Subject	Dresden Evaluation	Originator	STH	Date	6/14/94
Number		Verifier		Date	

MSLB with SSE (continued)

$$\alpha = \frac{-\frac{C}{M} \pm \sqrt{\frac{C^2}{M^2} - \frac{4k}{M}}}{2} = \frac{\frac{-5.373\times10^6}{496.1\times10^3} \pm \sqrt{\left(\frac{5.373\times10^6}{496.1\times10^3}\right)^2 - 4\frac{(3.64\times10^{10})}{(496.1\times10^3)}}}{2}$$

$$\alpha = \frac{-10.83 \pm 541.64i}{2} = \underline{-5.415 \pm 270.8i}$$

so $y(t) = Ce^{(-5.415 \pm 270.8i)t} = e^{-5.415t}\left[A\cos 270.8t + B\sin 270.8t\right]$

I.C. (1) $y(0) = 0 \Rightarrow \underline{A = 0}$

I.C. (2) $\dot{y}(0) = V = 7.71$ in/s

$$\Rightarrow 7.71 = -5.415e^{-5.415(0)}B\sin(0) + e^{-5.415(0)}(270.8)B\cos(0)$$

$$7.71 = 270.8\,B$$

$$\underline{B = 0.0285}$$

Now find y_{max} (maximum deflection):

$$\dot{y}(t) = 0 = 0.0285(-5.415e^{-5.415t}\sin 270.8t + 270.8e^{-5.415t}\cos 270.8t$$

$$5.415\sin 270.8t = 270.8\cos 270.8t \quad \text{for } e^{-5.415t} \neq 0$$

$$\tan 270.8t = 50.01$$

$$270.8t = 1.551 \text{ radians}$$

$$\underline{t = 0.00573 \text{ sec}}$$

$$y(0.00573) = y_{max} = 0.0285\,e^{-5.415(.00573)}\sin[270.8(0.00573)]$$

$$y_{max} = 0.0285\,(0.9694)(1.00)$$

$$\underline{y_{max} = 0.0276 \text{ in}} \rightarrow \text{maximum deflection due to shroud drop}$$

Subject	Dresden Evaluation	Originator	STH	Date	6/14/94
Number		Verifier		Date	

MSLB With SSE (continued)

$$F_{max} = K y_{max} = (3.64\times10^{10}\ \tfrac{\cancel{lbm}}{s^2})(0.0276\ in)\cdot\frac{ft}{12\ in}\cdot\frac{lbf\ s^2}{32.2\ lbm\ ft}$$

See Quad Cities Evaluation for k calculation of shroud support legs

$$F_{max} = 2.60\times10^{6}\ lbf$$

$$\sigma_{max} = \frac{F_{max}}{A_{TOT}}$$

$$A_{TOT} = 4A_{\substack{small\\leg}} + 2A_{\substack{large\\leg}}$$

(cross-sectional areas of shroud support legs)

$$A_{TOT} = 4(10.125\ in \times 2.3125\ in) + 2(20.21875\ in \times 2.3125\ in)$$

$$A_{TOT} = 187\ in^2$$

(assuming all shroud support legs take the force)

$$\sigma_{max} = \frac{F_{max}}{A_{TOT}} = \frac{2.84\times10^{6}\ lbf}{187\ in^2}$$

$$\sigma_{max} = 13.9\ ksi \sim \underline{14 ksi}$$

(stress on shroud support legs for MSLB with SSE)

Subject: Quad Cities Evaluation | Originator: STH | Date: 6/14/94
Number: | Verifier: | Date:

Main Steam Line Break With SSE

The worst-case scenario for Quad Cities is a Main Steam Line guillotine break with an SSE. For these conditions, the shroud may lift to a height of 7.696 in (Ref: "Safety Assessment of Core Shroud Indications for Cycle 13 Operation of Quad Cities Unit 2") Based upon this height, it has been determined (see attached calculations) that the maximum velocity of mass m_1 (the entire mass above H5 weld) is 2.83 ft/sec. Using this maximum velocity (even though this maximum velocity actually occurs slightly before the point of impact):

$$m v = M V \quad \Rightarrow \quad V = \frac{m}{M} v$$

$m_1 = 413.7 \times 10^3$ lbm (interpolated from Quad Cities screening criteria data for mass above H5 weld)
$v = 2.83$ ft/sec

$$M = m_1 + m_{\substack{\text{region between}\\\text{shroud support}\\\text{legs and H5}\\\text{weld}}} = m_1 + m_2$$

height of extra region $\approx$ 191.125 in $-$ $\underset{\text{approx}}{106 \text{ in}}$ $=$ 85.125 in

$M_{extra} \approx$ ratio of $\frac{\text{extra height}}{\text{shroud height}}$ * m_{shroud} (between 191.125 in. and 391.375 in.)
$\qquad 413.7 \times 10^3$ lbm $\qquad 219.9 \times 10^3$ lbm

$$M_{extra} = \frac{85.125 \text{ in} \rightarrow \text{see drawing}}{(391.375 \text{ in} - 191.125 \text{ in})} (413.7 \times 10^3 \text{ lbm} - 219.9 \times 10^3 \text{ lbm}) = 82.4 \times 10^3 \text{ lbm}$$

$$\Rightarrow M = 413.7 \times 10^3 \text{ lbm} + 82.4 \times 10^3 \text{ lbm} = 496.1 \times 10^3 \text{ l}$$

$$\Rightarrow V = \frac{413.7}{496.1} (2.83 \text{ ft/s}) = \underline{28.32}$$

Subject	Originator	Date
Quad Cities Evaluation	STH	6/14/94
Number	Verifier	Date

Main Steam Line Break With SSE (continued)

$$K_{TOTAL} = \underbrace{\sum \frac{AE}{L}}_{\text{shroud support legs}} = \underbrace{4\left(\frac{AE}{L}\right)_{\substack{small\\leg}} + 2\left(\frac{AE}{L}\right)_{\substack{large\\leg}}}_{\text{6 total legs}} + \underbrace{8\left(\frac{AE}{L}\right)_{stiffeners}}_{\text{stiffeners}}$$

Assume that $E_{leg} = E_{stiffener}$.

↑Quad Cities has two stiffener on each of the four small leg

$$K_{TOTAL} = K_{legs} + K_{stiffeners}$$

$$K_{legs} = \frac{E}{L}\left(4A_{small} + 2A_{large}\right)$$

Assumed for SB-168 material. (Actual value is 28.85×10^6 psi at 550°F. Ref: 1986 ASME Boiler and Pressure Vessel Code)

$$K_{legs} = \frac{28.35 \times 10^6 \text{ psi}}{56.375 \text{ in}}\left[4\left(10.125 \text{ in} \times 2.3125 \text{ in}\right) + 2\left(20.21875 \text{ in} \times 2.3125 \text{ in}\right)\right]$$

↙length of each leg

$$K_{legs} = 94.12 \times 10^6 \frac{\text{lbf}}{\text{in}} \cdot 32.2 \frac{\text{lbm ft}}{\text{lbf s}^2} \cdot 12 \frac{\text{in}}{\text{ft}} = 3.637 \times 10^{10} \text{ lbm/s}^2$$

→ This value is used for Dresden

$$K_{stiffeners} = 8\frac{AE}{L} = \frac{(8)(28.35 \times 10^6 \text{ psi})(2.125 \text{ in} \times 4 \text{ in})}{50.25 \text{ in}} \cdot 32.2 \frac{\text{lbm ft}}{\text{lbf s}^2} \cdot 12 \text{ in/ft}$$

$$K_{stiffeners} = 1.482 \times 10^{10} \text{ lbm/s}^2$$

$$K_{TOTAL} = K_{legs} + K_{stiffeners} = \underline{\underline{5.12 \times 10^{10} \text{ lbm/s}^2}}$$

→ This value is used for Quad Cities.

for shroud (from FSAR Table 3.7-1)

$$C = 2\lambda\sqrt{KM} = 2(0.02)\sqrt{(5.12 \times 10^{10} \text{ lbm/s}^2)(496.1 \times 10^3 \text{ lbm})}$$

$$\underline{\underline{C = 6.375 \times 10^6 \text{ lbm/s}}}$$

TABLE I-6.0
MODULI OF ELASTICITY *E* OF MATERIALS FOR GIVEN TEMPERATURES

Material	Modulus of Elasticity E = Value Given × 10^6 psi, for Temp. °F of										
	–325	–200	–100	70	200	300	400	500	600	700	800
Ferrous Materials											
Carbon steels with C ≤ 0.30%	31.4	30.8	30.2	29.5	28.8	28.3	27.7	27.3	26.7	25.5	24.2
Carbon steels with C > 0.30%	31.2	30.6	30.0	29.3	28.6	28.1	27.5	27.1	26.5	25.3	24.0
Carbon–molybdenum steels	31.1	30.5	29.9	29.2	28.5	28.0	27.4	27.0	26.4	25.3	23.9
Nickel steels	29.6	29.1	28.5	27.8	27.1	26.7	26.1	25.7	25.2	24.6	23.0
Chrome–molybdenum steels											
½–2 Cr	31.6	31.0	30.4	29.7	29.0	28.5	27.9	27.5	26.9	26.3	25.5
2¼–3 Cr	32.6	32.0	31.4	30.6	29.8	29.4	28.8	28.3	27.7	27.1	26.3
5–9 Cr	32.9	32.3	31.7	30.9	30.1	29.7	29.0	28.6	28.0	27.3	26.1
Straight chromium steels	31.2	30.7	30.1	29.2	28.5	27.9	27.3	26.7	26.1	25.6	24.7
Austenitic, precipitation hardened, and other high alloy steels	30.3	29.7	29.1	28.3	27.6	27.0	26.5	25.8	25.3	24.8	24.1
Nonferrous Materials High Nickel Alloys											
N02200 (200), N02201 (201)	32.1	31.5	30.9	30.0	29.3	28.8	28.5	28.1	27.8	27.3	26.7
N04400 (400), N04405 (405)	27.8	27.3	26.8	26.0	25.4	25.0	24.7	24.3	24.1	23.7	23.1
N07750 (750)	33.2	32.6	31.9	31.0	30.2	29.8	29.5	29.0	28.7	28.2	27.6
N07718 (718)	31.0	30.5	29.9	29.0	28.3	27.8	27.6	27.1	26.8	26.4	25.8
N06002 (X)	30.5	29.9	29.4	28.5	27.8	27.4	27.1	26.6	26.4	25.9	25.4
Inconel 600 → N06600 (600)	33.2	32.6	31.9	31.0	30.2	29.9	29.5	29.0	28.7	28.2	27.6
N06625 (625)	32.1	31.5	30.9	30.0	29.3	28.8	28.5	28.1	27.8	27.3	26.7
N08020 (20Cb–3)	30.0	29.4	28.8	28.0	27.3	26.9	26.6	26.2	25.9	25.5	24.9
N08800 (800), N08810 (800H)	30.5	29.9	29.4	28.5	27.8	27.4	27.1	26.6	26.4	25.9	25.4
N08825 (825)	30.0	29.4	28.8	28.0	27.3	26.9	26.6	26.2	25.9	25.5	24.9
N10001 (B)	33.3	32.7	32.0	31.1	30.3	29.9	29.5	29.1	28.8	28.3	27.7
N10665 (B-2)	33.6	33.0	32.3	31.4	30.6	30.1	29.8	29.3	29.0	28.6	27.9
N10276 (C-276)	31.9	31.7	30.7	29.8	29.1	28.6	28.3	27.9	27.6	27.1	26.5
Aluminum and Aluminum Alloys											
A03560 (356), A95083 (5083), A95086 (5086), A95456 (5456)	11.4	11.1	10.8	10.3	9.8	9.5	9.0	8.1	...	...	...

550°F operation

Ref: 1986 ASME Boiler and Pressure Vessel Code

Subject	Originator	Date
Quad Cities Evaluation	STH	6/14/94
Number	Verifier	Date

Main Steam Line Break Without SSE (continued)

$$\alpha = \frac{-\frac{c}{M} \pm \sqrt{\frac{c^2}{M^2} - \frac{4k}{M}}}{2} = \frac{\frac{-6.375\times10^6}{496.1\times10^3} \pm \sqrt{\left(\frac{6.375\times10^6}{496.1\times10^3}\right)^2 - \frac{4(5.12\times10^{10})}{496.1\times10^3}}}{2}$$

$$\alpha = \frac{-12.85 \pm 642.4i}{2} = \underline{-6.43 \pm 321.2i}$$

so $y(t) = Ce^{(-6.43\pm321.2i)t} = \left[A\cos 321.2t + B\sin 321.2t\right]e^{-6.43t}$

I.C. (1) $\quad y(0) = 0 \quad \Rightarrow \quad \underline{0 = A}$

I.C. (2) $\quad \dot{y}(0) = V = 28.32 \text{ in/s}$

$$\Rightarrow \quad 28.32 = -6.43e^{-6.43(0)} B\sin(0) + e^{-6.43(0)}(321.2)B\cos(0)$$

$$28.32 = 321.2B$$

$$\underline{B = 0.08817}$$

Now Find y_{max} (maximum deflection):

$$\dot{y}(t) = 0 = 0.08817\left(-6.43e^{-6.43t}\sin 321.2t + 321.2e^{-6.43t}\cos 321.2t\right)$$

$$6.43\sin 321.2t = 321.2\cos 321.2t \qquad \text{for } e^{-6.43t} \neq 0$$

$$\tan 321.2t = 49.95$$

$$321.2t = 1.551 \text{ radians}$$

$$\underline{t} = 0.00483 \text{ seconds}$$

$$y(0.00483) = y_{max} = 0.08817\sin[321.2(.00483)]e^{-6.43(.00483)}$$

$$y_{max} = 0.08817(1.0)(0.9694)$$

$\underline{y_{max} = 0.0855 \text{ in}}$ – maximum deflection due to shroud drop

Coul... results ...

Subject: Quad Cities Evaluation | Originator: STH | Date: 6/14/94
Number: | Verifier: | Date:

Main Steam Line Break With SSE (continued)

$$F_{max} = k y_{max} = \left(5.12 \times 10^{10} \frac{lbm}{s^2}\right)(0.0855 in) \cdot \frac{ft}{12 in} \frac{lbf\ s^2}{32.2 lbm\ ft}$$

$$F_{max} = 1.14 \times 10^7 \text{ lbf}$$

$$\sigma_{max} = \frac{F_{max}}{A_{TOT}}$$

$$A_{TOT} = 4A_{\substack{small\\leg}} + 2A_{\substack{large\\leg}} + 8A_{stiffeners}$$

(cross-sectional areas of shroud support legs and stiffeners)

$$A_{TOT} = 4(10.125 in \times 2.3125 in) + 2(20.21875 in \times 2.3125 in) + 8(2.125 in \times 4 in)$$

$A_{TOT} = 255.2 \text{ in}^2$ (assuming all shroud support legs and stiffeners take the force)

$$\sigma_{max} = \frac{1.14 \times 10^7 \text{ lbf}}{255.2 in^2} = \boxed{44.7 \text{ ksi}}$$

(Stress on shroud support legs for MSLB with SSE)

Note: This stress value is reached at $t = 4.8 ms$ after impact.

Table 3.7-1

VIBRATION DAMPING FACTORS FOR STRUCTURES AND ASSEMBLIES

Item	% of Critical Damping
Reinforced Concrete Structures	5.0
Steel Frame Structures	2.0 $\lambda = 0.02$
Bolted and Riveted Assemblies	2.0
Welded Assemblies	1.0
Vital Piping Systems	0.5
Standby Gas Treatment System Duct	1.0
Reactor Pressure Vessel	3.0
Masonry Walls	2.0

Subject	Quad Cities Evaluation	Originator	STH	Date	6/14/94
Number		Verifier		Date	

Main Steam Line Break Without SSE

As shown from previous calculations, the general solution for the spring-mass ODE model (for maximum deflection due to shroud drop) is

$$y(t) = [A \cos 321.2t + B \sin 321.2t]\, e^{-6.43t}$$

For MSLB without SSE, V_{max} was calculated to be 1.484 ft/s. Using this maximum velocity (even though the velocity at impact is actually lower);

Conserve linear momentum:

$$m_1 v = M V = (m_1 + m_2) V$$

$m_1 = 413.7 \times 10^3$ lbm (interpolated from Quad Cities Screening Criteria data for mass above HS grid)

$m_2 = 82.4 \times 10^3$ lbm (see QC calculation for MSLB with SSE)

$$\Rightarrow V = \frac{m}{M} v = \frac{413.7 \times 10^3 \text{ lbm}}{(413.7 + 82.4) \times 10^3 \text{ lbm}} (1.484 \text{ ft/s}) = \underline{14.85 \text{ in/s}} \rightarrow \text{Initial condition for ODE } \dot{y}(0) = V.$$

Subject: Quad Cities Evaluation	Originator	Date 6/14/94	
Number	Verifier	Date	

Main Steam Line Break Without SSE (continued)

I.C. (1) $y(0)=0 \Rightarrow 0 = A + B(0) \Rightarrow A = 0$

I.C. (2) $\dot{y}(0) = V = 14.85 \text{ in/s}$

$$\Rightarrow 14.85 = -6.43e^{-6.43(0)} B \cancel{\sin 0}^{\,0} + e^{-6.43(0)}(321.2)B\cos(0)$$

$$14.85 = 321.2 B$$

$$\underline{B = 0.04623}$$

Now find y_{max} (maximum deflection after shroud impact):

$$\dot{y}(t) = 0 = 0.04623(-6.43e^{-6.43t}\sin 321.2t + 321.2e^{-6.43t}\cos 321.2t)$$

$$6.43 \sin 321.2t = 321.2 \cos 321.2t \qquad \text{for } e^{-6.43t} \neq 0.$$

$$\tan 321.2t = 49.95$$

$$321.2t = 1.551 \text{ radians}$$

$$\underline{t = 0.004829 \text{ sec}} \rightarrow \text{when } y_{max} \text{ occurs.}$$

So
$$y_{max} = y(0.004829) = 0.04623 \sin[321.2(.004829)]e^{-6.43(.004829)}$$

$$y_{max} = 0.04623(1.000)(.9694) = \underline{0.04482 \text{ in}}$$

Maximum deflection due to shroud drop

Subject	Quad Cities Evaluation	Originator	STH	Date	6/14/94
Number		Verifier		Date	

Main Steam Line Break without SSE (continued)

$$F_{max} = K y_{max} = \left(5.12 \times 10^{10} \frac{lbm}{s^2}\right)(.04482\,in) \frac{ft}{12\,in} \cdot \frac{lbf\ s^2}{32.2\ lbm\,ft}$$

$$F_{max} = 5.943 \times 10^6\ lbf$$

$$\sigma_{max} = \frac{F_{max}}{A_{TOT}}$$

$$\sigma_{max} = \frac{5.943 \times 10^6\ lbf}{255.2\ in^2} = 2.329 \times 10^4\ psi$$

$$\boxed{\sigma_{max} \approx 23.3\ ksi}$$

(Stress on shroud support legs for MSLB without SSE

Note: This same result is obtained when the stress found for Quad Cities MSLB with SSE is scaled using the ratio of impact velocities.

$$\left(\text{i.e. } \sigma_{max} = \frac{1.484\ ft/s}{2.82\ ft/s} \cdot 44.7\ ksi = 23.4\ ksi \right)$$

Subject	Dresden/Quad Cities	Originator	STH	Date	6/9/94
Number		Verifier		Date	

Elastic Buckling Load of Shroud Support Legs (Dresden and Quad Cities)

Pinned - Pinned:

$$P_{cr} = \frac{\pi^2 E I}{L^2}$$

Find the critical buckling load for the weakest leg.

Dresden

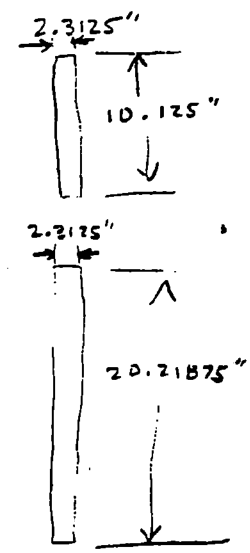

$$I = \frac{bh^3}{12}$$

Small shroud support leg (has no stiffeners):

$$I_{min} = \frac{1}{12}(10.125\,in)(2.3125\,in)^3 = \underline{10.4\,in^4}$$

Large shroud support leg:

$$I_{min} = \frac{1}{12}(20.21875\,in)(2.3125\,in)^3 = \underline{20.8\,in^4}$$

=> Minimum P_{cr} occurs for a small shroud support leg.

$$P_{cr} = \frac{\pi^2(28.35 \times 10^6\,psi)(10.4\,in^4)}{(56.375\,in)^2} = \underline{9.16 \times 10^5\ lbf} \quad \text{(elastic buckling load)}$$

length of shroud support leg

The corresponding stress is

$$\sigma_{cr} = \frac{P_{cr}}{A} = \frac{9.16 \times 10^5\ lbf}{(2.3125\,in)(10.125\,in)} = \underline{39.1\ ksi}$$

Subject	Quad Cities	Originator	STH	Date	6/9/94
Number		Verifier		Date	

Elastic Buckling Load of Shroud Support Legs

Quad Cities

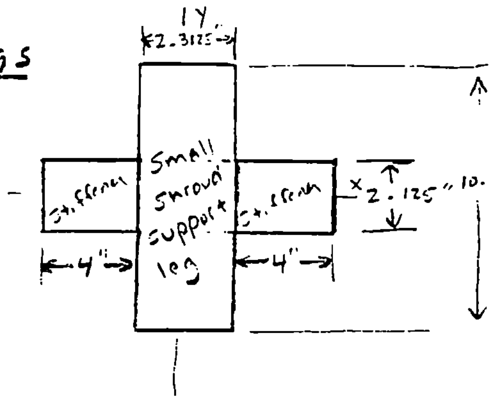

Small shroud support leg (with stiffeners):

$$I_x = \underbrace{\frac{1}{12}(2.3125\,in)(10.125\,in)^3}_{leg} + \underbrace{2\left[\frac{1}{12}(4\,in)(2.125\,in)^3\right]}_{stiffeners}$$

$$I_x = 200.0\,in^4 + 6.4\,in^4 = \underline{206.4\,in^4}$$

$$I_y = \underbrace{\frac{1}{12}(10.125\,in)(2.3125\,in)^3}_{leg} + \underbrace{\frac{1}{12}(2.125\,in)\left[(10.3125\,in)^3 - (2.3125\,in)^3\right]}_{stiffeners}$$

$$I_y = 10.4\,in^4 + 192.0\,in^4 = \underline{202.4\,in^4}$$

Large shroud support leg:

$$I_{min} = \frac{1}{12}(20.21875\,in)(2.3125\,in)^3 = \underline{20.8\,in^4}$$ ← smallest for Quad Cities

=> Minimum P_{cr} occurs for a large shroud support leg

$$P_{cr} = \frac{\pi^2 (28.35 \times 10^6 psi)(20.8\,in^4)}{(56.375\,in)^2} = \underline{1.83 \times 10^6\ lbf}$$ (elastic buckling load)

↓ length of shroud support leg

The corresponding stress is

$$\sigma_{cr} = \frac{P_{cr}}{A} = \frac{1.83 \times 10^6\,lbf}{(2.3125\,in)(20.21875\,in)} = \underline{39.1\ ksi}$$

Subject	Dresden / Quad Cities	Originator	STH	Date	6/14/9-
Number		Verifier		Date	

Stress on Shroud (due to shroud lift and drop above H5 weld)

$$\sigma_{shroud} = \frac{F_{max}}{A_{shroud}}$$

$A_{shroud} = \pi D t$ $t = 2"$ thickness (Dresden and Quad Cities)
$D = 199$ in (mean - Dresden and Quad Cities)

$\Rightarrow A_{shroud} = \pi (199 in)(2 in) = 1250 in^2$

Dresden
w/o SSE: (no shroud lift)
w/ SSE: $F_{max} = 2.64 \times 10^6$ lbf (see attached calculation

$$\Rightarrow \sigma_{shroud} = \frac{2.60 \times 10^6 \text{ lbf}}{1250 in^2} = \underline{2.08 \text{ ksi}}$$

Quad Cities
w/o SSE: $F_{max} = \frac{1.484 ft/s}{2.83 ft/s}(1.14 \times 10^7 \text{ lbf}) = \underline{5.98 \times 10^6 \text{ lbf}}$

$$\Rightarrow \sigma_{shroud} = \frac{5.98 \times 10^6 \text{ lbf}}{1250 in^2} = \underline{4.79 \text{ ksi}}$$

w/ SSE: $F_{max} = 1.14 \times 10^7$ lbf (see attached calculatio

$$\Rightarrow \sigma_{shroud} = \frac{1.14 \times 10^7 \text{ lbf}}{1250 in^2} = \underline{9.12 \text{ ksi}}$$

Subject	Dresden /Quad Cities	Originator	STH	Date	6/14/94
Number		Verifier		Date	

Elastic Limit Estimation

Assuming alloy SB-168:

$S_y = 28.8$ ksi (yield strength) at 500°F
$S_y = 27.9$ ksi at 600°F
$S_y = 35.0$ ksi at 100°F

Taken from ASME Boiler & Pressure Vessel Code, 1989 edition

$$\Rightarrow \sigma_y(550°F) = \frac{28.8\,ksi + 27.9\,ksi}{2} = \underline{\underline{28.35\,ksi}}$$

Assuming $\sigma_y \approx 44.8$ ksi (average value) for SB-168 at room temperature.
Ref: BWR Plant Materials Properties Handbook

$$S_y \approx 28.35\,ksi * \frac{44.8\,ksi}{35\,ksi} = \underline{36.29\,ksi}$$

35 ksi: Code minimum σ_y at room temp
Ref: 1989 edition, ASME Boiler and Pressure Vessel Code.

Assume Elastic Limit $\approx 0.75\,S_y = 0.75\,(36.29\,ksi)$

Elastic Limit = 27.2 ksi

Stresses below this limit are assumed to be within the elastic region for comparison with elastic buckling calculations.

GENERAL ELECTRIC
NUCLEAR ENERGY DIVISION

Y1002A050 REV 2 | SH NO. 21

Ni-Cr-Fe ALLOY 600

REVISION:
SOLID LINE:
AVERAGE (X̄) OR TYPICAL
--- STD. DEVIATION (NO.) OR BOUND
CATEGORY OF AVERAGE DATA: N/A
REFERENCE NO. 19
EQN. OF CURVE: N/A

PROPERTY CODE 2116 P 1.0

COMPRESSIVE STRENGTH

PRODUCT FORM (DATA) AND APPLICABLE

As noted

Product Form	Yield Strength (0.02% Offset), ksi	Yield Strength (0.2% Offset), ksi
Bar, Hot-Rolled, Annealed	40.0	44.8
Bar, Cold-Drawn, Stress-Relieved 1400 F/1 hr	74.4	87.7
Tubing, As-Extruded	27.9	32.5

This value was assumed as an average value at room temperature.

Ref: BWR Plant Materials Properties Handbook

Pressure Vessel Co[...]
1989 edition

TABLE I-2.2 (CONT'D)
YIELD STRENGTH VALUES S_y FOR AUSTENITIC STEELS, HIGH NICKEL ALLOYS, AND COPPER-NICKEL ALLOYS

Spec. No.	Nominal Composition	Type or Grade	Class	Product Form [Note (1)]	Specified Min. Yield Strength, ksi
High Nickel Alloys (Cont'd)					
SB-164	Ni–Cu	N04400	A	Bar	30
SB-164	Ni–Cu	N04405	B	Bar	35
SB-127	Ni–Cu	N04400	...	Plate	40
SB-164	Ni–Cu	N04400	A	Bar	40
SB-163	Ni–Cu	N04400	...	Smls. Tube	55
SB-165	Ni–Cu	N04400	...	Smls. Pipe & Tube	55
SB-167	Ni–Cr–Fe	N06600	...	Smls. Pipe & Tube	25
SB-167	Ni–Cr–Fe	N06600	...	Smls. Pipe & Tube	30
SB-163	Ni–Cr–Fe	N06600	...	Smls. Tube	35
SB-166	Ni–Cr–Fe	N06600	...	Bar	35
SB-167	Ni–Cr–Fe	N06600	...	Smls. Pipe & Tube	35
SB-168	Ni–Cr–Fe	N06600	...	Plate	35
SB-564	Ni–Cr–Fe	N06600	...	Forg.	35
SB-163	Ni–Cr–Fe	N06600 [Note (4)]	...	Smls. Tube	40
SB-163	Ni–Cr–Fe	N06690 [Note (4)]	...	Smls. Tube	40
SB-435	Ni–Cr–Mo–Fe	N06002	...	Sheet (< 3/16 in.)	40
SB-619	Ni–Cr–Mo–Fe	N06002	...	Wld. Pipe	40
SB-622	Ni–Cr–Mo–Fe	N06002	...	Smls. Pipe & Tube	40
SB-626	Ni–Cr–Mo–Fe	N06002	...	Wld. Tube	40
SB-435	Ni–Cr–Mo–Fe	N06002	...	Plate (≥ 3/16 in.)	35
SB-572	Ni–Cr–Mo–Fe	N06002	...	Bar	35
SB-443	Ni–Cr–Mo–Cb	N06625	...	Plate	55
SB-444	Ni–Cr–Mo–Cb	N06625	...	Smls. Pipe & Tube	60
SB-446	Ni–Cr–Mo–Cb	N06625	...	Bar ≤4 in.	60
SB-446	Ni–Cr–Mo–Cb	N06625	...	Bar >4 in.	50
SB-163	Ni–Fe–Cr–Mo–Cu	N08825	...	Smls. Tube	35
Copper–Nickel Alloys					
SB-111	Cu–Ni	N07715	...	Smls. Tube	18
SB-171	Cu–Ni	N07715	...	Plate	18
SB-171	Cu–Ni	N07715	...	Plate	20
SB-111	Cu–Ni	N07715	...	Smls. Tube	50

NOTES:
(1) The following are the abbreviations used for Product Forms : (a) Wld. — Welded; (b) Smls. — Seamless; (c) Forg. — Forging, Forged.
(2) For material annealed at 1925–1975°F.
(3) For material annealed at 2025–2075°F.
(4) SB-163 Supplementary Requirements S5 through S10 shall be met.

TABLE I-2.2 (CONT'D)
YIELD STRENGTH VALUES S_y FOR AUSTENITIC STEELS, HIGH NICKEL ALLOYS, AND COPPER-NICKEL ALLOYS

	Yield Strength, ksi, for Metal Temp., °F, Not Exceeding													
	100	200	300	400	500	600	650	700	750	800	850	900	950	1000
	High Nickel Alloys (Cont'd)													
	30.0	26.4	24.7	23.8	23.8	23.8	23.8	23.8	23.4	22.9	...	...	...	...
	35.0	30.9	28.8	27.8	27.8	27.8	27.8	27.8	27.3	26.7	...	...	...	...
	40.0	35.3	32.9	31.8	31.8	31.8	31.8	31.8	31.1	30.5	...	...	...	...
	55.0	48.5	45.3	43.7	43.7	43.7	43.7	43.7	42.8	41.9	...	...	...	...
	25.0	23.0	21.9	21.0	20.2	19.8	19.7	19.7	19.7	19.0	...	...	...	...
	30.0	28.0	26.6	25.6	24.7	23.9	23.5	23.2	22.8	22.4	...	...	...	...
					Averaged these two to get value at 550°F									
168	35.0	32.7	31.0	29.8	28.8	27.9	27.4	27.0	26.5	26.1	...	...	...	...
	40.0	36.8	34.6	33.0	31.8	31.1	30.9	30.6	30.3	30.0	...	...	...	...
	40.0	36.2	32.3	28.8	27.5	26.6	26.6	26.6	26.6	26.6	...	...	...	...
	35.0	31.7	28.3	24.9	24.0	23.3	23.3	23.3	23.3	23.3	...	...	...	...
	55.0	53.1	51.4	49.9	48.5	47.2	46.6	46.1	45.7	45.3	...	...	...	...
	60.0	57.9	56.1	54.1	52.9	51.5	50.9	50.3	49.8	49.4	...	...	...	...
	50.0	48.3	46.8	45.4	44.1	42.9	42.4	42.0	41.6	41.2	...	...	...	...
	35.0	32.5	30.5	29.0	27.7	27.0	26.5	26.0	25.8	25.6	...	...	...	...
	Copper-Nickel Alloys													
	18.0	17.0	16.2	15.5	14.9	...	...	...	...	...	...	...	...	...
	20.0	18.9	18.0	17.2	16.6	...	...	...	...	...	...	...	...	...
	50.0	47.6	46.2	44.9	43.8	...	...	...	...	...	...	...	...	...

Attachment ME-1-8 Summary of Table Movements

CORE SHROUD LOSS OF H5 WELD

Design Basis Accidents	Anticpated Movement			Rod Insertion	Core Reflood	Core Spray	SBLC
	Lateral	Vertical	Moment(Tip)				
Design Basis Earthquake (SSE)	None at the H5 weld location. 3/4" at the top of the shroud.	None	3/4" maximum displacement (laterally)	Rods Insert After Tipping, Timing Not Signifcantly Affected	Floodable Volume Maintained, ECCS Systems Available	System Function Not Affected	No Boron Density Change
Main Steam Line Break	None	4" Quad Cities 0" Dresden	None	Insertion Completed After Shroud Comes Down, Timing Not Significantly Affected	Floodable Volume Maintained	Dre. CS not Affected, QC Potential Failure OF CS Riser Or Sparger, Injection Into RPV Allows Long Term Cooling	No Boron Density Change
Recirculation Line Break	None	None	None	Rods Insert, Timing Not Affected	Very Small Gap 1-2 Mils, 40GPM Bypass Analysis Unaffected	Core Spray Not Affected	N/A

Additional Scenarios Considered	Anticpated Movement			Rod Insertion	Core Reflood	Core Spray	SBLC
	Lateral	Vertical	Moment(Tip)				
Main Steam Line Break Plus DBE	3/4" maximum displacement.	8" Quad Cities 2" Dresden	3/4" maximum displacement (laterally)	Rod Insertion Complete After and While Shroud Comes Down, Oscillitory Velocity Profile, Timing Affected	Floodable Volume Maintained	Dresden CS Function Not Affected, QC Potential Failure Of CS Riser Or Sparger, Injection Into RPV Will Allow Long Term Cooling	No Boron Density Change
Recirc. Line Break Plus DBE (Low PRA Without Adding Single Failure Criteria)	None at the H5 weld location. 3/4" at the top of the shroud.	None	3/4" maximum displacement (laterally)	Rods Insert After Tipping, Timing Not Significanly Affected	Bounded By Calc. Assuming 1/4" Open All Around (Bypass Flow Small)	Core Spray Function Not Affected	N/A

DRESDEN LIFT CALC

Sheet 9 of

Subject | Originator | Date
Number | Verifier E. C. Eckert | Date 5/1/94

Condition for maximum lift,

$$\frac{B}{1+ax} = 1$$

$$\therefore X_{max} = \frac{B-1}{a}$$ (see PB DRF Section for this formula)

$a = 0.1445$ inch

$$B = \frac{g_c A \Delta P_o}{M_s g}$$

Ref. 5. ECE 5/1/94

For H5 weld, $M_S = 413.74$ KIP

	El	Effective mass	Cummulative Wt
(H4) El	266.375	259.06 kip	?
	208.01		405.62 kip
(H5)	191.125	334.48	
	147.53		434.59

$$H5\ mass = 405.62 + \frac{(34.59 - 5.62)}{(208.01 - 147.53)}(208.01 - 191.125)$$

$$= 413.74\ kip$$

Subject	Originator	Date
Number	Verifier E.C. Eckert	Date 5/1/94

$$A = \frac{\pi}{4} D^2 = \frac{\pi}{4} \times (203.12)^2 = 32,403.75 \, in^2$$

<u>B values</u> <u>B</u>

$\Delta p = 7$ psi $\quad B = \dfrac{7 \times 32,403.75}{413.74 (10^3)} = 0.548$

ECE 5/1/94

$\Delta p = 12$ psi $\quad B = 0.94$

The effects of Drag force, Momentum, Buoyancy Force, Hydrodynamic mass are small, and canceles most of their effects each other.

No lift up to 12.77 psi of pressure drop.

Gives B = 1 ECE 5/1/94

GE Nuclear Energy
Engineering Calculation Sheet

		Sheet 11 of
Subject	Originator	Date
Number	Verifier E. C. Eckert	Date 5/1/94

Assume DBE

$W @ H5 = 306.76$ From Ref 5. ✓ EC 5/1/94

@ $\Delta P_0 = 12$ psi

$$B = \frac{12 \times 32,403.75}{306,760} = 1.27$$

$$X_{max} = \frac{1.27 - 1}{0.1445} = 1.85''$$

1.69" slack
.25" Thermal Exp
1.44" clearance

Assume OBE

$$B = \frac{12 \times 32,403.75}{334,480} = 1.1625$$

Ref. 5 EC 5/1/94

$$X_{max} = 1.13''$$

can be accommodated by the slack in the Core Spray line bracket

Prep: DKR
Verif: ECE

3. Lift Forces for Main Steam Line Break

From A00-05652, Sec. 15, (Dresden)

Condition for Max. Lift.

$$X = \frac{B-1}{a}$$; a = 0.1545 (inch) (See following Page for calculation of a)

$$B = \frac{g_c}{g} \frac{(A \Delta P)}{M_S}$$

Comparison of Masses between Dresden and QC in DRF-137-0010-7 shows M_S, A are same.

Thus, B is ratioed:

For Dresden, $\Delta p = 7$, $B = 0.548$

$\Delta p = 12$ $B = 0.94$

@ $\Delta p = 20$, $B = \frac{20}{12} * 0.94 = 1.567$

1. Break Only } $X_1 = \frac{1.567-1}{0.1545} = 3.67$ inches. (Only Break Loads)

2. Break (SSE) } M = 296,000 lb (DRF-137-0010-7)

$$B = \frac{20 * 32{,}403.75}{296{,}000} = 2.189$$

$$X_2 = \frac{2.189-1}{0.1545} = 7.696 \text{ inches.}$$

Prep: DKR

Verif: ECE

Lift Forces for MSLB with Earthquake

3. Break + OBE $\quad M = 329{,}000 \text{ lb}$

$$B = \frac{20 * 32{,}403.75}{329{,}000}$$

$$= 1.9698$$

$$X = \frac{1.9698 - 1}{0.1545} = 6.28 \text{ inches.}$$

Displacements are positive for

MSLB: 3.67 inches (Uses 3.7 inches)

MSLB+OBE: 6.28 inches (Use 6.3 inches)

MSLB+SSE: 7.696 inches (Use 7.7 inches)

—— x ——

Calculation of "a": $\quad a = \sqrt{C_1/C_2'}$

$$C_1 = \frac{\Delta p}{v_0 \, \dot{m}_{core}^2} \; ; \quad C_2' = \frac{K}{2g_c(\pi D)^2} * \frac{144}{3600^2}$$

Since only Δp is changed from 7 psid to 8 psid between Dresden and QC (See following pages)

$$C_1/C_2')_{QC} = C_1/C_2')_{Dresden} * 8/7$$

$$C_1/C_2')_{Dresden} = 0.1445^2 \; , \quad C_1/C_2')_{QC} = 0.1445^2 * 8/7$$

$$= 0.1445\sqrt{8/7} = 0.1545$$

Attachment ME-1-11 GENE-523-A92-0694

Safety Assessment of Core Shroud Indications for Cycle 14 Operation of Quad Cities Unit 1

Prepared by: ______________________
R. S. Daniel, Engineer

Verified by: ______________________
D. K. Rao, Senior Engineer

Approved by: ______________________ 6/24/94
S. Ranganath, Manager, for
Engineering and Licensing
Consulting Services

GE-NE Technical Services
GE Nuclear Energy
San Jose, California

IMPORTANT NOTICE REGARDING
CONTENTS OF THIS REPORT

TABLE OF CONTENTS

1. Introduction

Circumferential and axial crack indications have been reported at various locations in the core shroud assemblies of BWRs. GE Services Information Letter 572, Revision 1 (SIL-572), has been issued to assist utilities in their individual evaluation of this situation. SIL -572 recommends that shroud inspection be performed at the next scheduled refueling outage. The USNRC issued Information Notice 93-79 on this subject. Based on these recommendations, a shroud inspection was performed at Quad Cities Unit 1 during the current refueling outage.

The inspection indicated the presence of circumferential cracks in the Quad Cities Unit 1 (QC1) core shroud assembly. The visual inspections performed have shown the presence of cracks near the H3, H4, H5 and H6 welds for QC1. An engineering evaluation is sought by the Commonwealth Edison Company (ComEd) to justify operation of QC1 for one more cycle (Reference 1). The region near the H5 weld showed random indications of cracks in all areas inspected for QC1. The most severe indications are in the core support ring joined to the core shroud near the H5 weld and appear to be 360° circumferential cracking. Therefore, UT inspections were done at six locations of the H5 area using 60° dual R-L transmitters (Reference 2). The results used in this report are based on the current inspections and the following discussion is based on the results of the current inspections. If future inspections indicate that potentially larger cracks could exist, this assessment will have to be reviewed and amended appropriately.

The safety assessment for the QC1 core shroud in this report provides the engineering rationale for continued plant operation for the next QC1 fuel cycle. This safety assessment will have to be reviewed and updated if necessary when the QC1 core shroud is inspected during the next planned outage.

This report also qualitatively addresses the potential situation during normal operation, anticipated operational events, and design basis accidents, if unexpected significant crack growth occurs during plant operation. This assessment describes the symptoms and consequences expected if the shroud has degraded to the point that through-wall cracking has occurred in the core support ring in the H5 weld area, which was the most extensively cracked area on the QC1 shroud. A qualitative assessment is provided for other welds on the core shroud. The approach used in this assessment is to justify continued operation of QC1 for one more cycle.

GE Rapid Information Communication Services Information Letter (RICSIL) 068 has been issued (Reference 3) to assist ComEd and other utilities in the on-going evaluation of this situation. Previous communications about core shroud crack indications have included GE SIL 572 (Reference 4) and US-NRC Information Notice 93-79. Reference 4 states that current understanding of the root cause for shroud cracks is Intergranular

Stress Corrosion Cracking with apparent propagation by Irradiation Assisted Stress Corrosion Cracking.

2. Summary and Conclusions

The core shroud/core support ring cracking associated with the H5 weld at QC1 does not represent a threat to the safe operation of QC1 for the next cycle. The cracking is at the H5 weld, which was the most extensively cracked weld area in QC1.

1. The combination of high ductility, high toughness and low stresses makes the shroud extremely flaw tolerant. Even for this situation with the indications of 360 degree circumferential cracking, crack depths of 96% (2.88 inches) of the available material can be tolerated while maintaining the structural integrity for normal operation and postulated design basis accident conditions, including ASME Code safety factors. The available material considers the extra one inch of ligament provided by the weldment in addition to the two inch shroud wall thickness. The weld detail is shown in Figure 1.

2. The maximum crack depth observed by ultrasonic examinations in QC1 is approximately 1.24 inches, and is within the allowable crack depth of 2.88 inches. The postulated cracking in the QC1 core shroud maintains the structural integrity for normal operation and anticipated plant transients.

3. Discounting Hydrogen Water Chemistry (HWC) benefits that QC1 has had since 1990, and using the bounding crack growth rate of 5E-5 inch/hr (0.4 inch/year, assuming operating hours/year), as established in the BWROG Core Shroud Evaluation report for normal water chemistry, the crack depth is not expected to exceed the allowable crack depth in the next 24 months.

4. The weight of the core shroud above H5 is sufficient to hold the shroud in place even if the shroud assembly is postulated to have a 360° through-wall crack at the H5 weld, both under normal operating conditions and during anticipated plant transients. The shroud will not lift. Since the crack size is on the order of mils, any leakage flow through the crack is small and will not impact plant operations.

5. An evaluation of the design basis accident coupled with a seismic condition has been done with the shroud assembly postulated to have a 360° through-wall crack at the H5 weld. The evaluation was done to investigate the possibility of shroud movement. For recirculation line breaks, no shroud lifting occurs. Adequate long term cooling of the core will be maintained throughout the postulated event. For steamline breaks, shroud lifting is limited. Even if the shroud lifting causes the core spray line to fail, core spray water is delivered to the reactor vessel and adequate long term cooling of the core will be maintained throughout the postulated event. For both the recirculation and main steam line break events, safe reactor shutdown capability and long term core coolability is maintained.

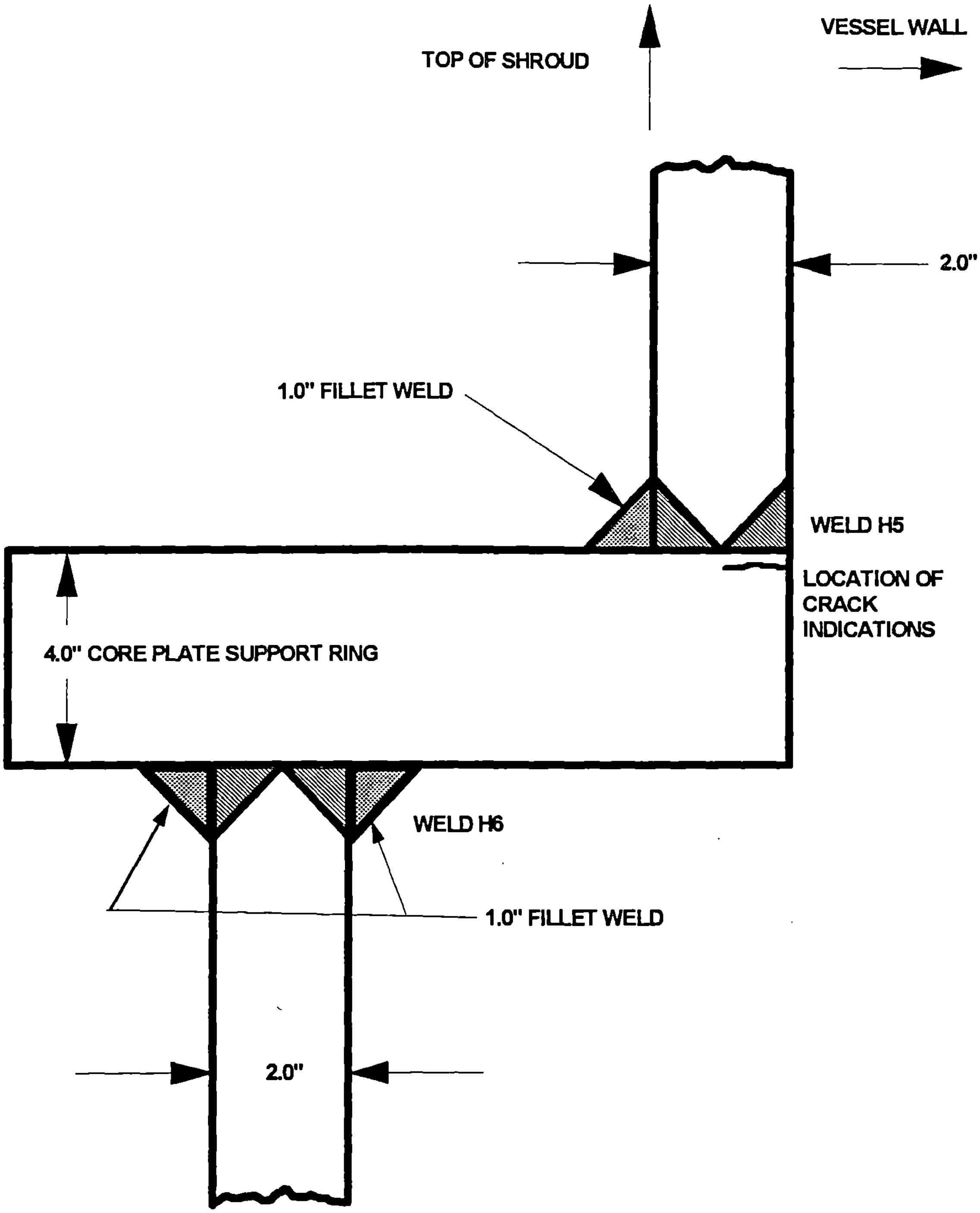

Figure 1 Shroud Weld Detail

3. Shroud Support, Shroud, and Top Guide Functions

The shroud support, shroud, core support, and top guide make up a stainless steel cylindrical assembly that provides lateral support for the core, vertical support for peripheral fuel bundles, and a partition between the core region and the downcomer annulus to separate the upward flow of coolant through the core from the downward recirculation flow. The shroud also provides (in conjunction with other components) a floodable region following a postulated recirculation line break. The shroud is not a primary pressure boundary component.

The top guide consists of a circular grid plate having square openings, which provide lateral support and guidance for fuel assemblies. The core support plate consists of a circular plate with openings and provides lateral support for the control rod guide tubes. The core support plate also provides vertical support for peripheral fuel assemblies. The majority of the fuel rests on fuel support castings that are supported by the control rod guide tubes. The fuel support castings are aligned by holes in the core support plate. The core support plate rests on the core support ring, which is welded to the shroud at the circumferential locations identified as H5 and H6.

4. Shroud Structural Evaluation

4.1 Shroud Loading Considerations

While the extent of the cracking reported at QC1 is not insignificant, there remains sufficient structural strength in the shroud to meet all of its design functions (Reference 5). The shroud is made of ductile material with high toughness properties even after accounting for any effects due to neutron fluence. The applied loading on the shroud is mainly from the differential pressure during normal operation, the transient differential pressure increase due to design basis accident loading, design basis seismic loads, and non-symmetric acoustic loads during the recirculation suction line break. These loads are generally small and well within the remaining structural integrity of the shroud.

The applied loads during normal operation, anticipated operational events, and the recirculation line break accident are in the downward direction. The applied load is in the upward direction when the main steam line break accident is assumed to occur alone or simultaneously with a safe shutdown earthquake (SSE). Reference 6 documents the design pressure drop loads of 8 psi on the upper part of the core shroud at normal, rated power conditions and 20 psi during the main steam line break accident.

The combination of high ductility and low applied stresses make the shroud extremely flaw tolerant. It has been calculated that 360° circumferential cracking of greater than 96% of the 3.0 inch available material can be tolerated while maintaining the industry accepted ASME Code allowable safety factors based on limit load method for the H5 area (Reference 16). The analysis that determines the 96% criterion conservatively ignores the available material of the extra one inch of ligament provided by the weldment in addition to the two inch shroud wall thickness. The maximum flaw depth is 1.24 inches or less than 42% of the 3.0 inch available material at QC1 (Reference 2).

Lateral loads on the core shroud due to an instantaneous break of the recirculation suction line and non-symmetric depressurization of the downcomer annulus are considered to be unrealistic in that it takes finite time (about 100 milliseconds) for the break to occur (Section 3.9.5.3.1.2 of the Quad Cities UFSAR). The asymmetric load is due to the time it takes for the pressure wave to travel from the broken suction line to the unbroken suction line. This duration is extremely short (about 5 milliseconds, as shown in Figure 3.9-12 of the Quad Cities UFSAR). This acoustic load affects the lower portion of the shroud (near H5) rather than the upper shroud (H2 and H3). Three areas that the acoustic load could affect are allowable crack length, crack depth, and lateral motion of the shroud assembly. Short duration loads of this type do not lead to significant deformation and are not included in the analysis of flaw sizes. The pressures due to the Main Steamline Break exceed those due to the Recirculation Line Break. Thus, from the standpoint of total loads, the steamline break with Safe Shutdown Earthquake is limiting. Lateral movement for the Main Steamline Break with SSE and the tipping motion of the shroud pivoted on one side of the H5 weld crack area during the Recirculation Suction Line Break are estimated to be less than 3/4 inch and the shroud would then return to its vertical position (Reference 19).

The low stresses and high material ductility under relatively low neutron fluence level ($3X10^{16}$ n/cm^2, Reference 16) make unrealistic the postulation of the separation of the core shroud assembly at H5 weld area during the present cycle based on the assumptions made and the information provided by ComEd (References 1 and 2).

4.2 Water Chemistry Considerations

The BWR oxidizing environment can provide the electrochemical driving force for intergranular stress corrosion cracking (IGSCC) of BWR structural materials. Also, the conductivity of the BWR coolant is sufficiently high to allow this corrosion reaction to occur (References 3, 7, and 8).

The crack growth rate depends on the water chemistry and the conductivity of reactor water. QC1 has been operated on Hydrogen Water Chemistry (HWC) continuously since the third quarter of 1990. The levels of hydrogen injected into QC1 have ranged from 1.4 to 1.5 ppm in the feedwater line with a corresponding concentration in the reactor vessel of approximately 180 ppb (Reference 9). The HWC system for QC1 was available for approximately 57% of the time the reactor was above 20% power. While this duration and availability is not high enough to protect reactor internals from IGSCC or IASCC, it could retard crack propagation. Conductivity measurements for QC1 show that the average conductivity through Cycle 12 for QC1 is 0.257 μS/cm (Reference 10).

Based on the information for QC1 inspection findings provided by ComEd, the maximum flaw depth for QC1 is 1.24 inches. Conservatively using the bounding crack growth rate of 5E-5 inch/hr (0.4 inch/year, assuming 8,000 operating hours/year), for normal water chemistry BWRs (Reference 20), the crack depth would be 2.04 inches in two years, which is beyond the planned end of the next cycle.

5. Normal Operation

As discussed in the preceding sections, the postulation of significant through-wall cracking, leakage, or separation of the core shroud assembly at H5 weld area is extremely improbable. The more likely, but still improbable scenario, would be for some bypass flow to occur from the core bypass region to the reactor downcomer annulus.

Even if the postulated cracking or separation were to occur, the weight of the core shroud above H5 weld is sufficiently high to hold the core shroud assembly in place during all normal operating conditions. The postulated leakage would occur through a gap much less than 0.001 to 0.002 inch. The estimated leakage flow is less than 35 gpm, assuming that a 0.002 inch gap exists around the entire circumference at 8 psid differential pressure. Leakage flow of this magnitude has no consequence on plant operation. It also would not be detectable by the plant operator because the leakage flow is small and the leakage temperature at this location is the same as the downcomer temperature.

6. Anticipated Operational Events

The previous sections show that cracks that grow through the shroud wall or cause complete separation of the shroud assembly at H5 area from the lower shroud are improbable. This section discusses anticipated operational occurrences that could increase shroud loads above those experienced during normal operation. The transients associated with such an occurrence are those that tend to depressurize the reactor vessel and those that increase core flow. The transients evaluated are: Pressure Regulator Failure - open, Recirculation Flow Control Failure - Increasing to Maximum Flow, and Inadvertent Actuation of the Automatic Depressurization System. The normal operating pressure drop across the upper shroud is 8 psid (Reference 6).

6.1 Pressure Regulator Failure - Open

This postulated Safety Analysis Report (SAR) event involves a failure in the pressure controls such that the turbine control valves and the turbine bypass valves are opened as far as the Maximum Combined Flow Limiter (MCFL) allows. For QC1, the bypass capacity is 40% of rated steam flow, the worst case involves inadvertently increasing the steam flow. The steam flow increase would be limited by the Maximum Combined Flow Limiter (MCFL) to 105% (Reference 17). A depressurization and cooldown occurs, followed by Main Steamline Isolation Valve (MSIV) closure. The steam flow increase is small enough that the increased force on the shroud head is offset by the weight of the core shroud above the H5 weld. Any leakage postulated may occur through a gap much less than 0.001 to 0.002 inch. Even if it is assumed that a momentary 20 psid pressure differential exists and that a 0.002 inch gap exists around the entire circumference, the postulated leakage flow is less than 60 gpm. A realistic flow, corresponding to a pressure differential of 10 psid, is less than 40 gpm. Leakage flows of this magnitude have no adverse consequences on plant operation.

6.2 Recirculation Flow Control Failure - Maximum Flow

This postulated event involves a recirculation control failure that causes both recirculation loops to increase to maximum flow. For this event, the pressure drop could change from a part-load condition to the high/maximum flow condition over a time period of several seconds. However, it should not significantly exceed the pressure drop expected for normal full power, high core flow operating conditions (8 psid). Normal operating procedures are considered sufficient to minimize the consequences of this potential transient.

6.3 Actuation of ADS

Inadvertent actuation of the Automatic Depressurization System (ADS) valves is another postulated event that could put an increased load on the upper shroud. The maximum steam flow and the depressurization rate occur over a period of about one second, spreading the effect of the change in load. There is a short-term increase in steam flow to approximately 130% of rated steam flow. The increase in the shroud ΔP resulting from the opening of the ADS valves is not expected to cause lifting of the shroud. Furthermore, inadvertent ADS is a very low probability event; it is classified in the ASME Emergency category.

7. Design Basis Accidents

Although the previous sections demonstrate that the probability of the postulated separation of the core shroud assembly at H5 weld area is extremely low, an accident occurring with a separated core shroud is addressed in this section.

The Main Steamline Break Accident imposes the largest potential lifting loads on the shroud head. Liquid breaks (up to and including the recirculation line break) do not impose significant pressure drops on the shroud head.

7.1 Main Steamline Break

The main steamline break inside primary containment is the postulated worst case because it results in the largest depressurization rate. During this SAR event, the reactor is rapidly depressurized as a result of a postulated instantaneous, double-ended break of the largest steamline. Thus, a larger than normal pressure difference could develop across the shroud as fluid flow is drawn from the core region toward the break. For QC1 the design basis pressure difference is 20 psid for the guillotine break of a main steam line (Reference 6).

The weight of the core shroud above H5 weld (Reference 5) is not high enough to hold the core shroud assembly in place during the main steam line break, and if the presence of the shroud ligament is totally neglected, the core shroud could lift momentarily by up to 4 inches while the reactor vessel is depressurizing. If the main steam line break occurs simultaneously with the safe shutdown earthquake (SSE), and 360° complete through-wall crack is postulated, the core shroud could lift momentarily by up to 8 inches while the reactor vessel is depressurizing. The estimated displacement is less for the OBE than for the SSE and is not discussed further. Since the break is in the main steamline, the core is capable of being reflooded up to and above two-third core height.

One of the key considerations of this postulated accident case is the ability of the control rods to insert before or during the postulated accident. Specifically, sufficient lifting of the top guide prior to control rod insertion could cause reorientation of the fuel bundles and thus impede the insertion of control rods.

The shroud head pressure drop characteristics calculated for the instantaneous, double-ended steamline break accident were evaluated generically (Reference 11). The conclusions, as described below, are applicable to QC1. The initial shroud head pressure drop loading is a result of the decompression wave which reduces system pressure overall, but would increase differential pressure across the shroud in the short term. The pressure loading increase is short-lived (less than two seconds) and decreases to below normal steady state loads. If it is even further postulated that the initial load pulse causes the shroud to separate, the last part of the pressure loading could cause the shroud assembly to lift. The flow path created by any separation reduces the upward lifting forces.

Scram is initiated during the main steamline break (inside containment) accident by the high drywell pressure trip signal. Drywell pressure exceeds the setpoint almost instantaneously, so the only delays in the rod insertion come from the sensors, the Reactor Protection System, and rod motion. For the main steamline break outside containment, shroud loads are lower, MSIV closure is initiated by high steam flow, and scram is initiated from the MSIV closure.

For all of the postulated steamline break scenarios, the insertion of all control rods will occur. Even if the first loading pulse causes the upper shroud assembly to break free, control rod motion will commence before the upper shroud assembly and top guide lift significantly. It is likely that the top guide will remain engaged with the tops of the fuel bundles. Any control rods that are partially inserted as part of the normal operation are already in position to initiate shutdown. Insertion of fully withdrawn control rods will occur by 0.9 second to 5% full stroke, which is early enough for the control rods to be moving up between the bundles before any significant lifting of the top guide can take place. The shroud assembly, if separated at H5, could shift laterally up to 3/4 inch (Reference 19). With the random displacement anticipated during seismic events, the CRD alignment in the core region would undergo intermittent periods of misalignment. Minimal scram performance degradation is expected. Even with 8 inches of lift during the main steam line break concurrent with the SSE, the fuel bundles and the top guide will stay engaged because the height of the top guide is approximately 14 inches (Reference 12) and an 8 inch lift retains the fuel bundles within the top guide. Friction between the fuel bundles and top guide is not high and the fuel bundles will slide against the top guide and stay within it. Control rod insertion will occur because the fuel will remain properly oriented. Reactor shutdown would thus be complete with all drives inserted. Even under the worst scenario discussed above, the control rods would fully insert and reactor shutdown would thus be achieved. In the very unlikely case that scram is not completed, the SLCS is available to provide shutdown capability.

Movement of the upper shroud assembly could affect the performance of the core spray system if it impacts the core spray line connection. If the lifting of the core shroud causes the core spray sparger or the riser to deflect, the coolant flow to the core from the core spray spargers could be affected. However, significant margins exist in the LOCA analysis results for QC1 (Reference 13, Table 5-3) even if a large deflection, resulting in a condition up to and including the failure of the core spray sparger or riser should occur. The core spray crack analysis (Reference 14) has shown that the core spray line crack is approximately 120° of the piping circumference. The effect of a deflection would tend to open the crack and allow water from the core spray system to enter the downcomer and thence to the core region. Such a condition would not prevent the entry of core spray system water into the reactor vessel. Therefore, even if the LPCI should fail to deliver water to the reactor vessel (Reference 15), the core spray water would be available and adequate long-term cooling would be available.

The main steamline break has also been evaluated for radiological release consequences in the SAR. For a main steamline break inside containment, the radiological consequences are bounded by the Loss of Coolant Accident. For the main steamline break outside containment, the magnitude of the pressure loads that potentially could lead to separation of the upper shroud are less than that for breaks inside the containment, due to attenuation of the depressurization wave along the steamline. MSIV closure is initiated before any potentially increased radiological release outside containment from such a scenario could occur. The radiological consequences of this main steamline break scenario are thus still bounded by the plant SAR results.

7.2 Recirculation Line Break

For the design basis recirculation line break combined with the SSE, the differential pressure across the upper shroud does not increase from the initial value as the reactor depressurizes, upward forces are reduced, and thus there is no significant threat to core shroud integrity in the vertical direction. The effect of lateral loads due to acoustic phenomena does not cause the shroud to move (see Section 4). Lateral movement due to tipping motion of the shroud does not exceed 3/4 inch and the shroud would then return to the vertical position. As described in Section 7.1, reactor shutdown would thus be complete with all drives inserted.

With the shroud integrity maintained, a floodable core region is also preserved. Even if the entire circumference is postulated to be cracked as done in the previous sections, the shroud assembly does not lift. The calculated leakage flow is very small compared to the emergency core cooling system flow capacity and there is no significant decrease in coolant to the core. Therefore, the recirculation line break analysis results are unchanged.

8. Emergency Operator Actions

The Quad Cities-specific Emergency Procedures (QGAs) are symptomatic in that they respond to detected symptoms and do not require diagnosis of the event by the operator. They address a wide range of events, both less severe and more severe than the design basis accidents.

The worst postulated event discussed above could result in separation of the shroud assembly from the lower shroud. However, this has minimal impact to scram performance because no disengagement of the fuel bundles from the top guide occurs. Therefore, no further consideration is necessary for the impact of this postulated event on the QGAs.

The QGAs provide instructions for reactor pressure, water level, and power control, as well as control of key primary containment parameters. Actions specified in the QGAs for reactor power control are to (1) insert control rods using a variety of methods, and (2) initiate the Standby Liquid Control System (SLCS) before pool temperature increases to the allowable value of 110 F (Reference 18). QGA instructions are for water level to be controlled below the high water level setpoint; thus there would not be dilution of the liquid boron by flooding to the steamline elevation or loss of vessel inventory out the break in case SLCS injection were to occur.

Water level would be controlled after the postulated event because the most challenging break is high in the vessel and water injection systems would be available to provide core cooling.

9. References

1. Letter form M.D.Lyster (ComEd), to W.D.Russell (NRC), dated 6/6/94. "Response to NRC Request for Additional Information Concerning Core Shroud Cracking at Dresden Units 2 & 3 and Quad Cities Units 1 & 2."

2. GE Rapid Information Communication Services Information Letter (RICSIL) 068, Revision 2, Update on Core Shroud Cracking, May 6, 1994.

3. GE Services Information Letter (SIL) 572, Revision 1, Core Shroud Cracks, October 4, 1993.

4. Evaluation and Screening Criteria for the Quad Cities 1 and 2 Shrouds, Dresden 3 Shroud Circ Flaw at H5, GE Design Record File, DRF-137-0010-7, Report Number GE-NE-523-02-0194..

5. Fax, Bob Walsh (ComEd) to Dilip Rao (GE), Received May 5, 1994. (Includes Pages from Updated Final Safety Analysis Report, Quad Cities Units 1 and 2, Tables 3.9-19 and 3.9-20).

6. M. Gordon et al, "Hydrogen Water Chemistry for BWRs-Materials Behavior-Final Report," EPRI TR-100304, Palo Alto, CA, February 1992.

7. E. Indig et al, "Investigation of the Protection Potential Against IASCC," Paper #71 presented at Corrosion 92, NACE, Nashville, April 1992.

8. Telecon, Dilip Rao (GE) and Tracy Finnegan (ComEd), May 5, 1994.

9. Internal Communication, Barry Gordon/Dilip Rao (GE), May 5, 1994.

10. Letter dated November 9,1993, from L. A. England to US NRC, "BWROG Safety Assessment - BWR Shroud Crack Indications"

11. GE drawings, 718E861 and 104R921

12. NEDC-31345P, "Quad Cities Nuclear Power Station Units 1 & 2 SAFER/GESTR LOCA Analysis," General Electric Company, June 1987.

13. GENE-523-A80-0594, "Core Spray Crack Analysis for Quad Cities Units 1 & 2."

14. Quad Cities Station UFSAR, Copy 40, Section 7.3.1.2.1.2, "Single Failure Criterion (IEEE 279, paragraph 4.2)."

15. GENE-523-A79-0594, "Evaluation of the Indications Found at the H5 Weld Location in the Quad Cities Unit 1 Shroud."

16. Fax, Mark Uhrich, ComEd, to Dilip Rao, GE, dated 6/1/94, "Comments on Safety Assessment."

17. QGA 200, Torus Temperature Control Methods.

18. GENE-A00-05652-03, Supplement 3, Revision 1, "Preliminary Safety Assessment of Core Shroud Indications for Cycle 14 Operation of Dresden Unit 2."

19. GE-NE-523-148-1193, April 1994, "BWR Core Shroud Evaluation."

GE-NE 523-A93-0694
DRF 137-0010-7
JUNE 1994

Safety Assessment of Core Shroud Indications for Cycle 14 Operation of Dresden Unit 3

Prepared by: ____________________
R. S. Daniel, Engineer

Verified by: ____________________
D. K. Rao, Senior Engineer

Approved by: ____________________
S. Ranganath, Manager 6/28/94
Engineering & Licensing Consulting Services

IMPORTANT NOTICE REGARDING
CONTENTS OF THIS REPORT

TABLE OF CONTENTS

1.0 Introduction

Circumferential crack indications have been observed in the Dresden 3 core shroud assembly during the current refueling outage. The visual inspections performed have indicated that crack indications are found near the H3, H4, and H5 welds. The most severe indications are in the core support ring joined to the core shroud near the H5 weld and appear to be 360° circumferential cracking (Reference 1). Initial ultrasonic (UT) inspections performed near the H5 weld have confirmed these indications to be cracks. Reference 2 indicates that the UT inspections were done at six locations of the H5 area, using automated UT. An engineering evaluation is sought by the Commonwealth Edison Company (ComEd) to justify operation of Dresden 3 for one additional cycle (18 to 24 months) before the final shroud fix is implemented.

This report also qualitatively addresses the potential situation during normal operation, anticipated operational events, and design basis accidents, if unexpected significant crack growth occurs during plant operation. This assessment describes the symptoms and consequences expected if the shroud has degraded to the point that through-wall cracking has occurred in the core support ring in the H5 weld area. A qualitative assessment is provided for other welds on the core shroud.

GE Rapid Information Communication Services Information Letter (RICSIL) 068 has been issued (Reference 3) to assist ComEd and other utilities in the on-going evaluation of this situation. Previous communications about core shroud crack indications have included GE SIL 572 (Reference 4) and the US-NRC Information Notice 93-79.

2.0 Summary and Conclusions

The core shroud/core support ring cracking associated with the H5 weld at Dresden Unit 3, which was the most extensively cracked weld area in Dresden 3, does not represent a threat to the safe operation for the next cycle:

1. The combination of high ductility, high toughness and low stresses makes the shroud extremely flaw tolerant. Even for this situation with the indications assumed to cover 360 degrees of the circumference, crack depths of up to 98% (2.94 inches) of the available material can be tolerated while maintaining the structural integrity for normal operation and postulated design basis accident conditions, including ASME Code safety factors. The available material considers the extra one inch of ligament provided by the weldment in addition to the two inch shroud wall thickness.

2. The maximum bounding crack depth determined by ultrasonic and visual examinations and boat sample analysis in Dresden 3 is 1.24 inches, and is within the allowable crack depth of 2.94 inches.

3. Using the bounding crack growth rate of 5 E-5 inch/hr (0.40 inch per year assuming 8,000 hours per year) for the BWR plant with normal water chemistry, the allowable crack depth is not expected to be exceeded within one fuel cycle based on the assumptions made and the information provided by ComEd. No BWR inspection to-date has found through-wall cracking.

4. If the shroud assembly is postulated to have 360° through-wall cracking, it would not lift during normal operations because the weight of the core shroud above H5 is sufficient to hold the shroud in place. The leakage flow is small, is not detectable because the leakage flow temperature near the H5 weld is almost the same as the downcomer annulus temperature, and does not impact plant operations.

5. In the unlikely occurrence of a design basis accident, safe reactor shutdown will be achieved, and no change in emergency core cooling function is anticipated, even with concurrent design basis earthquake.

3.0 Shroud and Top Guide Functions

The shroud support, shroud, core support, and top guide (see Figure 1) make up a stainless steel cylindrical assembly that provides lateral support for the core, vertical support for peripheral fuel bundles, and a partition between the core region and the downcomer annulus to separate the upward flow of coolant through the core from the downward recirculation flow. The shroud also provides (in conjunction with other components) a floodable region following a postulated recirculation line break. The shroud is not a primary pressure boundary component.

The top guide consists of a circular grid plate having square openings, and provides lateral support and guidance for fuel assemblies. The majority of the fuel rests on fuel support castings that are supported by the control rod guide tubes. The fuel support castings are aligned by holes in the core support plate. The core support plate rests on the core support ring, which is welded to the shroud at the circumferential locations identified as H5 and H6.

4.0 Shroud Structural Evaluation

While the extent of the cracking that has been reported at Dresden 3 is not insignificant, there remains sufficient structural strength in the shroud to meet all of its design functions (Reference 5). The shroud is made of ductile material with high toughness properties even after accounting for any effects due to neutron fluence. The applied loading on the shroud is mainly from the differential pressure during normal operation, the transient differential pressure increase due to design basis accident loading, and design basis seismic loads. These loads are generally small and well within the remaining structural integrity of the shroud.

The applied loads during normal operation, anticipated operational events, and the transient differential pressure loading due to a design basis accident are in the downward direction. The applied load is in the upward direction only when the main steam line break accident is assumed to occur simultaneously with a design basis earthquake. Reference 6 documents the design pressure drop loads of 7 psi on the upper part of the core shroud at normal, rated power conditions, and 12 psi during the main steam line break accident.

The combination of high ductility and low applied stresses make the shroud extremely flaw tolerant. It has been calculated that 360° circumferential cracking of greater than 98% of the 3.0 inch available material can be tolerated while maintaining the industry accepted ASME Code allowable safety factors based on limit load methods for the H5 area (Reference 5). The available material considers the extra one inch of ligament provided by the weldment in addition to the two inch shroud wall thickness. The maximum bounding flaw depth is 1.24 inches or 41% of the 3.0 inch available material at Dresden 3 (Reference 2).

The low stresses and high material ductility under relatively low neutron fluence level make unrealistic the postulation of the separation of the core shroud assembly at the H5 weld area during the next cycle. Using the upper bound crack growth rate of 5 E-5 inch/hr (0.40 inch per year assuming 8,000 hours per year) for the BWR plant with normal water chemistry, the allowable crack depth is not expected to be exceeded during the next fuel cycle based on the assumptions made and the information provided by ComEd (References 1 and 2).

5.0 Normal Operation

As discussed in the preceding sections, the postulation of significant through-wall cracking, leakage, or separation of the core shroud assembly at the H5 weld area is extremely improbable. The more likely but still improbable scenario would be for some bypass flow to occur from the core bypass region to the reactor downcomer annulus through the cracks.

Even if the postulated cracking or separation were to occur, the weight of the core shroud above the H5 weld is sufficiently high to hold the core shroud assembly in place during all normal operating conditions. The postulated leakage would occur through a gap much less than 0.001 to 0.002 inch. The estimated leakage flow is less than 30 gpm, assuming that a 0.002 inch gap exists around the entire circumference at 7 psid differential pressure. Leakage flow of this magnitude has no consequence upon the plant operation. It also would not be detectable by the plant operator because the leakage flow is small and the leakage temperature at this location is approximately the same as the downcomer temperature.

6.0 Anticipated Operational Events Related to Increased Shroud Head Pressure Loads

The previous sections demonstrate that cracks that grow through the shroud wall or cause complete separation of the shroud assembly at the H5 area from the lower shroud are improbable. This section discusses anticipated operational occurrences that could increase shroud loads above those experienced during normal operation: pressure regulator failure - open, recirculation flow control failure - increasing to maximum flow, and inadvertent actuation of the Automatic Depressurization System. The normal operating pressure drop across the upper shroud is 7 psid (Reference 6).

6.1 Pressure Regulator Failure - Open

This postulated Safety Analysis Report (SAR) event involves a failure in the pressure controls such that the turbine control valves and the turbine bypass valves are opened as far as the Maximum Combined Flow Limiter (MCFL) allows. For the Dresden units, with a bypass capacity of 40% of rated steam flow, the worst case involves inadvertently increasing the steam flow to about 150% of rated. This would not happen because the steam flow limit is set at 105%. A depressurization and cooldown occurs which is isolated by Main Steam Line Isolation Valve (MSIV) closure. This steam flow increase is small enough that the increased force on the shroud head (approximately 50% above the normal pressure drop) is less than the pressure differential of 12 psid due to the main steam line break (Reference 6). The weight of the core shroud above the H5 weld is sufficiently high to hold the core shroud assembly in place at 12 psid load. Any postulated leakage may occur through a gap much less than 0.001 to 0.002 inch. The postulated leakage flow is approximately less than 40 gpm, with the assumption that a 0.002 inch gap exists around the entire circumference at 12 psid pressure differential. The leakage flow of this magnitude has no consequence on plant operation.

6.2 Recirculation Flow Control Failure

This postulated event involves a recirculation control failure that causes both recirculation loops to increase to maximum flow. In this case, the pressure drop could change from a part-load condition to the high/maximum flow condition over a time period of several seconds, but it should not significantly exceed the pressure drop expected for normal full power, high core flow operating conditions (7 psid). Normal operating procedures are considered sufficient to minimize the consequences of this potential transient, and the force on the shroud head is within the inspected shroud capability (12 psid in Section 6.1).

6.3 Inadvertent Actuation of ADS

Inadvertent actuation of the Automatic Depressurization System (ADS) valves is another postulated event that could put an increased load on the upper shroud. The maximum steam flow and the depressurization rate are significantly smaller than for the postulated main steam line break, causing a short-term increase in steam flow of approximately 30% of rated steam flow. The increase in the shroud ΔP resulting from the opening of the ADS valves would occur over a period of about one second, spreading the effect of the change in load.

Inadvertent ADS is also a very low probability event; it is considered to be in the ASME Emergency category in the vessel thermal duty design. It has been used as the design basis Emergency event for the Dresden shroud. The effect of this event is bounded by Section 6.1.

7.0 Design Basis Accidents

Although the previous sections demonstrate that the probability of the postulated separation of the core shroud assembly at the H5 weld area is extremely low, an accident occurring with a separated core shroud is addressed in this section.

The Main Steam Line Break Accident imposes the largest potential lifting loads on the shroud head. Liquid breaks (e.g., recirculation line breaks) do not impose large pressure drops on the shroud head, and, in fact, the shroud pressure drop decreases from its initial value.

7.1 Main Steam Line Break

The main steam line break inside primary containment is the postulated worst case because it results in the largest depressurization rate. During this SAR event, the reactor is rapidly depressurized as a result of a postulated, instantaneous, double-ended break of the largest steam line. Thus, a larger than normal pressure difference could develop across the shroud as fluid flow is drawn from the core region towards the break. For Dresden 3, the design basis pressure difference is 12 psid for the guillotine break of a main steam line (Reference 6).

The weight of the core shroud above the H5 weld is sufficiently high to hold the core shroud assembly in place during the main steam line break, and the core shroud does not lift (Reference 5). The leakage may occur through a gap much less than 0.001 to 0.002 inch. The postulated leakage flow is less than 40 gpm, with the assumption that a 0.002 inch gap exists around the entire circumference at 12 psid pressure differential. The leakage flow of this magnitude has no consequence for the emergency core cooling performance.

If the main steam line break occurs simultaneously with the design basis earthquake, and 360° complete through-wall crack is postulated, the added load may cause separation of the upper shroud assembly near the H5 indications, leading to an upward displacement of the structure and the associated top guide. The amount of lifting and the potential effect of these postulated occurrences on emergency operation are described below.

One of the key considerations of this postulated accident case is the ability of the control rods to insert before or during the postulated accident. Specifically, sufficient lifting of the top guide prior to control rod insertion could cause reorientation of the fuel bundles and thus impede the insertion of the control rods.

The shroud head pressure drop characteristics calculated for the instantaneous, double-ended steam line break accident were evaluated for a typical BWR (Reference 7). The initial shroud head pressure drop loading is a result of the decompression wave which reduces system pressure overall, but would increase differential pressure across the shroud in the short term.

The pressure loading increase is short-lived (less than two seconds) and decreases to below normal steady state loads. Even if the remaining shroud ligament is small (see Section 4), the structural integrity of the shroud will remain intact for this postulated limiting event. If it is further postulated that the initial load pulse causes the shroud to separate, the last part of the pressure loading could cause the shroud assembly to lift. The flow path created by any separation reduces the upward lifting forces. For this postulated scenario, the core shroud assembly would not lift with the main steam line break alone, but would lift less than 2 inches if the main steam line break occurs simultaneously with the design basis earthquake.

The seismic acceleration is transmitted to the shroud assembly before the lift, but is no longer applicable once it is lifted. An evaluation has been done with the shroud assembly mounted on a frictionless roller. This analysis shows less than 0.6 inch lateral movement of the shroud during a main steam line break with SSE conditions. Based on this analysis, the maximum velocities of the shroud assembly, and engineering judgment, the lateral displacement is expected to be less than 3/4 inch. Displacement of this magnitude does not interfere with any reactor internals.

Scram is initiated during the main steam line break (inside containment) accident by the high drywell pressure trip signal. Drywell pressure would exceed the setpoint almost instantaneously, so the only delays in the rod insertion come from the sensors, the Reactor Protection System and rod motion. For the main steam line break outside containment, shroud loads are reduced, MSIV closure is initiated by high steam flow, and scram is initiated from the MSIV closure.

For either postulated steam line break scenario, the insertion of all control rods will occur within the required time. With the main steam line break alone, the core shroud assembly would not lift or move laterally, and no degradation of scram performance is expected. If the main steam line break occurs simultaneously with the design basis earthquake, the shroud assembly would lift less than 2 inches, and the lateral movement due to seismic excitation is less than 3/4 inch. Normal CRD alignment from the bottom end of the fuel bundles to CRD flange will be maintained and no binding within the CRD mechanisms is anticipated during a scram without seismic excitation. However, during a SSE, the shroud assembly, if separated at H5, could move laterally less than 3/4 inch. With the random displacement anticipated during seismic events, the CRD alignment in the core region would undergo intermittent periods of misalignment. Hence, the CRD scram speed would assume a somewhat oscillatory velocity profile, which is typically expected under seismic events. Even with 2 inches of lift anticipated during the main steam line break concurrent with a SSE, fuel bundles and the top guides stay engaged and the core lattice is maintained. The height of the top guide is 14 inches and a 2 inch lift retains the fuel bundles within the top guide cavity. The fuel bundles are not expected to be lifted by the top guide because the friction between the top guide and the fuel channel is not high, and the fuel bundles stay within the top guide cavity by gravity alone. Therefore, the core geometry is maintained during this event, minimal scram performance degradation is expected. Even under the worst condition, the control rods fully insert, and reactor shutdown would thus be achieved.

Movement of the upper shroud assembly (in the very unlikely case that it occurs) could affect the core spray system if it impacts the core spray line connection. The 2 inch lift can be easily accommodated by the 1.69 inch vertical clearance in the core spray line brackets and the compliance in the core spray line itself (Reference 8). Thus, coolant flow to the two core spray spargers is ensured. Therefore, no change is predicted in the emergency core cooling function.

The main steam line break has also been evaluated for radiological release consequences in the SAR. For a main steam line break inside the containment, the radiological consequences are bounded by the Loss of Coolant Accident. For the main steam line break outside of the containment, the magnitude of the pressure loads that potentially could lead to separation of the upper shroud are less than that for breaks inside the containment, due to attenuation of the depressurization wave along the steam line. MSIV closure is initiated before any potentially increased radiological release outside the containment from such a scenario could occur. The radiological consequences of this main steam line break scenario are thus still bounded by the plant SAR results.

7.2 Recirculation Line Break

For the design basis recirculation line break, the differential pressure across the upper shroud decreases from the initial value as the reactor depressurizes, upward forces are reduced, and thus there is no significant threat to core shroud integrity. With the shroud integrity maintained, a floodable core region is also preserved. Even if the entire circumference is postulated to be cracked as done in the previous sections, the shroud assembly does not lift, and the calculated leakage flow is very small compared to the emergency core cooling system flow capacity, and there is no significant decrease in coolant to the core. Therefore, the recirculation line break analysis results are unchanged.

The core shroud pressure drop during the recirculation suction line break under SSE seismic excitation does not lift the core shroud assembly above the H5 weld and allows substantial downward load, approximately 75 kips, even after the peak pressure difference across the shroud during a Safe Shutdown Earthquake (SSE) has been considered. Substantial resisting forces exist with the downward load due to the irregular mating surfaces along the crack both in the radial and circumferential directions. Therefore, the shroud assembly is not likely to move laterally. More likely, motion of the shroud assembly is rotational (tipping) motion of the assembly pivoted on one side of the H5 weld crack area. The lateral motion near the top of the shroud assembly due to this rotating motion is calculated to be less than 3/4 inch. The displacement of this magnitude does not interfere with any reactor internals.

The main contributor for the lateral motion or rotational (tipping) motion is caused by the seismic acceleration. The blowdown load caused by break flow through the recirculation suction line is primarily confined over the projected recirculation line area and is approximately 20,000 lbf (Reference 9 of GE-NE-A00-05652-03), and has a small effect on the shroud assembly above the H5 weld.

Acoustic load is due to an instantaneous break of the recirculation suction line. Such a load is unrealistic in the sense that it takes a finite time for the break to occur, at least 100 milliseconds. However, a hypothetical instantaneous break is considered as the source of a bounding load. The asymmetric load is caused by the fact that the sound wave takes finite time to travel from the broken suction line side to the unbroken suction line side of the annulus. The duration of the load is extremely short, about 5 milliseconds, as shown in Figure 3.9-6 of the Dresden UFSAR (Reference 6). The acoustic load has a higher load distribution on the lower portion of the shroud. However, the acoustic load distribution is assumed to be uniform between the jet pump base plate and the top of the shroud head. Above the shroud head, there is almost no acoustic load due to the large cross sectional area that attenuates the acoustic wave. Therefore, the assumption made provides a bounding lateral force and a bounding overturning moment to the shroud assembly above the H5 weld.

The result of this evaluation on the acoustic load indicates that the force acting on the shroud assembly above the H5 weld is less than 75 % of the total force calculated for the shroud. The total force on the shroud is provided as a function of time in Figure 3.9-6 of Reference 6. The point of application of the resultant horizontal acoustic load is less than 107 inches above the H5 weld. During the recirculation suction line break, the core shroud assembly does not lift and retains substantial downward load, approximately 75 kips, even after the pressure difference across the shroud under the SSE load has been considered. Substantial resisting forces exist with the downward load due to the irregular mating surfaces along the crack both in the radial and circumferential directions. Therefore, the shroud assembly is constrained from lateral movement. More likely, motion of the shroud assembly is rotational (tipping) motion of the assembly pivoted on one side of the H5 weld crack area. The resulting lateral motion near the top of the shroud assembly associated with this rotating motion is very small, approximately three thousandth of an inch, because the duration of the load is very short, the impulses are small. The restoring moment by the downward load of 75 kips sets back the shroud assembly in the vertical position. In conclusion,the lateral motion of the shroud assembly due to the acoustic load is essentially zero even if a 360° through-wall crack is present at the H5 weld. Practically, the addition of the acoustic load to seismic and other LOCA loads does not change the shroud motion.

Furthermore, it can be concluded that the acoustic load does not result in any plastic deformation of the shroud assembly.

8.0 Emergency Operator Actions

The Emergency Procedure Guidelines (EPGs) are the basis for plant specific Emergency Operating Procedures (EOPs). The EPGs are symptomatic in that they respond to detected symptoms and do not require diagnosis of the event by the operator. They address a very wide range of events, both less severe and more severe than the design basis accidents.

The worst postulated event discussed above could result in separation of the shroud assembly from the lower shroud, which has minimal impact to scram performance. Therefore, no further consideration is necessary for the impact of this postulated event on the EPGs.

The EPGs provide instructions for reactor pressure, water level, and power control, as well as control of key primary containment parameters. Actions specified in the EPGs for reactor power control are to (1) insert control rods using a variety of methods, and (2) initiate the Standby Liquid Control System (SLCS) before pool temperature increases to the allowable value (typically 110 °F). EPG instructions specify water level to be controlled below the high water level setpoint; thus, there would not be dilution of the liquid boron by flooding to the steam line elevation or loss of vessel inventory out the break in case SLCS injection were to occur.

Water level would be controlled after the postulated event because the break is high in the vessel and a large compliment of water injection systems would be available.

9.0 References

1. Telecons between Dave Rogowski and Dean Legler (ComEd) and G. L. Stevens, Hwang Choe, Gene Eckert, and John Nash (GE), April 27 and 28,1994

2. Ultrasonic Examination of Dresden Unit #3 Shroud Weld # H5, ComEd inspection report prepared by Brian F. Wilson, April 27, 1994

3. GE Rapid Information Communication Services Information Letter (RICSIL) 068, "Update on Core Shroud Cracking", April 8, 1994.

4. GE Services Information Letter (SIL) 572, Revision 1, "Core Shroud Cracks", October 4, 1993.

5. "Evaluation of the Indications Found at the H5 Weld Location in the Dresden Unit 3 Shroud", Report Number GE-NE-523-A69-0594, G. L. Stevens, June 1994.

6. Updated Final Safety Analysis Report, Dresden 2 and Dresden 3, Tables 3.9-19, and 3.9-20, and Figure 3.9-5

7. Letter dated November 9,1994, from L. A. England to US NRC, "BWROG Safety Assessment - BWR Shroud Crack Indications"

8. Evaluation and Screening Criteria for the Dresden Units 2 and 3 Shrouds, Report Number GE-NE-523-05-0194, W. F. Weitze, March 1994

9 Preliminary Safety Assessment of Core Shroud Indications for Cycle 14 Operation of Dresden Unit 2, Report Number GE-NE A00-05652-03, H. Choe, May 1994.

Subject Acoustic Load

Originator

Date

Number

Verifier

Date

Acoustic loads are created due to instantaneous guillotine break of a pipe, because the decompression wave from the recirculation suction nozzle goes through the downcomer annulus. Fig. 1 shows an experimental result, simulation BWR RPV + shroud geometry. One of the main reason that the pressure does not go down to the atmospheric pressure is that the subcooled water flashes when the pressure drops below the saturation pressure. The acoustic wave propagation for this application is modeled in "WHAM" code. WHAM prediction is known to be conservative. Fig. 2 shows the circumferential pressure distribution predict-

Subject | Originator | Date

Number | Verifier | Date

by WHAM code. There is a tendency that the depressurization is greater near the suction nozzle. This type of pressure distribution will create higher acoustic load distribution near the recirculation line suction nozzle.

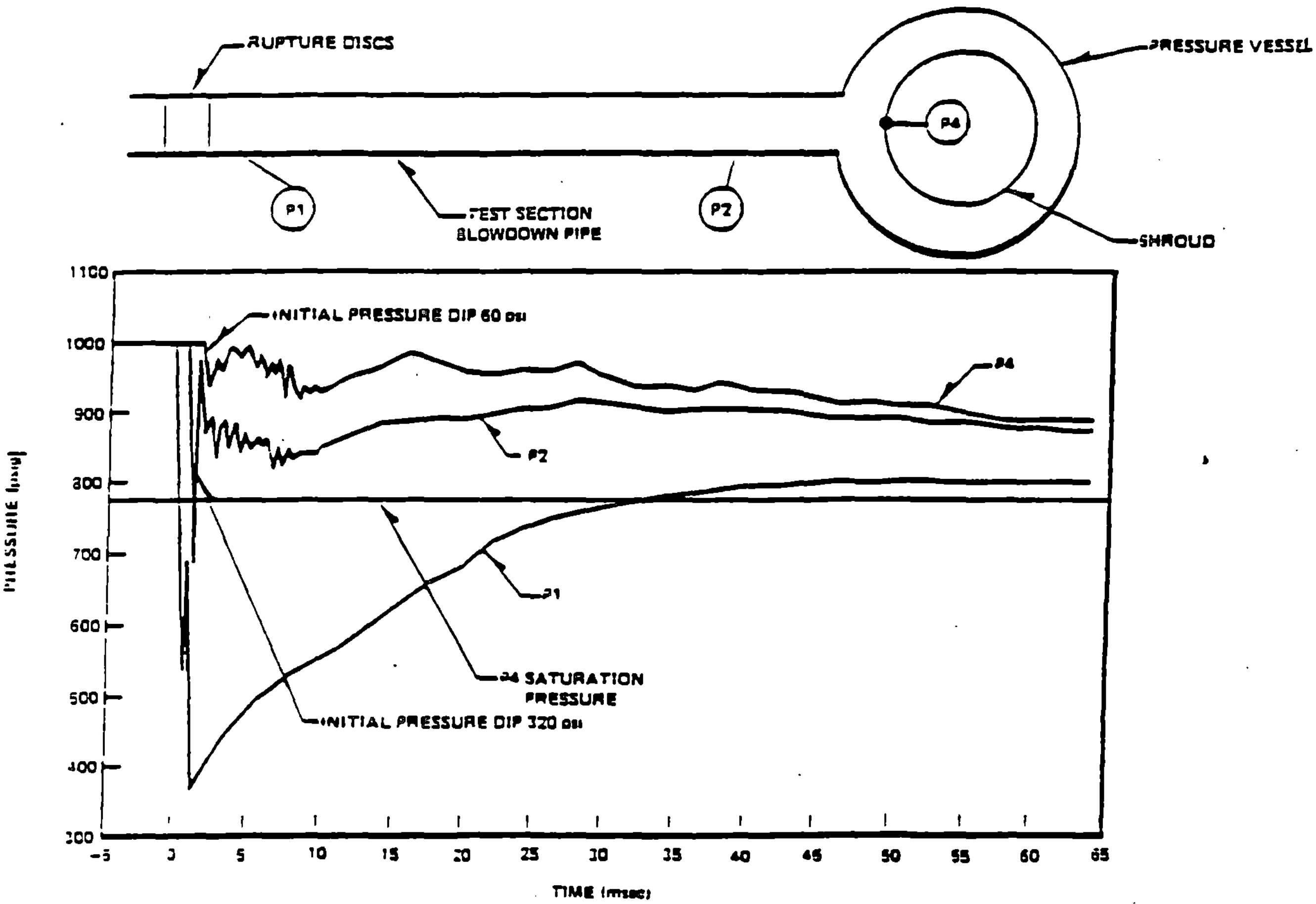

NOTE: 1 bar = 14.5 psi

Figure 1 Typical Measurements from Small Blowdown Test Apparatus with Shroud.

Figure 2

Acoustic Pressure Profiles on Shroud of a BWR/6-238.

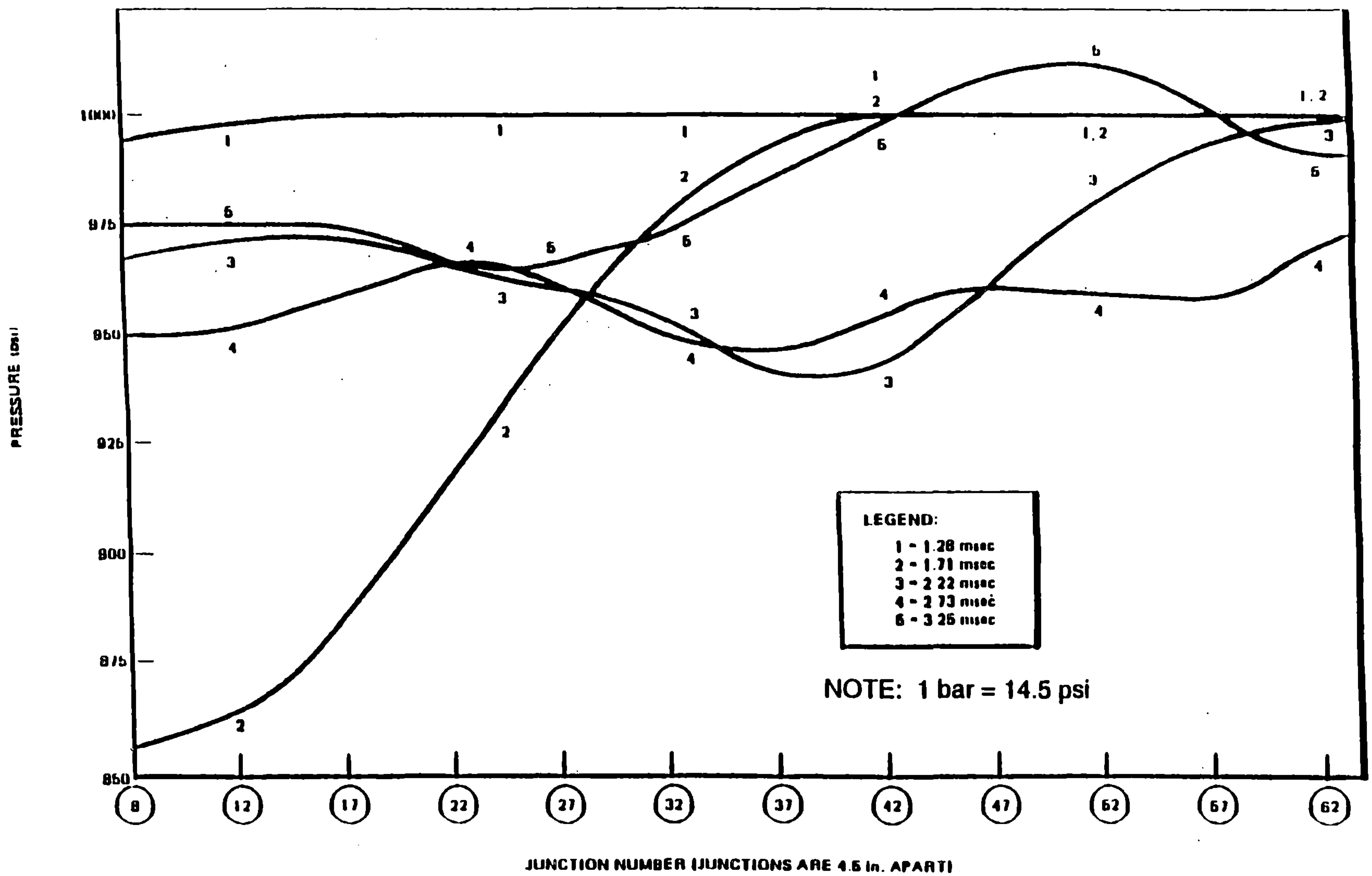

4 of 4

Subject Blowdown Load
Number
Originator
Date
Verifier
Date

The blowdown load is analyzed by ① examining expected flow pattern near the suction nozzle, ② Potential flow modeling assuming constant pressure across the down-comer annulus gap and using two-dimensional flow sinks (this is a very good approximation away from the suction nozzle, and ③ Potential flow modeling using three-dimensional flow sinks to simulate a point sink in front of an infinite plate

Figure 1 shows the expected flow pattern. This shows that the static pressure on the shroud wall would be quite different from the static pressure on the RPV wall or suction nozzle as the flow approaches the suction nozzle. For this reason, the static pressure below H5 near the suction nozzle is assumed to be constant & is approximately the same as at H5. Inside the flow separation region, velocity is very low and pressure does not vary much.

A. 2-D Potential Flow Model.

Assumptions

① Viscosity effect is ignored. It is a small effect.

② Annulus gap is assumed to be constant, the same as at H5. Actual annulus gap changes, but the constant gap assumption provides an accurate result for the blowdown load for the shroud assembly above H5. The annulus gap change at H3 does not affect the resul much because H3 is far enough away from the suction nozzle.

③ All flow properties ($p, \vec{V}$) are constant across the annulus gap.

Subject	Originator	Date
Number	Verifier	Date

④ The annulus is modeled as a repeated two dimensional plane

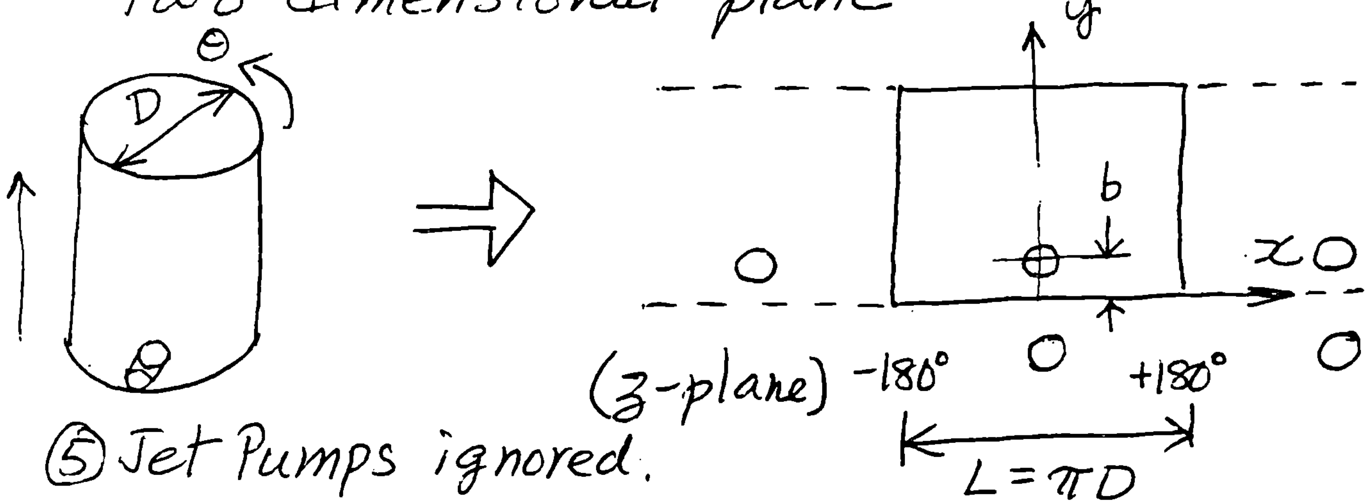

⑤ Jet Pumps ignored.

For two-dimensional potential flows, complex potential function can be used. For the flow sinks with strength, q, separated by π, and located at $\pm n\pi$ on x-axis, we have

$$\phi = -\frac{q}{2\pi} \log \sin z \quad , \quad z = x + iy$$

when our problem is approximated by flow sinks located at $(\pm n\pi, b)$ and $(\pm n\pi, -b)$ to satisfy the boundary condition at the jet pump base plate,

Subject	Originator	Date
Number	Verifier	Date

we have

$$\phi = -\frac{Q/W}{2\pi}\left\{\log \sin\left[\frac{\pi}{L}(z-bi)\right] + \log \sin\left[\frac{\pi}{L}(z+bi)\right]\right\}$$

where

Q = Total volume flow
W = annulus gap
q = volume flow / unit thickness

Now $\bar{V} = V_x - iV_y = \frac{d\phi}{dz}$

$$\therefore \bar{V} = -\frac{Q/W}{2\pi D}\left\{\cot\left(\frac{z-bi}{D}\right) + \cot\left(\frac{z+bi}{D}\right)\right\}$$

$$= -\frac{V_\infty}{4}\left\{\frac{\sin\left(\frac{2x}{D}\right) - i\sinh\left\{\frac{2(y-b)}{D}\right\}}{\sin^2\left(\frac{x}{D}\right) + \sinh^2\left(\frac{y-b}{D}\right)} + \frac{\sin\left(\frac{2x}{D}\right) - i\sinh\left\{\frac{2(y+b)}{D}\right\}}{\sin^2\left(\frac{x}{D}\right) + \sinh^2\left(\frac{y+b}{D}\right)}\right\}$$

The following relations were used in the above calculation

$$\cot(x+iy) = \frac{1}{2}\,\frac{\sin 2x - i\sinh 2y}{\sin^2 x + \sinh^2 y}$$

$$V_\infty = \frac{Q}{\pi D W}$$

Now $P_0 = P_s + \rho\frac{V^2}{2g_c}$

Subject	Originator	Date
Number	Verifier	Date

$$\therefore \quad P_o - P_s = \frac{\rho V^2}{2g_c} = \frac{\rho V_\infty^2}{2g_c}\left(\frac{V^2}{V_\infty^2}\right)$$

Now

$$\frac{P_o - P_s}{\left(\frac{\rho V_\infty^2}{2g_c}\right)} = \left(\frac{V}{V_\infty}\right)^2, \text{ non-dimensionalized pressure distribution}$$

$$= \frac{V_x^2 + V_y^2}{V_\infty^2}$$

$\left(\frac{V}{V_\infty}\right)^2$ is calculated at 10° interval in the annulus (x-direction), and with the same interval in y-direction. This is shown on pages 1 and 3 of the spread sheet.

The pressure obtained is integrated to calculate the net force. Due to the symmetry with respect to (0°-180°) y-direction forces all cancels out, and the net x-direction forces are calculated

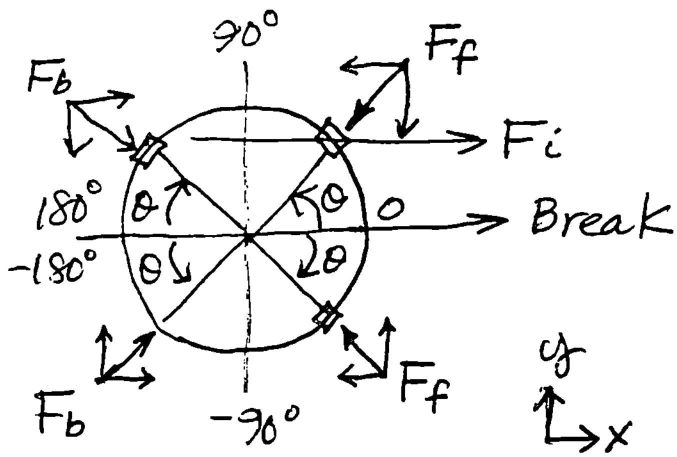

$$F_i = (F_b - F_f)\cos\theta$$

The pressure is integrated above H5 and below H5 separately for each 10° segment, and the total resulting force is calculated for the shroud above H5 and below H5. The result is shown in pages 5 and 7.

$$F(180° \text{ half}) = \int_{HALF}\int_{H5}^{TOP} (p\,dy) \cdot \cos\theta \cdot dx$$

$$\simeq \Sigma (F_b - F_p)_i \cos\theta_i = \Sigma F_i$$

In order to calculate the application pt of the force, the moment is calculated with the axis of rotation at H5.

$$\text{Moment} = F \cdot Y$$

$$= \int_{HALF}\int_{H5}^{TOP} (p\,y\,dy)\,dx \cos\theta$$

For each 10° section,

$$\int_{H5}^{TOP} p\,y\,dy = y_i \underbrace{\int_{H5}^{TOP} p\,dy}_{F_i} = y_i F_i$$

y_i = moment arm for each 10° section.

Subject	Originator	Date
Number	Verifier	Date

$\therefore$ Moment $= F \cdot Y$

$$\approx \sum F_i y_i$$

and $Y = \dfrac{\sum F_i y_i}{F}$

This result is shown in spread sheet pages 6 and 8.

Summary of Results

F = 17.2 Kips above H5
Y = 61.7 inches
Moment = 1060 Kips-inches

Note: QC & Dresden Restoring Moment after ΔP inside the shroud and seismic acceleration (upward) are considered

QC: 37 Kips x 100 inches = 3700 Kips-in

Dresden: 75 Kips x 100 in = 7500 Kips-in

Subject | Originator | Date
Number | Verifier | Date

B. 3-D Potential Flow Model

For the point flow sink, the potential function is

$$\phi = -\frac{Q}{4\pi}\frac{1}{r}, \quad \text{wher } r = |x\vec{i} + y\vec{j} + z\vec{k}|$$

and

$$V_x = \frac{\partial \phi}{\partial x}, \quad V_y = \frac{\partial \phi}{\partial y}, \quad V_z = \frac{\partial \phi}{\partial z}$$

Now assume that two sinks are separated by $2W$,

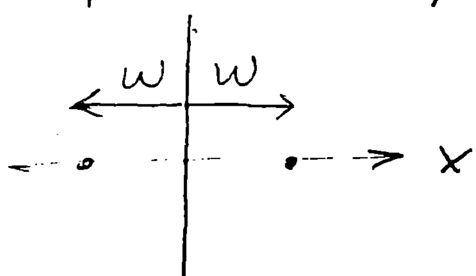

$$\phi = -\frac{Q}{4\pi}\left(\frac{1}{r - W\vec{i}} + \frac{1}{r + W\vec{i}}\right)$$

$\vec{i}$ is used to denote this apply to axis

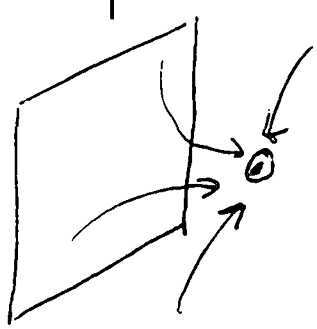

when infinite number of sinks are considered (located at $(2n-1)W$ along the x-axis

$$\phi = -\frac{Q}{4\pi}\sum \frac{1}{r - (2n-1)W\vec{i}}$$

$$V_x = \frac{Q}{4\pi}\sum \frac{x - (2n-1)W}{|r - (2n-1)W\vec{i}|^3}$$

$$V_y = \frac{Q}{4\pi}\sum \frac{y}{|r - (2n-1)W\vec{i}|^3}$$

$$V_Z = \frac{Q}{4\pi} \sum \frac{\cdot Z}{|r-(2n-1)Wi|^3}$$

These velocities are for the following flow field $(X=0)$ $(X=W)$ $(X=2W)$

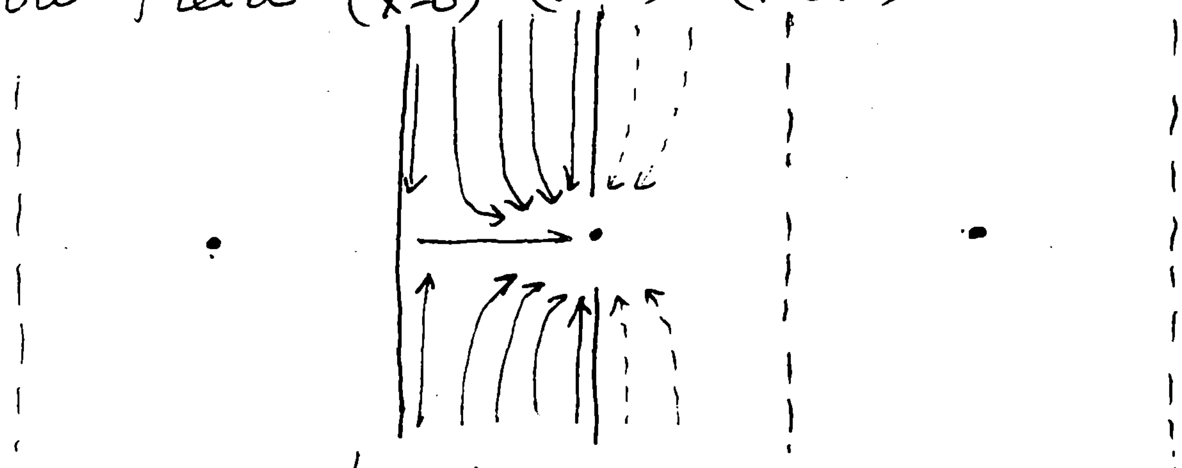

Now Blowdown flow, Q_B, is half the sink flow, Q. $\therefore Q = Q_B * 2$

Also pressure distribution the shroud wall is calculated

$$P_0 = P_S + \frac{\rho V^2}{2g_c}$$

$$(P_0 - P_S) = \frac{\rho V^2}{2g_c}$$

Numerical computation becomes quite complicated.

Subject | Originator | Date
Number | Verifier | Date

To understand the behavior near suction nozzle, the most simplest case was considered, i.e. $\boxed{\text{sinks at } x = -W \text{ and } +W}$

at $x=0$, (on the shroud wall)

$V_x = 0$, $\quad V^2 = V_y^2 + V_z^2$

also introduce $V_\infty = Q_B / \pi D \cdot W$

and $Q = 2 Q_B$

$$\therefore \frac{P_0 - P}{\left(\frac{\rho V_\infty^2}{2 g_c}\right)} = \frac{1}{4} \frac{W^2 D^2 a^2}{(W^2 + a^2)^3}$$

where $a^2 = y^2 + z^2$

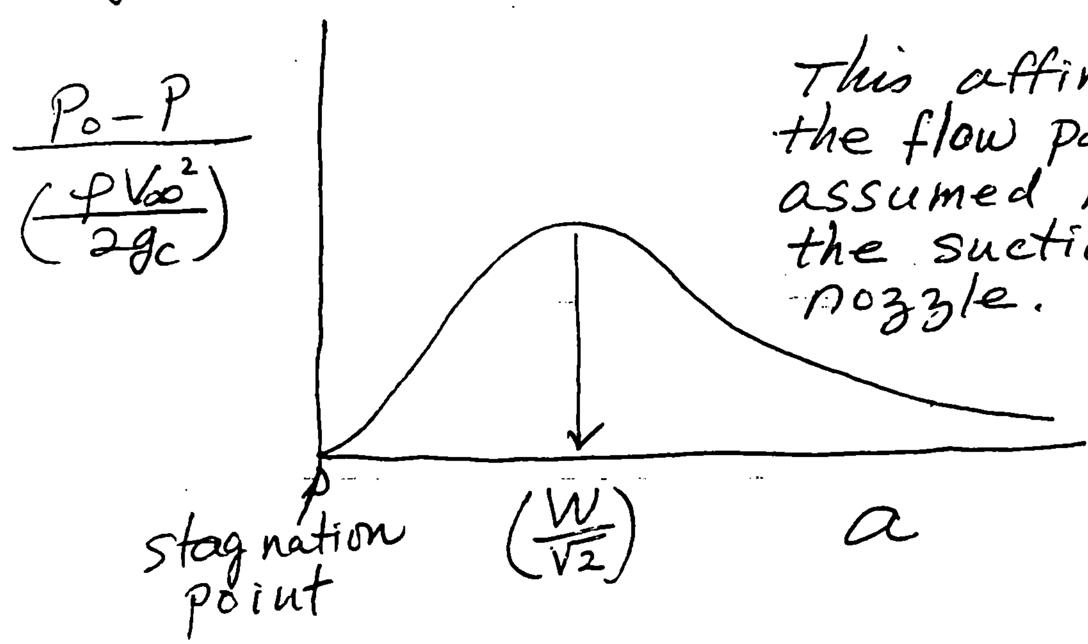

This affirms the flow pattern assumed near the suction nozzle.

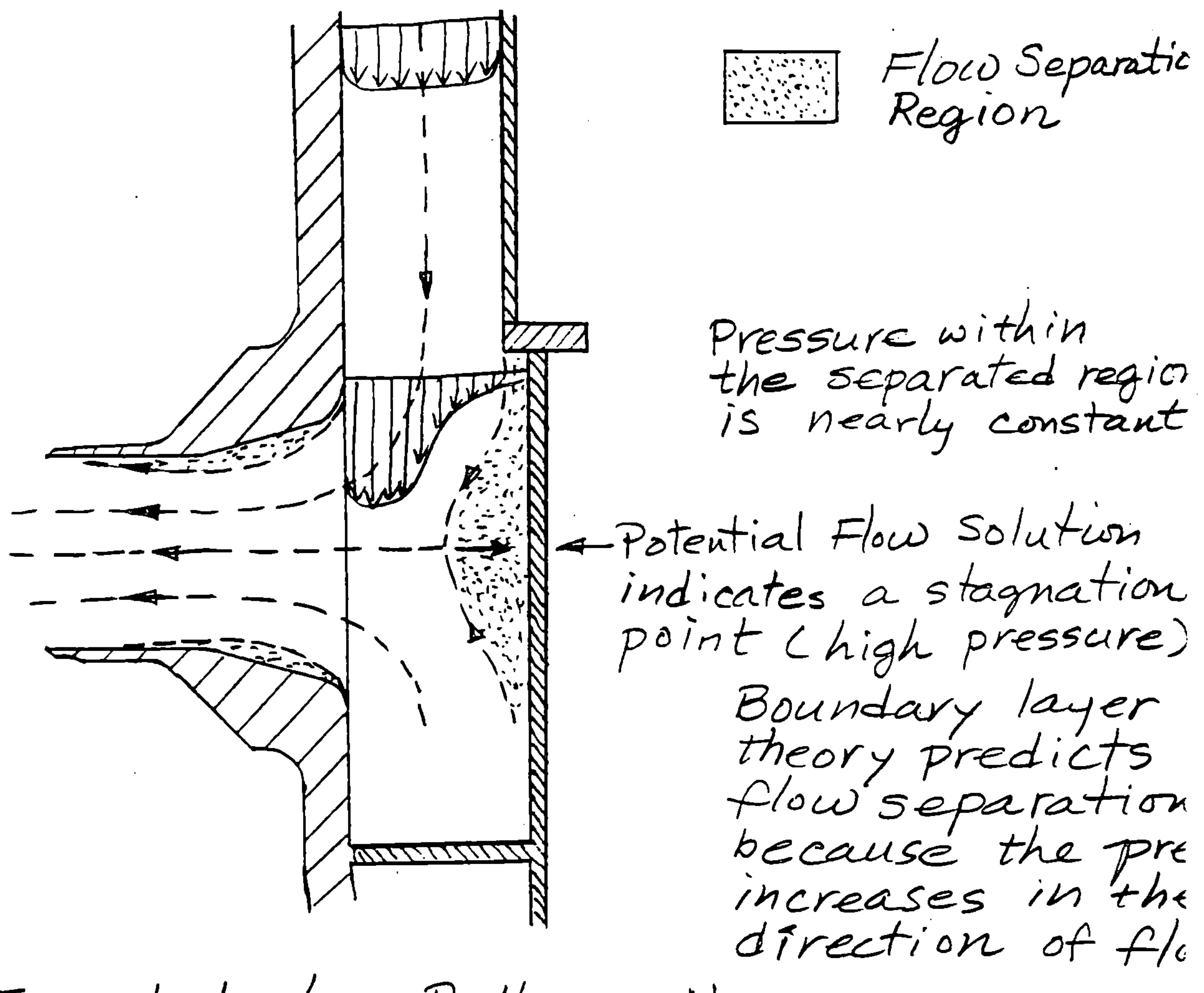

Expected Flow Pattern Near
the Recirculation Suction Nozzle

Fig. 1

blowdown force

ANGLE (DEG)	0	10	20	30	40	50	60	70	80
			C1(pi/36) =	0.087		D (inches) =	229.063	b (inches) =	40.625
	X/D =		Y (H5, inch) =	191.125	Y(H3,inch)=	354.875	Ymax(inch)=	407.000	Y(H5)/D =
Y/D =	0.000	0.087	0.175	0.262	0.349	0.436	0.524	0.611	0.698
0.000	0.000	4.861	7.623	6.406	4.667	3.314	2.361	1.696	1.225
0.087	13.190	12.212	9.473	6.738	4.702	3.303	2.351	1.691	1.225
0.175	30905.684	37.790	12.698	7.175	4.692	3.247	2.313	1.676	1.224
0.177		38.261	12.753	7.179	4.688	3.244	2.312	1.675	1.224
0.262	51.063	26.272	11.859	6.806	4.454	3.107	2.241	1.646	1.221
0.307	25.000	17.904	10.196	6.297	4.235	3.000	2.190	1.625	1.218
0.349	15.812	12.938	8.608	5.729	3.989	2.882	2.133	1.602	1.214
0.436	8.342	7.606	6.060	4.581	3.444	2.612	2.002	1.547	1.203
0.524	5.419	5.139	4.458	3.665	2.941	2.342	1.864	1.486	1.188
0.611	3.941	3.807	3.455	2.996	2.527	2.099	1.731	1.423	1.170
0.698	3.082	3.007	2.802	2.517	2.202	1.893	1.611	1.364	1.151
0.785	2.534	2.488	2.359	2.171	1.952	1.725	1.508	1.309	1.133
0.873	2.164	2.133	2.046	1.916	1.759	1.590	1.421	1.262	1.115
0.960	1.901	1.880	1.819	1.725	1.609	1.481	1.349	1.220	1.099
1.022	1.760	1.743	1.694	1.619	1.524	1.417	1.305	1.195	1.089
1.047	1.710	1.694	1.649	1.580	1.492	1.393	1.289	1.185	1.085
1.134	1.565	1.554	1.520	1.468	1.400	1.323	1.240	1.155	1.073
1.222	1.455	1.446	1.420	1.380	1.327	1.266	1.199	1.130	1.062
1.249	1.426	1.418	1.394	1.356	1.307	1.250	1.188	1.123	1.059
1.309	1.369	1.362	1.342	1.310	1.268	1.219	1.165	1.109	1.052
1.396	1.301	1.296	1.280	1.254	1.221	1.181	1.137	1.091	1.044
1.484	1.247	1.243	1.230	1.210	1.183	1.151	1.115	1.076	1.037
1.571	1.203	1.200	1.190	1.173	1.151	1.125	1.096	1.064	1.031
3.142	1.008	1.008	1.007	1.007	1.006	1.005	1.004	1.003	1.001
Gm =	8000.000	lbm/sec.ft^2		A (ft^2) =	3.451		mdot(lm/sec)=	27607.757	
A(anl.,ft^2)=	109.630	V (ft/sec) =	5.475	VHead(psi)=	0.149		rho(lm/ft^3)=	46.000	
		v (ft/sec) =	173.913	VHead(psi)=	150.029		Q (ft^3/sec)=	600.169	
BLOWDOWN F=	30231.984	lmf		ratio =	1009.193				

 (continue to page 3)

90	100	110	120	130	140	150	160	170	180
b/D =	0.177	W (inches) =	21.938	d (inches) =	25.154				
0.307	Y(H3)/D =	1.022	Ymax/D =	1.249					
0.785	0.873	0.960	1.047	1.134	1.222	1.309	1.396	1.484	1.571
0.884	0.634	0.447	0.307	0.202	0.123	0.067	0.029	0.007	0.000
0.887	0.639	0.453	0.313	0.208	0.130	0.074	0.036	0.014	0.007
0.896	0.653	0.470	0.333	0.229	0.151	0.095	0.057	0.035	0.028
0.896	0.653	0.471	0.333	0.229	0.152	0.096	0.058	0.036	0.029
0.908	0.675	0.498	0.363	0.261	0.184	0.128	0.091	0.069	0.062
0.916	0.688	0.515	0.382	0.281	0.205	0.150	0.112	0.091	0.084
0.923	0.702	0.533	0.402	0.302	0.227	0.173	0.135	0.114	0.106
0.938	0.732	0.573	0.448	0.352	0.279	0.225	0.188	0.167	0.160
0.951	0.764	0.615	0.498	0.406	0.335	0.283	0.248	0.227	0.220
0.963	0.794	0.658	0.549	0.462	0.395	0.345	0.311	0.291	0.284
0.972	0.823	0.699	0.599	0.518	0.455	0.408	0.375	0.356	0.350
0.980	0.849	0.738	0.647	0.573	0.514	0.470	0.439	0.421	0.415
0.985	0.871	0.774	0.692	0.624	0.571	0.530	0.501	0.484	0.478
0.989	0.891	0.806	0.733	0.672	0.623	0.586	0.559	0.544	0.539
0.992	0.903	0.826	0.759	0.703	0.658	0.623	0.598	0.584	0.579
0.992	0.908	0.834	0.769	0.715	0.672	0.638	0.614	0.599	0.595
0.995	0.923	0.858	0.802	0.754	0.715	0.685	0.663	0.650	0.646
0.996	0.935	0.880	0.831	0.789	0.754	0.728	0.708	0.697	0.693
0.997	0.939	0.886	0.839	0.799	0.766	0.740	0.721	0.710	0.706
0.997	0.945	0.898	0.856	0.819	0.789	0.765	0.748	0.738	0.735
0.998	0.954	0.914	0.877	0.846	0.819	0.799	0.784	0.775	0.772
0.999	0.962	0.927	0.896	0.869	0.846	0.828	0.815	0.807	0.804
0.999	0.968	0.938	0.912	0.889	0.869	0.853	0.842	0.835	0.833
1.000	0.999	0.997	0.996	0.995	0.994	0.993	0.993	0.992	0.992

13 of 17

		F (lmf) =	11482.553	(FORCE INTEGRAL)					
		0.287		0.579		0.268		0.155	
BOTTOM	0.000	6.574	4.853	6.739	7.594	3.266	6.339	2.056	4.544
*	25.000	5.484	12.198	5.995	9.437	2.522	6.664	1.489	4.572
*	25.000	3.302	37.755	3.815	12.641	1.559	7.080	0.889	4.540
*	25.000	3.231	38.225	3.708	12.695	1.523	7.083	0.869	4.536
*	25.000	1.120	26.203	0.988	11.768	0.490	6.678	0.288	4.270
H5	24.916		17.814		10.084		6.147		4.030
	(B-T)	(180-0)	(C-S)	(170-10)	(D-R)	(160-20)	(E-Q)	(150-30)	(F-P)
H5	24.916	0.000	17.814	0.000	10.084	0.000	6.147		4.030
	15.705	0.861	12.825	0.649	8.473	0.393	5.556	0.248	3.762
	8.182	1.903	7.439	1.533	5.872	1.019	4.356	0.681	3.165
	5.199	2.487	4.912	2.072	4.210	1.459	3.382	1.018	2.605
	3.658	2.873	3.516	2.440	3.144	1.780	2.651	1.281	2.132
	2.732	3.152	2.651	2.709	2.427	2.023	2.109	1.489	1.747
	2.119	3.364	2.067	2.915	1.920	2.213	1.701	1.655	1.437
	1.685	3.530	1.649	3.077	1.545	2.364	1.386	1.790	1.188
	1.363	3.663	1.336	3.207	1.260	2.486	1.140	1.900	0.986
H3	1.182	3.741	1.160	3.284	1.096	2.559	0.996	1.966	0.866
	1.115	3.771	1.095	3.313	1.036	2.586	0.942	1.991	0.821
	0.919	3.859	0.903	3.400	0.857	2.669	0.783	2.066	0.685
	0.762	3.933	0.749	3.473	0.712	2.737	0.652	2.129	0.573
TOP	0.719	3.953	0.707	3.493	0.672	2.756	0.616	2.146	0.541
		0.172		0.300		0.226		0.162	
		F (lmf) =	8601.958	(FORCE ABOVE H5)					

* Near the recirculation suction nozzle, flow separation occurs on the outer wall of the shroud. The pressure within the flow separated region is nearly constant and close to the pressure at H5 weld location.

The forces are calculated for the half section of the shroud assembly.

 (continued to page 7)

blowdown force

0.091		0.052		0.026		0.011		0.003
1.366	3.113	0.919	2.055	0.605	1.249	0.369	0.591	0.175
0.968	3.095	0.648	2.037	0.426	1.238	0.260	0.586	0.123
0.571	3.019	0.381	1.981	0.251	1.205	0.153	0.571	0.073
0.558	3.015	0.372	1.978	0.246	1.204	0.150	0.571	0.071
0.186	2.847	0.125	1.878	0.083	1.149	0.051	0.546	0.024
	2.719		1.807		1.111		0.530	
(140-40)	(G-O)	(130-50)	(H-N)	(120-60)	(I-M)	(110-70)	(J-L)	(100-80)
	2.719		1.807		1.111		0.530	
0.165	2.580	0.112	1.731	0.075	1.070	0.046	0.512	0.022
0.467	2.260	0.323	1.554	0.218	0.975	0.135	0.470	0.065
0.719	1.936	0.507	1.366	0.346	0.871	0.216	0.424	0.104
0.926	1.637	0.662	1.182	0.457	0.765	0.287	0.376	0.139
1.095	1.375	0.794	1.013	0.553	0.664	0.350	0.329	0.170
1.234	1.153	0.904	0.861	0.634	0.571	0.404	0.284	0.196
1.349	0.965	0.997	0.730	0.704	0.488	0.450	0.244	0.219
1.443	0.809	1.074	0.616	0.763	0.415	0.489	0.208	0.239
1.501	0.714	1.121	0.546	0.798	0.369	0.513	0.186	0.251
1.522	0.678	1.139	0.519	0.812	0.351	0.523	0.177	0.256
1.588	0.568	1.193	0.437	0.854	0.297	0.551	0.150	0.270
1.643	0.477	1.239	0.368	0.889	0.250	0.575	0.127	0.282
1.658	0.451	1.251	0.349	0.899	0.237	0.581	0.120	0.286
0.111		0.070		0.039		0.017		0.004

15-H17

blowdown force

MOMENT INTEGRAL

	(B-T)	(180-0)	(C-S)	(170-10)	(D-R)	(160-20)	(E-Q)	(150-30)	(F-P)
H5	0.000	0.000	0.000	0.000	0.000	0.000	0.000	0.000	0.000
	0.666	0.014	0.544	0.012	0.359	0.008	0.235	0.005	0.159
	1.061	0.089	0.964	0.077	0.761	0.056	0.565	0.040	0.410
	1.128	0.185	1.065	0.166	0.913	0.130	0.734	0.097	0.565
	1.113	0.283	1.070	0.259	0.956	0.211	0.806	0.164	0.648
	1.069	0.378	1.038	0.351	0.950	0.294	0.826	0.235	0.684
	1.015	0.469	0.990	0.439	0.919	0.376	0.814	0.307	0.688
	0.954	0.555	0.933	0.523	0.875	0.454	0.785	0.376	0.672
	0.890	0.635	0.873	0.602	0.823	0.528	0.744	0.443	0.644
H3	0.845	0.689	0.829	0.655	0.784	0.578	0.712	0.488	0.619
	0.826	0.710	0.811	0.676	0.767	0.598	0.698	0.506	0.608
	0.761	0.779	0.748	0.744	0.709	0.662	0.648	0.565	0.567
	0.697	0.843	0.686	0.806	0.652	0.721	0.597	0.619	0.524
TOP	0.678	0.862	0.667	0.825	0.634	0.739	0.581	0.635	0.510
	Yi =	0.218		0.236		0.268		0.296	
	Fi*Yi =	0.038		0.071		0.061		0.048	
	MOMENT =	530452.27							
	Y =	61.666	inches						

The moment is calculated for the half of the shroud assembly.

 (Continue to page 8)

blowdown force

(140-40)	(G-O)	(130-50)	(H-N)	(120-60)	(I-M)	(110-70)	(J-L)	(100-80)
0.000	0.000	0.000	0.000	0.000	0.000	0.000	0.000	0.000
0.003	0.109	0.002	0.073	0.002	0.045	0.001	0.022	0.000
0.028	0.293	0.020	0.201	0.014	0.126	0.008	0.061	0.004
0.071	0.420	0.051	0.296	0.035	0.189	0.022	0.092	0.011
0.124	0.498	0.091	0.360	0.064	0.233	0.041	0.114	0.020
0.182	0.538	0.136	0.396	0.097	0.260	0.062	0.129	0.030
0.242	0.552	0.184	0.412	0.132	0.273	0.085	0.136	0.042
0.301	0.546	0.232	0.413	0.168	0.276	0.109	0.138	0.054
0.359	0.528	0.279	0.403	0.204	0.271	0.133	0.136	0.066
0.397	0.510	0.311	0.391	0.228	0.264	0.150	0.133	0.074
0.413	0.502	0.324	0.385	0.238	0.260	0.156	0.131	0.077
0.464	0.470	0.366	0.362	0.271	0.246	0.178	0.124	0.089
0.512	0.436	0.406	0.337	0.301	0.229	0.199	0.116	0.099
0.526	0.425	0.417	0.328	0.310	0.223	0.205	0.113	0.102
0.317		0.334		0.345		0.353		0.358
0.035		0.023		0.014		0.006		0.002

17 of 17

BOUNDING LATERAL SHROUD DISPLACEMENT RELATIVE TO RPV DUE TO ASYMMETRIC ACOUSTIC LOAD AND TO SEISMIC SSE

(Alternate Calculation)

PURPOSE

The purpose of this calculation is to verify the upper bound shroud lateral displacements relative to the RPV given in Section 15 of DRF A00-05652 "Asymmetric Load Analysis for Core Shroud Assembly without H5 Weld", for Dresden and Quad Cities.

Bounding relative displacements are calculated for: (1) Asymmetric Acoustic Load due to recirculation suction line break, and (2) Seismic SSE excitation.

ASYMMETRIC ACOUSTIC LOAD

Methodology. Based on a fundamental structural dynamics principle, it first demonstrated that the displacement of the shroud due to the acoustic load is small. Then based on a very conservative calculation, an upper bound value for the small lateral displacement is obtained.

Deamplification. As has been demonstrated ad infinitum, both theoretically by anal and empirically by dynamic test, the structural responce is significantly deamplified relative to the input excitation whenever a low frequency structure is excited b a high frequency excitation. The extent of the deamplification is dependen on the ratio of the dominant characteristic frequency of the excitation to th predominant (generally fundamental) natural frequency of the structure an or the ratio of the duration of the impulse to the dominant natural period of the structure.

The acoustic load resultant force time history on the shroud due to a recirculation suction line break for Dresden 2 and 3 is given in Figure 3.9-6 of the Dresden 2 & 3 USAR. The USAR figure is given in Figure 1 of this calculation. Figure 1 is representative of both Dresden and Quad Cities for purpose of the present evaluation.

From Figure 1, it is observed that the resultant acoustic load on the shroud corresponds to an impulse load with a characteristic frequency $f_c > 50$ Hz; i. $f_c = 1/T = 1/0.02 = 50$ Hz.

The shroud fundamental frequency for the uncracked weld condition is 6.69 H and that for a 360° through-wall crack for weld H5 is 0.073 Hz. These values come from eigen-analyses of the seismic, licensing basis, primary structure model for Quad Cities 1 & 2. The values are representative of both Quad Cites and Dresden for the present evaluation.

The eigen summary table for the uncracked weld case is given by Table 1. The summary table for a 360° through-wall crack at H5 with the shrou pin-connected at H5 is given by Table 2 and with the shroud on a roller at H5 by Table 3.

Denoting the characteristic frequency of the acoustic impulse by Ω, (>50) and the duration by t_d, ($\cong 0.020$ sec), and the structurally dominant natural (fundamental) frequency and natural period of the shroud by ϖ, (< 0.073 Hz), and T, ($> 1/0.073 = 13.7$ sec); respectively, we have

$$\Omega/\varpi \geq 50/0.073 = 685 \quad \ldots (1)$$

and

$$t_d/T \leq 0.020/13.7 = 0.0015 \quad \ldots (2)$$

Subject | Originator DKHenrie | Date 6/11/94
Number | Verifier | Date

The maximum possible structural dynamic amplification occurs for harmonic excitation of a Simple Harmonic Oscillator (SHO) in which the excitation frequency is equal to oscillator frequency. In addition, the excitation must be for a sufficient number of cycles to allow for the resonant build-up. As discussed above, the response of the SHO is deamplified relative to that of the harmonic input motion if the driving frequency is sufficiently high relative to the oscillator frequency. The corresponding dynamic amplification curve, taken from Bigg's "Introduction to Structural Dynamics", is given in Figure 2.

The dynamic amplification from Figure 2 for the frequency ratio calculated in Eq. (1) is essentially zero. If the same SHO was excited by the acoustic force time history impulse in Figure 1, the dynamic amplification would be even lower. Farthermore, the dynamic amplification of the cracked shroud excited by the acoustic impulse is even lower than that for the SHO excited by the acoustic impulse.

Figures 3 and 4, also taken from Biggs, give the dynamic amplifications of a SHO excited by impulses more nearly representative of the acoustic impulse. Figure 4 provides the closest approximation of the two. Again, the dynamic amplification of a SHO excited by any of the impulse loads of Figures 3 and 4 is essentially zero for the period ratio calculated in Eq. (20). The dynamic amplification of the shroud excited by any of the Figure 3 and 4 impulse loads would be even lower. Since the Figure 3 and 4 impulse loa[ds] are approximately representative of the acoustic load, it follows that the dyn[amic] amplification of the shroud, excited by the acoustic load, is also essentially zero.

<u>Conclusion.</u> Based on the foregoing discussion, it follows that the dynamic amplification of the Dresden or Quad Cities shroud is approximately zero when excited by the acoustic impulse time history given in Figure 1. Therefore, the expected displacement of the shroud due to the acoustic loading is also close to zero.

Subject	Originator DKHenrie	Date 6/11/94
Number	Verifier	Date

Shroud Bounding Lateral Displacement. The following calculations provide an independent demonstration of the foregoing conclusion.

From Newtons 2nd Law:

$$\vec{F} = \frac{d\vec{p}}{dt} \qquad \ldots (3)$$

Integrating with-respect-to (wrt) time,

$$\vec{p} - \vec{p}_0 = \int_{t_0}^{t} \vec{F}(t)\,dt \qquad \ldots (4)$$

Assuming system (i.e., shroud) at rest at $t = t_0$ implies $\vec{p}_0 = \vec{0}$. Then

$$\vec{p} = \int_{t_0}^{t} F(t)\,dt \ , \quad (= \text{Impulse}) \qquad \ldots (5)$$

From Figure 1., the impulse is conservatively calculated by

$$\int_{t_0}^{t} F(t)\,dt < (240{,}000\ \text{lb}) \times (0.020\,\text{sec})$$
$$= 4{,}800\ \text{lb-sec} \qquad \ldots (6)$$

The momentum $\vec{p}$ is given by

$$\vec{p} = m\dot{x} = \frac{413{,}000}{386}\dot{x} = \left(1070\ \frac{\text{lb-sec}^2}{\text{in}}\right)\dot{x} \qquad \ldots (7)$$

Subject | Originator DK Henrie | Date 6/11/94
Number | Verifier | Date

Substitute (7) and (6) into (5),

$$1070\left(\frac{\text{lb-sec}^2}{\text{in}}\right) \dot{x} < 4800 \text{ lb-sec} \qquad \ldots (8)$$

$$\rightarrow \quad \dot{x} < 4800/1070 \text{ in/sec} = 4.49 \text{ in/sec.} \qquad \ldots (9)$$

Then very conservatively assuming that the shroud had this upper bound velocity at the beginning of the acoustic loading, the shroud maximum lateral displacement at the end of the idealized rectangular impulse; i.e., after 0.020 seconds is

$$\begin{aligned} x &< \dot{x} \times (0.020) \\ &= (4.49) \times 0.02 \\ &= 0.090 \text{ in.} \end{aligned} \qquad \ldots (10)$$

The actual lateral displacement is much less the conservative upper bound value given by (10). In addition to: (1) the assumed rectangular impulse, (2) the maximum velocity $\dot{x} = 4.49$ in/sec assumed to occur uniformly throughout the entire acoustic loading, and (3) the assumption of rigid body (actually particle) mechanics, the surface traction along the cracked weld surface as well as all fluid drag forces and all restoring spring forces due to piping, etc. were neglected in the calculation. Only the acoustic loading was considered.

It can be concluded at this point that an upper bound on the shroud displacement relative to the RPV is well below 90 mils and that minimal benefit will be obtained by trying to more precisely quantify this higher order effect. However, based on the conservative, simplifying assumptions, it is expected that the upper bound displacement will be less than 20 mils.

Subject	Originator DK Henrie	Date 6/11/94
Number	Verifier	Date

SEISMIC SSE DISPLACEMENTS

The Quad Cities 1 & 2 primary structure seismic model was modified to account for a 360° through-wall crack of Weld H5. Two shroud configurations were analyzed to bound the H5 weld crack condition. The first configuration assumed that only the shroud shear could be transmitted through the cracked weld. Consequently, the shroud was pin-connected at the weld location.

In the second shroud configuration, it was assumed that neither the shro shear nor the shroud moment could be transfered across the crack weld. Consequently, the shroud was roller connected in the horizontal direction at the H5 weld location in the second configuration.

Both shroud configurations resulted in model instability. In order to circumvent the corresponding analytical singularities in the liner time history analyses, the models were farther modified to include soft elastic links between the shroud and the RPV. In turn, two configurations each were selected for both the pin-connected and the roller-connected shroud configuration. In the first configuration, an elastic link was assumed between that shroud and the RPV at the top guide elevation only. In the second configuration, elastic links were assumed at both the top guide and core support plate elevations.

The stiffness of the shroud-to-RPV elastic links were initially selected low enough such that insignificant changes resulted in the eigendata set when the soft springs were added to the original (benchmark) primary structure model with no cracked welds. The elastic link stiffness were farther reduced to more realistically reflect the actual stiffness of connecting piping between the shroud and the RPV.

Subject		Originator D.K. Henrie	Date 6/11/94
Number		Verifier	Date

The modified primary structure models were subjected to the Quad Cities licensing basis free-field, seismic SSE acceleration time history; i.e., 1957 Golden Gate Park, S 80°E, normalized to 0.25g.

Conclusion. The maximum lateral displacement of the shroud relative to the RPV for the pin-connected shroud configuration model is 0.53" (Computer Run 2865V) and for the roller-connected shroud configuration model the maximum relative displacement is 0.68" (Computer Run 2866V)

FIGURE 1. Acoustic Load Resultant Time History

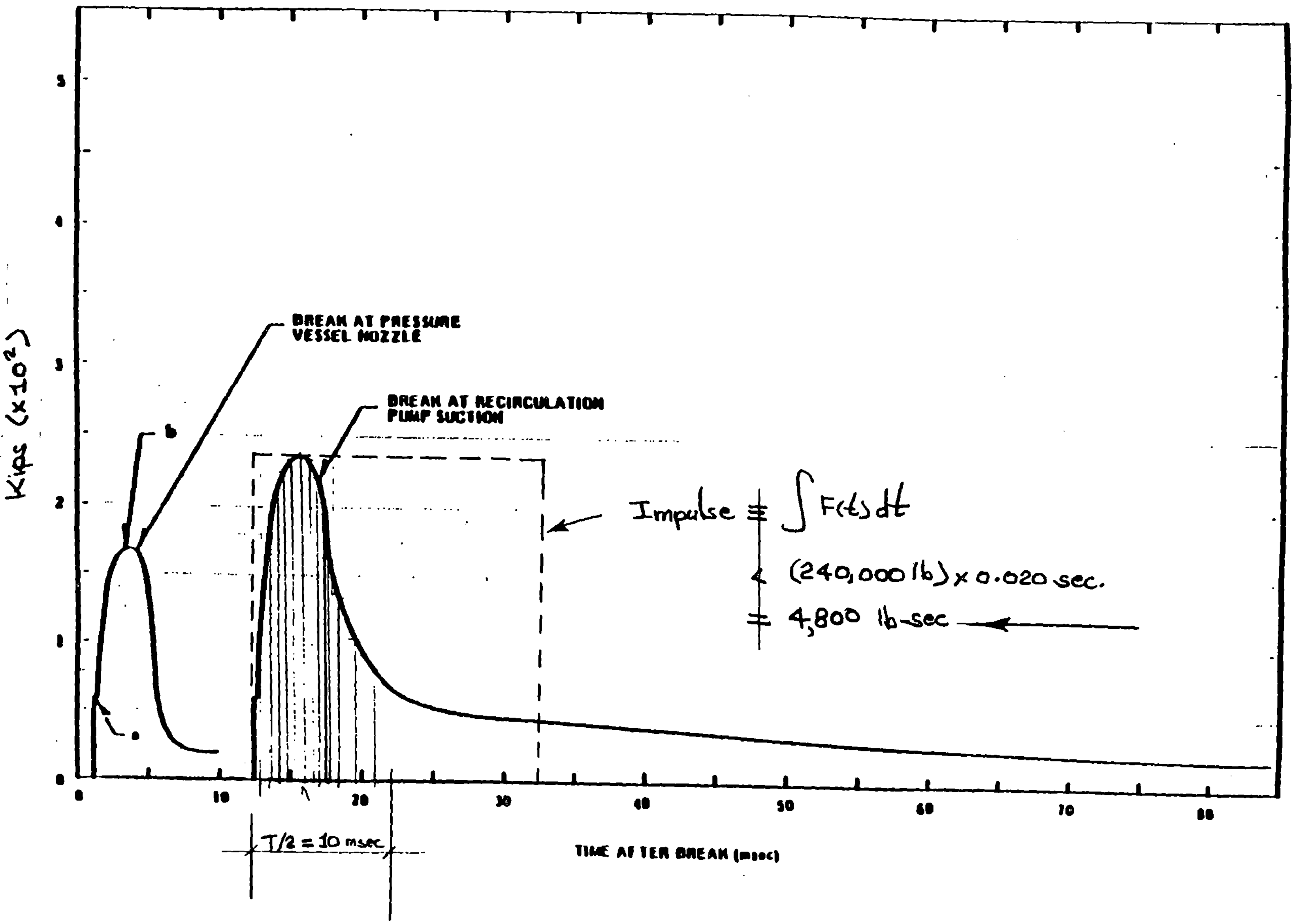

DRESDEN STATION
UNITS 2 & 3
REACTOR VESSEL SHROUD FORCE FOLLOWING RECIRCULATION LINE BREAK
FIGURE 3.9-6

Sheet 9 of 14

Peak values occur at damped natural frequencies!

$$\frac{\Omega}{\omega_d} = \frac{\Omega}{\omega\sqrt{1-\lambda^2}}$$

Then $\frac{\Omega}{\omega_d} = 1$

$$\Rightarrow \frac{\Omega}{\omega} = \sqrt{1-\lambda^2}$$

NOTE:

FIG. 2.18 GIVES THE FORCED PART; i.e., PARTICULAR SOLUTION, DLF. THUS THE RESPONSE IS AT THE DRIVING FREQUENCY Ω.

$\lambda = \beta/\omega$ = FRACTION CRITICAL DAMPING

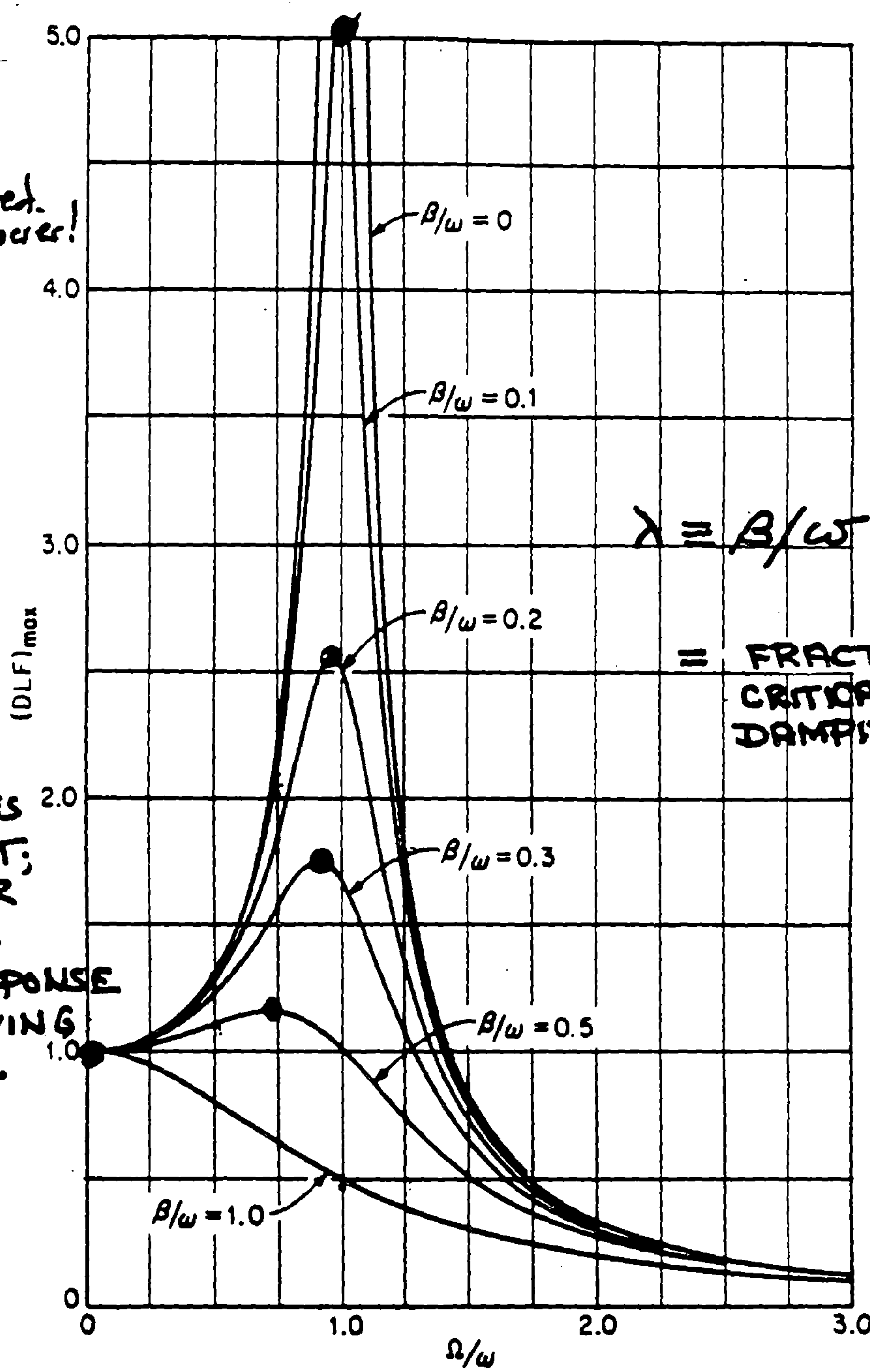

FIGURE 2.18 Maximum dynamic load factor for sinusoidal load, $F_1 \sin \Omega t$, damped systems.

FIGURE 2.

Sheet 10 of 14

FIGURE 3.

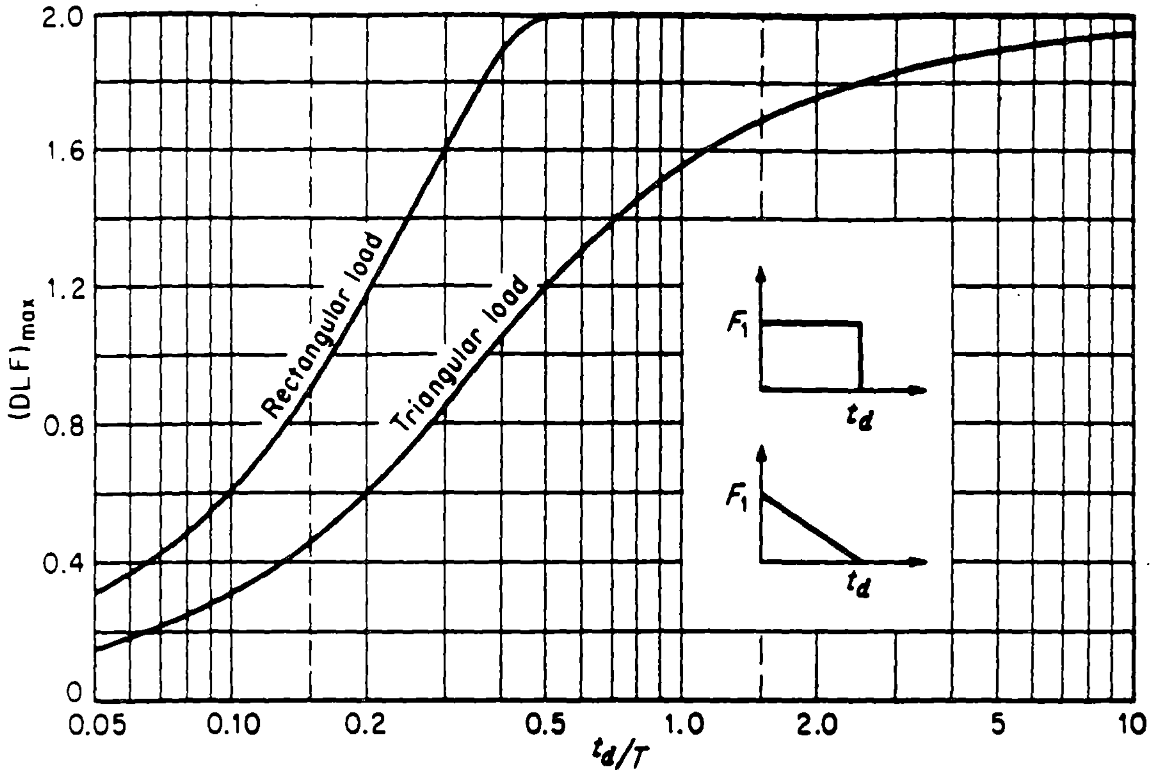

(a)

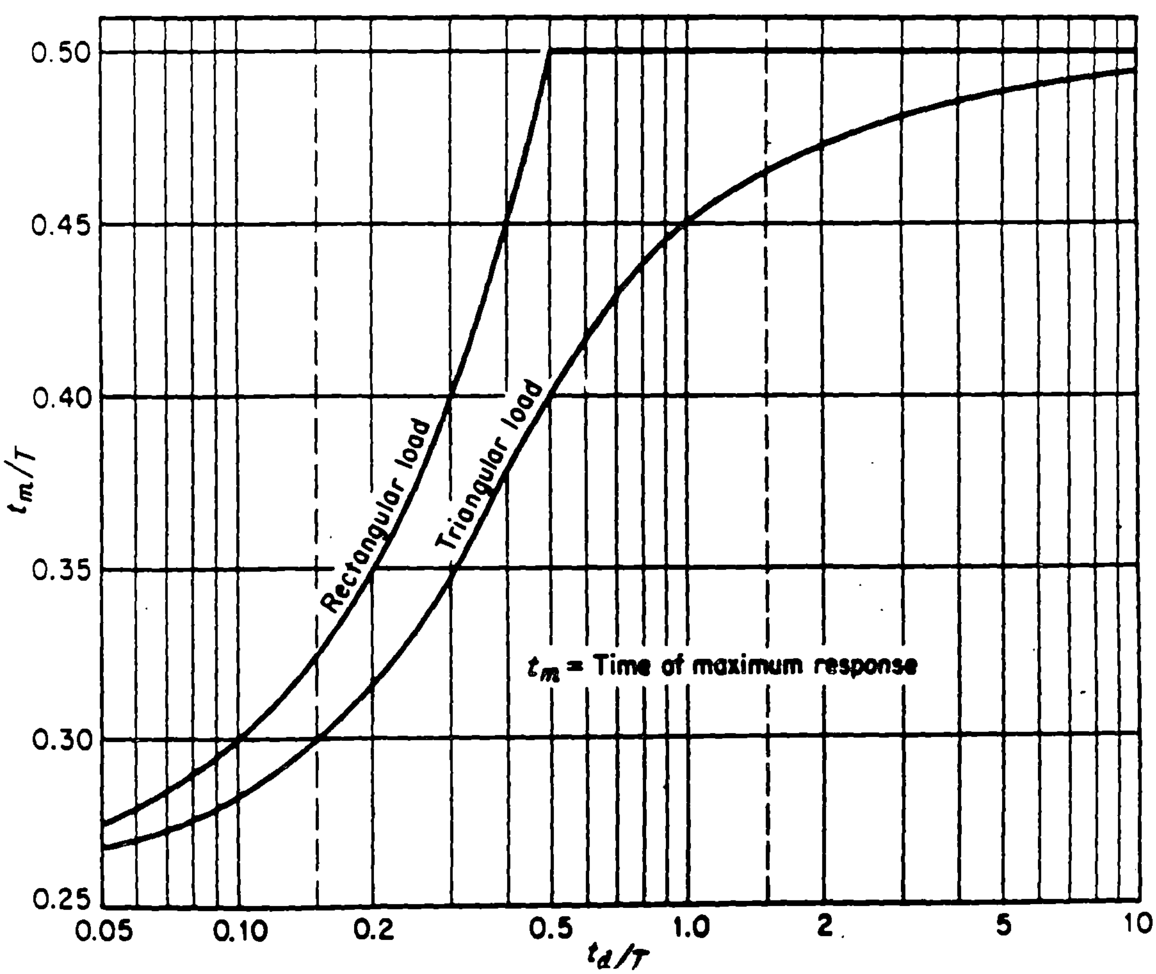

FIGURE 4. Sheet 11 of 14

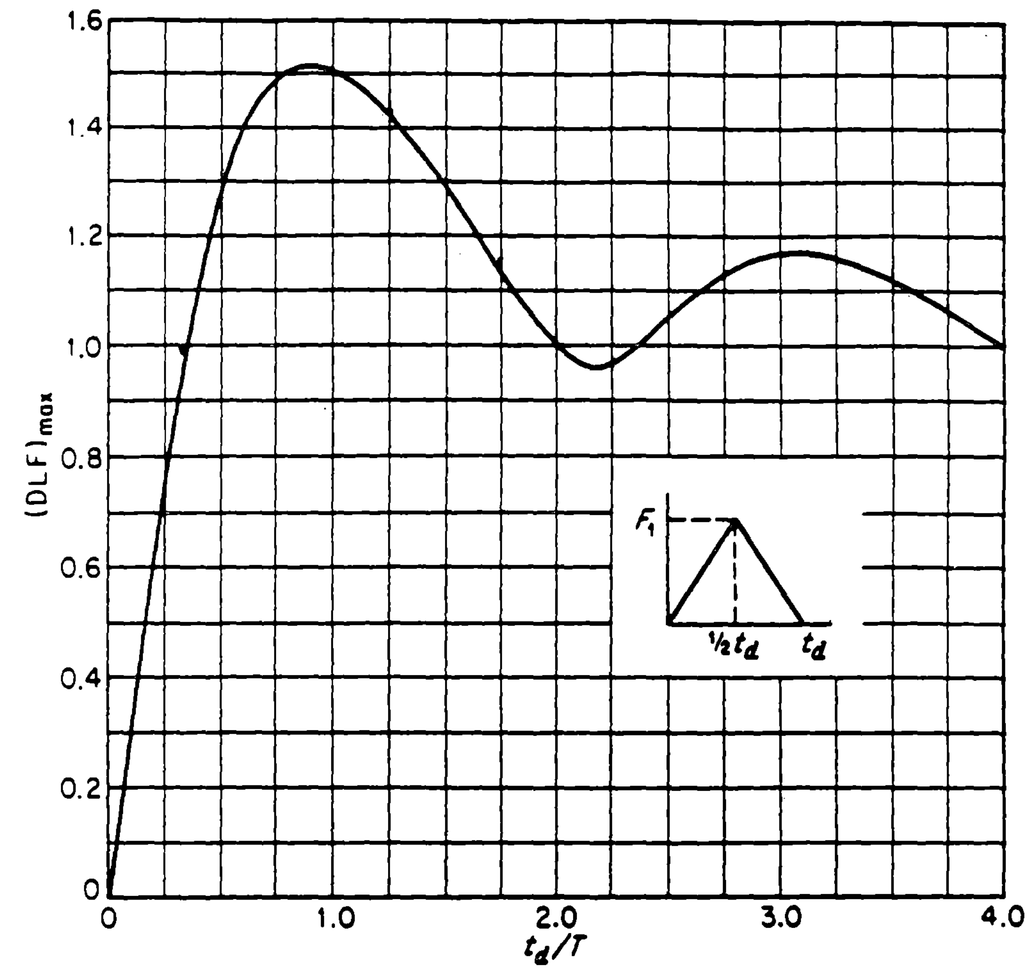

(a)

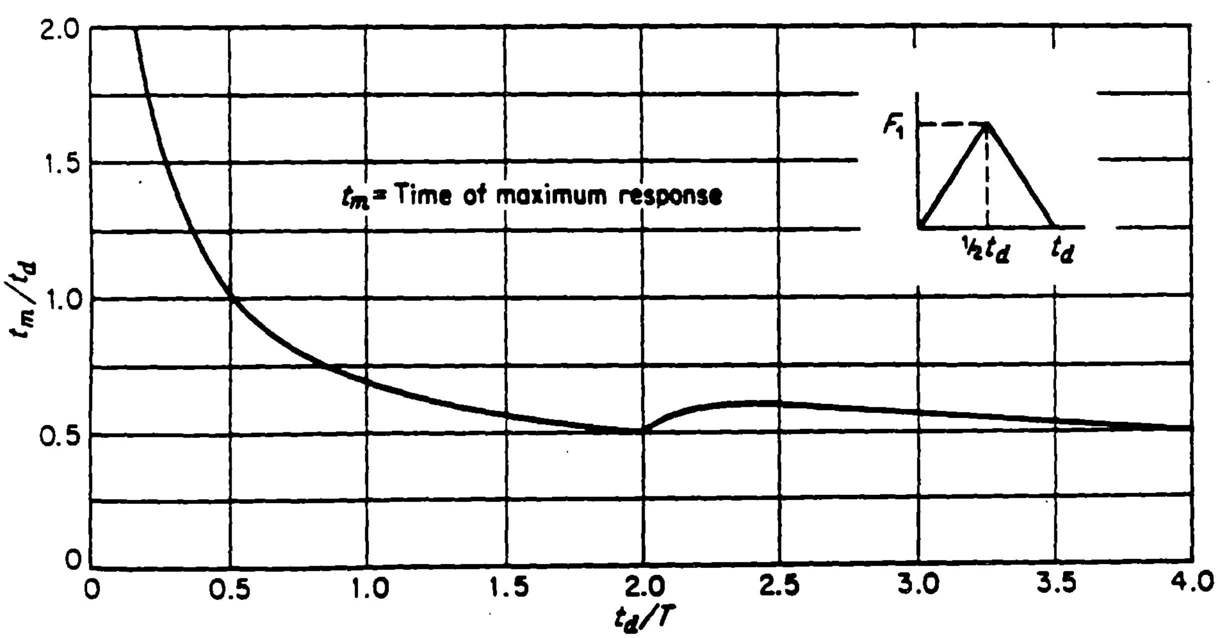

(b)

FIGURE 2.8 Maximum response of one-degree elastic systems (undamped) subjected to equilateral triangular load pulse.

TABLE 1.

*** M O D A L D I S P L A C E M E N T S U M M A R Y T A B L E ****

CASE 1

$K_{s/y} = 0$

(Benchmark)

IODE IBER	CIRCULAR FREQUENCY (RAD/TIME)	FREQUENCY (HERTZ)	PERIOD (TIME)	MAX MODAL AMPLITUDE	NODE NUMBER	DEG OF FREEDOM	MAX DYN DISPLACEMT	NODE NUMBER	DEG OF FREEDOM	MAX DYN ROTATION
1	1.8963E 01	3.0180E 00	3.3135E-01	1.9449E-01	29	1	3.9537E-02	19	5	1.8065E-05
2	2.5909E 01	4.1236E 00	2.4251E-01	1.3483E-01	24	1	8.4481E-02	24	5	1.0541E-02
3	2.6184E 01	4.1674E 00	2.3996E-01	1.6381E-01	18	1	4.6212E-02	19	5	5.5007E-03
4	3.4011E 01	5.4130E 00	1.8474E-01	7.6171E-01	38	1	8.0162E-02	24	5	1.8427E-03
5	3.9900E 01	6.3502E 00	1.5747E-01	5.0037E-01	38	1	5.1821E-02	17	5	4.3276E-03
6	4.2061E 01	6.6942E 00	1.4938E-01	1.1850E-01	11	1	3.2798E-02	17	5	5.9091E-03
7	5.5201E 01	8.7855E 00	1.1382E-01	4.8440E-02	30	1	1.2317E-02	17	5	1.0687E-04
8	6.2457E 01	9.9404E 00	1.0060E-01	5.5853E-03	11	1	7.0311E-04	17	5	1.1321E-04
9	7.6608E 01	1.2193E 01	8.2017E-02	3.5618E-03	40	1	1.1647E-03	24	5	3.4457E-07
10	8.9587E 01	1.4258E 01	7.0135E-02	1.7852E-02	1	1	3.9470E-03	24	5	1.9710E-04
11	9.6861E 01	1.5416E 01	6.4868E-02	3.1681E-02	1	1	1.3577E-03	11	5	7.0294E-05
12	1.0540E 02	1.6775E 01	5.9613E-02	2.6925E-04	21	1	7.4142E-05	20	5	1.1331E-05
13	1.1994E 02	1.9089E 01	5.2386E-02	4.0948E-05	19	1	1.3713E-05	18	5	5.6726E-06
14	1.2248E 02	1.9494E 01	5.1298E-02	1.6247E-03	21	1	1.1800E-04	20	5	1.4718E-05
15	1.3445E 02	2.1399E 01	4.6732E-02	1.3143E-03	21	1	1.0436E-03	20	5	1.1868E-04
16	1.3789E 02	2.1946E 01	4.5566E-02	3.0356E-04	39	1	1.1726E-04	11	5	4.8105E-07
17	1.3829E 02	2.2010E 01	4.5434E-02	2.5718E-04	11	1	1.2057E-04	11	5	1.9835E-05
18	1.5303E 02	2.4356E 01	4.1058E-02	8.6455E-03	21	1	5.9016E-04	24	5	1.2903E-04
19	1.7157E 02	2.7306E 01	3.6621E-02	9.9160E-05	23	1	5.0252E-05	24	5	2.6356E-05
20	1.8608E 02	2.9616E 01	3.3766E-02	3.1996E-04	31	1	1.7025E-04	24	5	5.7790E-07

TABLE 2.

****** M O D A L D I S P L A C E M E N T S U M M A R Y T A B L E ******

MODE NUMBER	CIRCULAR FREQUENCY (RAD/TIME)	FREQUENCY (HERTZ)	PERIOD (TIME)	MAX MODAL AMPLITUDE	NODE NUMBER	DEG OF FREEDOM	MAX DYN DISPLACEMT	NODE NUMBER	DEG OF FREEDOM	MAX DYN ROTATION
~~1~~	~~4.6289E-01~~	~~7.3671E-02~~	~~1.3574E 01~~	~~2.0813E-01~~	11	~~1~~	~~8.4700E-02~~	~~19~~	~~5~~	~~3.1530E-03~~
2	1.8963E 01	3.0180E 00	3.3135E-01	1.9447E-01	29	1	3.9532E-02	17	5	1.3841E-05
3	2.5928E 01	4.1266E 00	2.4233E-01	1.0803E-01	24	1	7.0556E-02	24	5	8.8180E-03
4	3.0956E 01	4.9268E 00	2.0297E-01	4.0632E-01	18	1	1.2131E-01	17	5	2.3162E-02
5	3.4159E 01	5.4366E 00	1.8394E-01	8.0811E-01	38	1	8.5816E-02	17	5	1.1780E-02
6	4.0087E 01	6.3801E 00	1.5674E-01	4.2656E-01	38	1	4.4231E-02	17	5	3.5226E-03
7	5.5201E 01	8.7854E 00	1.1382E-01	4.8427E-02	30	1	1.2311E-02	17	5	1.1748E-04
8	6.1774E 01	9.8316E 00	1.0171E-01	4.3202E-03	15	1	5.2869E-04	17	5	1.0706E-04
9	7.1421E 01	1.1367E 01	8.7974E-02	3.4139E-03	11	1	6.3966E-04	19	5	7.9477E-05
10	7.6608E 01	1.2193E 01	8.2017E-02	2.8427E-03	40	1	9.2955E-04	24	5	2.7444E-07
11	8.9596E 01	1.4260E 01	7.0128E-02	1.9230E-02	1	1	4.2654E-03	24	5	2.1332E-04
12	9.6861E 01	1.5416E 01	6.4868E-02	3.1006E-02	1	1	1.3385E-03	11	5	7.6208E-05
13	1.0588E 02	1.6851E 01	5.9343E-02	1.9649E-04	21	1	5.9658E-05	20	5	8.4309E-06
14	1.2068E 02	1.9207E 01	5.2064E-02	3.3044E-05	19	1	1.0815E-05	18	5	4.5364E-06
15	1.2248E 02	1.9494E 01	5.1298E-02	1.8217E-03	21	1	1.2960E-04	20	5	1.6328E-05
16	1.3485E 02	2.1462E 01	4.6594E-02	1.4224E-03	21	1	1.0964E-03	20	5	1.2960E-04
17	1.3789E 02	2.1946E 01	4.5566E-02	2.8654E-04	39	1	1.1070E-04	20	5	4.2231E-07
18	1.5302E 02	2.4354E 01	4.1061E-02	8.6461E-03	21	1	5.5250E-04	24	5	1.1966E-04
19	1.7079E 02	2.7182E 01	3.6789E-02	9.4143E-05	23	1	4.7045E-05	24	5	2.4676E-05
20	1.8607E 02	2.9614E 01	3.3768E-02	3.2690E-04	31	1	1.7341E-04	11	5	6.8776E-07

TABLE 3.

**** M O D A L D I S P L A C E M E N T S U M M A R Y T A B L E ****

MODE NUMBER	CIRCULAR FREQUENCY (RAD/TIME)	FREQUENCY (HERTZ)	PERIOD (TIME)	MAX MODAL AMPLITUDE	NODE NUMBER	DEG OF FREEDOM	MAX DYN DISPLACEMT	NODE NUMBER	DEG OF FREEDOM	MAX DYN ROTATION
1	4.5919E-01	7.3082E-02	1.3683E 01	1.8615E-01	11	1	7.9714E-02	11	5	3.1841E-03
2	8.5306E-01	1.3577E-01	7.3655E 00	1.4828E-01	61	1	5.7085E-02	11	5	3.4728E-03
3	1.8963E 01	3.0180E 00	3.3135E-01	2.1766E-01	29	1	4.4248E-02	17	5	1.5430E-05
4	2.5928E 01	4.1266E 00	2.4233E-01	9.0982E-02	24	1	5.9420E-02	24	5	7.4262E-03
5	3.1020E 01	4.9370E 00	2.0255E-01	5.6689E-01	18	1	1.6866E-01	17	5	3.2461E-02
6	3.4168E 01	5.4380E 00	1.8389E-01	7.3037E-01	38	1	7.7567E-02	17	5	1.1053E-02
7	4.0092E 01	6.3808E 00	1.5672E-01	5.1380E-01	38	1	5.3232E-02	17	5	4.3625E-03
8	5.5201E 01	8.7854E 00	1.1382E-01	4.2025E-02	30	1	1.0684E-02	17	5	1.0263E-04
9	6.1878E 01	9.8482E 00	1.0154E-01	4.7986E-03	11	1	6.4968E-04	17	5	1.1562E-04
10	7.6608E 01	1.2193E 01	8.2017E-02	2.8494E-03	40	1	9.3174E-04	24	5	2.9334E-07
11	8.1525E 01	1.2975E 01	7.7071E-02	8.3019E-03	15	1	1.4493E-03	19	5	2.4562E-04
12	9.0340E 01	1.4378E 01	6.9551E-02	1.8247E-02	1	1	4.2738E-03	18	5	2.8280E-04
13	9.6897E 01	1.5422E 01	6.4844E-02	2.9455E-02	1	1	1.5265E-03	18	5	1.0650E-04
14	1.0718E 02	1.7058E 01	5.8622E-02	9.9554E-05	21	1	3.5319E-05	20	5	4.5519E-06
15	1.2195E 02	1.9409E 01	5.1523E-02	1.5122E-05	19	1	4.8092E-06	18	5	2.0252E-06
16	1.2249E 02	1.9495E 01	5.1296E-02	2.1267E-03	21	1	1.2042E-04	18	5	2.5874E-05
17	1.3786E 02	2.1942E 01	4.5576E-02	9.1815E-04	39	1	3.2009E-04	20	5	3.6136E-05
18	1.3802E 02	2.1966E 01	4.5525E-02	1.2545E-03	21	1	8.4088E-04	20	5	1.0350E-04
19	1.5313E 02	2.4371E 01	4.1033E-02	7.9067E-03	21	1	6.9704E-04	24	5	1.5746E-04
20	1.7207E 02	2.7386E 01	3.6515E-02	1.0848E-04	23	1	5.4462E-05	24	5	2.8562E-05